Characterisation of the role of AMP-activated protein kinase in 3T3-L1 adipocytes

Pamela Jane Logan

Thesis submitted for the Degree of Doctor of Philosophy

September 2009

Division of Biochemistry and Cell Biology
Faculty of Biomedical and Life Sciences
University of Glasgow

Abstract

AMP-activated protein kinase (AMPK) has been proposed to be a therapeutic target for patients with type 2 diabetes and the metabolic syndrome. In skeletal muscle AMPK stimulates glucose uptake and fatty acid oxidation, whereas in liver it inhibits fatty acid and cholesterol synthesis. The Rab GTPase activating proteins Akt substrate of 160 kDa (AS160) and tre-2/USP6, BUB2, cdc16 domain family member 1 (TBC1C1) have been identified as potential targets of both protein kinase B (PKB, also known as Akt) and AMPK which mediate glucose transporter 4 (GLUT4) translocation to the plasma membrane in response to insulin and 5-aminoimidazole-4-carboxamide riboside (AICAR) respectively in muscle. Previous work in our laboratory has demonstrated that AICAR modestly stimulates basal glucose transport, yet inhibits insulin-stimulated glucose transport in 3T3-L1 adipocytes, which is in contrast to the effect of AICAR in skeletal muscle. Currently the role of AMPK in adipocytes remains poorly characterised despite the importance of fat tissue in energy homeostasis.

To address this, the molecular mechanism of AMPK activation by known stimuli, the acute effect of various AMPK activators on glucose transport, the effect of AMPK inhibition and knockdown on AICAR mediated inhibition of insulin-stimulated glucose transport and the effect of acute AICAR treatment on PKB substrate phosphorylation in 3T3-L1 adipocytes was investigated. In addition the effect of sustained AMPK activation on glucose transport and insulin signaling in 3T3-L1 adipocytes, and the effect of sustained AMPK activation on insulin signaling in human adipose tissue was also investigated.

The AMPK activators; sorbitol, metformin, rosiglitazone, arsenite, azide, hydrogen peroxide and isoproterenol were all shown to stimulate AMPK activity in the presence of the Ca^{2+}/Calmodulin dependent protein kinase kinase (CaMKK) inhibitor STO-609, suggesting that these activators activate AMPK via a CaMKK-independent pathway in 3T3-L1 adipocytes. However, A23187-stimulated AMPK activity was abrogated in the presence of STO-609. Isoproterenol, sodium azide and rosiglitazone, were all shown to cause an increase in the ADP/ATP ratio in 3T3-L1 adipocytes compared to control as assessed by high performance liquid chromatography, suggesting that they stimulate AMPK activity in an LKB1-dependent manner. These results suggest a possible role for CaMKK as an upstream AMPK kinase in 3T3-L1 adipocytes, in addition to LKB1. There may also exist other upstream AMPK kinases in 3T3-L1 adipocytes that are both nucleotide and calcium independent since sorbitol, metformin, arsenite, hydrogen peroxide

and leptin were found to activate AMPK independently of CaMKK and also showed no significant effect on adenine nucleotide ratios.

Sorbitol, rosiglitazone, AICAR, isoproterenol and A769662 all significantly inhibited insulin-stimulated glucose transport. Furthermore, in the presence of the AMPK inhibitor, Compound C, the inhibitory effect of AICAR on insulin-stimulated glucose transport was no longer apparent. However, AICAR still displayed a tendency to inhibit insulin-stimulated glucose transport in 3T3-L1 adipocytes infected with adenoviruses expressing a dominant negative AMPK mutant.

The effect of AICAR on basal and insulin-stimulated AS160/TBC1D1 phosphorylation at phospho-Akt substrate (PAS) sites, was assessed. AICAR did not alter AS160/TBC1D1 phosphorylation compared to basal levels, nor perturb insulin-stimulated AS160/TBC1D1 phosphorylation at PAS sites. In addition, AICAR did not appear to alter the phosphorylation of any other proteins at PAS sites.

Prolonged AMPK activation by AICAR in 3T3-L1 adipocytes also significantly inhibited insulin-stimulated glucose transport and was not associated with altered PKB protein expression or insulin-stimulated PKB Ser473 phosphorylation. In addition, chronic AMPK activation by metformin in adipose tissue of type 2 diabetic subjects was not associated with altered expression of three key insulin signalling molecules; PKB, the phosphoinositide 3-kinase (PI3K) p85 subunit and insulin receptor substrate 1 (IRS-1).

Overall these results suggest a prominent role for LKB1 as an AMPK kinase and a potential role for CaMKK as an AMPK kinase in adipocytes. This study also suggests that both acute and prolonged AMPK activation in adipocytes inhibits insulin-stimulated glucose uptake, however the precise mechanism of inhibition has yet to be elucidated.

Table of Contents

Abstract 2
List of Tables 8
List of Figures 9
Acknowledgements 11
Declaration 12
Abbreviations 13
Chapter 1 - Introduction 20
1.1 Adipose Tissue 20
1.1.1 Adipose Tissue Structure 20
1.1.2 Lipogenesis 20
1.1.3 Lipolysis 22
1.2 Adipose Tissue Related Disorders 23
1.2.1 Obesity 23
1.2.2 Type 2 diabetes 24
1.2.2.1 Insulin secretion 24
1.2.2.2 Insulin-stimulated glucose transport 25
1.2.2.3 Other actions of insulin 29
1.2.3 Lipotoxicity 30
1.2.4 Lipodystrophies 31
1.3 Adipocytokines 32
1.3.1 The adipocyte and adipocytokines 32
1.3.2 Leptin 33
1.3.3 TNFα 34
1.3.4 IL-6 35
1.3.5 Adiponectin 35
1.4 AMPK 36
1.4.1 Reversible phosphorylation 36
1.4.2 Discovery of AMPK 38
1.4.3 AMPK overview 38
1.4.4 AMPK Structure 39
1.4.5 Naturally Occurring AMPK mutations 42
1.4.6 Regulation of AMPK by AMP and phosphorylation 43
1.4.7 AMPK Function 45
1.4.8 Activators of AMPK 46
1.4.9 AMPK Targets 51
1.4.10 Role of AMPK in glucose homeostasis 52
1.4.11 Role of AMPK in lipid metabolism 53
1.4.12 Role of AMPK and adipocyte differentiation 55
1.4.13 Role of AMPK and adipokine secretion 56
1.4.14 Role of AMPK in mitochondrial biogenesis 57
1.4.15 Role of AMPK in protein synthesis 57
1.5 Aims 59
Chapter 2 – Materials and methods 61
2.1 Materials 61
2.1.1 List of materials and suppliers 61
2.1.2 List of specialist equipment and suppliers 65
2.1.3 List of antibodies and conditions of use 66
2.1.3.1 Primary antibodies for Western blotting 66
2.1.3.2 Secondary detection agents for Western blotting 70
2.1.4 Standard solutions 71
2.2 Methods 75
2.2.1 Cell Culture Procedures 75
2.2.1.1 Cell culture plastic ware 75

2.2.1.2 Cell culture growth media for 3T3-L1 preadipocytes....75
2.2.1.3 Cell culture growth media for HEK 293 cells....75
2.2.1.4 Preparation of 3T3-L1 fibroblast differentiation medium....75
2.2.1.5 3T3-L1 fibroblast differentiation protocol....76
2.2.1.6 Passaging of 3T3-L1 fibroblasts....76
2.2.1.7 Passaging of HEK 293cells....76
2.2.1.8 Resurrection of frozen 3T3-L1 cell stocks from liquid nitrogen....77
2.2.1.9 Resurrection of frozen HEK 293 cell stocks from liquid nitrogen....77
2.2.1.10 Preparation of 3T3-L1 murine fibroblast cells for freezing....77
2.2.1.11 Preparation of HEK 293 for freezing....78
2.2.2 Preparation of 3T3-L1 lysates....78
2.2.3 Protein concentration determination....78
2.2.4 Immunoprecipitation....79
2.2.4.1 Immunoprecipitation of AMPK α1, AMPK α2 and CaMKK β from 3T3-L1 adipocytes....79
2.2.4.2 Immunoprecipitation of AS160 and TBC1D1 from 3T3-L1 adipocytes....79
2.2.5 AMPK Assay....80
2.2.6 SDS-Polyacrylamide Gel Electrophoresis....80
2.2.7 Western Blotting of Proteins....81
2.2.7.1 Electrophoretic transfer of proteins from gels onto nitrocellulose membranes....81
2.2.7.2 Blocking of membranes and probing with antibodies....81
2.2.7.3 Immunodetection of proteins using western blotting and the ECL detection system....82
2.2.7.4 Stripping of nitrocellulose membranes....82
2.2.7.5 Densitometric quantification of protein bands....82
2.2.8 2-deoxy-D-glucose uptake assay....82
2.2.9 Nucleotide extraction and analysis....83
2.2.9.1 Nucleotide extraction....83
2.2.9.2 Reversed-phase chromatography....83
2.2.9.3 Preparation of TEA phosphate buffer....84
2.2.10 Recombinant adenoviruses....84
2.2.10.1 AMPK adenoviruses....84
2.2.10.2 Adenovirus propagation....84
2.2.10.3 Adenovirus purification....84
2.2.10.4 Adenovirus titration....85
2.2.10.5 3T3-L1 adipocyte adenovirus infection....85
2.2.11 Albumin and IgG depletion....86
2.2.12 Statistical Analysis....86
Chapter 3 - Activation parameters and mechanism of AMPK activation by various stimuli in 3T3-L1 cells....87
3.1 Introduction....87
3.1.1 Known activators of AMPK in adipocytes....87
3.1.2 Role for LKB1 as an AMPK kinase in adipocytes....87
3.1.3 AMPK subunit isoform expression....88
3.1.5 Aims....88
3.2 Results....90
3.2.1 Investigating the expression of LKB1, CaMKKα, CaMKKβ, ACC1 and ACC2 in 3T3-L1 adipocytes....90
3.2.2 AMPK subunit isoform expression during adipogenesis....93
3.2.3 Investigating catalytic α-subunit isoform specific AMPK activity during adipogenesis....102
3.2.4 Investigating AMPK activation parameters by various stimuli in 3T3-L1 adipocytes....104

3.2.5 Investigation of the molecular mechanism of AMPK activation by various stimuli in 3T3-L1 adipocytes 119
3.2.5.1 Effect of STO-609 on AMPK activity in response to various stimuli 119
3.2.5.2 Effect of various stimuli on the AMP/ATP and ADP/ATP ratios 121
3.3 Discussion 130
Chapter 4 - Role of acute AMPK activation in adipocyte insulin action 139
4.1 Introduction 139
4.1.1 Insulin-stimulated glucose uptake 139
4.1.2 Insulin indepedent glucose uptake 139
4.1.3 The role of AS160 and TBC1D1 in glucose transport 140
4.1.4 Rab proteins 143
4.1.5 Aims 144
4.2 Results 146
4.2.1 Effect of various AMPK activators on basal and insulin-stimulated glucose transport 146
4.2.2 Investigating whether the inhibition of insulin-stimulated glucose transport by AICAR is dependent on AMPK activation 146
4.2.2.1 Effect of Compound C on AICAR mediated inhibition of insulin-stimulated glucose uptake 146
4.2.2.2 Effect of a DN AMPK mutant on AICAR mediated inhibition of insulin-stimulated glucose transport 147
4.2.3 Investigating the mechanism of AICAR mediated inhibition of insulin-stimulated glucose uptake in 3T3-L1 adipocytes. 151
4.2.3.1 Specificity of anti-AS160 and anti-TBC1D1 antibodies 151
4.2.3.2 Effect of AICAR on basal and insulin-stimulated AS160 phosphorylation at PAS sites and association of 14-3-3 proteins. 151
4.2.3.3 Effect of AICAR on basal and insulin-stimulated TBC1D1 phosphorylation at PAS sites. 154
4.2.3.4 Effect of AICAR on PKB substrate phosphorylation 154
4.3 Discussion 157
Chapter 5 - Effect of sustained AMPK activation on adipocyte insulin action 167
5.1 Introduction 167
5.1.1 Aims 167
5.2 Results 169
5.2.1 Effect of sustained AMPK activation on basal and insulin-stimulated glucose transport in 3T3-L1 adipocytes. 169
5.2.1.1 Effect of 24 hr and 48 hr incubation of 3T3-L1 adipocytes with AICAR on AMPK expression, ACC expression, AMPK Thr12 phosphorylation and ACC Ser79 phosphorylation 169
5.2.1.2 Effect of 24 hr and 48 hr incubation of 3T3-L1 adipocytes with metformin on AMPK expression, ACC expression, AMPK Thr12 phosphorylation and ACC Ser79 phosphorylation 169
5.2.1.3 Effect of 24 hr and 48 hr incubation of 3T3-L1 adipocytes with AICAR on insulin-stimulated glucose transport 172
5.2.1.4 Effect of 24 hr and 48 hr incubation of 3T3-L1 adipocytes with metformin on insulin-stimulated glucose transport 172
5.2.1.5 Effect of overexpression of a constitutively active AMPK mutant on basal and insulin-stimulated glucose transport in 3T3-L1 adipocytes. 172
5.2.1.6 Effect of 24 hr and 48 hr incubation of 3T3-L1 adipocytes with AICAR on PKB expression and insulin-stimulated PKB phosphorylation 176
5.2.1.7 Effect of 24 hr and 48 hr incubation of 3T3-L1 adipocytes with metformin on PKB expression and insulin-stimulated PKB phosphorylation 176
5.2.2 Effect of chronic AMPK activation in human adipose tissue 179

5.2.2.1 Effect of prolonged treatment of type 2 diabetic subjects with metformin on AMPK activity in human adipose tissue. 179
5.2.2.2 Effect of prolonged treatment of type 2 diabetic subjects with metformin on the expression of GAPDH in human adipose tissue 181
5.2.2.3 Effect of prolonged treatment of type 2 diabetic subjects with metformin on the expression of PI3K in human adipose tissue. 181
5.2.2.4 Depletion of albumin from human adipose tissue samples 181
5.2.2.5 Effect of prolonged treatment of type 2 diabetic subjects with metformin on the expression of IRS-1 and PKB in human adipose tissue. 185
5.2.2.6 Effect of prolonged treatment of type 2 diabetic subjects with metformin on FAS expression in human adipose tissue. 185
5.3 Discussion 189
Chapter 6 – Final discussion 195
List of References 202

List of Tables

Table 1-1: Classification of lipodystrophy syndromes. 31
Table 1-2: Bioactive proteins secreted by adipose.....32
Table 2-1: Primary antibodies used for western blotting.....66
Table 2-2: Secondary detection agents for western blotting.....70
Table 5-1: Clinical and metabolic parameters of test subjects.....179

List of Figures

Figure 1-1: Cellular compartments of the adipose tissue. 20
Figure 1-2: Regulation of lipogenesis in adipocytes. 22
Figure 1-3: Hormonal control of adipocyte lipolysis. 23
Figure 1-4: The stimulus-secretion coupling pathway of glucose-dependent insulin exocytosis. 25
Figure 1-5: Insulin receptor signalling 28
Figure 1-6: A model that depicts the transport of GLUT4 in insulin-responsive cells 29
Figure 1-7: Leptin stimulates decreased feeding and increased energy expenditure. 33
Figure 1-8: Domain structure of AMPK subunit isoforms and slice variants 41
Figure 1-9: The positions of known mutations that cause cardiac disease are marked on the γ2 subunit. 42
Figure 1-10: Role of AMPK in regulating energy balance at the cellular level. 45
Figure 1-11: Role of AMPK in regulating energy balance at the whole-body level. 46
Figure 1-12: Model for the stimulatory effect of AMPK on fatty acid oxidation in muscle. 47
Figure 1-13: Model for activation of AMPK by A-769662 or AMP 50
Figure 1-14: Targets for AMPK. 51
Figure 1-15: Regulation of protein synthesis and cell growth by AMPK and PKB/Akt by the mTOR pathway. 58
Figure 3-1: LKB1, CaMKKα, CaMKKβ and LKB1 expression in 3T3-L1 adipocytes. 91
Figure 3-2: ACC1 and ACC2 expression in 3T3-L1 adipocytes. 92
Figure 3-3: AMPK α1 subunit expression during adipogenesis 95
Figure 3-4: AMPK α2 subunit expression during adipogensis. 96
Figure 3-5: AMPK β1 subunit expression during adipogenesis 97
Figure 3-6: AMPK β2 subunit expression during adipogenesis. 98
Figure 3-7: AMPK γ1 subunit expression during adipogenesis 99
Figure 3-8: AMPK γ2 subunit expression during adipogenesis 100
Figure 3-9: AMPK γ3 subunit expression during adipogenesis 101
Figure 3-10: Contribution of the AMPK α1 and AMPK α2 subunits to total AMPK activity throughout adipogenesis 103
Figure 3-11: Effect of 0.6 M sorbitol on AMPK activity and Thr172 phosphorylation. 105
Figure 3-12: Effect of 2 mM AICAR on AMPK activity and Thr172 phosphorylation 106
Figure 3-13: Effect of 100 μM arsenite on AMPK activity and Thr172 phosphorylation. 108
Figure 3-14: Effect of 5 μM A23197 on AMPK activity and phosphorylation. 109
Figure 3-15: Effect of 100 μM rosiglitazone on AMPK activity and phosphorylation. 110
Figure 3-16: Effect of 1 mM metformin on AMPK activity and phosphorylation. 111
Figure 3-17: Effect of 1 μM isoproterenol on AMPK activity in 3T3-L1 adipocytes 114
Figure 3-18: Effect of 5 mM sodium azide on AMPK activity and phosphorylation 115
Figure 3-19: Effect of 1 mM hydrogen peroxide on AMPK activity and phosphorylation. 116
Figure 3-20: Effect of 0.1 μM leptin on AMPK activity and phosphorylation 117
Figure 3-21: Effect of 300 μM A769662 on AMPK activity and phosphorylation. 118
Figure 3-22: Effect of STO-609 on AMPK activity, stimulated by different AMPK activators. 120
Figure 3-23: Elution times of AMP, ADP and ATP. 122
Figure 3-24: Elution time of adenosine. 123
Figure 3-25: Elution time of cAMP. 124
Figure 3-26: Elution time of ZMP. 125
Figure 3-27: Identification of a ZMP peak in a nucleotide extract from AICAR treated cells using HPLC. 126

Figure 3-28: Identification of an AICAR peak in a nucleotide extract from AICAR treated cells using HPLC. 127
Figure 3-29: The effect of various AMPK activators on the ADP/ATP ratio. 128
Figure 3-30: The effect of various AMPK activators on the AMP/ATP ratio....129
Figure 3-31: Effects of various stimuli on AMPK activity versus ADP/ATP ratio....137
Figure 3-32: Mechanism of acute AMPK activation in 3T3-L1 adipocytes....138
Figure 4-1: The Rab GTPase cycle. 144
Figure 4-2: Effect of various AMPK activators on basal and insulin-stimulated glucose transport....148
Figure 4-3: Effect of Compound C on AICAR mediated inhibition of insulin-stimulated glucose transport. 149
Figure 4-4: Effect of overexpression of a dominant negative AMPK mutant on AICAR mediated inhibition of insulin stimulated glucose transport in 3T3-L1 adipocytes....150
Figure 4-5: Specificity of anti-AS160 and anti-TBC1D1 antibodies. 152
Figure 4-6: Effect of AICAR on basal and insulin-stimulated AS160 phosphorylation at PAS sites and association with 14-3-3 proteins. 153
Figure 4-7: Effect of AICAR on basal and insulin-stimulated TBC1D1 phosphorylation at PAS sites. 155
Figure 4-8: Effect of AICAR on PKB substrate phosphorylation. 156
Figure 4-9: Fold increase in AMPK activity versus % inhibition of insulin-stimulated glucose transport. 160
Figure 5-1: Effect of 24 hr and 48 hr incubation of 3T3-L1 adipocytes with AICAR on AMPK expression, ACC expression, AMPK Thr172 phosphorylation and ACC Ser79 phosphorylation. 170
Figure 5-2: Effect of 24 hr and 48 hr incubation of 3T3-L1 adipocytes with metformin on AMPK expression, ACC expression, AMPK Thr172 phosphorylation and ACC Ser79 phosphorylation. 171
Figure 5-3: Effect of 24 hr and 48 hr incubation of 3T3-L1 adipocytes with AICAR on basal and insulin-stimulated glucose transport. 173
Figure 5-4: Effect of 24 hr and 48 hr incubation of 3T3-L1 adipocytes with metformin on basal and insulin-stimulated glucose transport. 174
Figure 5-5: Effect of overexpression of a constitutively active AMPK mutant on basal and insulin stimulated glucose transport in 3T3-L1 adipocytes. 175
Figure 5-6: Effect of 24 hr and 48 hr incubation of 3T3-L1 adipocytes with AICAR on PKB expression and insulin-stimulated PKB phosphorylation. 177
Figure 5-7: Effect of 24 hr and 48 hr incubation of 3T3-L1 adipocytes with AICAR on PKB expression and insulin-stimulated PKB phosphorylation. 178
Figure 5-8: Effect of prolonged treatment of type 2 diabetic subjects with metformin on AMPK activity and expression in human adipose tissue. 180
Figure 5-9: Effect of prolonged treatment of type 2 diabetic subjects with metformin on GAPDH expression in human adipose tissue....182
Figure 5-10: Effect of prolonged treatment of type 2 diabetic subjects with metformin on the expression of the PI3K p85 subunit in adipose tissue. 183
Figure 5-11: Albumin depletion from adipose tissue sample. 184
Figure 5-12: Effect of prolonged treatment of type 2 diabetic subjects with metformin on the expression of IRS-1 in adipose tissue. 186
Figure 5-13: Effect of prolonged treatment of type 2 diabetic subjects with metformin on the expression of PKB in adipose tissue. 187
Figure 5-14: Effect of prolonged treatment of type 2 diabetic subjects with metformin on the expression of FAS in adipose tissue....188
Figure 6-1: Proposed mechanism of acute AMPK activation and subsequent inhibition of insulin-stimulated glucose transport in 3T3-L1 adipocytes. 196

Acknowledgements

I should firstly like to thank my supervisor Dr. Ian Salt for his endless patience, consistent reassurance and guidance throughout the last three years, for which I am sincerely grateful.

To all members of Lab 241 past and present, thank you for your advice throughout and for making my time in the lab both memorable and enjoyable. In particular, I would like to thank Stephen Miller from the Glasgow Cardiovascular Research Centre for his technical assistance with the HPLC machine, and Dr Colin Moran from the Faculty of Biomedical Life Sciences for his advice regarding statistical analysis of human adipose biopsies.

Thanks to Christopher for his emotional support and motivational talks throughout, and for tolerating in depth accounts of my laboratory work over the last few years.

Thanks also to my two sisters, Charlotte and Lucinda, for the many times that they volunteered to provide a test audience for presentations.

Finally and most importantly, I would like to thank my parents Agnes and Eric for their love, patience, support and encouragement – this thesis is dedicated to them.

Funding for this project was provided by the Biotechnology and Biological Sciences Research Council.

Declaration

I declare that the work presented in this thesis has been carried out by myself, unless otherwise stated. It is entirely of my own composition and has not, in whole or in part, been submitted for any other degree.

Pamela Jane Logan

September 2009

Abbreviations

4E-BP1	Elongation factor-4E binding protein 1
α-MSH	α-Melanocyte-stimulating hormone
ACC	Acetyl-CoA carboxylase
Ad.α1^{312}	Adenovirus encoding a constitutively active AMPK mutant
Ad.α1-DN	Adenovirus encoding a dominant negative AMPK mutant
ADP	Adenosine diphosphate
AgRP	Agouti related peptide
AICAR	5-aminoimidazole-4-carboxamide riboside
AMP	Adenosine monophosphate
AMPK	AMP-activated protein kinase
AMPKK	AMP- activated protein kinase kinase
APS	Ammonium peroxydisulphate
ART	Arcuate nucleus
AS160	Akt substrate of 160 kDa
ASC	Association with Snf-1 complex
ATP	Adenosine triphosphate
BSA	Bovine serum albumin
C3G	Crk SH3 binding Guanine-nucleotide releasing Factor

CaMKK	Ca^{2+}/Calmodulin dependent protein kinase kinase
cAMP	Cyclic adenosine monophosphate
CBS	Cystathionine β-synthase
C/EBPα	CAAT/enhancer-binding protein alpha
CPT1	Carnitine palmitoyl transferase 1
CRKII	CT10 sarcoma oncogene cellular homolog II
DAB	Diaminobenzidin
DG	Diglyceride
DMEM	Dulbecco's modified Eagle's medium
DMSO	Dimethyl sulphoxide
DTT	Dithiothreitol
DYRK	Dual specificity tyrosine phosphorylation regulated kinase
ECL	Enhanced chemiluminescence
EDTA	Diaminoethanetetra-acetic acid, disodium salt
eEF2	Eukaryotic elongation factor 2
EGFR	Epidermal growth factor receptor
EGTA	Ethylene glycol-bis (β-amino-ethylether)-N,N,N',N'-tetraacetic acid
ERK	Extracellular signal-regulated kinase
FAS	Fatty acid synthase
FAT	Fatty acid translocase

FCS	Foetal calf serum
G6Pase	Glucose-6-phosphatase
Gab1	GRB2-associated binding protein 1
GAP	GTPase activating protein
GAPDH	Glyceraldehyde 3-phosphate dehydrogenase
GBD	Glycogen binding domain
GDP	Guanosine diphosphate
GFP	Green fluorescent protein
GH	Growth hormone
GLUT	Glucose transporter
GMP	Guanosine monophosphate
GS	Glycogen synthase
GSK-3	Glycogen synthase kinase-3
GTP	Guanosine triphosphate
HA	Haemagglutinin
HEK	Human embryonic kidney cells
HEPES	N-2-hydroxyethylpiperazine-N' 2-ethane sulphonic acid
HIPK2	Homeodomain-interacting protein kinase 2
HMGR	3-Hydroxy-3-methylglutaryl-CoA reductase
HPLC	High performance liquid chromatography

HRP	Horseradish peroxidase
HSL	Hormone sensitive lipase
IBMX	Isobutylxanthine
IgG	Immunoglobulin gamma
Il-	Interleukin
IMP	Inosine monophosphate
IP	Immunoprecipitation
IR	Insulin receptor
IRS-1	Insulin receptor substrate-1
KIS	Kinase-interacting sequence
KRH	Krebs-Ringer HEPES
KRP	Krebs-Ringer phosphate
Lck	Leukocyte-specific protein tyrosine kinase
MAP	Mitogen activated protein
MC4R	Melanocortin 4 receptor
MEF-2	Myocyte enhancer factor-2
MELK	Maternal embryonic leucine zipper kinase
MG	Monoglyeride
MGL	Monoglyceride lipase
MLCK	Myosin light chain kinase

MNK-1	MAP kinase-interacting kinase-1
NCS	Newborn calf serum
NEFA	Non-esterified fatty acid
NHE-1	Na^+/H^+ exchanger-1
NPY	Neuropeptide Y
OCT	Organic cation transporter
PAS	Phospho Akt/PKB substrate
PBS	Phosphate buffered saline
PD	pleckstrin-homology
PDE3B	Phosphodiesterase 3B
PDK-1	Protein dependent kinase-1
PEPCK	Phosphoenolpyruvate carboxykinase
PFK-1	Phospho-fructose kinase-1
PFK-2	Phospho-fructose kinase-2
PGC1a	Peroxisome-proliferator-activated receptor (PPAR)γ co-activator 1a
PHK	Phosphorylase kinase
PI3K	Phosphoinositide 3-kinase
PKA	Protein kinase A
PKB	Protein kinase B
PKC	Protein kinase C

PLD	Phospholipase D
POMC	Proopiomrlanocortin
PPARγ	Peroxisome proliferator-activated receptor gamma
PTB	Phospho tyrosine binding
PtdIns	Phosphatidylinositol
PtdInsP2	Phosphatidylinositol 4,5 bisphosphate
PtdInsP3	Phosphatidylinositol 3,4,5-trisphosphate
PVN	Paraventricular nucleus
PYK2	Proline-rich tyrosine kinase 2
RICTOR	rapamycin insensitive companion of mTOR
S6K1	Ribosomal protein S6 kinase
SBTI	Soybean trypsin inhibitor
SDS	Sodium dodecyl sulphate
SDS-PAGE	SDS-polyacrylamide gel electrophoresis
Ser	Serine
SNARE	Soluble N-ethylmaleimide-sensitive-factor attachment protein receptor
SNS	Sympathetic nervous system
SDS	Sodium dodecyl sulphate
SOCS-3	Suppressor of cytokine signalling-3
Src	Sarcoma kinase

SREBP-1	Sterol regulatory element binding protein-1
TG	Triglyceride
TAK-1	Transforming growth factor-beta activated kinase
TBC1D1	tre-2/USP6, BUB2, cdc16 domain family member 1
TBS	Tris buffered saline
TBST	Tris buffered saline + Tween 20
TC10	GTP-binding protein TC10
TEA	Triethylamine
TEMED	N, N, N', N'-tetramethylenediamine
Thr	Threonine
TNF	Tumour necrosis factor
TOR	Target of rapamycin
Tris	Tris(hydroxymethyl)aminoethane
TSC	Tuberous sclerosis complex
Tye	Tyrosine
TZD	Thiazolidinedione
UCP-1/2	Un-coupling protein-1/2
UMP	Uridine monophosphate
ZMP	5-Aminoimidazole-4-carboxamide riboside monophosphate

Chapter 1 - Introduction

1.1 Adipose Tissue

1.1.1 Adipose Tissue Structure

Adipose tissue is constructed of different components including; adipocytes, connective tissue matrix, nerve tissue, stromovascular cells and immune cells (Fig. 1.1).

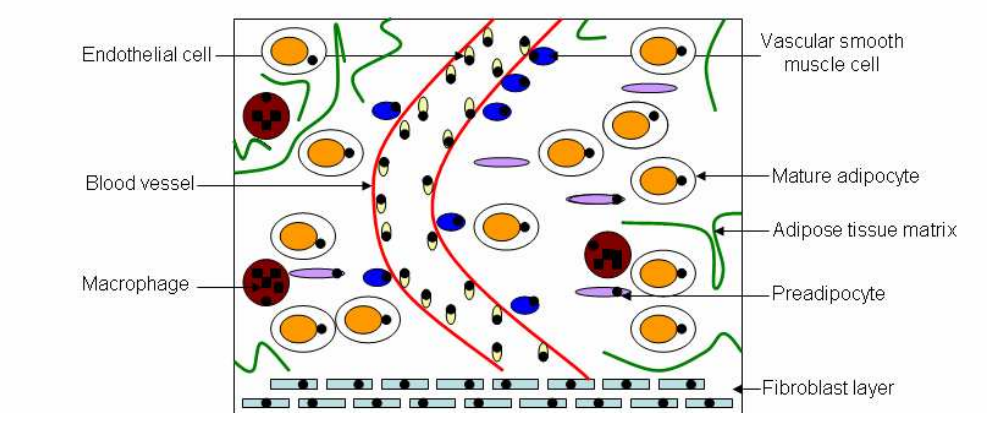

Figure 1-1: Cellular compartments of the adipose tissue.

One role of adipocytes in adipose tissue is to store triglyceride (TG) during periods of caloric excess and to mobilize this reserve when energy expenditure exceeds intake. Adipocytes regulate the amount of stored fat in adipose tissue through the mechanisms of lipogenesis and lipolysis.

1.1.2 Lipogenesis

Lipogenesis is stimulated by insulin during the fed state in adipocytes (Fig. 1.2). Insulin increases the uptake of glucose (Fig. 1.2) in the adipose cell via recruitment of glucose transporters to the plasma membrane (Saltiel and Kahn 2001). In the cytosol glucose enters into glycolysis, where it is converted to pyruvate. Pyruvate is then converted to acetyl-CoA in the mitochondria by pyruvate dehydrogenase (Patel and Roche 1990). Acetyl-CoA produced in the mitochondria is condensed with oxaloacetate to form citrate, which is then transported into the cytosol and broken down to yield acetyl-CoA by citrate lyase (Srere 1959). Acetyl-CoA carboxylase (ACC), a biotin-dependent enzyme, then catalyses the carboxylation of acetyl-CoA to malonyl-CoA (Tong 2005). Fatty acids are synthesized from acetyl-CoA and malonyl-CoA by fatty acid synthase (FAS) (Wakil *et al* 1983, Wakil

1989), an enzyme system consisting of a multifunctional polypeptide. The first step in the synthesis of TG is the synthesis of phosphatidate which is formed by the addition of two fatty acids to glycerol-3-phosphate. Fatty acids must first be activated via esterification, by fatty acyl CoA synthetase (Watkins 1997), with Coenzyme A before they can be utilized in the synthesis of TG. Glycerol phosphate acyltransferase catalyses the acylation of glycerol 3-phosphate to lysophoshophatidate, and the subsequent acylation of lysophoshophatidate to phosphatidate (Coleman and Lee 2004, Gimeno and Cao 2008). Finally in the synthesis of TG, phosphatidate is hydrolysed by a phosphatase to generate diglyceride (DG) which is acylated to a TG by diglyceride acyltransferase (Coleman and Lee 2004, Gimeno and Cao 2008).

In addition to stimulating glucose uptake, insulin also increases the expression of lipogenic enzymes (Assimacopoulos-Jeannet *et al* 1995) (Fig. 1.2). In liver, insulin is thought to increase the expression of genes connected with lipogenesis via the transcription factor sterol regulatory element binding protein-1 (SREBP-1) (Horton and Shimomura 1999, Kersten 2001). However, currently the regulation of gene expression by insulin via SREBP-1 has yet to be clearly defined in adipocytes (Kersten 2001). The nuclear hormone receptor, peroxisome proliferator-activated receptor gamma **(**PPARγ), is an important transcription factor in adipocytes involved in the differentiation of preadipocytes into mature fat cells. Expression of PPARγ, which regulates the expression of various lipid metabolism genes in adipocytes including; adipocyte fatty acid binding protein, lipoprotein lipase, fatty acid transport protein and acyl-CoA synthetase (Kersten *et al* 2000, Yoon *et al* 2000), has been shown to be increased by both insulin (Vidal-Puig *et al* 1997) and SREBP-1 (Fajas *et al* 1999). This suggests that in adipocytes insulin may regulate the expression of lipogenic enzymes primarily via elevated PPARγ expression.

Growth hormone (GH) is also involved in the regulation of lipogenesis in adipose tissue. GH has been shown to reduce lipogenesis by reducing insulin sensitivity, resulting in down-regulation of fatty acid synthase expression in adipose tissue (Yin *et al* 1998).

Leptin, synthesised by adipocytes, is another hormone which has been shown to regulate lipogenesis. Leptin (Fig. 1.2) has been shown to inhibit lipogenesis (Wang and Sul 1997), by down-regulating the expression of genes involved in fatty acid and triglyceride synthesis, (Soukas *et al* 2000). Leptin is thought to mediate these changes in gene expression by reducing SREBP-1 expression (Soukas *et al* 2000).

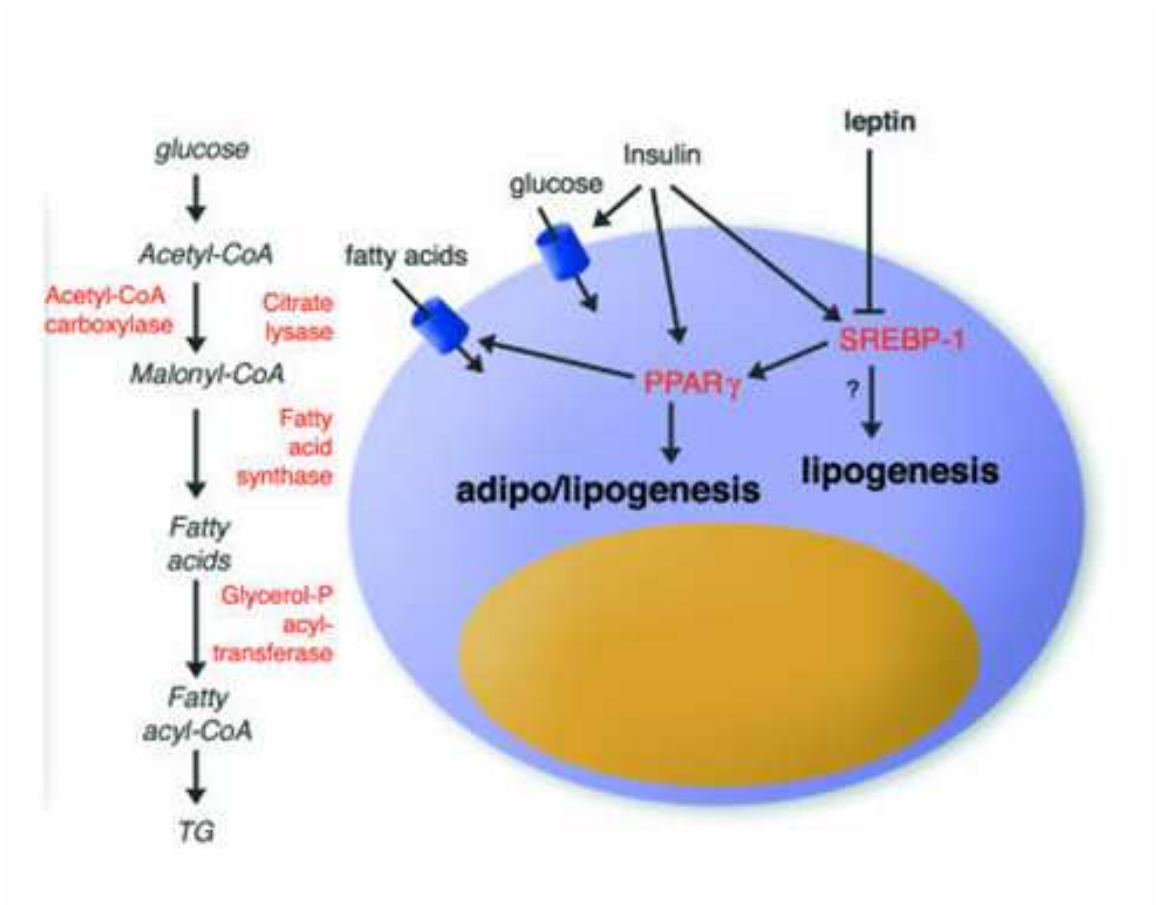

Figure 1-2: Regulation of lipogenesis in adipocytes (adapted from Kersten 2001).
PPARγ = peroxisome proliferator-activated receptor gamma, SREBP-1 = sterol regulatory element binding protein-1. TG = triglyceride

1.1.3 Lipolysis

Lipolysis is a catabolic pathway, where by stored TG is hydrolysed to yield non-esterified fatty acids (NEFAs), and glycerol. This process is activated in adipose tissue during fasting and is regulated by the hormones noradrenaline and insulin. Binding of noradrenaline to β-adrenergic receptors (Fig. 1.3), coupled to adenylate cyclase via the stimulatory G_s-protein, leads to an increased production of cyclic adenosine monophosphate (cAMP) and subsequent activation of protein kinase A (PKA) (Holm *et al* 2000, Holm *et al* 2003, Collins *et al* 2004). PKA subsequently phosphorylates target proteins including hormone sensitive lipase (HSL) and perilipins. Perilipins are characteristic proteins in mature adipocytes, which cover lipid droplets in the adipocyte thereby preventing HSL activity (Londos *et al* 1999). However, phosphorylation of perilipins by PKA abolishes their ability to inhibit HSL. PKA phosphorylates HSL at three serine residues, Ser563, Ser659 and Ser660 (rat HSL) (Anthonsen *et al* 1998). Once active, HSL migrates to the lipid droplet surface where it cleaves the first fatty acid from TG yielding diglyceride (DG) (Fredrikson

et al 1986). Diglyceride lipase then cleaves the second fatty acid from DG to yield monglyceride (MG) (Fredrikson *et al* 1986). Finally monoglyceride lipase (MGL) exerts its lipase activity and cleaves MG yielding the final fatty acid and glycerol (Fredrikson *et al* 1986). NEFAs and glycerol are exported to muscle and liver respectively. Insulin antagonises lipolysis (Fig. 1.3) by reducing PKA activity via a reduction in cAMP levels, mediated via activation of phosphodiesterase 3B (PDE3B) (Shakur *et al* 2001).

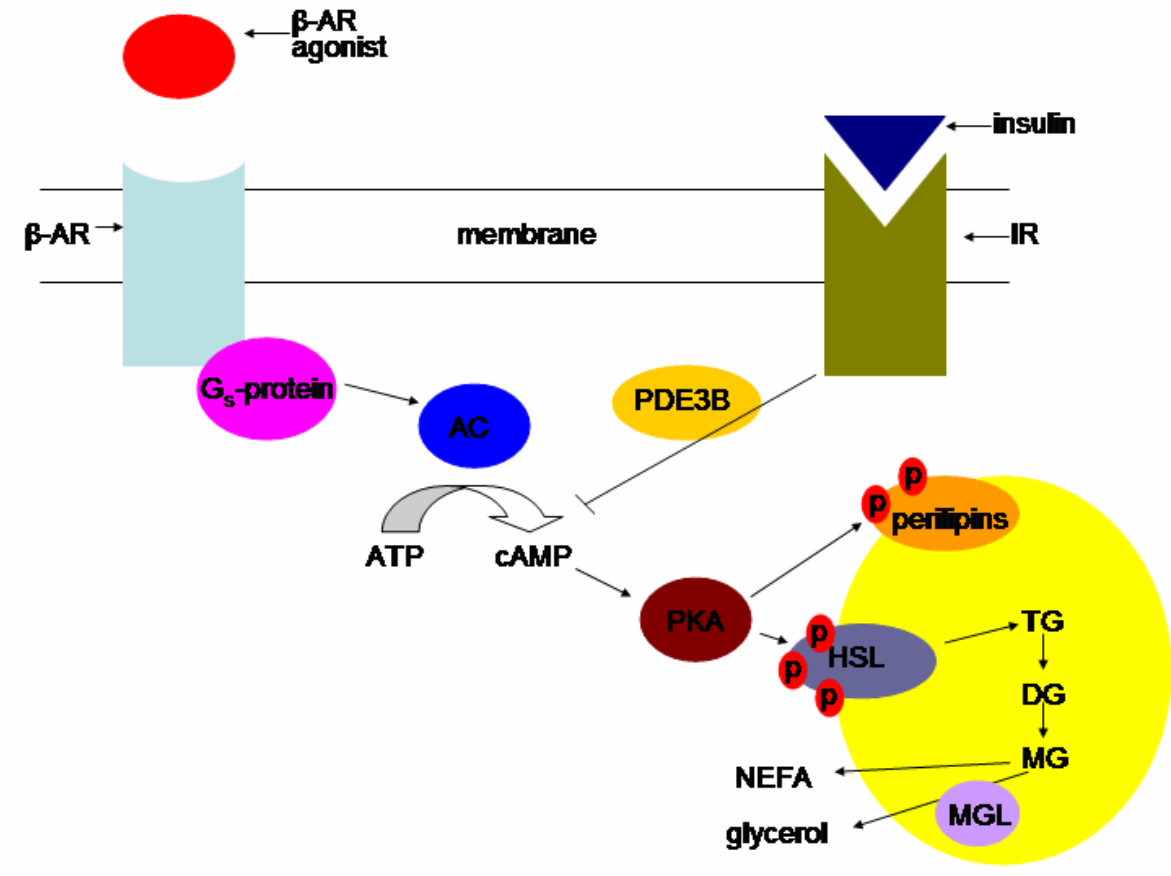

Figure 1-3: Hormonal control of adipocyte lipolysis.
β-AR = beta adrenergic receptor, AC = adenylate cyclase, PKA = protein kinase A, HSL = hormone sensitive lipase, TG = triglyceride, DG = diglyceride, MG = monoglyceride, MGL = monoglyceride lipase, NEFA = non-esterified fatty acid, IR = insulin receptor, PDE3B = phosphodiesterase 3B.

1.2 Adipose Tissue Related Disorders

1.2.1 Obesity

Adipose tissue has a fundamental role in regulating energy balance and metabolism, thus a normal amount of adipose tissue is necessary for maintaining metabolic homeostasis.

Excess or loss of adipose tissue is detrimental to health, and results in obesity and lipodystrophy respectively.

Obesity results from an increase in adipose tissue mass. Currently obesity has reached epidemic proportions. The world health organisation projects that by 2015 2.3 billion adults will be overweight, and at least 700 million of them will be clinically obese (World Health Organisation, 2009). Obesity and overweight increases the risk of chronic diseases including; type 2 diabetes, cardiovascular disease, hypertension, stroke, hypercholesterolaemia, hypertriglyceridaemia, arthritis, asthma and some cancers (Mokdad *et al* 2003), thereby increasing morbidity and mortality.

1.2.2 Type 2 diabetes

1.2.2.1 Insulin secretion

Insulin, a hormone produced in the pancreas, lowers blood glucose levels by stimulating the uptake of glucose into target tissues. Diabetes is a disease in which the body does not produce enough insulin, or respond properly to insulin, and is characterized by elevated fasting blood glucose levels. Type 1 diabetes is an autoimmune disease that results in the destruction of insulin-producing β-cells in the pancreas (Marino and Grey 2008). Type 2 diabetes is characterized by a fasting hyperglycemia due to the combination of insulin resistance in peripheral tissue and an insulin secretory defect of the β-cell. Type 2 diabetes is the most common form of diabetes mellitus and is associated with a family history of diabetes (American Diabetes Association, 2000), obesity (Sinha *et al* 2002) and older age (Pagano *et al* 1984).

After feeding, in the healthy individual, elevated blood glucose levels trigger exocytosis of the insulin secretory vesicles and release of insulin into the bloodstream (Fig. 1.4). Glucose transporter 2 (GLUT2), facilitates the entry of glucose into the pancreatic β-cells (1). Once inside the cell glucose is phosphorylated by glucokinase to glucose 6-phosphate (2), and metabolized with a resultant increase in the adenosine triphosphate / adenosine diphosphate (ATP/ADP) ratio (3) (Kennedy *et al* 1999**)**, triggering closure of the ATP-gated potassium channels (4) in the cellular membrane and depolarization (5) (Cook and Hales 1984). Membrane depolarization of the β-cell opens voltage dependent calcium channels (VDCC) (6) resulting in an influx of calcium into the β-cell. The increased

intracellular calcium concentration (7) subsequently triggers exocytosis of insulin granules into the bloodstream (8) (Rorsman *et al* 2000) (Fig. 1.4).

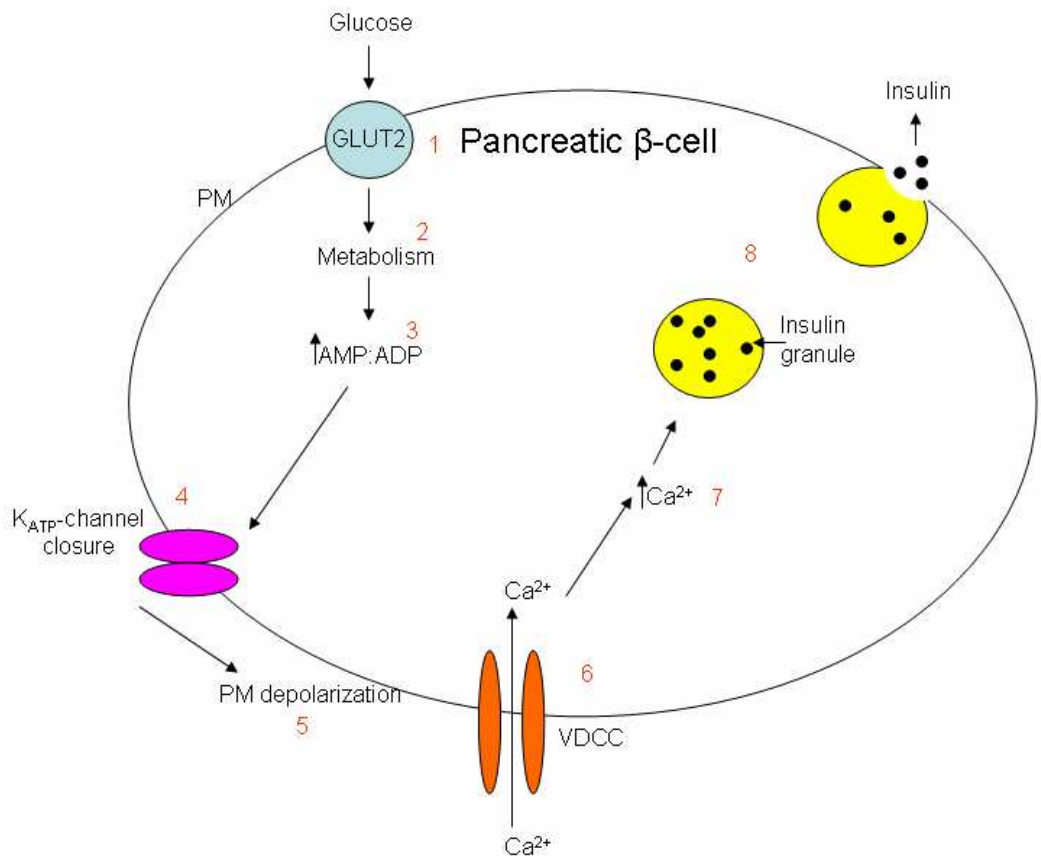

Figure 1-4: The stimulus-secretion coupling pathway of glucose-dependent insulin exocytosis.
VDCC = voltage dependent calcium channels, GLUT2 = glucose transporter 2, PM = plasma membrane.

1.2.2.2 Insulin-stimulated glucose transport

In normal insulin signalling (Fig. 1.5), insulin stimulates glucose transport in muscle and adipocytes via the regulated translocation of vesicles containing the glucose transporter GLUT4 to the plasma membrane. The complete mechanism by which insulin regulates the translocation of GLUT4 vesicles to the plasma membrane remains currently incompletely defined. However, the mechanism established to date is discussed below.

The initial step in insulin-stimulated GLUT4 translocation to the plasma membrane involves the binding of insulin to its receptor. The insulin receptor (IR) is a transmembrane receptor, composed of two α-subunits and two β-subunits linked by disulphide bonds. The α-subunits are entirely extracellular and contain insulin binding domains, while the linked β-subunits penetrate through the plasma membrane into the cytosol (Lee and Pilch 1994).

The binding of insulin to its receptor causes a conformational change in the α-subunits. This in turn induces a conformational change in the β-subunits which promotes tyrosine autophosphorylation of the β-subunits of the insulin receptor (IR). This occurs through an intramolecular trans-autophosphorylation mechanism in which one β-subunit tyrosine kinase domain phosphorylates the adjacent β-subunit resulting in the activation of the intrinsic substrate kinase activity of the insulin receptor (Ullrich and Schlessinger 1990, Czech and Corvera 1999, Ward and Lawrence 2009).

Substrates of the IR are termed insulin receptor substrate (IRS) proteins. IRS proteins are characterized by the presence of an NH2-terminal pleckstrin-homology (PH) domain adjacent to a phosphotyrosine binding (PTB) domain, followed by a variable-length COOH-terminal tail that contains numerous tyrosine and serine phosphorylation sites (Sun and Liu 2009). IRS proteins bind to phosphorylated IR Tyr960 via the PTB domain (White 1998). In addition, the IRS protein PH domain is also thought to mediate specific interactions with the IR kinase (Burks *et al* 1997). Once bound to the IR, IRS is phosphorylated on tyrosine residues by the IR (Ward and Lawrence 2009). At least three IRS proteins occur in humans, including IRS-1 and IRS-2, which are widely expressed, and IRS-4, which is limited to the thymus, brain, and kidney and possibly β-cells (Bernal *et al* 1998, Uchida *et al* 2000). Both IRS-1 and IRS-2 have key roles in insulin-stimulated glucose uptake in fat and muscle, and the independent genetic ablation of either isoform leads to peripheral insulin resistance (White 2002). Mechanistically the insulin-dependent tyrosine phosphorylation of IRS proteins generates docking sites for the Src homology 2 (SH2)-domain-containing downstream effector phosphatidylinositol 3'-kinase **(**PI3K) (Whitehead *et al* 2000).

PI3Ks are a family of related intracellular signal transduction enzymes which phosphorylate the 3 position hydroxyl group of the inositol ring of phosphatidylinositol (PtdIns). The PI3K family is divided into three different classes based on their sequence homology. Class I PI3Ks are further divided between IA and IB subsets based on their structure and mechanism of activation (Vanhaesebroeck *et al* 1997). Class-1A PI3Ks are heterodimers composed of a regulatory p85 subunit and a catalytic p110 subunit. The p85 subunit contains SH2 domains that bind phosphotyrosine residues in IRS proteins, which allosterically regulates the activity of the p110 catalytic subunit **(**Vanhaesebroeck *et al* 1997, Shepherd 2005). Class-1A PI3Ks preferentially phosphorylate phosphatidylinositol 4,5-bisphosphate (PtdInsP2) to form phosphatidylinositol 3,4,5-trisphosphate (PtdInsP3) at the plasma membrane **(**Vanhaesebroeck *et al* 1997). Accumulation of this lipid leads to the

PH-domain-dependent recruitment of 3-phosphoinositide-dependent protein kinase-1 (PDK1) and protein kinase B (PKB), two PH-domain-containing enzymes involved in GLUT4 translocation to the plasma membrane (Brazil *et al* 2004, Currie *et al* 1999, (Calleja *et al* 2009).

PKB (also known as Akt) is a serine/threonine kinase, which in mammals comprises three highly homologous members known as PKBα, PKBβ, and PKBγ (Scheid and Woodgett 2003). Activation of PKB requires phosphorylation at two sites. PDK1 phosphorylates PKB at Thr308, a residue located in its kinase-domain activation loop (Alessi *et al* 1997). In addition, Ser473 in the C-terminal hydrophobic motif of PKB is also phosphorylated, however the identity of the kinase responsible has been controversial, with several enzymes having been proposed as candidates to mediate this phosphorylation event (Bayascas *et al* 2005). However, studies by Hresko and co-workers, and Sarbassov and co-workers have provided evidence that an enzyme complex consisting of mTOR (mammalian target of rapamycin) and RICTOR (rapamycin insensitive companion of mTOR) mediates the phosphorylation of PKB at Ser473 (Hresko and Mueckler 2005, Sarbassov *et al* 2005). Various studies have strongly linked PKBβ to GLUT4 translocation. In 3T3-L1 adipocytes depletion of PKBβ by RNAi was reported to inhibit insulin responsiveness in 3T3L1 adipocytes (Jiang *et al* 2003). In addition knockout of PKBβ in mice has been reported to result in impaired glucose uptake in skeletal muscle and hepatic insulin resistance (Cho *et al* 2001). Furthermore, a mutation in PKBβ was recently identified in a human family with severe insulin resistance and diabetes (George *et al* 2004).

At the start of this project a Rab GTPase activating protein (GAP), termed Akt substrate of 160 kDa **(**AS160), had been identified as a downstream target of PKB (Sano *et al* 2003). More recently another Rab GAP, tre-2/USP6, BUB2, cdc16 domain family member 1 (TBC1D1), was also identified as a downstream target of PKB (Roach *et al* 2007). It is thought that PKB phosphorylation inhibits Rab-GAP activity, leading to a higher proportion of Rabs in the guanosine triphosphate (GTP)-bound state (Sakamoto K, Holman GD 2008), which via a currently poorly characterised mechanism, involving SNARE (soluble N-ethylmaleimide-sensitive-factor attachment protein receptor) proteins, promotes exocytosis of GLUT4 vesicles to the plasma membrane (Bryant *et al* 2002).

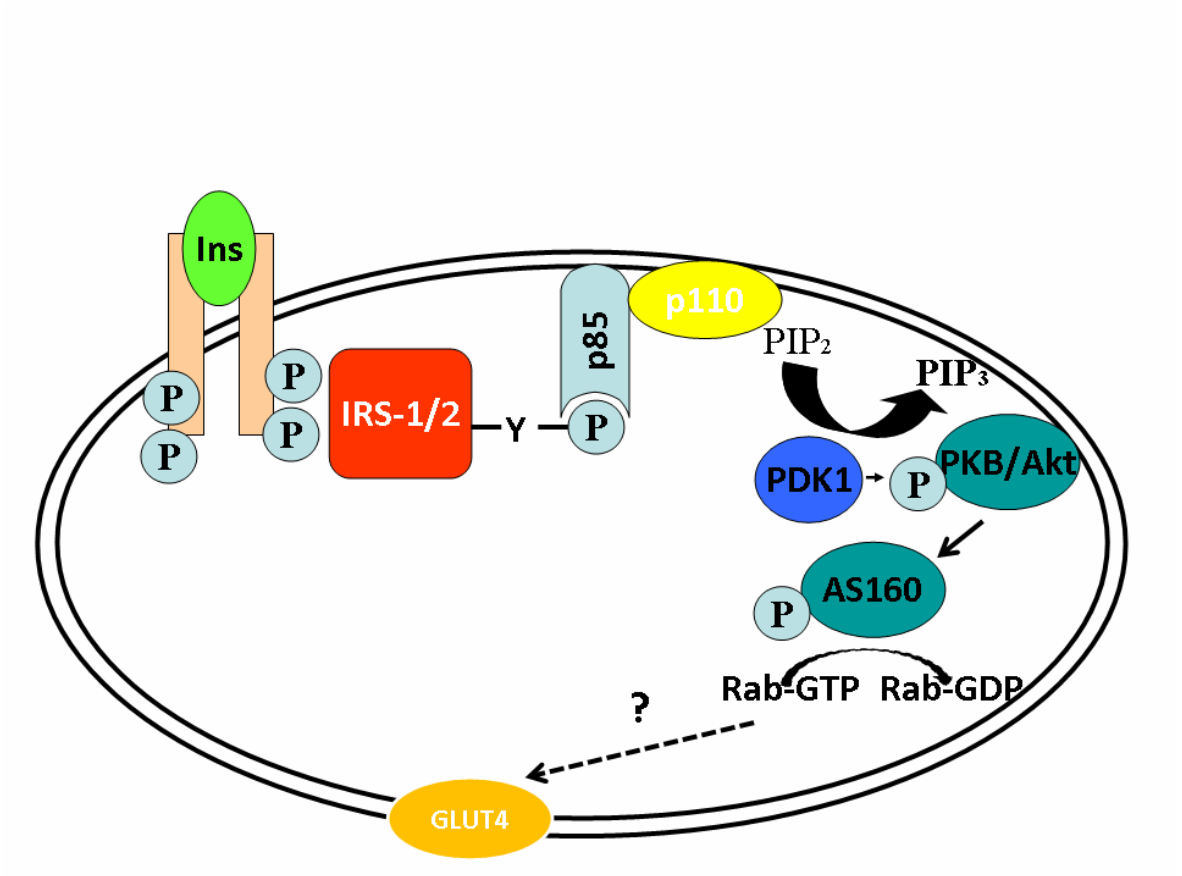

Figure 1-5: Insulin receptor signalling.
IRS = insulin receptor substrate, PIP_2 = phosphatidylinositol 4,5 bisphosphate, PIP_3 = phosphatidylinositol 3,4,5-trisphosphate, PKB = protein kinase B, PDK1 = protein dependent kinase 1, AS160 = Akt substrate of 160 kDa .

In addition, a parallel insulin-signalling pathway has been reported to contribute to GLUT4 translocation. Insulin-stimulated phosphorylation of Cbl activates the small GTP-binding protein TC10, which functions to stimulate trafficking of GLUT4 vesicles due to actin rearrangement (Saltiel and Pessin 2002).

Current models have proposed that GLUT4 populates two inter-related endosomal cycles (the fast cycle 1 and the slow cycle 2) involving the trans-golgi network and a population of vesicles called GLUT4-storage vesicles (Fig. 1.6). In the absence of insulin, GLUT4 is thought to be sequestered away from the cell surface into the fast cycling endosomal system (cycle 1). Once there, unique sequences within GLUT4 direct it into a slowly recycling pathway (cycle 2). The selective routing of GLUT4 into this slowly recycling pathway results in the effective sequestration of GLUT4 away from the cell surface, in a population of vesicles available for rapid mobilisation upon insulin binding (Bryant *et al* 2002).

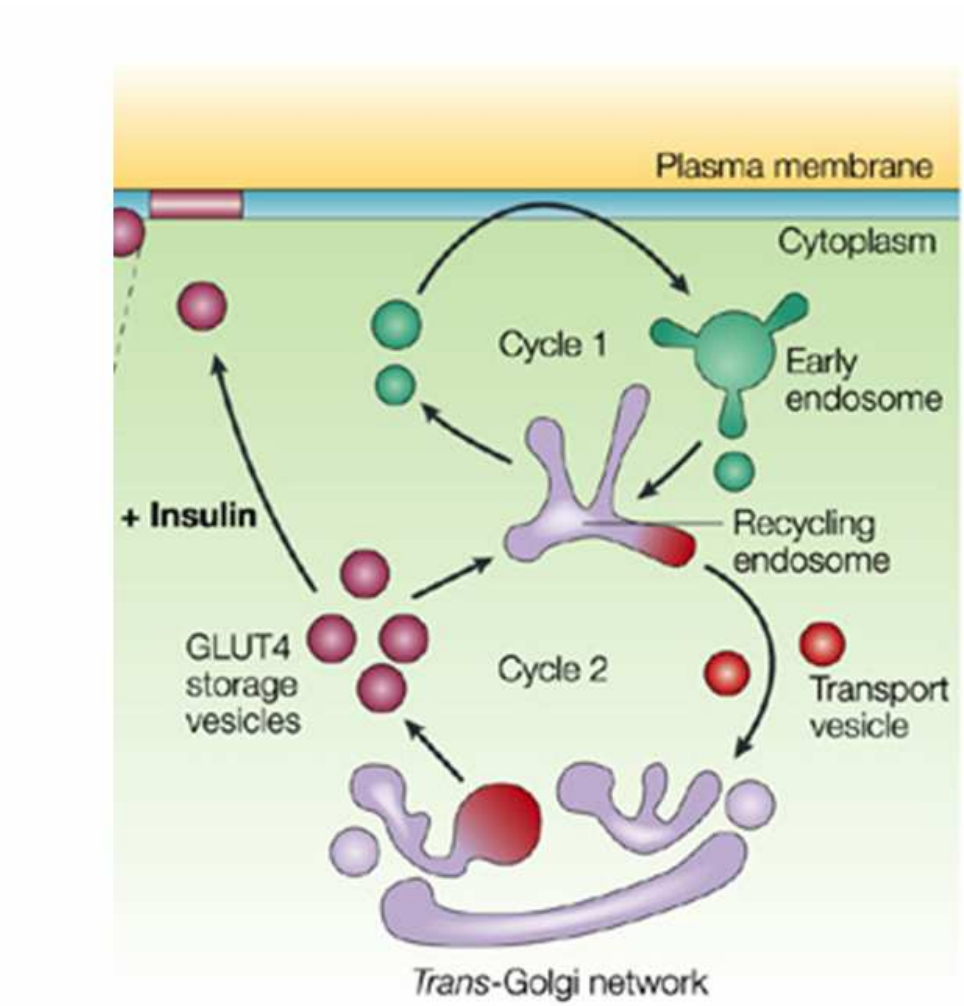

Figure 1-6: A model that depicts the transport of GLUT4 in insulin-responsive cells (adapted Bryant *et al* 2002)

1.2.2.3 Other actions of insulin

Insulin stimulates glycogen synthesis in muscle by inhibiting glycogen synthase kinase-3 (GSK-3), and increasing the activity of glycogen synthase (GS) (Cross *et al* 1995, Borthwick *et al* 1995). Gluconeogenesis in the liver is inhibited by insulin via suppression of the genes for the key gluconeogenic enzymes phosphoenolpyruvate carboxykinase (PEPCK) and glucose-6-phosphatase (G6Pase) (Agati *et al* 1998, Dickens *et al* 1998). As previously described, insulin also inhibits lipolysis by reducing cyclic AMP levels via PKB mediated activation of PDE3B (Shaker *et al* 2001).

1.2.3 Lipotoxicity

Lipotoxicity is characterised by the build up of fatty acids in tissues other than adipose. Circulating NEFA concentrations are higher in obese individuals than in lean people (Campbell *et al* 1994) and are proposed to cause insulin resistance through inhibition of the insulin signalling transduction system (Shulman 2000).

For example, it has been shown that the decrease in insulin-induced IRS-1 tyrosine phosphorylation mediated by NEFAs is linked to an increase in the activity of protein kinase C (PKC) theta in rat skeletal muscle (Griffin *et al* 1999). Active PKC results in phosphorylation of IRS-1 at Ser 307 which inhibits the interaction of IRS-1 with the insulin receptor (Aguirre *et al* 2000, Aguirre *et al* 2002). In addition, it has also been shown that elevated concentrations of NEFAs inhibit insulin stimulation of PKB in muscle cells (Chavez *et al* 2003). It has been proposed that ceramides produced from the metabolism of NEFAs could activate protein phosphatase 2A, which dephosphorylates and inactivates PKB, thus inducing insulin resistance in target tissues (Chavez *et al* 2003). Thus impaired insulin action, induced by elevated NEFAs, results in an increase in hepatic gluconeogenesis, an increase in lipolysis and reduction of glucose uptake in adipose tissue, and a reduction in glucose uptake and glycogen synthesis in muscle.

Elevated plasma NEFAs after a meal are transported into the β-cell via fatty acid binding protein 2. In the cytosol the NEFAs are converted to their acyl-CoA derivatives which have been shown to stimulate insulin secretion (Newgard and McGarry 1995, Prentki and Corkey 1996). Carnitine palmitoyl transferase 1 (CPT1) is associated with the mitochondria outer membrane and mediates the transport of long chain fatty acids across the membrane where they are subsequently oxidized. An increase in glucose levels after feeding leads to an increase in malonyl-CoA concentration within the β-cell. Malonyl-CoA inhibits CPT1, thus increasing cystolic fatty acyl-CoAs (Prentki and Corkey 1996). Thus it has been proposed (Prentki and Corkey 1996) that NEFAs work in tandem with glucose to stimulate insulin secretion. However, long term elevated NEFA levels have a detrimental effect on insulin secretion by the pancreatic β-cells. Chronic exposure to elevated NEFAs in human β-cells *in vitro* (Zhou and Grill 1995) and *in vivo* (Kashyap *et al* 2002) resulted in β-cell dysfunction characterized by enhanced insulin secretion at low glucose concentration, depletion of insulin stores and an impaired response of the β-cell to stimulatory concentrations of glucose. It has been demonstrated that apoptosis is increased in islets of obese Zucker diabetic fatty rats that are progressing through the pre-diabetic

and diabetic stages of their disease. The β-cell apoptosis is thought to be induced by NEFAs via *de novo* ceramide formation and increased nitric oxide (NO) production (Shimabukuro *et al* 1998). In addition, incubation of human β-cells with elevated levels of NEFAs also resulted in β-cell apoptosis (Lupi *et al* 2002), thought to be the result of caspase activation, partially dependent on the ceramide pathway and possibly Bcl-2 regulation.

1.2.4 Lipodystrophies

Lipodystrophies are characterized by selective loss of body fat. They are classified according to their origin, either genetic or acquired, and on the extent of fat loss, either generalized or partial (Table 1.1). Interestingly, lipodystrophies pre-dispose to similar metabolic complications associated with obese patients including insulin resistance, type 2 diabetes, hepatic steatosis (fatty liver) and dyslipidemia.

Inherited (genetic) lipodystrophies
Autosomal recessive
Congenital generalized lipodystrophy, types 1 and 2
Lipodystrophy associated with mandibuloacral dysplasia, types A and B
Lipodystrophy associated with SHORT syndrome
Lipodystrophy associated with neonatal progeroid syndrome
Autosomal dominant
Familial partial lipodystrophies (*LMNA*, *PPARG* and *AKT2* mutations)
Lipodystrophy associated with SHORT syndrome
Lipodystrophy associated with Hutchinson–Gilford progeria syndrome
Pubertal-onset generalized lipodystrophy
Acquired lipodystrophies
Lipodystrophy in HIV-infected patients
Acquired partial lipodystrophy
Acquired generalized lipodystrophy
Localized lipodystrophies

Table 1-1: Classification of lipodystrophy syndromes (Garg *et al* 2006).

1.3 Adipocytokines

1.3.1 The adipocyte and adipocytokines

Historically the adipocyte was considered a passive tissue for the storage of excess energy in the form of fat. However, it has become apparent that adipocytes secrete a number of bioactive proteins called adipocytokines thus establishing adipose tissue as an endocrine organ (Table 1.2).

Protein	**Reference**
Leptin	[Campfield *et al* 1995]
Adiponectin	[Scherer *et al* 1995; Hu *et al* 1996; Maeda *et al* 1996]
IL-6	[Mohaamed-Ali *et al* 1997]
TNF-α	[Kern *et al* 1995]
resistin	[Steppan *et al* 2001]
Plasminogen activator-inhibitor	[Wiman *et al* 1984]
Adipsin	[Cook *et al* 1985]
Acylation-stimulating protein	[Maslowska *et al* 1997]
IL-8	[Bruun *et al* 2001]
Agouti protein	[Manne *et al* 1995]
Transforming growth factor-β	[Samad *et al* 1996, Jones *et al* 1997]
Adipophilin	[Heid *et al* 1998]
Apelin	[Castan-Laurell *et al* 2005]
Omentin	[Schaffler *et al* 2005]
Visfatin	[Fukuhara *et al* 2005]
Chemerin	[Bozaogula *et al* 2007]

Table 1-2: Bioactive proteins secreted by adipose.

Leptin, tumour necrosis factor alpha (TNFα), interleukin (IL)-6 and adiponectin are some of the best characterized adipocytokines and are discussed below. They appear to play an important role in insulin resistance. In obesity the secretion levels of these adipocytokines are altered. Thus, there is intense interest in the role of adipocytokines in the pathogenesis of obesity related disorders such as type 2 diabetes.

1.3.2 Leptin

Leptin is predominantly expressed in adipose tissue (Green *et al* 1995). It is the protein product of the *ob* (obese) gene and was discovered in 1994 after positional cloning of the monogenic mutant responsible for the morbidly obese phenotype observed in the obese (*ob/ob*) mouse (Zhang *et al* 1994).

Leptin serves to inform the hypothalamus of the quantity of stored fat. In adults leptin crosses the blood brain barrier via a saturable transport system. In the arcuate nucleus (ARH) leptin stimulates the proconvertase 1-dependent cleavage of proopiomrlanocortin (POMC) neurons, to produce the anorexigenic peptide α-melanocyte-stimulating hormone (α-MSH) (Rouille *et al* 1995) which is an agonist of the melanocortin 4 receptor (MC4R). Also, in the ARH, leptin inhibits neurons which co-express the orexigenic peptides, neuropeptide Y (NPY) and agouti related peptide (AgRP), which is an antagonist of MC4R (Zigman and Elmquist 2003). This consequently results in the activation of the MC4R in the paraventricular nucleus (PVN) consequently resulting in a decrease in feeding and an increase in energy expenditure (Fig. 1.7). Thus, conversely a decrease in leptin levels results in a decrease in energy expenditure and an increase in food intake (Adan *et al* 1994) (Hwa *et al* 2001).

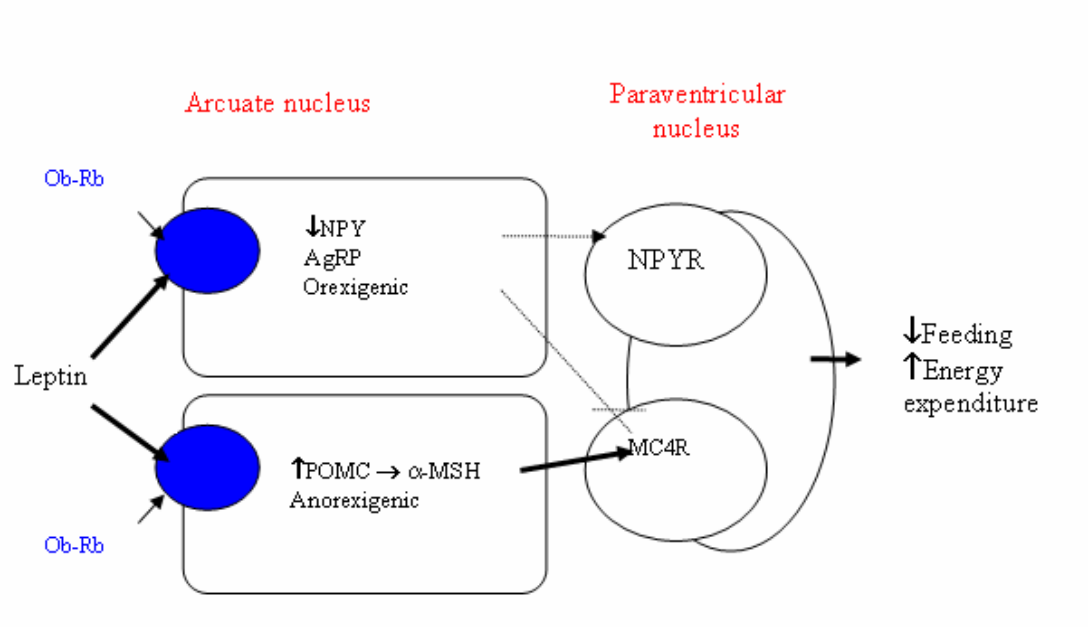

Figure 1-7: Leptin stimulates decreased feeding and increased energy expenditure.
POMC = proopiomrlanocortin, α-MSH = α-melanocyte-stimulating hormone, MC4R = melanocortin 4 receptor, NPYR = neuropeptide Y receptor, AgRP = agouti related peptide, MC4R = melanocortin 4 receptor, PVN = paraventricular.

Spontaneous mutations in leptin or in the leptin receptor result in obesity in mice and in humans (Chen *et al* 1996, Zhang *et al* 1994, Montague *et al* 1997, Clement *et al* 1998). Leptin deficient mice and humans were shown to be successfully treated with leptin (La Campfield *et al* 1995, Farooqi *et al* 1999). This finding fuelled excitement that leptin could be used to treat obese patients. Unfortunately the level of leptin secreted from adipocytes is proportional to body fat stores (Maffei *et al* 1995), with greater secretion occurring from subcutaneous adipose tissue compared with visceral adipose tissue (Fain *et al* 2004, Wajchenberg 2000). Thus, obese individuals have high levels of circulating leptin in their blood stream due to increased amounts of leptin-secreting adipose tissue (Considine *et al* 1996). In fact most obese patients appear to be leptin resistant as treatment with exogenous leptin does not ameliorate their obesity (Bjorbaek and Kahn 2004, Flier 2004). Leptin resistance is thought to be due to saturable transport across the blood-brain barriers or due to abnormalities of the leptin receptor activation and / or signal transduction (El-Haschimi *et al* 2000).

In addition to regulating appetite and bodyweight leptin has also been shown to be involved in other processes. Leptin appears to play a role in immune responsiveness by modulating the T-cell immune response (Gainsford *et al* 1996, Lord *et al* 1998), inhibit bone formation (Ducy *et al* 2000) and correct sterility in leptin deficient mice (Chehab *et al* 1996, Chehab *et al* 1997, Ahima *et al* 1997).

1.3.3 TNFα

TNFα is an inflammatory cytokine which can stimulate the production of other cytokines e.g IL-1 and IL-6 (Warne *et al* 2003, Wajant *et al* 2003). TNFα is produced by many different tissues including adipose (Kern *et al* 1995, Wajant *et al* 2003).

Adipose tissue TNFα expression is increased in obese rodents and humans and positively correlates with adiposity and insulin resistance (Ruan and Lodish 2003, Hotamisligil 2003, Fernandez-Real and Ricart 2003). Targeted knock out of the TNFα gene in obese mice resulted in improved insulin sensitivity (Uysal *et al* 1997). In addition, in rat models of obesity and insulin resistance, neutralizing TNFα with injections of a soluble TNF-receptor-immunoglobulin gamma (IgG) fusion protein, resulted in increased insulin sensitivity (Hotamisligil *et al* 1993). However the effects of neutralizing TNFα using an engineered human anti-TNFα antibody appeared to have no significant effects on insulin sensitivity in patients with type 2 diabetes (Ofei *et al* 1996).

1.3.4 IL-6

IL-6 is another cytokine which positively correlates with body mass index (Vgontzas *et al* 1997). As much as a third of total circulating concentrations of IL-6 is thought to originate from adipose tissue (Mohamed-Ali *et al* 1997, Xing *et al* 1997).

Elevated levels of IL-6 are associated with obesity and insulin resistance (Fernandez-Real and Ricart 2003). TNFα whose expression is elevated in obesity has been shown to increase IL-6 production in 3T3-L1 adipocytes (Grunfeld and Feingold 1991). Peripheral administration of IL-6 was shown to induce hyperlipidemia, hyperglycemia and insulin resistance in rodents and humans (Fernandez-Real and Ricart 2003). In rats peripheral administration of IL-6 induced hypertriglyceridemia by stimulating hepatic triglyceride secretion (Nonogaki *et al* 1995), and in humans an IL-6 infusion resulted in an increase in NEFA concentration (Stouthard *et al* 1995). In addition IL-6 has been shown to inhibit insulin signalling by inducing suppressor of cytokine signalling-3 (SOCS-3), a negative regulator of insulin signalling (Senn *et al* 2003).

1.3.5 Adiponectin

Adiponectin is expressed exclusively in adipocytes (Weyer *et al* 2001). Adiponectin exists in plasma as trimeric, hexameric and higher order polymeric structures (Pajvani *et al* 2003). Adiponectin is the only adipocytokine whose secretion is decreased in the obese state. Further more, adiponectin has been shown to be able to inhibit the secretion of inflammatory cytokines including IL-6 and IL-8 by human adipocytes (Sell *et al* 2006).

Reduced adiponectin levels are documented in obese, insulin resistant and type 2 diabetes patients (Hotta *et al* 2000). Analysis of a Pima Indian population showed that the development of type 2 diabetes was associated with lower plasma adiponectin levels prior to diagnosis of type 2 diabetes (Lindsay *et al* 2002). Overexpression of adiponectin in mice resulted in improved insulin sensitivity, glucose tolerance and serum NEFAs (Combs *et al* 2004). Conversely adiponectin deficient mice exhibit insulin resistance, glucose intolerance and increased serum NEFAs (Kubota *et al* 2002, Maeda *et al* 2002).

1.4 AMPK

1.4.1 Reversible phosphorylation

In 1992 Krebs and Fischer were awarded a Nobel Prize for 'their discoveries concerning reversible protein phosphorylation as a biological regulatory mechanism' (Kresge *et al* 2005). Reversible protein phosphorylation regulates many cellular signal transduction pathways, which underlie many biological processes, including metabolism, growth, differentiation, membrane trafficking, muscle contraction, immunity, and memory (Manning *et al* 2002). Reversible phosphorylation involves the phosphorylation of a target protein by a protein kinase and subsequent dephosphorylation of that protein by a protein phosphatase.

Protein kinases are one of the largest families of genes in eukaryotes. The human genome contains about 500 protein kinase genes, which accounts for approximately 2% of all human genes (Manning *et al* 2002).

Approximately 30% of human proteins can be modified by kinases (Hubbard and Cohen, 1993). Protein kinases phosphorylate target substrate proteins by catalyzing the transfer of the γ phosphate from ATP to a target amino acid residue. In eukaryotes, phosphorylation usually occurs on serine (Ser), threonine (Thr) and tyrosine (Tyr) residues. Phosphorylation of these residues is mediated by Ser/Thr-specific kinases such as PKA, PKB and PKC (Filippa *et al* 1999, Newton *et al* 1995), Tyr-specific kinases such as epidermal growth factor receptor (EGFR) and IR (Carpenter *et al* 2000) and dual specificity kinases such as mitogen activated protein (MAP) kinase kinases (MAPKK) (Dhanasekaran and Reddy 1998) which phosphorylate Ser/Thr and Tyr. Interestingly, of the ~500 protein kinases encoded by the human genome, the majority, ~400, encode Ser/Thr kinases, while only ~90 encode Tyr kinases and ~40 encode dual-specificity protein kinases (Manning *et al* 2002).

Phosphorylation on other amino acid residues such as histidine, arginine and lysine occurs mostly in prokaryotic proteins (Cozzon 1988, Stock *et al* 1989).

Eukaryotic protein kinases are structurally similar (Hanks *et al* 1988). The catalytic domain contains an N-terminal lobe of β-sheets and a larger C-terminal lobe of α-helices (Knighton *et al* 1991, Lowe *et al* 1997). This lobe structure forms an ATP-binding cleft

that constitutes the active site. ATP binds in a clef between the two lobes. It is orientated with adenosine sitting in a hydrophobic pocket and the hydrophilic phosphate chain pointing outwards away from the hydrophobic pocket. The substrate binds along the cleft and conserved residues within the kinase catalytic domain catalyse the removal of the γ phosphate from ATP and the covalent attachment of it to a free hydroxyl group on either Ser/Thr or Tyr residues. Despite the fact that kinases share a common fold, they can still selectively phosphorylate their target substrates. Specificity can be determined by the structure of the catalytic cleft of the kinase, local interactions between the cleft and the substrate phosphorylation site, and distal binding between the kinase and the substrate (Ubersax and Ferrell 2007).

Phosphorylation of a protein can alter the protein activity, subcellular location, half-life and the association of that particular protein with other proteins. Thus, multisite phosphorylation of a protein can allow several of these effects to operate in the same protein (Cohen 2000).

It is well established that protein kinases are themselves phosphorylated. Thus giving rise to protein kinase cascades, such as the AMPK signalling cascade (Hardie 2004a) and the MAPK signalling cascades (Seger and Krebs 1995), which are formed when two or more proteins act in series.

Interestingly, the human genome encodes ~200 protein phosphatases, comprising of ~40 Ser/Thr, ~100 Tyr and ~50 dual specificity (Alonso *et al* 2004, Arena *et al* 2005, Moorhead *et al* 2007). Thus is comparison to the number of protein kinases (~500) there are substantially less protein phosphatases.

It has become apparent that each Ser/Thr phosphatase must regulate many more substrates than each Ser/Thr kinase since there are only ~40 Ser/Thr kinases compared to ~400 Ser/Thr kinases. Specificity of Ser/Thr phosphatases is thought to occur through the association of phosphates catalytic domains with particular regulatory subunits, which target the catalytic core to different cellular locations and target substrates (Cohen 2002).

In comparison, there are similar numbers of Tyr phosphatases and Tyr kinases. Thus, unlike Ser/Thr phosphatases, Tyr phosphatases do not require different regulatory subunits. They exist mostly as modular proteins with separate catalytic and targeting domains (Alonso *et al* 2004).

1.4.2 Discovery of AMPK

AMP-activated protein kinase (AMPK) was initially discovered three decades ago. Two separate groups showed that preparations of two enzymes involved in liver fat metabolism; ACC (Carlson and Kim 1973) and 3-hydroxy-3-methylglutaryl-CoA reductase (HMGR) (Beg *et al* 1978) became inactivated in the presence of ATP. This effect was concluded by both groups to be due to the contamination of the enzyme preparation with a protein kinase. It was later shown that the kinases responsible for the inhibitory effects on ACC and HMGR were stimulated by 5'-adenosine monophosphate (AMP) (Yeh *et al* 1980) (Ferrer *et al* 1985). Subsequently, it was discovered that the inactivation of both ACC and HMGR was catalysed by the same single protein kinase (Carling *et al* 1987). It soon became apparent that the protein kinase initially termed HMGR kinase was in fact a multisubstrate kinase, thus it was renamed AMP-activated protein kinase after its allosteric activator 5'-AMP (Munday *et al* 1988).

1.4.3 AMPK overview

AMPK is a conserved sensor of cellular energy status and is present in all eukaryotes. AMPK is activated when there is a decrease in cellular energy level i.e an increase in the cellular AMP/ATP ratio. Metabolic stresses which activate AMPK include muscle contraction (Hutber *et al* 1997) which increases ATP consumption, and deprivation of oxygen (Kudo *et al* 1995, Marsin *et al* 2000) or glucose (Salt *et al* 1998b) which depletes ATP levels. AMPK exists as a heterotrimeric complex consisting of a catalytic α subunit and regulatory β and γ subunits. The β subunit contains a glycogen binding domain and the γ subunit contains cystathionine β-synthase (CBS) motifs which bind the two nucleotides; AMP and ATP (Towler and Hardie, 2007). AMPK is regulated by phosphorylation by upstream kinases. The tumour suppressor LKB1 (Hawley *et al* 2003; Woods *et al* 2003) and Ca^{2+}/Calmodulin dependent protein kinase kinase (CaMKK) (Hawley *et al* 2005) are two well characterized AMPK kinases. Active AMPK stimulates ATP-producing pathways such as glycolysis and fatty acid oxidation, while inhibiting ATP consuming pathways such as gluconeogenesis, fatty acid synthesis and cholesterol synthesis (Hardie 2004a). AMPK mediates these effects via phosphorylation of downstream metabolic enzymes (Hardie 2004a) and by effects on gene (Foretz *et al* 1998) and protein expression (Winder *et al* 2000). In addition to regulating energy balance at the cellular level it has become apparent that AMPK also regulates food intake and energy expenditure at the whole body

level, in particular by mediating the effects of hormones and cytokines such as leptin (Minokoshi *et al* 2002, Minokoshi *et al* 2004) and adiponectin (Yamauchi *et al* 2002).

1.4.4 AMPK Structure

AMPK exists as a heterotrimer comprising of a catalytic α subunit and a regulatory β and γ subunit (Hardie *et al* 2003). In mammals there are two genes encoding isoforms of both the α and β subunits; α1, α2, β1 and β2, and three genes encoding isoforms of the γ subunit; γ1, γ2, and γ3 (Hardie *et al* 1998, Stapleton *et al* 1996, Stapleton *et al* 1997, Woods *et al* 1996a/b). Along with splice variants and different combinations of isoforms there exists a diverse array of different complexes. Expression levels of the subunit isoforms vary between different tissues and cellular localization (Salt *et al* 1998a, Thornton *et al* 1998, Stapleton *et al* 1996, Mahlapuu *et al* 2004).

AMPK appears to be a fundamental feature of all eukaryotic cells, as genes encoding orthologues of the α, β and γ subunits are present in all eukaryotic species whose genome sequence has been determined. Indeed orthologues of AMPK have been found in the yeast *Saccharomyces cerevisiae* and the parasite *Giardia lamblai* (Carling 2004, Hardie *et al* 2003).

The α1 and α2 mammalian subunits share 90% identity at their N-terminal catalytic domains, but only 60% identity at their C-terminal domains (Stapleton *et al* 1996). The C-terminal domain has been shown to be required to form a complex with the non-catalytic subunits β and γ (Fig. 1.8) (Crute *et al* 1998).

The β subunits contain two conserved regions (Fig. 1.8). These regions were originally termed kinase-interacting sequence (KIS) and association with Snf-1 complex (ASC) domains. Based on two hybrid analysis in yeast it was originally thought that the KIS domain was required for interacting with the α subunit, while the ASC domain was required for interaction with the γ subunit (Jiang and Carlson 1997). However, it has since been discovered that only the ASC domain is required for complex formation. The KIS domain is actually a glycogen binding domain (GBD) (Hudson *et al* 2003). This domain is present in enzymes which metabolize the α1→ 6 branch points in α1→ 4 linked glucans such as starch and glycogen (Hudson *et al* 2003, Polekhina *et al* 2003). GBD has been shown to cause association of AMPK with glycogen particles, where one of its substrates GS is located (Hudson *et al* 2003). Interestingly, prior glycogen loading of skeletal muscle

suppresses activation of AMPK by exercise in humans (Wojtaszewshi *et al* 2003). In addition, glycogen has also been shown to inhibit AMPK in cell-free assays, an effect that is dependent on binding to the GBD and varies according to the branching content of the glycogen i.e glycogen branch points inhibit AMPK activity (McBride *et al* 2009). Thus it has been proposed by McBride and co-workers that in muscle containing a high glycogen content, AMPK may be bound to the non-reducing ends at the surface of glycogen, sequestering AMPK away from other downstream targets. This is thought to account for the reduced apparent activation of AMPK in response to exercise (Wojtaszewshi *et al* 2003) when muscle is in a glycogen-loaded state. Since the outer chains prevent access of AMPK to the internal glycogen branch points, AMPK would not be inhibited and thus would phosphorylate and inhibit GS. In contrast, exposure of the glycogen branch points by phosphorylase after contraction would inhibit AMPK. Thus, GS would no longer be phosphorylated and inhibited by AMPK, which would allow glycogen re-synthesis. Thus essentially the GBD may function as a regulatory domain which allows AMPK to act as a glycogen sensor *in vivo*.

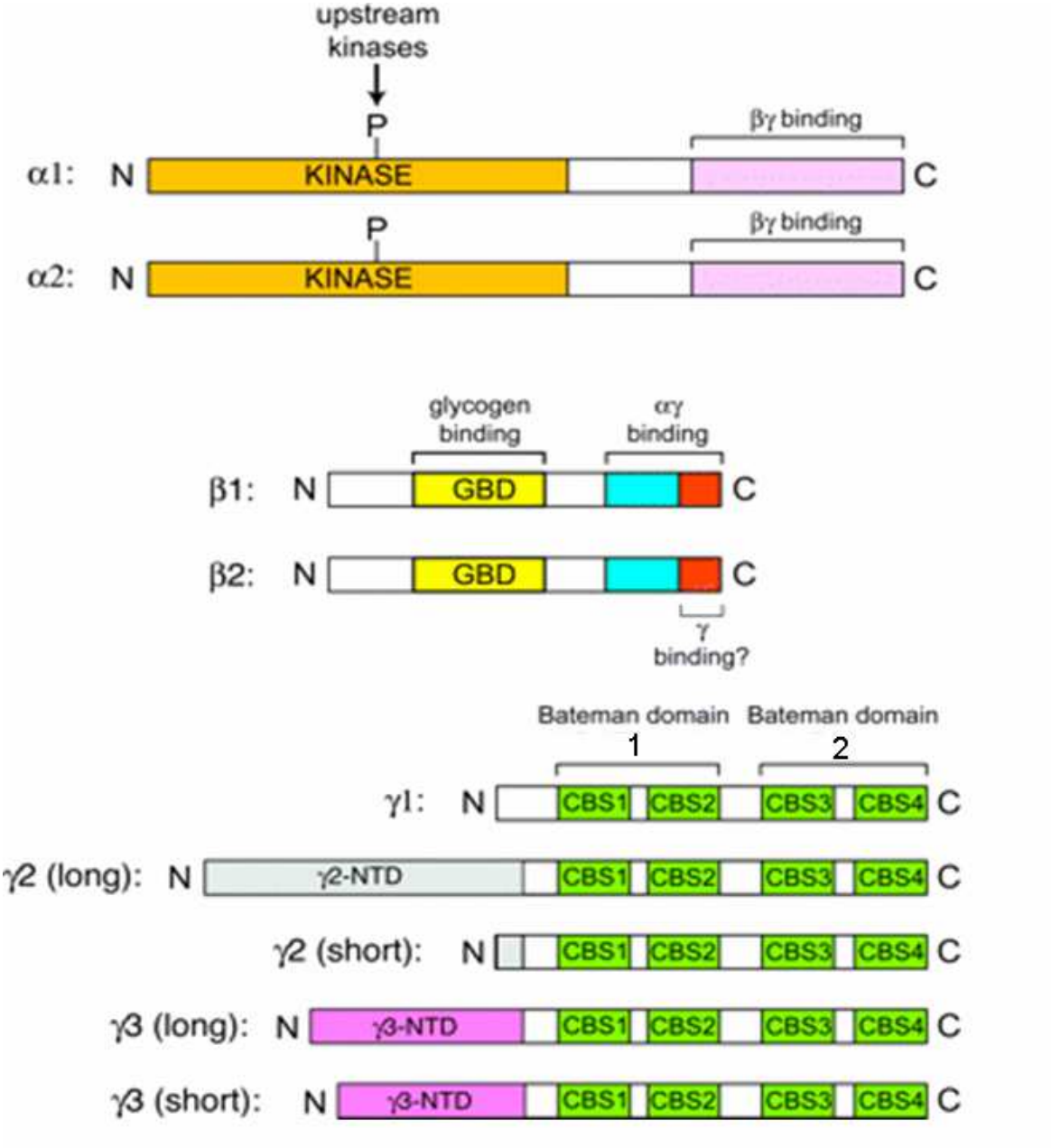

Figure 1-8: Domain structure of AMPK subunit isoforms and splice variants
Regions shown in the same colour are related, and their functions, where known, are indicated (amended from Towler and Hardie 2007).

There exist three γ isoforms, with splice variants creating both long and short forms of γ2 and γ3. The γ subunits differ from each other in the length of their N-terminal sequence, but they all contain conserved CBS motifs (Fig. 1.8). Bateman discovered the CBS motifs, which are named after the enzyme cystathionine β-synthase which contains a pair of such motifs at the C-terminus (Bateman 1997). These motifs occur as tandem pairs, therefore the term 'Bateman domain' was derived to describe the structure formed by two tandem CBS motifs (Kemp 2004). The recent determination of the crystal structure of the regulatory core of mammalian AMPK revealed that there was a nucleotide binding site on three of the four CBS motifs in the γ subunit. Two of these sites can bind AMP or ATP

with approximately equal affinity, and the third site contains a tightly-bound AMP that appears to be non-exchangeable (Xiao *et al* 2007).

1.4.5 Naturally Occurring AMPK mutations

Currently, a total of five missense mutations and an insert mutation in the γ2 subunit of AMPK have been detected in different families with the hereditary heart disease in humans called Wolff-Parkinson-White syndrome. Four of these mutations affect the N-terminal Bateman domain, while the other two affect the C-terminal Bateman domain (Fig. 1.9) (Gollob *et al* 2001, Arad *et al* 2002, Gollob *et al* 2002, Blair *et al* 2001). These mutations cause both defective activation of the intact AMPK complex by AMP (Daniel and Carling 2002) and defective binding of AMP to the isolated Bateman domains (Scott *et al* 2004). Interestingly, the mutations also decrease the binding of the inhibitor ATP (Scott *et al* 2004). Therefore, although the mutations prevent activation by AMP, they also appear to increase the basal activity (Burwinkel *et al* 2005). In addition, these studies provide strong evidence that the Bateman domains are indeed the regulatory AMP and ATP binding sites.

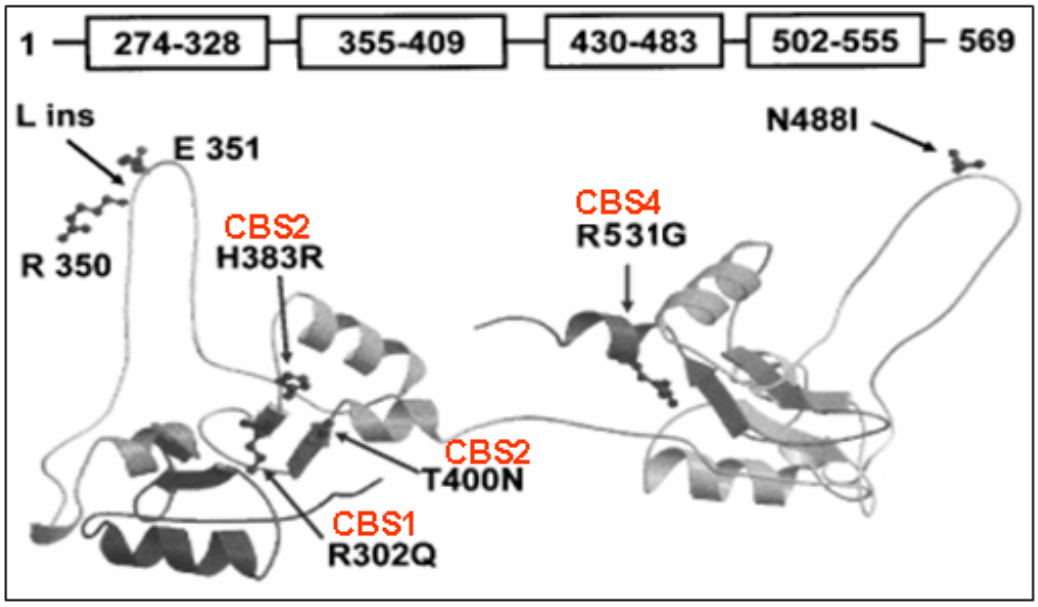

Figure 1-9: The positions of known mutations that cause cardiac disease are marked on the γ2 subunit (adapted from Kemp *et al* 2003).

A feature of Wolff-Parkinson-White syndrome is elevated storage of glycogen in cardiac myocytes (Burwinkel *et al* 2005). Thus the dominant effect of the mutations to increase basal AMPK phosphorylation has led to the proposal that elevated AMPK activity leads to

a higher basal glucose uptake into the myocytes. This would result in excessive glycogen storage, thought to underlie the cardiomyopathy (Arad *et al* 2007).

1.4.6 Regulation of AMPK by AMP and phosphorylation

AMPK is stimulated by an elevated AMP/ATP ratio. As eukaryotic cells have significant levels of adenylate kinase to maintain the reaction: 2 ADP ↔ ATP + AMP close to equilibrium, the AMP/ATP ratio varies approximately with the square of the ADP/ATP ratio (Hardie and Hawley 2001) making the AMP/ATP ratio extremely sensitive to cellular energy levels.

It is thought that under physiological conditions, AMPK exists in its inactive form in complex with the much more abundant ATP, with only a small proportion binding AMP (Xiao *et al* 2007). Xiao and co-workers have proposed that a 2-3 fold increase in the AMP concentration (low μM range) results in a similar fold increase in the proportion of AMP bound enzyme in the presence of a much higher (mM range) concentration of ATP (Xiao *et al* 2007).

AMPK is regulated by AMP by two distinct mechanisms. Firstly, AMP causes allosteric activation of AMPK (Hardie *et al* 1999). Secondly, the binding of AMP to AMPK makes it a worse substrate for protein phosphatases, especially protein phosphatase-2C (Davies *et al* 1995). These effects by AMP are antagonised by high concentrations of ATP, demonstrating that the system responds to the AMP/ATP rather than to just AMP levels (Corton *et al* 1995, Hawley *et al* 1996, Davies *et al* 1995).

AMPK is activated by an upstream kinase, AMPK kinase (AMPKK). Phosphorylation occurs in the α subunit at Thr172 which lies in the activation loop (Hawley *et al* 1996). The major breakthrough in identifying upstream kinases came from the study of the regulation of the AMPK orthologue, Snf-1 in *Saccharomyces cerevisiae*. Snf-1 was shown to be phosphorylated and activated by three closely related kinases, Elm 1, Pak 1 and Tos 3 (Hong *et al* 2003). Database searches with these yeast sequences revealed that LKB1 and CaMKK α and β were closely related mammalian kinases.

LKB1 is encoded by the Peutz-Jegher syndrome tumour suppressor gene (Jenne *et al* 1998). Peutz-Jegher syndrome is an autosomal dominant disorder, characterised by a predisposition to gastrointestinal neoplasms marked by a high risk of benign and malignant

pancreatic tumours (Hemminki 1999). AMPK kinase purified from rat liver was found to correspond to LKB1 (Hawley *et al* 2003, Woods *et al* 2003). In addition, cells which lacked LKB1 were shown to have a reduced AMPK activity compared to cells expressing LKB1, and AMPK was not found to be activated by stimuli which normally activate it (Shaw *et al* 2004, Hawley et al 2003, Woods *et al* 2003). These findings provided evidence that LKB1 is an AMPKK. The discovery that LKB1 is not regulated by stimuli which activate AMPK in cells (Lizcano *et al* 2004, Woods *et al* 2003) or in skeletal muscle (Sakamoto *et al* 2004), and that it is not directly activated by AMP (Hawley *et al* 2003, Woods *et al* 2003) suggested that LKB1 is 'constitutively active' and that the regulation of AMPK phosphorylation is regulated by effects on AMPK itself.

Initially it was thought that AMP also made AMPK a better substrate for the upstream kinase LKB1 (Hawley *et al* 1995). However, subsequent work has shown that this is not the case (Sanders *et al* 2007b). Earlier results indicating that AMP stimulates phosphorylation of AMPK by LKB1 can be plausibly explained by the presence of endogenous protein phosphatase 2C in the preparations of the rat liver kinases used in the study i.e AMP inhibited dephosphorylation of AMPK by the phosphatase, rather than increasing phosphorylation of AMPK by LKB1.

The current AMP-dependent AMPK activation model proposed by Sanders and co-workers (Sanders *et al* 2007b) suggests that in addition to the allosteric effect of AMP on AMPK, when there is an increases in the AMP/ATP ratio, dephosphorylation of AMPK is inhibited. Since LKB1 functions as a constitutively active kinase, inhibition of the dephosphorylation reaction leads to an increase in AMPK Thr172 phosphorylation and activation of AMPK. Thus, AMPK phosphorylation by LKB1 occurs in response to decreased dephosphorylation following a rise in the AMP/ATP ratio.

CaMKKα/β are also important intracellular AMPKKs which phosphorylate and activate AMPK in the presence of an increased calcium concentration, independently of an increase in AMP concentration. Hawley and co-workers showed that there is significant basal activity and phosphorylation of AMPK in LKB1-deficient cells that can be stimulated by Ca^{2+} ionophores, and studies using the CaMKK inhibitor STO-609 and CaMKK isoform-specific siRNAs show that CaMKKβ is required for this effect (Hawley *et al* 2005). K^{+}-induced depolarization in rat cerebrocortical slices, which increases intracellular Ca^{2+} without disturbing cellular adenine nucleotide levels, was also shown to activate AMPK, and to be blocked by STO-609 (Hawley *et al* 2005). It was also shown that CaMKKβ

appears to activate AMPK much more rapidly than CaMKKα in cell-free assays (Hawley *et al* 2005). However, 2-deoxyglucose- and ionomycin-stimulated AMPK activity and phosphorylation, was reported to be reduced in HeLa cells transfected with small interfering RNAs specific for both CaMKKα and CaMKKβ (Hurley *et al* 2005).

Recently transforming growth factor-β activated kinase (TAK1) was identified as a possible candidate for a novel AMPK kinase in mammalian cells (Momcilovic *et al* 2006). TAK1 was shown to activate the Snf1 protein kinase *in vivo* and *in vitro* and co-expression of TAK1 and its binding partner TAB1 in HeLa cells stimulated AMPK Thr172 phosphorylation.

1.4.7 AMPK Function

Active AMPK can inhibit ATP consuming pathways and stimulate ATP producing pathways. Historically AMPK was thought to act as a regulator of energy balance primarily at the cellular level (Fig. 1.10). However, it has since been shown to have a

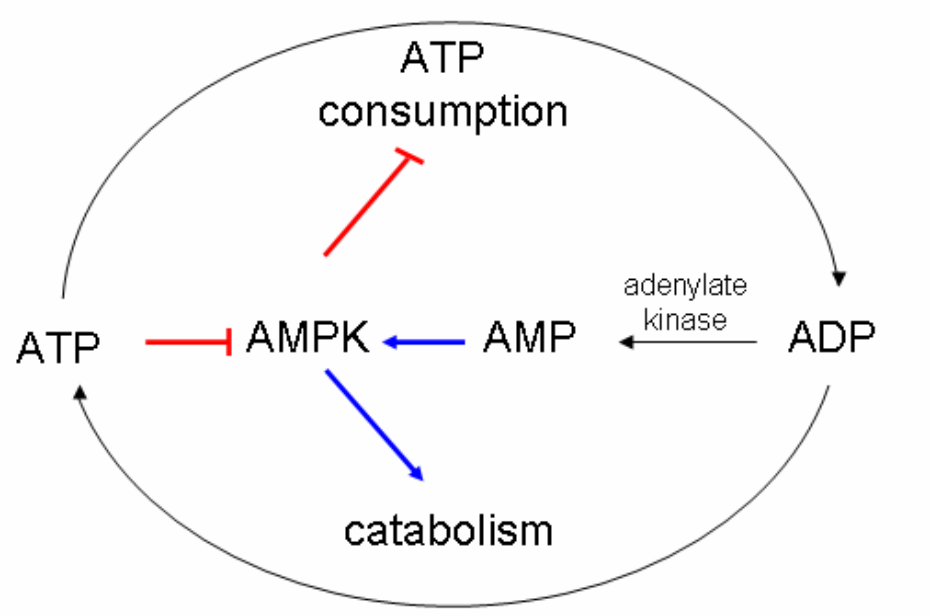

Figure 1-10: Role of AMPK in regulating energy balance at the cellular level.

fundamental role in regulating energy balance at the level of the whole organism (Fig. 1.11). Active AMPK results in many changes including glucose uptake and metabolism by muscle and other tissues, reduced glucose production in the liver and reduced synthesis and increased oxidation of fatty acids. All of these effects are beneficial to people with type 2 diabetes and the metabolic syndrome, thus making AMPK an attractive therapeutic target.

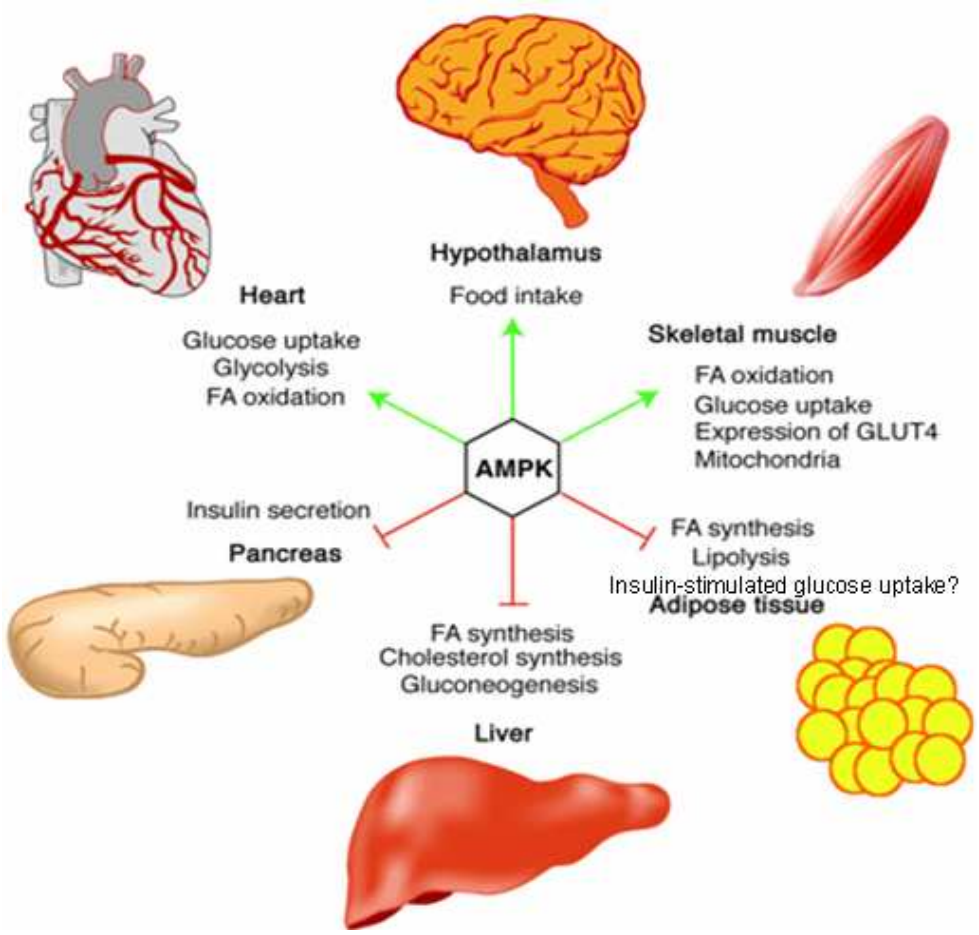

Figure 1-11: Role of AMPK in regulating energy balance at the whole-body level (adapted from Hardie 2004b).

1.4.8 Activators of AMPK

Metabolic poisons such as arsenite, an inhibitor of the tricarboxylic acid cycle (Corton *et al* 1994), antimycin A and azide, inhibitors of the respiratory chain (Witters *et al* 1991), oligomycin, an inhibitor of mitochondrial ATP synthase (Marsin *et al* 2000) and dinitrophenol, an uncoupler of oxidative phosphorylation (Witters *et al* 1991) all activate AMPK by depleting cellular ATP levels.

Pathological stresses can activate AMPK by increasing the AMP/ATP ratio. These include glucose deprivation (Salt *et al* 1998b), ischemia (Kudo *et al* 1995, Marsin *et al* 2000) and oxidative stress (Choi *et al* 2001). Interestingly, hyperosmotic stress, induced by sorbitol, in muscle cells was shown to activate AMPK without altering the cellular AMP/ATP ratio (Fryer *et al* 2002b).

Exercise (Winder and Hardie 1996) or contraction in skeletal muscle (Hutber *et al* 1997) activates AMPK by increasing ATP consumption. In muscle the level of activation of AMPK depends on both the intensity and duration of the work.

Leptin activates AMPK in muscle by direct effects via the leptin receptor and indirectly via the hypothalamic-sympathetic nervous system (SNS) axis through α-adrenergic receptors (Fig. 1.12). A decrease in cellular energy levels (AMP/ATP) is thought to occur during direct AMPK activation by leptin, but not during the indirect activation in muscle (Minokoshi *et al* 2002).

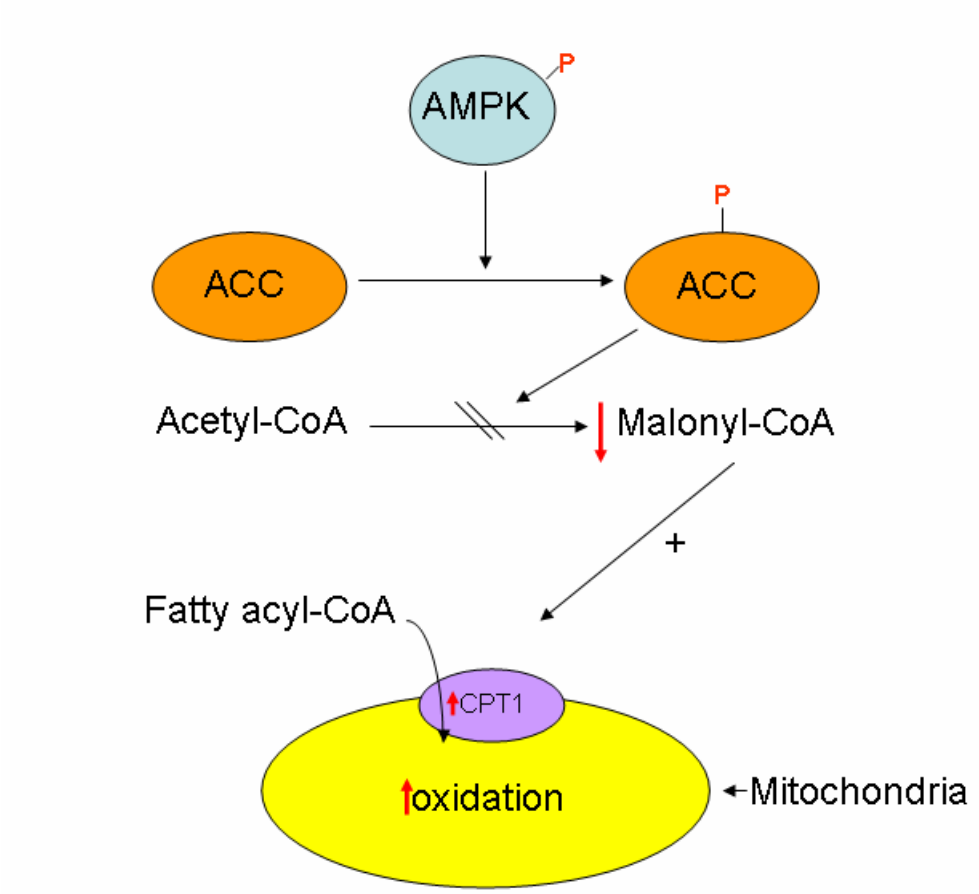

Figure 1-12: Model for the stimulatory effect of AMPK on fatty acid oxidation in muscle.
ACC = acetyl CoA carboxylase, CPT1 = carnitine palmitoyl transferase 1.

In skeletal muscle, phosphorylation and activation of AMPK by leptin (Minokoshi *et al* 2002), results in fatty-acid oxidation via phosphorylation and inhibition of ACC (discussed further in the text 1.4.11). Briefly, inhibition of ACC leads to a decrease in malonyl-CoA levels, which prevents inhibition of CPT1, subsequently allowing the uptake of fatty acids into the mitochondria where they are oxidized (Fig. 1.12).

As previously mentioned leptin has an anorexigenic action in the hypothalamus. This effect is mediated by inhibition of AMPK activity in the ART and PVN (Minokoshi *et al* 2004). Decreased AMPK activity in the ART results in the inhibition of the orexigenic peptides NPY/AgRP. It would appear that that MC4Rs are required for the physiological and hormonal regulation of AMPK in the paraventricular hypothalamus as an agonist for this receptor which inhibits food intake also inhibits AMPK activity in the paraventricular nucleus, and mice lacking the MC4R are hyperphagic and obese and are unable to inhibit AMPK activity in response to feeding or leptin (Minokoshi *et al* 2004).

In muscle and liver, *in vivo* and *in vitro*, adiponectin has been demonstrated to stimulate AMPK phosphorylation and activation (Yamauchi *et al* 2002). The activation of AMPK in muscle that occurs five minutes after adiponectin treatment may result from an increase in the concentration of cellular AMP (Yamauchi *et al* 2002). In parallel with its activation of AMPK, adiponectin stimulates phosphorylation of ACC, fatty-acid oxidation, glucose uptake and lactate production in myocytes, phosphorylation of ACC and reduction of molecules involved in gluconeogenesis in the liver, and reduction of glucose levels *in vivo*. Blocking AMPK activation by a dominant-negative mutant inhibits each of these effects demonstrating that the stimulation of glucose utilization and fatty acid oxidation by adiponectin occurs through activation of AMPK (Yamauchi *et al* 2002). In addition AMPK can also be activated in adipocytes by adiponectin, however the biological effect has yet to be determined (Wu *et al* 2003).

The thiazolidinediones (TZDs) are a class of drugs used to treat type 2 diabetes. They stimulate PPARγ mediated adipocyte differentiation and increase the number of small adipocytes (Okuno *et al* 1998). This is associated with reduced serum NEFAs and reduced TNFα expression, which increases insulin sensitivity in the liver and skeletal muscle (Quinn *et al* 2008). In addition, TZDs can also elevate levels of adiponectin. This is achieved in part via the generation of the small adipocytes which abundantly express and secrete adiponectin (Yamauchi *et al* 2001) and by the up-regulation of adiponectin via direct effects of TZDs on adiponectin gene transcription (Iwaki *et al* 2003). As discussed, above, activation of AMPK by adiponectin results in reduced gluconeogenesis in the liver and increased fatty acid oxidation and glucose uptake in muscle. Therefore, TZDs are able to activate AMPK indirectly via adiponectin. In addition, the TZD, rosiglitazone (Fryer *et al* 2002b) has been shown to increase the activity of AMPK after 30min in H-2K^b muscle cells, suggesting that TZDs can also directly activate AMPK.

The biguanides are another class of drugs used for the treatment of type 2 diabetes. This class of drug primarily acts to inhibit hepatic gluconeogenesis. Metformin has been shown to stimulate AMPK activity in cultured primary rat and human hepatocytes (Zhou *et al* 2001) and 3T3-L1 adipocytes (Huypens *et al* 2005). In addition another biguanide, phenformin, has been shown to activate AMPK in isolated rat adipocytes (Daval *et al* 2005).

The TZDs (Brunmair *et al* 2004) and metformin (El-Mir *et al* 2000) have also been reported to inhibit Complex 1 in the mitochondrial electron transport chain. In addition TZDs (Fryer *et al* 2002b, Saha *et al* 2004) have been reported to increase the intracellular AMP/ATP ratio, however this has not yet been demonstrated with metformin (Fryer *et al* 2002b, Hawley *et al* 2002).

Many studies of AMPK have utilised 5-aminoimidazole-4-carboxamide riboside (AICAR), which is a cell permeable molecule that is taken up readily by cells and phosphorylated by adenosine kinase (Bontemps *et al* 1986) to 5-aminoimidazole-4-carboxamide riboside monophosphate (ZMP), which functions as a cellular mimetic of AMP. Unfortunately ZMP is not a specific activator of AMPK in that it also mimics the effects of AMP on other molecules or processes. For example AICAR has been shown to suppress gluconeogenesis by inhibiting fructose-1, 6-bis phosphatase in isolated rat hepatocytes (Vincent *et al* 1991) and *in vivo* (Vincent *et al* 1996), and increase glycogenolysis by increasing glycogen phosphorylase activity in rat muscle preparations *in vitro* (Young *et al* 1996).

Recently, a novel AMPK activator, A769662, was discovered (Cool *et al* 2006). This new AMPK activator, directly activates native rat AMPK by mimicking both effects of AMP, *i.e.* allosteric activation and inhibition of dephosphorylation (Göransson *et al* 2007). In addition, A769662 has been shown to have no direct effect on the ability of the LKB1 or CaMKK to phosphorylate AMPK (Sanders *et al* 2007a). However, the mechanism of AMPK activation by A769662 is thought to be distinct from that of AMP. AMP is unable to activate AMPK containing a mutation in the γ subunit, whereas A769662 can (Sanders *et al* 2007a). Also, A769662 stimulated AMPK activity was shown to be inhibited by a mutation in the β1 AMPK subunit (Ser108 to Ala), an autophosphorylation site within the GBD, however the same mutation only partially reduces AMPK activation by AMP (Sanders *et al* 2007a). Sanders and co-workers have proposed a model of AMPK activation by A769662 (Fig 1.13). They suggest that binding of A769662 to AMPK stabilizes a conformation that is resistant to dephosphorylation of Thr172. This conformation requires

phosphorylation of Ser108 within β1, and phospho-Ser108 is thought to then interact with another region of the AMPK heterotrimer **(**Sanders *et al* 2007a**).** Scott and co-workers showed that A769662 appears to exclusively activate AMPK containing the β1 subunit isoform (Scott *et al* 2008). Furthermore the activation of AMPK by A769662 appears to involve the interaction of the β1 subunit GBD and residues from the γ subunit that are not involved in AMP binding (Scott *et al* 2008). Currently, the mechanism of AMPK activation by A769662 is not completely understood, although the mechanism does not appear to involve the binding of A769662 to the GBD or the nucleotide binding sites on the γ subunit (Scott *et al* 2008).

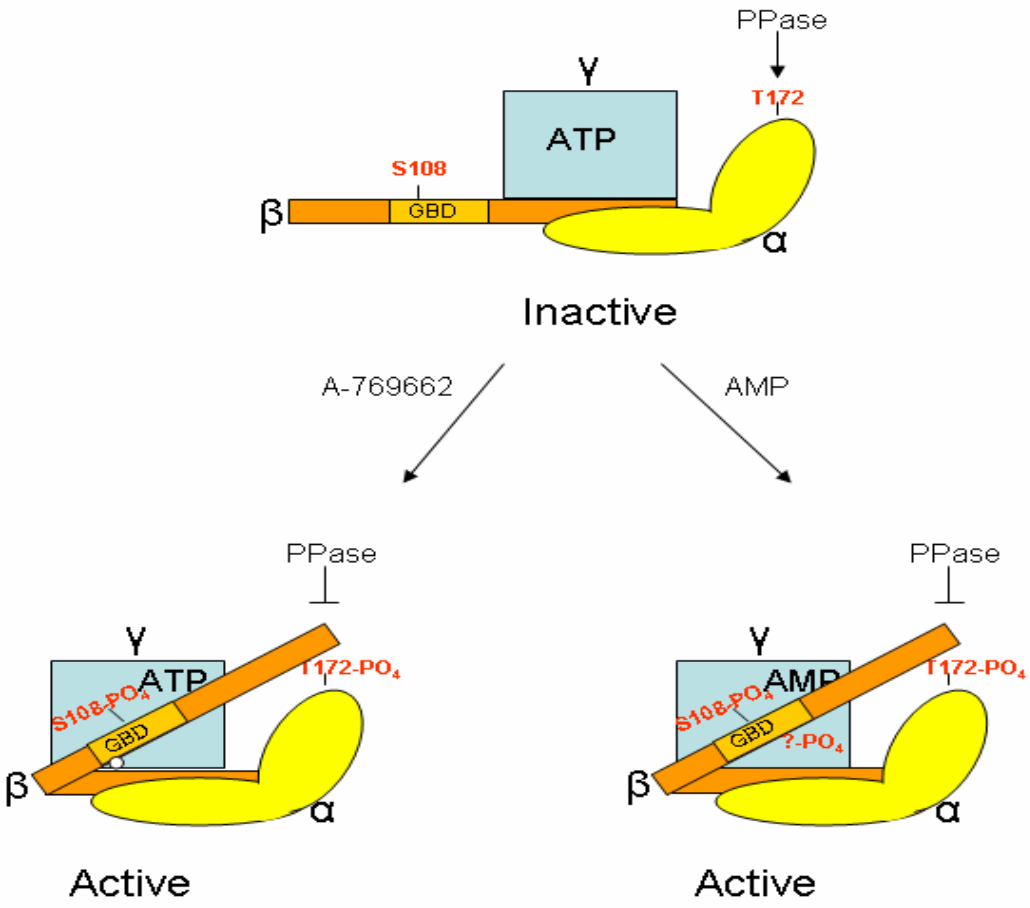

Figure 1-13: Model for activation of AMPK by A-769662 or AMP.
In the inactive conformation, ATP is bound to the γ subunit, and Thr172 within the catalytic subunit (α) is freely accessible to protein phosphatases (PPase). In this conformation, Thr172 is maintained predominantly in the unphosphorylated form. Binding of A-769662 (denoted by the small white circle) stabilises a conformation of AMPK that inhibits dephosphorylation of Thr172, depicted here as steric hindrance by the β subunit. This conformation requires phosphorylation of Ser108 in the GBD of the β subunit. The active conformation is also promoted when AMP displaces ATP from the γ subunit. In this case, however, phosphorylation of Ser108 alone is not sufficient to maintain the conformation, and additional phosphorylation sites (within either α or β) may be required to maintain the active form (shown here by ?-PO_4).

1.4.9 AMPK Targets

AMPK targets many different proteins and pathways in different tissues. The well-established downstream protein targets are summarized below (Fig. 1.14).

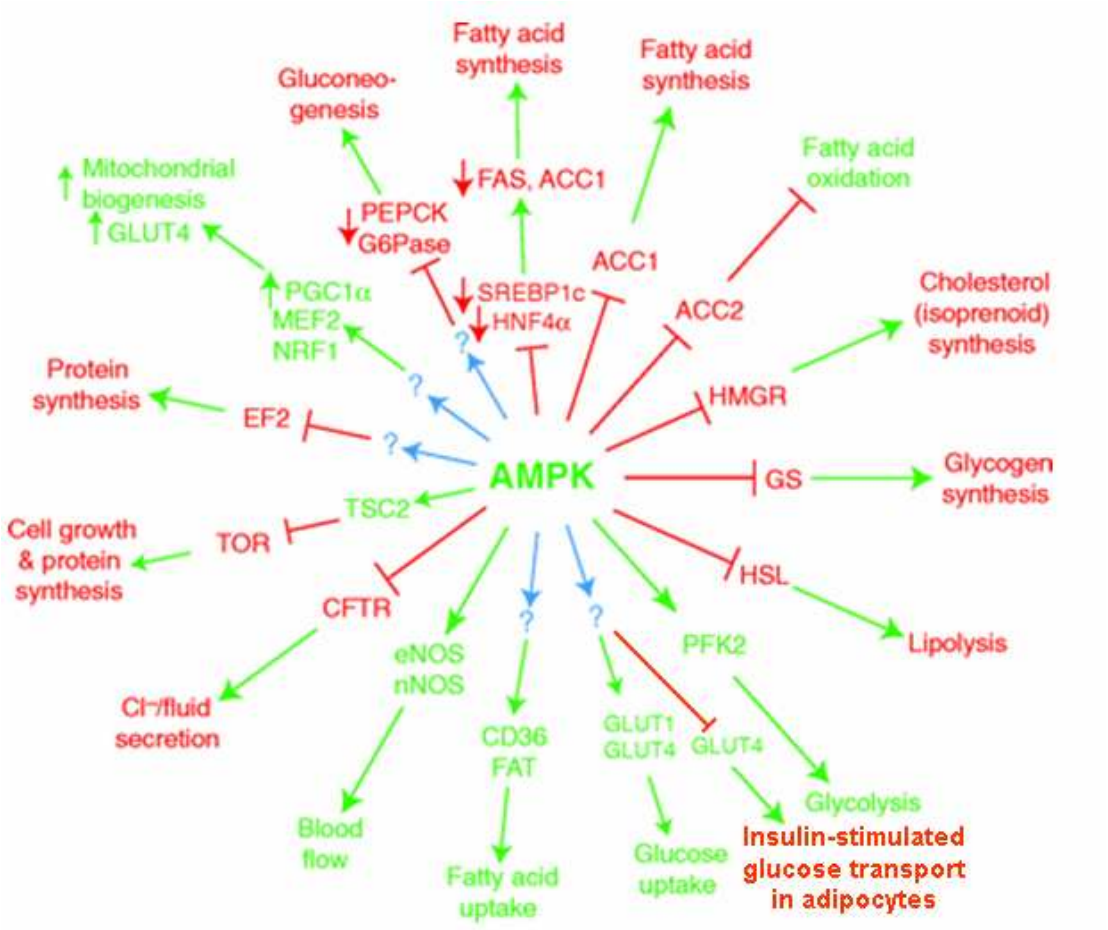

Figure 1-14: Targets for AMPK (adapted from Hardie 2004a).
Target proteins and processes activated by AMPK activation are shown in green, and those inhibited by AMPK activation are shown in red. Where the effect is caused by a change in gene expression, an upward-pointing green arrow next to the protein indicates an increase, whereas a downward-pointing red arrow indicates a decrease in expression. Abbreviations: ACC1/ACC2, 1 (α) and 2 (β) isoforms of acetyl-CoA carboxylase; CD36/FAT, CD36/fatty acid translocase; CFTR, cystic fibrosis transmembrane regulator; EF2, elongation factor-2; eNOS/nNOS. endothelial/neuronal isoforms of nitric oxide synthase; FAS, fatty acid synthase; G6Pase, glucose-6-phosphatase; GLUT1/4, glucose transporters; GS, glycogen synthase; HMGR, 3-hydroxy-3-methyl-CoA reductase; HSL, hormone-sensitive lipase; MEF2, myocyte-specific enhancer factor-2; NRF1, nuclear respiratory factor-1; PEPCK, phosphoenolpyruvate carboxykinase; PGC1α, peroxisome proliferator-activated receptor-γ co-activator-1α; TOR, mammalian target of rapamycin.

1.4.10 Role of AMPK in glucose homeostasis

AMPK plays an important role in the regulation of glycogen synthesis, glycolysis, gluconeogenesis and glucose transport.

It has been shown that AMPK can phosphorylate and inactivate the muscle isoform of GS (Carling and Hardie 1989) which is the key regulatory enzyme in glycogen synthesis.

Phospho-fructose-kinase-2 (PFK-2) stimulates the production of fructose-2, 6-bisphosphate which is a physiological activator of a key enzyme in glycolysis, 6-phosphofructo-1-kinase, also known as phospho-fructose-kinase-1 (PFK-1). In ischemic cardiac muscle, AMPK has been shown to stimulate glycolysis by phosphorylating and activating PFK-2 (Marsin *et al* 2000).

The AMPK activator AICAR has been shown to reduce the expression of the genes for the gluconeogenic enzymes PEPCK and G6Pase in hepatoma cells (Lochhead *et al* 2000).

As discussed, the IRS-1 is phosphorylated by the active insulin receptor and then acts as a binding site for PI3K leading to the uptake of glucose by cells. Interestingly AMPK has been shown to phosphorylate the IRS-1 protein in the muscle cell line C2C12 in response to the AMPK activator AICAR (Jakobsen *et al* 2001). Thus potentially in muscle AMPK may play a role in increasing insulin sensitivity, thus consequently lowering blood glucose levels.

In muscle AICAR, was shown to increase glucose uptake by promoting GLUT4 translocation to the cell surface (Kurth-Kraczek *et al* 1999, Russell *et al* 1999, Ojuka *et al* 2000) and GLUT4 gene transcription (Zheng *et al* 2001). In addition GLUT1 and GLUT4 transport to the plasma membrane was also shown to be increased in the presence of a constitutively active AMPK mutant in a skeletal muscle cell line (Fryer *et al* 2002a). Furthermore, AICAR has been shown to potentiate insulin-stimulated glucose transport in isolated rat muscle (Bergeron *et al* 1999, Hayashi *et al* 1998**).** In 3T3-L1 adipocytes AICAR was found to stimulate basal glucose transport (Salt *et al* 2000, Yamaguchi *et al* 2005) and inhibit insulin-stimulated glucose uptake and GLUT4 translocation to the plasma membrane (Salt *et al* 2000) which is in contrast to the effect of AICAR in muscle.

In contrast, another study reported that overexpression of a dominant negative mutant of AMPK in 3T3-L1 adipocytes treated with AICAR abolishes AMPK activation without affecting the increase in glucose uptake, suggesting that AICAR-induced glucose uptake by 3T3-L1 adipocytes is independent of AMPK activation (Sakoda *et al* 2002).

1.4.11 Role of AMPK in lipid metabolism

AMPK has been shown to phosphorylate and inhibit ACC activity (Park *et al* 2002**,** Kim *et al* 1989, Davies *et al* 1990*).* ACC is the rate-controlling step in the conversion of acetyl-CoA to malonyl CoA (Tong 2005). The product of ACC, malonyl-CoA, is both a precursor for the biosynthesis of fatty acids (Wakil *et al* 1983) and a potent inhibitor of fatty acid oxidation because it inhibits CPT1 (McGarry 1995) and, thereby, the transport of long-chain fatty acids into the mitochondrial matrix. In mammals there are two isoforms of ACC. ACC1 (265kDa) is expressed predominantly in lipogenic tissues such as liver, adipose and lactating mammary gland (Ha *et al* 1996, Abu-Elheiga *et al* 2005), and is reported to primarily regulate the biosynthesis of long-chain fatty acids (Ruderman *et al* 2003). In contrast ACC2 (280kDa) is predominantly expressed in cardiac and skeletal muscle (Ha *et al* 1996, Abu-Elheiga *et al* 2005), and is reported primarily to regulate fatty acid oxidation (Merrill *et al* 1997).

In adipocytes, ACC has been shown to be phosphorylated and inhibited by AICAR and overexpression of a constitutively active AMPK mutant (Sullivan *et al* 1994, Daval *et al* 2005). Sullivan and co-workers also showed that this inhibition of ACC was concomitant with a decrease in the lipogenic rate (Sullivan *et al* 1994). In addition, Gaidhu and co-workers also showed that AICAR stimulated AMPK activation inhibited lipogenesis in isolated rat adipocytes, (Gaidhu *et al* 2006**)**. It has been proposed that inhibition of lipogenesis would conserve ATP under conditions of cellular stress (Gaidhu *et al* 2006**)**.

In skeletal muscle and liver it has been established that activation of AMPK results in increased mitochondrial import and oxidation of fatty acids to provide ATP as a fuel (Ruderman *et al* 1999, Chien *et al* 2000). Some studies suggest that AMPK activation in adipose tissue may also drive fatty acid oxidation. Overexpression of un-coupling protein 1 (UCP-1) in white fat was reported to be associated with an increase in the AMP/ATP ratio, activation of AMPK and increased lipid oxidation (Matejkova *et al* 2004). In addition, in hyper-leptinized rats there is an increase in UCP-1 and UCP-2 expression, AMPK activity and inactivation of ACC (Orci *et al* 2004) in rat epididymal fat pads. However, in contrast

AICAR stimulated AMPK activation and subsequent inhibition of ACC in isolated rat adipocytes was shown to inhibit fatty acid oxidation (Gaidhu, *et al* 2006**)**. Gaidhu and co-workers proposed that suppression of fatty acid oxidation would spare fatty acids for exportation to other tissues where oxidation is crucial for energy production (Gaidhu, *et al* 2006**).** Interestingly, a recent study by Gaidhu and co-workers showed that prolonged AICAR-induced AMPK activation promotes energy dissipation by activating fatty acid oxidation (Gaidhu *et al* 2008).

As discussed, the β-adrenergic signalling pathway regulates triglyceride breakdown, acting via the accumulation of cAMP and subsequent PKA-dependent phosphorylation of HSL. The AMPK activator AICAR and was shown to antagonise isoproterenol induced lipolysis by phosphorylating HSL, which inhibits phosphorylation and activation of HSL by PKA in isolated adipocytes (Corton *et al* 1995, Sullivan et al 2004, Daval *et al* 2005, Dagon *et al* 2006). In addition, overexpression of a constitutively active AMPK in rat adipocytes was also shown to inhibit isoproterenol-induced lipolysis, whereas overexpression of a dominant negative form of AMPK had a converse effect (Daval *et al* 2005). Gauthier and co-workers also showed that AMPK is activated as a consequence of lipolysis in adipocytes (Gauthier *et al* 2008). When the rate at which fatty acids are being produced by lipolysis exceeds the rate at which they are being exported from the cell, they are re-esterified back into TG in an energy dependent manner. Thus, it has been proposed that AMPK activation and subsequent inhibition of lipolysis by AMPK would prevent futile cycling and depletion of ATP (Hardie *et al* 2007, Gauthier *et al* 2008).

Contrary to the above findings, Yin and co-workers have shown that adrenergic stimulation results in AMPK phosphorylation and activation which results in the stimulation of lipolysis in 3T3-L1 adipocytes (Yin *et al* 2003). It has been proposed that upon β-adrenergic stimulation, AMPK is phosphorylated and activated via an intermediary rise in cAMP, and this activation contributes to lipolysis, possibly by phosphorylating HSL at Ser565 and promoting HSL translocation to the lipid droplet (Yin *et al* 2003). Yin and co-workers also showed that overexpression of a dominant negative form of AMPK inhibits isoproterenol-induced lipolysis suggesting, rather, a lipolytic action of AMPK activation (Yin *et al* 2003). However, AMPK activity was not measured in these conditions and thus final conclusions from these experiments are difficult to draw.

It has been reported that the duration of AMPK stimulation may be important with respect to lipolysis, as Gaidhu and co-workers found that lipolysis was first suppressed in

adipocytes, but then increased both *in vitro* and *in vivo* with prolonged AICAR treatment (Gaidhu *et al* 2008).

Other potential targets of AMPK include fatty acid translocase (FAT), which plays an important role in long-chain fatty acid uptake in adipocytes. FAT knock out mice showed increased serum fasting levels of NEFAs and showed reduced uptake of oleate in isolated adipocytes (Febbraio *et al* 1999). Interestingly, signalling through AMPK has been proposed to mediate FAT translocation to the membrane in rat cardiac myocytes (Luiken *et al* 2003). Finally, cholesterol and isoprenoid biosynthesis, for which HMG-CoA reductase (HMGR) catalyses the rate limiting step is also influenced by AMPK activity. Active AMPK can phosphorylate and inactivate HMGR resulting in reduced cholesterol and isoprenoid synthesis (Beg *et al* 1978).

1.4.12 Role of AMPK and adipocyte differentiation

There is some evidence to suggest that AMPK activation can inhibit preadipocyte differentiation. Studies investigating the role of AMPK in adipogenesis have reported that AMPK activation by AICAR inhibits differentiation of 3T3-L1 preadipocytes into adipocytes and blocks the expression of the early adipogenic transcription factors PPARγ, CAAT/enhancer-binding protein alpha (C/EBPα), CAAT/enhancer-binding protein beta (C/EBPβ) and the late adipogenic markers such as FAS and ACC (Habinowski and Witters 2001, Giri *et al* 2006, Tong *et al* 2008). Thus it has been suggested by these studies that AMPK activation inhibits differentiation of preadipocytes by turning off anabolic adipose-specific gene expression. However, intra-peritoneal administration of AICAR to a mouse diet induced obesity model, blocked body weight gain and reduced total epididymal fat in these mice. The reduction in adipose tissue content was due to reduced lipid accumulation in the pre-existing adipocytes and by activating expression of peroxisome-proliferator-activated receptor (PPAR)γ co-activator 1a (PGC1a) without reducing adipocyte-specific transcription factors such as C/EBPα and PPARγ in the diet induced obesity model mice (Giri *et al* 2006).

Furthermore, other studies concluded that AMPKα2 does not regulate adipocyte differentiation *in vivo*. AMPKα2 knockout mice were subjected to a high-fat diet to examine the effect of AMPK on adipose tissue formation. These mice were found to exhibit higher body weight, with a specific increase in adipose tissue compared to wild type mice. However the expression of genes that control adipogenesis, including C/EBPα

and PPARγ were found not to be changed in the AMPKα2 knockout mice suggesting that the increased adipose tissue mass is not due to an enhancement of preadipocyte differentiation into adipocytes and therefore that AMPKα2 does not regulate adipocyte differentiation *in vivo*. The augmentation in adipose tissue mass in AMPKα2 knockout mice is thought to be due to the enlargement of pre-existing adipocytes, with an increase in triglyceride accumulation (Villena *et al* 2004).

Thus it is currently not clear whether AMPK has a physiological regulatory function in adipocyte differentiation.

1.4.13 Role of AMPK and adipokine secretion

The biguanide metformin is used to treat type 2 diabetic patients. In these patients metformin lowers blood glucose levels by reducing hepatic glucose production and facilitating glucose utilization in skeletal muscle (Bailey *et al* 1996, Galuska *et al* 1991, Hundal *et al* 1992, Hundal *et al* 2000). These effects appear to be mediated through inhibition of complex I in the mitochondrial respiratory chain (Owen *et al* 2000, El-Mir *et al* 2000) and / or stimulation of AMPK (Zhou *et al* 2001). In 3T3-L1 adipocytes, metformin was shown to activate AMPK and suppress adiponectin expression and secretion (Huypens *et al* 2005). Since treatment of 3T3-L1 adipocytes with AICAR (Huypens *et al* 2005) also caused a decrease in adiponectin expression and secretion it has been proposed that metformin induced suppression involves AMPK activation. However, as metformin is a metabolic poison and not a specific AMPK activator, the role of AMPK is uncertain. In addition, there has been no observed change in adiponectin serum concentration or adiponectin mRNA concentration in adipose tissue of type 2 diabetic patients treated with metformin (Phillips *et al* 2003, Tiikkainen *et al* 2004). Conversely, AICAR has been shown to increase the expression of adiponectin in human adipose tissue (Sell *et al* 2006, Lihn *et al* 2004). AICAR has also been shown to inhibit the expression and secretion of the pro-inflammatory cytokines TNFα and IL-6 in human adipose tissue (Lihn *et al* 2004, Sell *et al* 2006). Given that adiponectin has also been shown to decrease the secretion of pro-inflammatory cytokines (Sell *et al* 2006), it has been proposed that AICAR may mediate its effects on the pro-inflammatory cytokines via adiponectin. Thus, the inhibition of secretion of these pro-inflammatory cytokines by AMPK could be beneficial, as inflammation contributes to disorders such as cardiovascular disease and insulin resistance, which are associated with obesity.

1.4.14 Role of AMPK in mitochondrial biogenesis

Studies have shown that in rodent muscle AMPK activation correlates with increased DNA binding by the transcription factors nuclear respiratory factor-1 (NRF-1) (Bergeron *et al* 2001) and myocyte enhancer factor-2 (MEF-2) (Zheng *et al* 2001) which results in increased mitochondrial biogenesis. In addition AMPK activation was also shown to correlate with the up-regulation of the expression of the co-activator PGC1α (Terada *et al* 2002) which may also be involved in the increased expression of mitochondrial genes in muscle (Zong *et al* 2002).

1.4.15 Role of AMPK in protein synthesis

AMPK has been shown to inhibit protein synthesis and cell growth in cultured cells. Translational elongation is blocked through the activation of eukaryotic elongation factor-2 (eEF-2) kinase, which phosphorylates and inhibits eEF2, allowing protein translocation to pause until ATP levels are restored. Hypoxia inhibits protein synthesis in hepatocytes and is mediated by AMPK-dependent activation of eEF2 kinase and subsequent phosphorylation of eEF2 (Horman *et al* 2002).

The target of rapamycin (TOR) pathway is activated by growth factors and amino acids and is a major positive stimulus for protein synthesis, cell growth and cell size (Fig. 1.15) (Schmelzle and Hall 2000). Tuberous sclerosis complex 1/2 (TSC1/TSC2) form a stable complex in the cells, with mutations in either leading to the human disease tuberous sclerosis (Young and Povey 1998). Recent genetic studies in *Drosophilia* demonstrated that TSC1/TSC2 complex acts to negatively regulate cell growth and cell size and have shown that it acts downstream of PKB/Akt in the insulin-signalling pathway

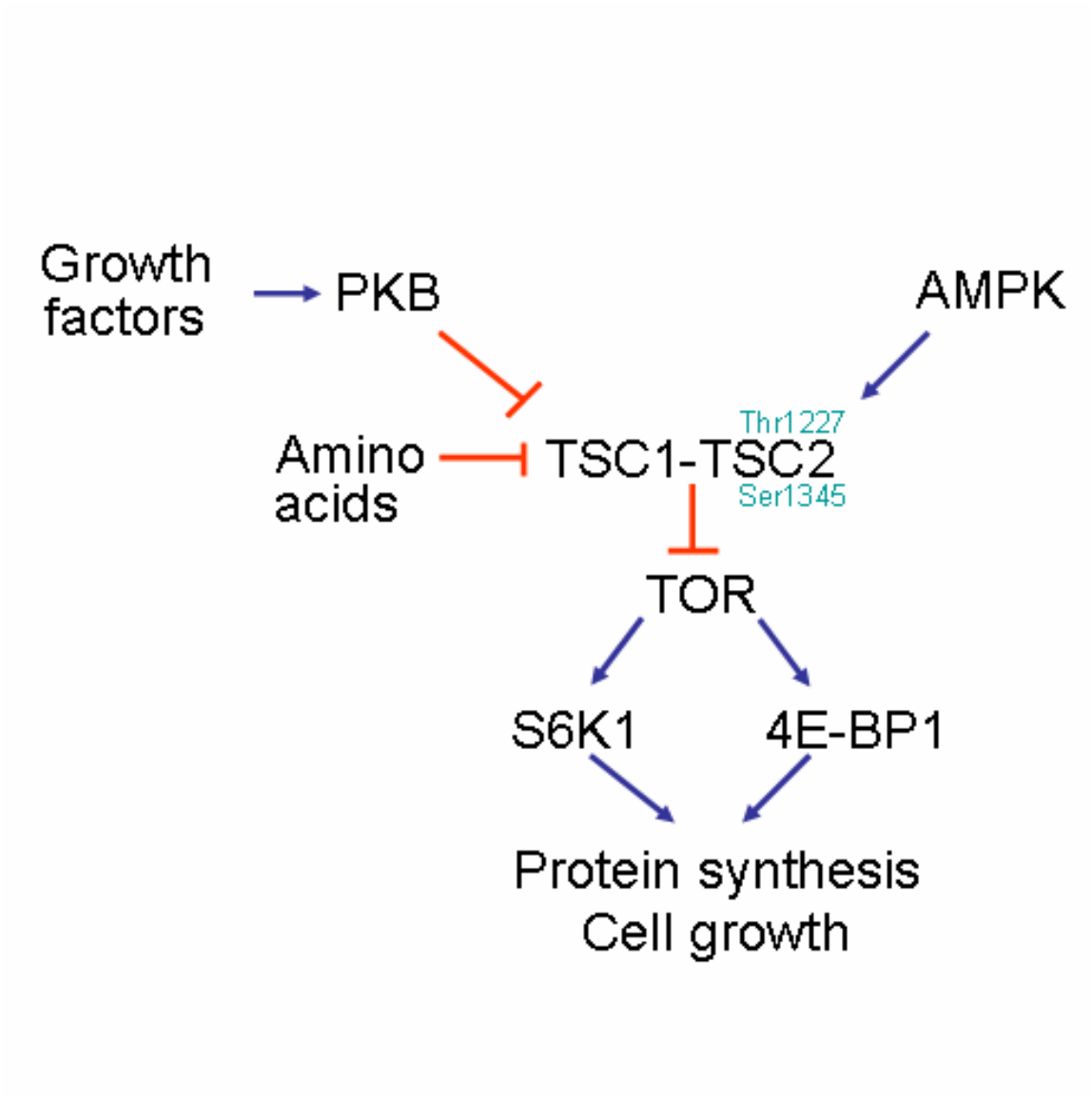

Figure 1-15: Regulation of protein synthesis and cell growth by AMPK and PKB/Akt by the mTOR pathway.
AMPK = AMP-activated protein kinase, PKB = protein kinase B, TSC1/2 = Tuberous sclerosis complex 1/2, TOR = target of rapamycin, S6K1 = ribosomal protein S6 kinase, 4E-BP1 = elongation factor-4E binding protein 1.

and upstream of mammalian TOR (Gao and Pan 2001, Gao *et al* 2002, Tapon *et al* 2001). AMPK phosphorylates TSC2 at two sites, Thr1227 and Ser1345. Activation of TSC2 by AMPK-dependent phosphorylation results in activation of the TSC1/TSC2 complex and subsequent inhibition of the TOR pathway, thus inhibiting protein synthesis and cell growth through ribosomal protein S6 kinase (S6K1) and elongation factor-4E binding protein 1 (4E-BP1) (Inoki *et al* 2003).

1.5 Aims

The overall aim of this study was to characterise the role of AMPK in adipocytes. Although AMPK activation has been previously reported in adipose tissue and cultured adipocytes, a thorough investigation of the expression of components of the AMPK cascade, kinetics/mechanism of AMPK stimulation and role of AMPK in adipocyte insulin action has yet to be undertaken.

The initial aim of this study was to investigate the expression of the upstream AMPK kinases; LKB1 and CaMKKα/β, and the downstream AMPK substrates ACC1/2 in 3T3-L1 adipocytes. Since AMPK has been shown to play a role in the regulation of adipogenesis and 3T3-L1 cells are widely used as a model system to study the differentiation of preadipocytes to adipocytes, the expression of AMPK subunit isoforms and the relative contribution of the catalytic AMPKα subunits to total AMPK activity throughout development from fibroblasts to adipocytes in 3T3-L1 cells was also investigated.

The parameters of AMPK activation in 3T3-L1 in response to various stimuli; AICAR, arsenite, azide, metformin, rosiglitazone, leptin, sorbitol, hydrogen peroxide, A23187, isoproterenol and A769662 were then determined. In addition, the mechanism by which each activator stimulates AMPK activity in 3T3-L1 adipocyte was investigated using the CaMKK inhibitor STO-609 and high performance liquid chromatography (HPLC) to detect changes in cellular energy levels.

Acute AICAR treatment has previously been shown in our laboratory to modestly stimulate basal glucose transport and inhibit insulin stimulated glucose transport in 3T3-L1 adipocytes (Salt *et al* 2000), which is in contrast to the effect of AICAR in muscle Bergeron *et al* 1999) . In order to further characterise the role of AMPK in the inhibition of insulin-stimulated glucose transport the acute effect of various other AMPK activators on basal and insulin stimulated glucose uptake was assessed using 2-[^{3}H] deoxy-D-glucose. The effect of AMPK inhibition and knockdown, using Compound C and Ad.α1DN respectively, on AICAR stimulated basal glucose transport and inhibition of insulin-stimulated glucose transport was also assessed to determine whether the effects of AICAR on glucose transport are dependent on AMPK activation.

Previous work in our laboratory also showed that AICAR did not alter IRS-1 phosphorylation, PI3K association with IRS-1 or PKB activity in 3T3-L1 adipocytes (Salt

et al 2000). During the course of this project AS160 and TBC1D1 have emerged as Rab GAPs (Thong *et al* 2007, Roach *et al* 2007) involved in the regulation of glucose transport. Therefore another aim of this study was to investigate the mechanism by which AICAR inhibits insulin-stimulated glucose transport in adipocytes, with particular attention being paid to the effect of AICAR on basal and insulin-stimulated AS160/TBC1D1 phosphorylation at phospho-Akt/PKB (PAS) sites.

Finally the effect of sustained AMPK activation on glucose transport and insulin signaling in 3T3-L1 adipocytes was also to be determined. In addition, the effects of sustained AMPK activation on insulin signaling in human adipose tissue was investigated.

Chapter 2 – Materials and methods

2.1 Materials

2.1.1 List of materials and suppliers

American Type Culture Collection, Manassas, Virginia, USA

3T3-L1 preadipocytes

AXXORA (UK) Ltd, Bingham, Nottingham, UK

Rosiglitazone

Gliclazide

BDH Laboratory Supplies, Poole, UK

Calcium chloride ($CaCl_2$)

Coomassie Brilliant Blue G-250

Dipotassium hydrogen phosphate (K_2HPO_4)

Hydrogen peroxide (H_2O_2)

Magnesium chloride ($MgCl_2$)

Magnesium sulphate ($MgSO_4$)

Potassium chloride (KCl)

Sodium chloride (NaCl)

Tetrasodium pyrophosphate ($Na_4P_2O_7$)

Cambridge Bioscience Ltd, Cambridge, UK

Quick Titer^{TM} Adenovirus Titer Immunoassay kit

Dundee University, Dundee, UK

A-769662 (AMPK activator), was a generous gift from Prof. D.G. Hardie.

Eastman Kodak Company, Rochester, New York, USA

Kodak Medical X-ray film

Fisher Scientific UK Ltd, Loughborough, Leicestershire, UK

Corning tissue culture T75/ T150 flasks

D-Glucose

Ethanol

Glycine

HEPES (N-2-hydroxyethylpiperazine-N' 2-ethane sulphonic acid**)**

Potassium dihyrogen phosphate (KH_2PO_4)

Tris base (tris(hydroxymethyl)aminoethane)

GE Healthcare, Little Chalfont, Buckinghamshire, UK

Protein A-sepharose beads

Protein G-sepharose beads

Hopkin and Williams, Chadwell Health, Essex, UK

Sodium azide (NaN_3)

Inverclyde Biologicals, Bellshill, Lanarkshire, UK

Nitrocellulose transfer membrane, 0.45 μm pore size

Invitrogen (GIBCO Life Technologies Ltd), Paisley, UK

Dulbecco's modified Eagles media (DMEM)

Foetal calf serum (FCS) (USA origin)

Newborn calf serum (NCS) (EU origin)

Penicillin/streptomycin

L-glutamine

Trypsin

Premier International Foods, Cheshire, UK

Dried skimmed milk

Melford Laboratoried Ltd, Chelsworth, Ipswich, Suffolk, UK

Dithiothreitol (DTT)

Merck Chemicals Ltd, Nottingham, UK

Compound C

A23187

National Diagnostics (UK) Ltd, Hessle, East Riding of Yorkshire, UK

Ecosint A

New England Biolabs, Hertfordshire, UK

Prestained protein markers (broad range 6-175kDa)

Novo-Nordisk, Bagsvaerd, Denmark

Porcine insulin

Pepceuticals, Leicester, UK

SAMS peptide (HMRSAMSGLHLVKRR)

PeproTech, London, UK

Leptin

Perkin Elmer, Beaconsfield, Buckinghamshire, UK

2-[^{3}H]-deoxy-D-glucose

[γ-^{32}P] ATP

Pierce, Perbio Science, UK Ltd, Tattenhall, Cheshire, UK

10,000 MWCO slide-a-lyzer

Severn Biotech Ltd, Kidderminster, Hereford, Worcester, UK

Acrylamide:Bisacrylamide (37.5:1; 30% (w/v) Acrylamide)

Sigma-Aldrich (Steinheim, Germany; Seelze, Germany; St Louis, MO, USA)

5-Amino-2,3-dihydro-1,4-phthalazinedione (luminol)

Adenosine 5'-diphosphate (ADP)

Adenosine 5'-monophosphate (AMP)

Adenosine 5'-triphosphate (ATP)

Ammonium peroxydisulphate (APS)

Bovine serum albumin (BSA)

Benzamidine

p-Coumaric acid

Cytochalasin B

Dexamethasone

Dimethyl sulphoxide (DMSO)

Disodium hydrogen phosphate (Na_2HPO_4)

D-mannitol

Ethylenediamine tetraacetic acid (EDTA)

Ethylene glycol-bis (β-amino-ethylether)-N,N,N',N'-tetraacetic acid (EGTA)

Glycerol

Isobutylxanthine (IBMX)

Metformin

Methanol

ProteoPrep Blue Albumin and IgG Depletion Kit

Sodium flouride (NaF)

Sodium hydrogen carbonate ($NaHCO_3$)

Sodium dihydrogen phosphate (NaH_2PO_4)

Sodium orthovanadate (Na_4VO_3)

Soybean trypsin inhibitor (SBTI)

Sodium dodecyl sulphate (SDS)

N,N,N′,N′-Tetramethylethylenediamine (TEMED)

Triethylamine (TEA)

Triton X-100

Tween-20

Tocris Cookson Ltd, Fouth Way, Avonmouth, UK

STO-609

Toronto Research Chemicals Inc, Ontario, Canada

AICAR (5-aminoimidazole-4-carboxamide-1-beta-4-ribofuranoside)

Varian, California, USA

Chrom Spher C18 octadecylsilane (5 µm)

VWR, Lutterworth, Leicestershire, UK

Falcon tissue culture 10 cm dishes and 6/12 well plates

Whatman P81 phosphocellulose paper

2.1.2 List of specialist equipment and suppliers

Beckman Coulter™ High Wycombe, UK

Optima™ XL-80K ultracentrifuge

SW40 rotor

Multi-Purpose scintillation counter LS 6500

Bio-Rad Laboratories, Hemel Hempstead, UK

Protein gel casting and Western blotting equipment (Mini Protean III)

Fisher Scientific, Loughborough, UK

Polycarbonate freezing container

Optika Microscopes, Ponteranica, Italy

XDS-1B light microscope

WPA, Cambridge, UK

S2000 spectrophotometer

Varian Limited, Oxford, UK

Varian ProStar 410 high performance liquid chromatography (HPLC) AutoSampler

Stainless-steel column (250 x 4.6 mm I.D) packed with Chrom Spher C18 octadecylsilane (ODS)

2.1.3 List of antibodies and conditions of use

2.1.3.1 Primary antibodies for Western blotting

Table 2-1: Primary antibodies used for western blotting
n/a: not applicable. All antibodies were incubated overnight at 4°C.

Epitope	Clonality	Host species	Dilution	Diluent (w/v in TBST)	Source
14-3-3	polyclonal	rabbit	1:1000	5% milk	Abcam, Cambridge, UK. (#9093)
ACC1 N-term (cDEP)	polyclonal	sheep	1:1000	5% milk	A generous gift from Prof. D.G. Hardie, University of Dundee, Dundee, UK. CDEPSPLAKTLELNQ (C + residues 2-15 of rat ACC coupled to KLH.
ACC2 (146)	polyclonal	sheep	1:1000	5% milk	A generous gift from Prof. D.G. Hardie, University of Dundee, Dundee, UK. CEDKKQAPIKRQLMT (C + residues 146-159 of rat ACC2 coupled to KLH.
ACC Ser79	polyclonal	rabbit	1:1000	5% BSA	New England Biolabs, Hertfordshire, UK. (#3661)

AMPKα1	polyclonal	sheep	1:1000	5% milk	A generous gift from Prof. D.G. Hardie, University of Dundee, Dundee, UK (Woods *et al* 1996b).
AMPKα2	polyclonal	sheep	1:1000	5% milk	A generous gift from Prof. D.G. Hardie, University of Dundee, Dundee, UK (Woods *et al* 1996b).
AMPK Pan α1/ α2	polyclonal	sheep	1:500	5% milk	A generous gift from Prof. D.G. Hardie, University of Dundee, Dundee, UK. CDPMKRAT(phospho)IKDIRE (C + residues 252-264 of rat alpha-1).
AMPK T172	polyclonal	rabbit	1:1000	5% BSA	New England Biolabs, Hertfordshire, UK. (#2531)
AMPKβ1	polyclonal	sheep	1:1000	5% milk	A generous gift from Prof. D.G. Hardie, University of Dundee, Dundee, UK (Woods *et al* 1996a).
AMPKβ2	polyclonal	sheep	1:1000	5% milk	A generous gift from Prof. D.G. Hardie, University of Dundee,

					Dundee, UK (Woods *et al* 1996a).
AMPKγ1	polyclonal	sheep	1:1000	5% milk	A generous gift from Prof. D.G. Hardie, University of Dundee, Dundee, UK (Cheung *et al* 2000).
AMPKγ2	polyclonal	sheep	1:1000	5% milk	A generous gift from Prof. D.G. Hardie, University of Dundee, Dundee, UK DLEGSGKHSSRKVD (residues 51-63 human gamma 2).
AMPKγ3	polyclonal	sheep	1:1000	5% milk	A generous gift from Prof. D.G. Hardie, University of Dundee, Dundee, UK LSPAGIDPSGPEKI (residues 479-492 human gamma 3).
AS160	polyclonal	rabbit	1:1000	5% BSA	New England Biolabs, Hertfordshire, UK. (#2447)
CaMKKα	monoclonal clone: F-2	mouse	1:200	5% milk	Santa Cruz, Biotechnology, California. (#17827)

CaMKKβ	polyclonal	goat	1:200	5% milk	Santa Cruz, Biotechnology, California. (#9629)
FAS	monoclonal clone: 23	mouse	1:250	5% milk	BD transduction laboratories, Oxford science park, Oxford, UK. (#610962)
GAPDH	monoclonal clone: 6C5	mouse	1:40000	5% milk	Ambion, Ermine Business Park, Cambridgeshire, UK. (#4300)
IRS1	polyclonal	rabbit	1:1000	5% BSA	New England Biolabs, Hertfordshire, UK. (#2382)
LKB1	polyclonal	sheep	1:500	5% milk	A generous gift from Prof. D.G. Hardie, University of Dundee, Dundee, UK. LKB1 antibody was raised against the whole protein in sheep and was purified using protein G.
myc	monoclonal clone: 9E10	mouse	1:1000	5% milk	Sigma, St Louis, MO, USA. (#5546)

PAS	monoclonal clone:110B	rabbit	1:1000	5% BSA	New England Biolabs, Hertfordshire, UK. (#9614)
PKB	ploYclonal	rabbit	1:1000	5% milk	New England Biolabs, Hertfordshire, UK. (#9272)
PKB Ser473	polyclonal	rabbit	1:1000	5% BSA	New England Biolabs, Hertfordshire, UK. (#9271)
TBC1D1	polyclonal	sheep	1:1000	5% BSA	A generous gift from Prof. C. Mackintosh University of Dundee, Dundee, UK, (Chen *et al* 2008).

2.1.3.2 Secondary detection agents for Western blotting

Table 2-2: Secondary detection agents for western blotting

Linked molecule	Epitope	Host species	Dilution	Diluent (w/v in TBST)	Source
HRP	mouse IgG	sheep	1:1000	5% milk or BSA	GE Healthcare, Little Chalfont, Buckinghamshire, UK. (#NA931)
HRP	rabbit IgG	donkey	1:1000	5% milk or BSA	GE Healthcare, Little Chalfont, Buckinghamshire,

					UK. (#NA934)
HRP	streptococcus sp. Protein G	n/a	1:1000	5% milk or BSA	Sigma, St Louis, MO, USA. (#P8170)

2.1.4 Standard solutions

Unless stated otherwise, all buffers and reagents were made up with distilled water.

Bradford's reagent

35.0 mg/L coomassie brilliant blue

5.0% (v/v) ethanol

5.1% (v/v) orthophosphoric acid

Bradford's reagent was filtered and stored in the dark.

Coomassie stain

0.05% (w/v) coomassie brilliant blue

50% (v/v) methanol

10% (v/v) acetic acid

Coomassie stain was filtered.

Coomassie de-stain

10% (v/v) methanol

10% (v/v) acetic acid

Enhanced chemiluminescence (ECL) detection reagents

Solution 1

0.1 mM Tris-HCl, pH 8.5

450 mg/L luminol in 2% (v/v) DMSO

130 mg/L coumaric acid in 1% (v/v) DMSO

Solution 2

0.1 mM Tris-HCl , pH 8.5

0.02% (v/v) H_2O_2

HEPES Brij-35 buffer

50 mM HEPES, pH 7.4 at 4˚C

1 mM DTT

0.02% (v/v) Brij-35

Immunoprecipitation (IP) buffer

50 mM Tris-HCl, pH 7.4 at 4˚C

150 mM NaCl

50 mM NaF

5 mM $Na_4P_2O_7$

1 mM EDTA

1 mM EGTA

1% (v/v) Triton X-100
1% (v/v) glycerol
1 mM DTT
0.1 mM benzamidine
0.1 mM PMSF
5 µg/ml SBT1
1 mM Na_3VO_4
} added on day of use

Krebs-Ringer HEPES (KRH) buffer

119.0 mM NaCl

20.0 mM HEPES-NaOH, pH 7.4

5.0 mM $NaHCO_3$

10.0 mM glucose

4.8 mM KCl

2.5 mM $CaCl_2$

1.2 mM $MgSO_4$

1.2 mM NaH_2PO_4

0.1 mM L-Arginine

Krebs-Ringer phosphate (KRP) buffer

130 mM NaCl

4.8 mM KCl

5 mM NaH_2PO4, pH 7.4

1.25 mM $MgSO_4$

1.25 mM $CaCl_2$

Lysis buffer

50 mM Tris-HCl, pH 7.4 (at 4°C)

50 mM NaF

1 mM $Na_4P_2O_7$

1 mM EDTA

1 mM EGTA

1% (v/v) Triton X-100

250 mM mannitol

1 mM DTT

1 mM Na_3VO_4

0.1 mM benzamidine

0.1 mM PMSF

5 μg/ml SBTI

} added on day of use

Phosphate-buffered saline (PBS) (pH 7.2)

85 mM NaCl

1.7 mM KCl

5 mM Na_2HPO_4

0.9 mM KH_2PO_4

Ponceau S Stain

0.2% (w/v) ponceau S

1% (v/v) acetic acid

SDS-polyacrylamide gel electrophoresis (SDS-PAGE) Running buffer

190 mM glycine

62 mM Tris base

0.1% (w/v) SDS

4 X SDS-PAGE sample buffer

200 mM Tris-HCl, pH 6.8

8% (w/v) SDS

40% (v/v) glycerol

0.4% (w/v) bromophenol blue

200 mM DTT

Transfer buffer

25 mM Tris base

192 mM glycine

20% (v/v) ethanol

Tris buffered saline (TBS)

20 mM Tris-HCl, pH 7.5

137 mM NaCl

Tris buffered saline + Tween 20 (TBST)

20 mM Tris-HCl, pH 7.5

137 mM NaCl

0.1% (v/v) tween 20

2.2 Methods

2.2.1 Cell Culture Procedures

2.2.1.1 Cell culture plastic ware

3T3-L1 cells were cultured in Corning T75 flasks and Falcon 10 cm dishes, 6 well plates and 12 well plates.

Human embryonic kidney (HEK) 293 cells, a generous gift from Dr. S. Yarwood, University of Glasgow, were cultured in Corning T75 flasks, T150 flasks, and 24 well plates.

2.2.1.2 Cell culture growth media for 3T3-L1 preadipocytes

Preadipocytes were maintained as fibroblasts (passage 2-12) in Dulbecco's modified Eagle's medium (DMEM) supplemented with 10% (v/v) newborn calf serum (NCS) and 200 IU penicillin and 200 μg streptomycin/500ml. Cells were cultured at 37˚C in a humidified atmosphere of 10% (v/v) CO_2 in media replaced every 48 hr.

2.2.1.3 Cell culture growth media for HEK 293 cells

HEK 293 cells were maintained in DMEM supplemented with 5% (v/v) foetal calf serum (FCS), 2 mM glutamine and 200 IU penicillin and 200 μg streptomycin/500ml. Cells were cultured at 37˚C in a humidified atmosphere of 5% (v/v) CO_2 in media replaced every 48 hr.

2.2.1.4 Preparation of 3T3-L1 fibroblast differentiation medium

Differentiation was initiated using DMEM medium containing 10% (v/v) FCS, 0.5 mM methyl isobutylxanthine (IBMX), 0.25 μM dexamethasone, and porcine insulin (1 μg/ml), prepared as outlined below.

A 2.5 mM sterile solution of dexamethasone in ethanol was diluted 1:20 with 10% (v/v) FCS/DMEM medium immediately prior to use yielding a 500X stock solution. A 500X concentrated sterile solution of IBMX was also prepared by dissolving 110 mg IBMX in 2

ml of 1 M KOH. Insulin (1 mg/ml) was then prepared in 0.01 M HCl. Sterile solutions of dexamethazone, IBMX and insulin were achieved by passing through a 0.22 µm filter.

3T3-L1 differentiation medium was prepared by diluting both the dexamethasone and IBMX solutions to a 1X concentration in 10% (v/v) FCS/DMEM and then adding insulin to a final concentration of 1 µg/ml.

2.2.1.5 3T3-L1 fibroblast differentiation protocol

To differentiate the 3T3-L1 fibroblast cells into adipocytes, the cells were grown to confluency in 10% (v/v) NCS/DMEM. At 48 hr post confluence, cell medium was aspirated and replaced with differentiation medium consisting of 10% (v/v) FCS/DMEM containing 0.25 µM dexamethasone, 0.5 mM IBMX and insulin (1 µg/ml). After a further two days this medium was aspirated and replaced with 10% (v/v) FCS/DMEM containing 1 µg/ml insulin. The cells were incubated in this medium for two days, and then the medium was aspirated and replaced with 10% (v/v) FCS/DMEM. At 8-12 days post-induction of differentiation, cells were used for experimentation.

2.2.1.6 Passaging of 3T3-L1 fibroblasts

When cells in T75 flasks were 70-80% confluent, DMEM growth medium was aspirated and 5 ml of sterile trypsin (0.05% (v/v) in diaminoethanetetra-acetic acid, disodium salt **(**EDTA)) was added to each T75 flask. Flasks were then incubated at 37˚C until the cells began to lift off. Trypsin was titurated over the surface of the flask until all of the cells were detached. An appropriate amount of DMEM growth medium was then added to the 5 ml of trypsin and used to seed 10 cm cell culture plates, 12 well plates, 6 well plates and T75 flasks.

2.2.1.7 Passaging of HEK 293cells

When cells in T75 flasks were 70-80% confluent, DMEM growth medium was aspirated and 5 ml of sterile trypsin (0.05% (v/v) in EDTA) was added to each T75 flask. Flasks were then incubated at 37˚C until the cells began to lift off. Trypsin was titurated over the surface of the flask until all of the cells were detached. 10-15 ml of DMEM was added to neutralize the trypsin. The trypsinised cells were then transferred to a 50 ml falcon tube. Cells were centrifuged at 2000 x g for 5 min. The media was then aspirated and the cells

re-suspended in the appropriate amount of media to seed T75, T150 flasks and 12 well plates.

2.2.1.8 Resurrection of frozen 3T3-L1 cell stocks from liquid nitrogen

Cell cryogenic vials were removed from liquid nitrogen and incubated in a water bath at 37°C until the cells were thawed. Vials were then transferred to a cell culture sterile flow hood where the following procedure was performed.

The cells were transferred to a T75 flask containing 15 ml of 10% (v/v) NCS/DMEM. 3T3-L1 cells were then maintained in an incubator at 37°C in an atmosphere of 10% CO_2. The following day the medium was aspirated to remove dead cell debris and was replaced with fresh medium.

2.2.1.9 Resurrection of frozen HEK 293 cell stocks from liquid nitrogen

Cell cryogenic vials were removed from liquid nitrogen and incubated in a water bath at 37°C until the cells were thawed. Vials were then transferred to a cell culture sterile flow hood where the following procedure was performed.

The cells were transferred to a T75 flask containing 15 ml of 5% (v/v) FCS/DMEM. HEK 293 cells were then maintained in an incubator at 37°C in an atmosphere of 5% CO_2. The following day the medium was aspirated to remove dead cell debris and was replaced with fresh medium.

2.2.1.10 Preparation of 3T3-L1 murine fibroblast cells for freezing

DMEM medium was aspirated from T75 flasks and 5 ml of trypsin (0.05% (v/v) in EDTA) was added to each flask. Flasks were then incubated at 37˚C for 3-5 min until the cells were just beginning to lift off the flask. The trypsin solution was gently titurated over the surface of the flask until all of the cells were detached. 5 ml of 10% (v/v) NCS/DMEM was added to each flask. The cell suspension was then transferred to a 15 ml universal tube. The trypsin/cell mix was then centrifuged at 2000 x g for 3 min and the trypsin supernatant aspirated. The cell pellet was then re-suspended in 1 ml of freeze medium; 10% (v/v) NCS/DMEM containing 10% (v/v) dimethyl sulphoxide **(**DMSO). The re-suspended cell pellet was then transferred into 1.8 ml polypropylene cryogenic tubes and

left for 10 min at room temperature. The cryogenic tubes were then placed into a polycarbonate container and stored overnight at -80˚C. The following morning the vials were transferred to liquid nitrogen and stored until required.

2.2.1.11 Preparation of HEK 293 for freezing

DMEM medium was aspirated from T75 flasks and 5ml of trypsin (0.05% (v/v) in EDTA) was added to each flask. Flasks were then incubated at 37˚C for 3-5 min until the cells were just beginning to lift off the flask. The trypsin solution was gently titurated over the surface of the flask until all of the cells were detached. 5 mls of 5% (v/v) FCS/DMEM was added to each flask containing HEK 293 cells. The cell suspension was then transferred to a 15 ml universal tube. The trypsin/cell mix was then centrifuged at 2000 x g for 3 min and the trypsin supernatant aspirated. The cell pellet was then re-suspended in 1 ml of freeze medium; 5% (v/v) FCS/DMEM containing 10% (v/v) DMSO. The re-suspended cell pellet was then transferred into 1.8 ml polypropylene cryogenic tubes and was left for 10 min at room temperature. The cryogenic tubes were placed into a polycarbonate container and stored overnight at -80˚C. The following morning the vials were transferred to liquid nitrogen and stored until required.

2.2.2 Preparation of 3T3-L1 lysates

3T3-L1 cells cultured on 10 cm diameter Falcon tissue culture dishes were incubated for 2 hr at 37˚C in 5 ml Krebs-Ringer HEPES (KRH) per dish. After incubating the cells in fresh KRH, test substances were then added to the dishes for various durations at 37˚C. The medium was removed and 0.4 ml lysis buffer was added to the dishes on ice. The cell extract was scraped off using a cell lifter and transferred into pre-cooled 1.5 ml microcentrifuge tubes. The extracts were vortex-mixed and centrifuged (21,910 x g, 3 min, 4˚C) on a bench top centrifuge. The supernatants were stored at -80˚C.

2.2.3 Protein concentration determination

Spectrophotometric analysis of 3T3-L1 lysates according to the Bradford method (Bradford 1976**)** was carried out at 595 nm in a spectrophotometer using disposable plastic cuvettes. Duplicates of 2 μg, 4 μg and 6 μg bovine serum albumin (BSA) were made up to 100 μl with H_2O and utilised as reference standards. Lysates, analysed in duplicate, were diluted (1:10) using distilled water. 5 μl of diluted lysate was then added to 95 μl of

distilled water in a cuvette. To all samples and reference standards, 1 ml Bradford's reagent was added and spectrophotometric analysis performed in a WPA S2000 spectrophotometer within 10 min of reagent addition. The mean absorbance for each sample duplicate was calculated and the protein concentration determined by comparison to the calculated mean A_{595} / µg BSA derived from the linear portion of the BSA reference standard curve.

2.2.4 Immunoprecipitation

2.2.4.1 Immunoprecipitation of AMPK α1, AMPK α2 and CaMKK β from 3T3-L1 adipocytes

10 µl (per sample) of protein G-sepharose beads were washed three times in screw cap microcentrifuge tubes using 1 ml of immunoprecipitation (IP) buffer (21,910 x g, 1 min at 4˚C). AMPK α1 (2 ug/sample), AMPK α2 (2 ug/sample) or CaMKKβ (2 ug/sample) were then added to the beads. 250 µl of IP buffer was added to the mixture and mixed by rotation for 1 hr at 4˚C. The beads were pelleted (21,910 x g, 1 min at 4˚C) and re-suspended in IP buffer (25% v/v). In 1.5 ml microcentrifuge tubes, 3T3-L1 adipocyte lysate (200 µg) was added to 20 µl of the protein G-sepharose bead slurry pre-bound to sheep anti-AMPK α1, sheep anti-AMPK α2 antibody or goat anti-CaMKKβ antibody. The volume was made up to 300 µl with IP buffer and was mixed for 4 hr at 4˚C on a rotating mixer. The beads were then pelleted (21,910 x g, 1 min at 4˚C) and the supernatant aspirated. The pellet was washed twice (21,910 x g, 1 min at 4˚C) with 1 ml of high salt (1 M NaCl) IP buffer and twice (21910 x g, 1 min at 4˚C) with 1 ml of IP buffer. For AMPK IPs the pellets were washed (21910 x g, 1 min at 4˚C) with 1 ml of HEPES Brij-35. The pellets were stored at -20˚C.

2.2.4.2 Immunoprecipitation of AS160 and TBC1D1 from 3T3-L1 adipocytes

Using 1.5 ml microcentrifuge tubes, 3T3-L1 adipocyte lysate (200 µg) was added to 6 µl of rabbit anti-AS160 antibody (1:12) or (1.5 µg/sample) of sheep anti-TBC1D1 antibody and mixed by rotation overnight at 4˚C in screw cap micocentrifuge tubes. The following morning 10 µl (per sample) of protein A-sepharose beads or protein G-sepharose beads were washed three times (21,910 x g, 1 min at 4˚C) with 1 ml of IP buffer. The beads were then re-suspended in IP buffer (25% v/v). 20 µl of the protein A-sepharose bead slurry was added to the lysate/anti-AS160 antibody mixture and 20 µl of the protein G-sepharose bead

slurry was added to the lysate/anti-TBC1D1 antibody mixture. The mixture was then mixed by rotation for 3 hr at 4˚C. The beads were then pelleted (21,910 x g, 1 min at 4˚C) and the supernatant aspirated. The pellet was washed twice with 1 ml of high salt (1 M NaCl) IP buffer (21,910 x g for 1 min at 4˚C), except when looking for 14-3-3 co-immunoprecipitation, before washing three times with 1 ml of IP buffer (21,910 x g for 1 min at 4˚C). The pellets were stored at -20˚C.

2.2.5 AMPK Assay

AMPK activity in immunocomplexes was determined by phosphorylation of the peptide HMRSAMSGLHLVKRR [SAMS]. The AMPK pellets were re-suspended in 20 μl of HEPES Brij-35 buffer. Reaction mixtures (20 μl) containing 5 μl of HEPES Brij-35 buffer, 5 μl of 1 mM SAMS peptide in HEPES Brij-35 buffer, 5 μl of 1 mM AMP in HEPES Brij-35 buffer and 5 μl of immunoprecipitate re-suspended in HEPES Brij-35 buffer, were prepared in 1.5 ml microcentrifuge tubes on ice and the reaction initiated by the addition of 5 μl of MgATP solution (1 mM [γ-^{32}P] ATP, 250 - 500 c.p.m./pmol; 25 mM $MgCl_2$ in HEPES Brij-35 buffer). Reaction mixtures were then incubated on a vibrating platform in an air incubator at 30°C for 10 min. Assay mixtures (15 μl) were spotted onto P81 phosphocellulose paper, and rinsed, with gentle stirring to remove free ATP, for 5 min in 1% (v/v) phosphoric acid. A further 2 x 5 min water washes were performed on the phosphocellulose paper, before a final 5 min wash with 1% (v/v) phosphoric acid. A Beckman Multi-Purpose scintillation counter LS 6500 was used to measure [^{32}P]-labelled substrate. 3 ml of scintillation fluid was used per sample. Results were corrected for radioactivity recovered in blank reactions lacking the SAMS peptide. One unit of AMPK activity is that required to incorporate 1 nmol of ^{32}P into the SAMS substrate peptide/min/mg protein.

2.2.6 SDS-Polyacrylamide Gel Electrophoresis

Sodium dodecyl sulphate-polyacrylamide gel electrophoresis (SDS-PAGE) was performed using 1.5 mm thick vertical slab gels containing either 6% or 10% acrylamide.

Slab gels were prepared using Bio-Rad mini-Protean III gel units, with a stacking gel of approximately 2 cm deep. The stacking gel consisted of 5% acrylamide/0.136% bisacrylamide in 125 mM Tris-HCl, pH 6.8, 0.1% SDS, polymerized with 0.1% (w/v)

ammonium peroxidisulphate (APS) and 0.05% (v/v) tetramethylethylenediamine (TEMED).

Cell lysate samples were mixed 3:1 with 4 X SDS-containing sample buffer and heated to 95°C in a heating block for 5 min prior to separation by SDS-PAGE on Tris buffered gels. Prestained broad range (6-175 kDa) protein markers, were used as a standard.

Gels were electrophoresed using the Bio-Rad Protean III system at a constant voltage of 80 V for stacking and 150 V through the separating gel. Gels were electrophoresed until the tracking dye had migrated to the bottom of the gel and good separation of the molecular weight markers had been obtained.

2.2.7 Western Blotting of Proteins

2.2.7.1 Electrophoretic transfer of proteins from gels onto nitrocellulose membranes

Proteins were separated by SDS-PAGE as previously described (2.2.6). The gels were removed from the plates and placed on top of an equal-sized sheet of nitrocellulose (0.45 μm pore size), pre-wet with transfer buffer and then placed between 2 layers of 3 MM filter paper also pre-wet with transfer buffer. The 'sandwich' was then inserted between the plates of the gel holder cassette and transfer was performed using a Bio-Rad mini Protean III trans-blot electrophoretic transfer cell at a constant current of 40 mA overnight or at 60 V for 2 hr. The nitrocellulose membranes were then removed from the transfer cassette and the efficiency of transfer determined by the presence and intensity of pre-stained molecular weight standards. Membranes were also briefly stained with Ponceau to check for equal loading of the gels.

2.2.7.2 Blocking of membranes and probing with antibodies

Non-specific sites on the nitrocellulose membranes were blocked by incubation with shaking in tris buffered saline (TBS)/5% (w/v) milk for 30 min at room temperature. After washing (3 x 5 min) the membrane in tris buffered saline tween (TBST), the primary antibody was applied to the blot and incubated, with shaking, overnight at 4°C in TBST/5% (w/v) milk or TBST/5% (w/v) BSA. After washing (3 x 5 min) in TBST the membranes were incubated, with shaking, for 1 hr at room temperature with the

appropriate horseradish peroxidase (HRP)-conjugated secondary antibody in TBST/5% (w/v) milk or TBST/5% (w/v) BSA. The membranes were then washed (5 x 5 min) in TBST. If required, membranes were further washed (3 x 5 min) in high salt (0.5 M NaCl) TBST and then washed (2 x 5 min) in TBST.

2.2.7.3 Immunodetection of proteins using western blotting and the ECL detection system

Enhanced chemiluminescence (ECL) is a light emitting non-radioactive method for the detection of immobilized specific antigens, conjugated directly or indirectly with HRP-labeled antibodies. HRP is used to catalyze the oxidation of luminol in the presence of hydrogen peroxide. Immediately after the oxidation, the luminol is in an excited state which decays to ground state via a light emitting pathway.

Equal volumes of 'detection reagent 1' and 'detection reagent 2' were mixed and the membranes, prepared as described in 2.2.7.2, were immersed in the mix with shaking for 60 seconds. The detection reagents were then removed, membranes wrapped in cling-film and exposed to Kodak film. Finally the films were developed using the X-OMAT processor.

2.2.7.4 Stripping of nitrocellulose membranes

Nitrocellulose membranes were incubated in 50 mM glycine, pH 2.5 with shaking for 5 min. Membranes were then washed in TBST for 5 mins.

2.2.7.5 Densitometric quantification of protein bands

The antibody-detected bands on the developed film were scanned on a Mercury 1200c scanner, using Adobe Photoshop software. The intensity of the immuno-detected protein bands on the film was measured using ImageJ software.

2.2.8 2-deoxy-D-glucose uptake assay

Glucose uptake was measured by the uptake of 2-[^{3}H]-deoxy-D-glucose according to the method of Gibbs (Gibbs *et al* 1988). Cells were cultured on 12 well plates and incubated at 37˚C in 1 ml of serum free DMEM for 2 hr prior to use. Cells were subsequently incubated at 37˚C in 475 µl/well of Krebs-Ringer phosphate (KRP) for 1 hr and test substances added

to the plates for various durations at 37°C. The cells were then stimulated with 10 nM insulin for 15 min. Glucose transport was initiated by the addition of 2-[^{3}H]-deoxy-D-glucose (final concentration 50 μmol/l and 1 μCi/ml) to each well. The reaction was terminated after 3 min by inverting the plates rapidly to remove the incubation buffer, and then by immersing them sequentially in 2 x 2l and 1l of ice-cold phosphate buffered saline (PBS). After air drying the plates for 1 hr, 0.5 ml of 1% (v/v) Triton X-100/H2O was added to the cell monolayers. A Beckman Multi-Purpose scintillation counter LS 6500 was used to measure 2-[^{3}H]-deoxy-D-glucose uptake. 5 ml of scintillation fluid was used per sample. Non-specific association of radioactivity was determined in parallel incubations in the presence of 10 μmol/l cytochalasin B.

2.2.9 Nucleotide extraction and analysis

2.2.9.1 Nucleotide extraction

3T3-L1 cells cultured in 10 cm diameter dishes were incubated for 2 hr at 37°C in 5 ml of KRH buffer. Test substances were added at 37°C for various durations. The buffer was removed and 500 μl of 5% (w/v) ice cold perchloric acid added to the dishes on ice. The extract was scraped off with a cell scraper and transferred to a screw cap microcentrifuge tube. Precipitated protein was removed by centrifugation of the extract at 21,910 x g for 3 min in a microcentrifuge at 4°C. The supernatant was then extracted twice to remove perchloric acid with 10% excess (by volume) of a 1:1 mixture of tri-n-octylamine and 1,1,2-trichlorotrifluoroethane. Nucleotides were separated by reversed-phase chromatography adapted from the method published by Uesugi (Uesugi *et al* 1997).

2.2.9.2 Reversed-phase chromatography

Neutralised perchloric acid extracts were prepared as described (see 2.2.9.1). All analyses were performed on a stainless-steel column (250 x 4.6 mm I.D) packed with Chrom Spher C18 octadecylsilane (ODS) (5 μm) attached to a Varian Prostar HPLC system. The column was equilibrated (30-60 min) with the eluent 0.1 M triethylamine (TEA) phosphate buffer pH 8 and methanol (96:4, v/v) at a flow rate of 1.0 ml/min for 25 min at ambient temperature (22-23°C) prior to sample injection. Nucleotides were detected by their absorbance at 259 nm, and compared with the elution position of standards; AMP, ADP and ATP. Retention times were measured from the time between the injection point (50 μl sample) and the peak maximum on the chromatogram.

The concentration of each nucleotide was determined by quantifying the area under the peaks, after calibration using standards of a known concentration.

2.2.9.3 Preparation of TEA phosphate buffer

Stock solutions of 0.1 M TEA and a mixture of 0.1 M TEA and 0.1 M phosphoric acid were filtered through a 0.45 μM filter and kept at 4°C. The pH of the TEA phosphate buffer was adjusted to pH 8 by admixing both of the stock solutions at 23°C.

2.2.10 Recombinant adenoviruses

2.2.10.1 AMPK adenoviruses

Adenovirus encoding a dominant negative AMPK mutant (Ad.α1-DN) was constructed from cDNA encoding AMPKα1 containing a mutation that alters aspartic acid residue 157 to alanine (D157A), and adenovirus encoding a constitutively active AMPK mutant (Ad.$\alpha1^{312}$) was constructed from cDNA encoding residues 1-312 of AMPKα1, containing a mutation that alters threonine 172 to an aspartic acid (T172D) as described previously (Woods *et al* 2000). These AMPK adenoviruses were a generous gift from Dr. F. Foufelle, Centre Biomédical des Cordeliers, Paris.

2.2.10.2 Adenovirus propagation

HEK 293 cells in T75 flasks were cultured in DMEM growth media (see 2.2.1.5) and passaged at 70-80 % confluency (see 2.2.1.7). Each T75 flask was split into 5 x T150 flasks. Once 30 x T150 flasks were obtained, and grown to 70-80% confluency, recombinant adenoviruses were propagated in the HEK 293 cells. Detached cells were then pelleted in 50 ml falcon tubes (5 min at 2000 x g). 100 ml of the supernatant was retained to infect more HEK 293 cells, and the pellets pooled and re-suspended in 5 ml of sterile PBS.

2.2.10.3 Adenovirus purification

In order to lyse the HEK 293 cells containing the adenovirus particles, 5 ml of Arklone P (trichlorotrifluroethane) was added to the HEK 293 cell suspension (2.2.10.2) and mixed gently by inverting the tube for about 10 seconds. The mixture was left at room temperature for 3 min and then centrifuged at 2000 x g for 10 min. The upper layer

containing virus was separated from cell debris (interface) and the Arklone P layer (bottom layer). 2.5 ml sterile CsCl dissolved in Tris/EDTA (5 mM Tris-HCl, 1 mM EDTA pH 7.8) at a density of 1.33 g/ml was added to a sterile centrifuge tube. This was underlaid with 1.5 ml of sterile 1.45 g/ml CsCl. The virus layer was loaded on the CsCl gradient and centrifuged at 100,000 x g in a SW40 rotor using an Optima^{TM} XL-80K ultracentrifuge at 8°C for 90 min. The tube was then punctured just below the virus band with a 21 guage needle, and withdrawn into a 2.5 ml syringe. The virus was transferred to a 10 micron Slide-A-Lyzer cassette and dialysed against cold Tris/EDTA buffer at 4°C overnight, and against fresh buffer containing 10% (v/v) glycerol for a further 2 hr the following morning. The purified virus was removed and stored at -80°C.

2.2.10.4 Adenovirus titration

The Quick Titer^{TM} Adenovirus Titer Immunoassay kit was used to titre the virus. Briefly, HEK cells were plated onto a 24 well plate. After 1 hr 100 µl of 10^{-3}, 10^{-4}, 10^{-5} and 10^{-6} diluted virus solutions were added to the wells. The cells were then incubated for 48 hr at 37°C, 5% (v/v) CO_2. To fix the cells the media was removed and replaced with 0.5 ml cold methanol and incubated for 20 min at 20°C. Cells were washed three times in PBS prior to blocking with PBS containing 1% (w/v) BSA at room temperature for 1 hr. 250 µl of anti-Hexon antibody was added to each well and incubated for 1 hr at room temperature. The cells were then washed three times in PBS prior to the addition of 250 µl of the HRP-conjugated secondary antibody to each well and incubated for 1 hr at room temperature. The cells were then washed five times in PBS. 250 µl of diaminobenzidine (DAB) was added to each well and incubated for 10 min at room temperature. DAB was then aspirated and the wells were washed twice with PBS. 1 ml of PBS was added to each well. The positive stained cells were counted for at least five separate fields per well using a light microscope and 10X objective. Calculation of adenovirus titre was determined (Infectious Units/ml).

2.2.10.5 3T3-L1 adipocyte adenovirus infection

6 days post differentiation 500 µl of serum free DMEM was added to 3T3-L1 adipocytes cultured on 12 well plates. Adenovirus was added (600 ifu/cell) to the dishes and incubated for 6 hr at 37°C in a humidified atmosphere of 10% (v/v) CO_2. 500 µls of DMEM / 20% FCS was added to the cells for a further 24 hr. The media was replaced with 1 mls DMEM

/ 10% FCS and incubated for a further 24 hr before 3T3-L1 cell lysates were prepared (see 2.2.2) or a glucose transport assay performed (2.2.8).

2.2.11 Albumin and IgG depletion

Albumin and immunoglobulin gamma (IgG), two abundant proteins in serum, were depleted from human adipose samples collected by Dr J Boyle, University of Glasgow, using the ProteoPrep Blue Albumin and IgG Depletion Kit.

2.2.12 Statistical Analysis

Results are expressed as mean +/- SEM. Statistically significant differences were determined using a one or two-tailed Student's *t* test (two-sample assuming unequal variance), or one-way ANOVA where appropriate, with $p < 0.05$ as significant.

The statistics package, Minitab, was used for data analysis of results obtained from human adipose tissue samples (chapter 5). Each data set was tested separately for normality using the Ryan-Joiner test and subsequently (when required) transformed by logarithmic ($\log_{10}$) or square route (sqrt) transformation. The mean and 95% confidence intervals of the mean were calculated using transformed data; however, for presentation results were back transformed. Statistically significant differences were determined using a paired T-test, with $p < 0.05$ as significant.

Chapter 3 - Activation parameters and mechanism of AMPK activation by various stimuli in 3T3-L1 cells

3.1 Introduction

3.1.1 Known activators of AMPK in adipocytes

AMPK has been shown to be activated by some AMPK activators in adipocytes and adipose tissue. The adipocytokines leptin (Orci *et al* 2004) and adiponectin (Wu *et al* 2003) have both been shown to activate AMPK in rat white fat tissue and isolated rat adipocytes respectively. AICAR has been shown to activate AMPK in isolated rat adipocytes and 3T3-L1 adipocytes (Corton *et al* 1995, Salt *et al* 2000). The biguanides metformin and phenformin have been reported to activate AMPK in 3T3-L1 adipocytes and isolated rat adipocytes respectively (Huypens *et al* 2005, Daval *et al* 2005). In addition the TZD, pioglitazone has also been shown to activate AMPK *in vivo* in rat adipose tissue (Saha *et al* 2004). Furthermore, the β adrenergic agonist, isoproterenol, has been shown to stimulate AMPK activity in isolated rat adipocytes (Moule and Denton 1998) and in 3T3-L1 adipocytes (Yin *et al* 2003, Gauthier *et al* 2008).

3.1.2 Role for LKB1 as an AMPK kinase in adipocytes

Indirect arguments suggest that the upstream kinase LKB1 is involved in AMPK activation in adipocytes. Phenformin can induce AMPK activation in isolated rat adipocytes by decreasing the ATP concentration (Daval *et al* 2005) and AICAR, which is converted to ZMP, a cellular mimetic of AMP, activates AMPK in isolated rat adipocytes and 3T3-L1 adipocytes (Corton *et al* 1995, Salt *et al* 2000). In addition, in transgenic mice expressing UCP1 in white adipose tissue, the AMP/ATP ratio is increased and AMPK is activated (Matejkova *et al* 2004). However, a potential role for CaMKK in AMPK activation has yet to be demonstrated in adipocytes.

3.1.3 AMPK subunit isoform expression

AMPK is a heterotrimeric complex containing two α, two β, and three γ subunit isoforms of which the expression level of each varies between different tissues. The liver predominantly expresses the α1 subunit (Stapleton *et al* 1996) and β1 subunit (Thornton *et al* 1998), where as skeletal muscle predominantly expresses the α2 subunit (Stapleton *et al* 1996) and β2 subunit (Thornton *et al* 1998). Expression profiling of the AMPK γ subunit expression across different tissues in human, rat and mouse found that the γ3 subunit appears to be predominantly expressed in skeletal muscle, while the γ1 and γ2 subunits showed broad tissue distributions (Cheung *et al* 2000, Mahlapuu *et al* 2004**).** In 3T3-L1 adipocytes both the α1 and α2 catalytic subunits have been shown to be expressed (Salt *et al* 2000).

In addition to tissue distribution, subunit isoforms can also exhibit preferential cellular localization. Salt and co-workers showed that the α2 subunit was clearly localized in the nucleus of both INS-1 cells and CCL13 cells, while both α subunit isoforms could be found in the cytoplasm (Salt *et al* 1998a).

3.1.5 Aims

Although AMPK activation has been previously reported in adipose tissue and cultured adipocytes, a thorough investigation of expression of components of the AMPK cascade and kinetics of AMPK stimulation has yet to be undertaken.

AMPK has been shown to be involved in the regulation of adipogenesis (Habinowski and Witters 2001, Dagon *et al* 2006, Giri *et al* 2006, Tong *et al* 2008), however the AMPK subunit isoform expression throughout adipogenesis remains unknown.

The 3T3-L1 cell line is derived from disaggregated Swiss mouse embryos. The cell line isolated and cloned by Green and Kehinde have a fibroblast like morphology, but, under appropriate conditions, the cells differentiate into cells resembling adipocytes which synthesise and store TG (Green and Hehinde 1974, Green and Hehinde 1975, Green and Hehinde 1976). 3T3-L1 fibroblasts, once confluent, convert to adipocytes in the presence of IBMX, dexamethasone, and insulin. Thus, 3T3-L1 cells are used widely as a model system to study the differentiation of preadipocytes to adipocytes.

In the current study the expression of the upstream AMPK kinases; LKB1 and CaMKKα/β, and the downstream AMPK substrates ACC1/2 in 3T3-L1 adipocytes, was investigated. In addition, the expression of AMPK subunit isoforms and the relative contribution of the catalytic AMPKα subunits to total AMPK activity throughout development from fibroblasts to adipocytes was determined using 3T3-L1 cells as a model system. Finally, the parameters and molecular mechanism of AMPK activation by various stimuli in 3T3-L1 adipocytes was investigated.

3.2 Results

3.2.1 Investigating the expression of LKB1, CaMKKα, CaMKKβ, ACC1 and ACC2 in 3T3-L1 adipocytes

The expression of molecules both upstream and downstream of AMPK in the AMPK signalling cascade was investigated. The presence of the upstream AMPK kinases; LKB1, CaMKKα and CaMKKβ and the downstream substrates of AMPK; ACC1 and ACC2 were determined by western blotting analysis of 3T3-L1 adipocyte lysates.

The tumour suppressor LKB1, is expressed in 3T3-L1 adipocytes as demonstrated by the presence of two bands (splice variants of LKB1) situated between the 62kDa and 47.5kDa molecular weight markers (Fig. 3.1A). These two bands are not present in HeLa cells, which lack LKB1. CaMKKα is expressed in 3T3-L1 adipocytes as demonstrated by the presence of a band at approximately 63kDa in 3T3-L1 cell lysates (Fig. 3.1B) which corresponds to a band present in rat brain extract which is rich in CaMKKα. It appears that CaMKKβ is also expressed in 3T3-L1 adipocytes, as there appears to be a faint band at approximately 66kDa (Fig. 3.1C) in the 3T3-L1 cell lysate immunoprecipitated with anti-CaMKKβ antibody corresponding to a band present in rat brain extract, which is abundant in CaMKKβ.

Using anti-ACC antibodies, the presence of a band at approximately 260kDa (Fig. 3.2A) in the 3T3-L1 cell lysate, corresponds to a band present in rat liver extract which is rich in ACC1, indicating that 3T3-L1 adipocytes express ACC1.

3T3-L1 cell lysate probed with anti-ACC2 antibody displays a doublet at approximately 280kDa (Fig. 3.2B). Muscle is rich in ACC2, yet the band detected by the anti-ACC2 antibody in the rat muscle extract, runs at a molecular weight in between the doublet in the 3T3-L1 lysate. In addition, the single band in the rat muscle extract (assumed to be ACC2), corresponds to the lower molecular weight band, from the doublet, in the rat liver extract. Thus the higher molecular weight band, from the rat liver doublet, may be a non-specific band and the lower band may correspond to ACC2.

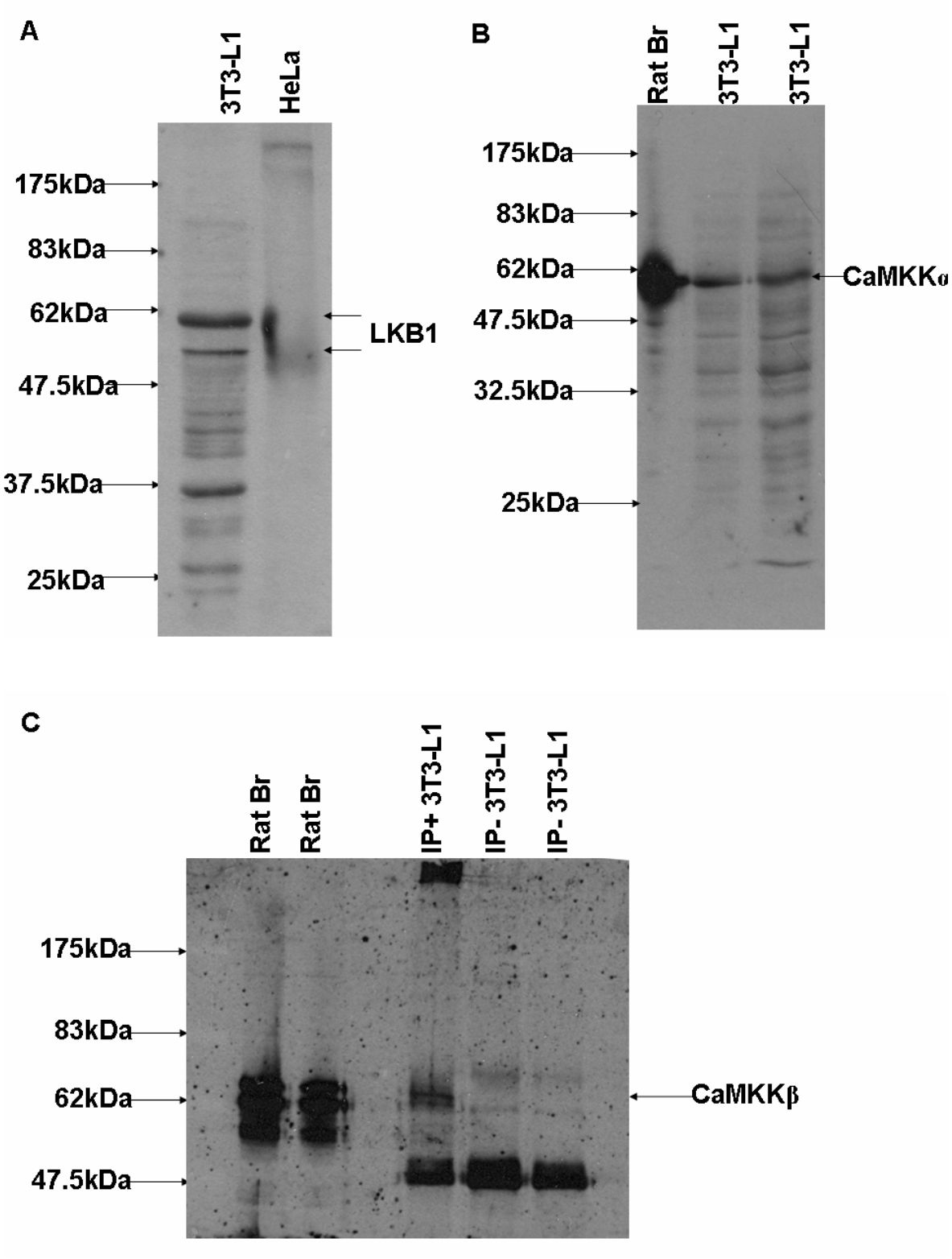

Figure 3-1: LKB1, CaMKKα, CaMKKβ and LKB1 expression in 3T3-L1 adipocytes.
3T3-L1 lysate (25 μg) was resolved by 10% SDS-PAGE, transferred to nitrocellulose, and probed with (A) anti-LKB1 antibody or (B) anti-CaMKKα antibody. (C) 3T3-L1 lysate (200 μg) was immunoprecipitated using anti-CaMKKβ antibody, resolved by 6% SDS-PAGE, transferred to nitrocellulose, and probed with anti-CaMKKβ antibody. Negative control for LKB1 was HeLa cell lysate. Br = rat brain extract. IP+ = immunoprecipitation using anti-CaMKKβ antibody in the presence of 3T3-L1 lysate. IP- = immunoprecipitation using anti-CaMKKβ antibody in the absence of 3T3-L1 lysate. The positions of the molecular weight markers are shown to the left of the gels.

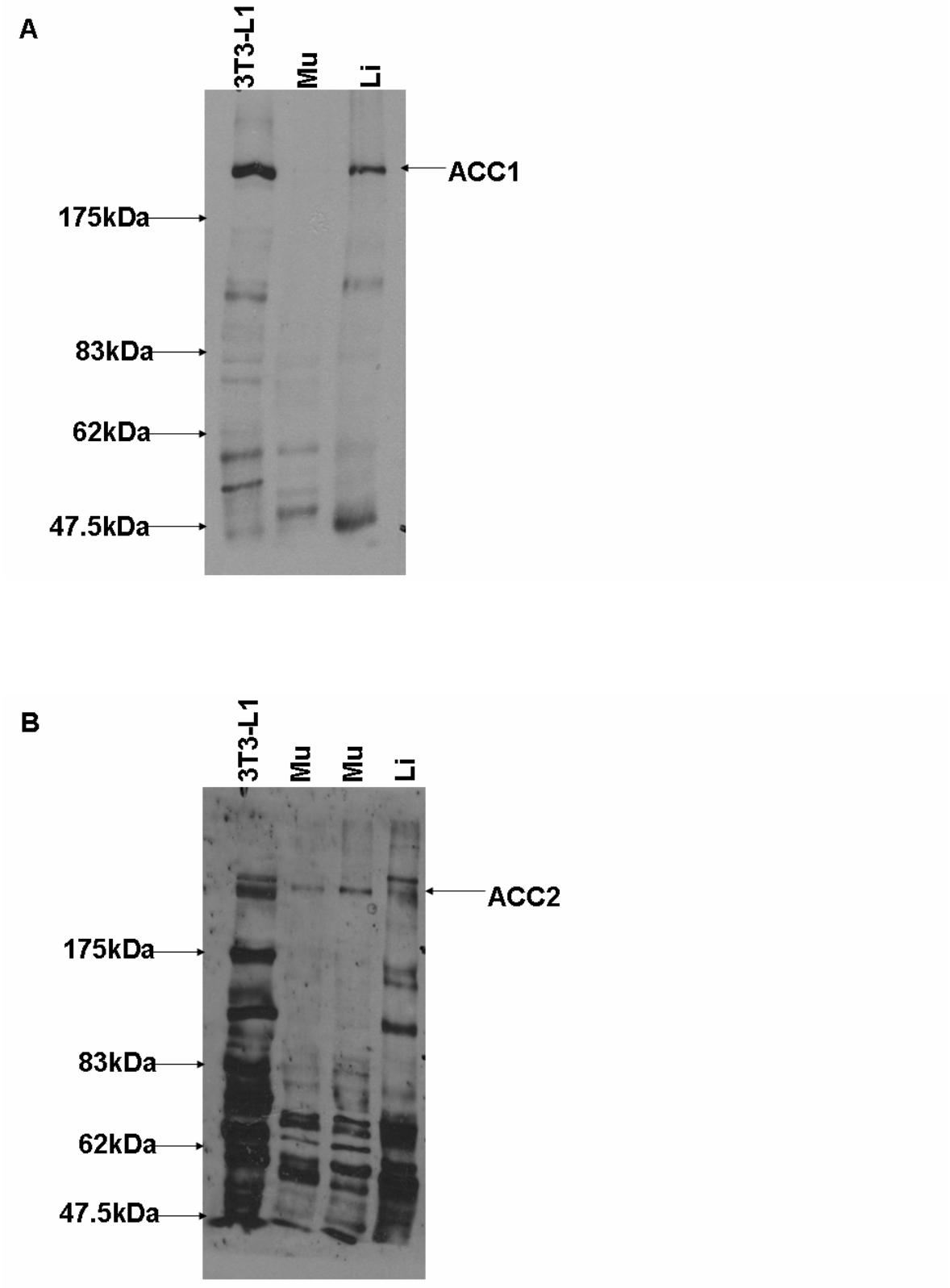

Figure 3-2: ACC1 and ACC2 expression in 3T3-L1 adipocytes.
3T3-L1 lysate (60 µg) was resolved by 6% SDS-PAGE, transferred to nitrocellulose, and probed with (A) anti-ACC1 antibody or (B) anti-ACC2 antibody. Li = rat liver extract, Mu = rat muscle extract. The position of the molecular weight markers are shown to the left of the gel.

3.2.2 AMPK subunit isoform expression during adipogenesis

To investigate AMPK subunit isoform expression during adipogenesis, lysates obtained from 3T3-L1 cells every 48 hr post differentiation were analysed by western blotting.

As shown below (Fig. 3.3) the α1 subunit isoform expression level was not significantly altered throughout adipogenesis.

Unfortunately, densitometric analysis for α2 expression could not be accurately performed on fibroblasts (day 0) due to smearing in most blots. The α2 subunit isoform expression level (Fig. 3.4) is undetectable at 2 days post differentiation. Modest expression levels of α2 were detected at 4 days post differentiation, however a significant ($p < 0.05$) increase, compared to 2 days post differentiation, in α2 expression was observed at 6, 8, 10 and 12 days post differentiation. Interestingly, there is also an intense band recognised by the anti-AMPK α2 antibody resolving with a higher molecular mass than that of α2 which appears to decrease throughout adipogenesis.

β1 is expressed in fibroblasts, however expression levels (Fig. 3.5) are significantly ($p < 0.05$) decreased throughout differentiation. The maximum significant ($p < 0.05$) reduction in expression level, compared to fibroblasts at day 0, was 74 +/- 3.5 % which was observed after 8 days post differentiation.

β2 (Fig. 3.6) is also expressed in fibroblasts, however there is a general increase in β2 expression levels throughout adipogenesis. A maximum 1.66 +/- 0.2 fold increase in expression levels, of β2 was observed at 10 days post differentiation, compared to fibroblasts at day 0.

γ1 (Fig. 3.7) is expressed in fibroblasts, and expression levels were found to increase during adipogenesis with significant ($p < 0.05$) increases, compared to fibroblasts, in expression levels at 10 and 12 days post differentiation. A maximum significant ($p < 0.05$), 2.55 +/- 0.31 fold increase in expression levels of γ1 was observed at 12 days post differentiation, compared to fibroblasts at day 0.

γ2 (Fig. 3.8) and γ3 (Fig. 3.9) are both expressed in fibroblasts. It should be noted that the doublet (52/54 kDa) recognised by the anti-AMPK γ3 antibody corresponds to different splice variants of the γ3 isoform. Unfortunately, densitometric analysis could not be

accurately performed on fibroblasts (day 0) due to smearing. In general, the expression levels of both γ2 and γ3 are decreased through out adipogenesis. Significant ($p < 0.05$) reductions in γ3 expression levels occurred at 8, 10 and 12 days post differentiation, with a maximum significant ($p < 0.05$) 51 +/- 13 % reduction in expression occurring at 12 days post differentiation, compared to 2 days post differentiation.

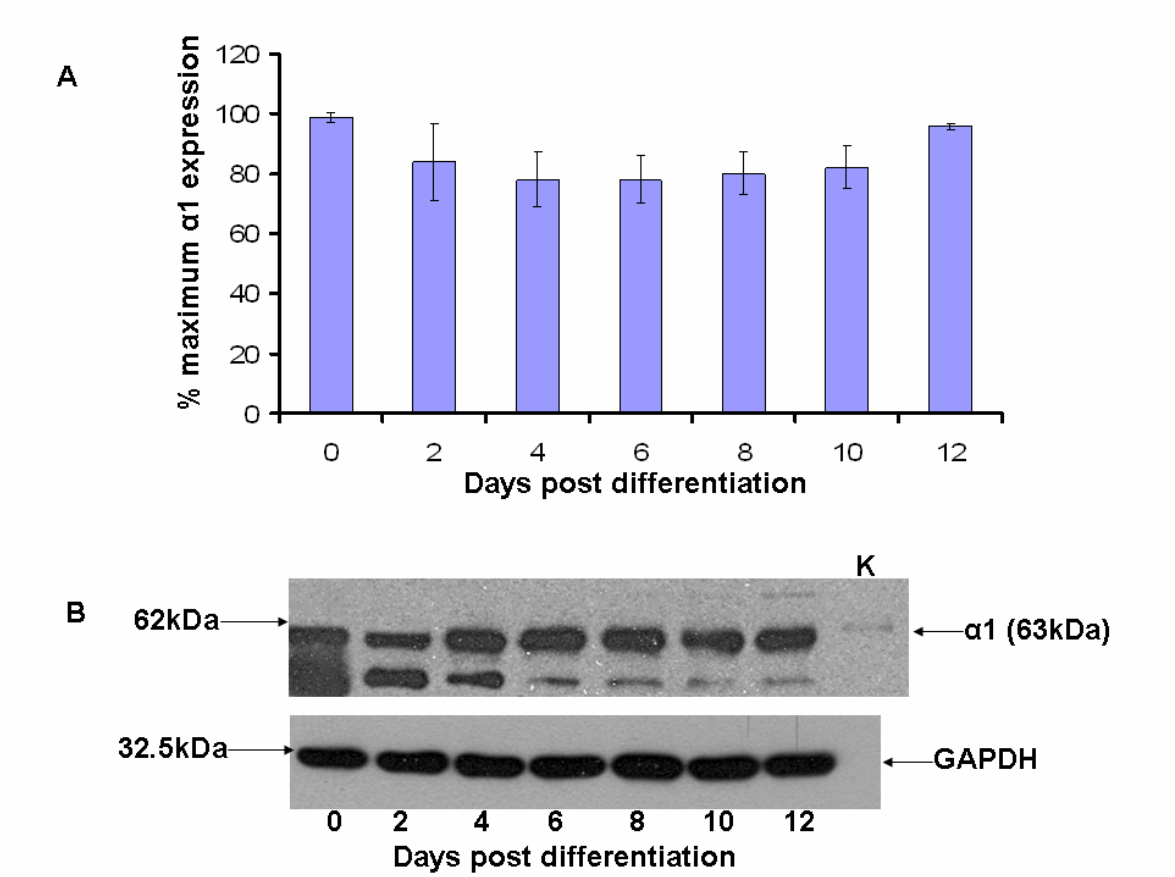

Figure 3-3: AMPK α1 subunit expression during adipogenesis

Lysates (15 µg) obtained from cells at various time points post differentiation were resolved by 10% SDS-PAGE, transferred to nitrocellulose, and probed with anti-AMPK α1 and anti-GAPDH antibodies. K = purified rat liver AMPK (positive control). (A) Quantification of AMPK α1 expression was determined by comparison with total GAPDH by densitometric analysis. Data shown represents the mean % maximum +/- S.E.M of three independent experiments. (B) Representative blots from three independent experiments. The position of the molecular weight markers are shown to the left of the gel.

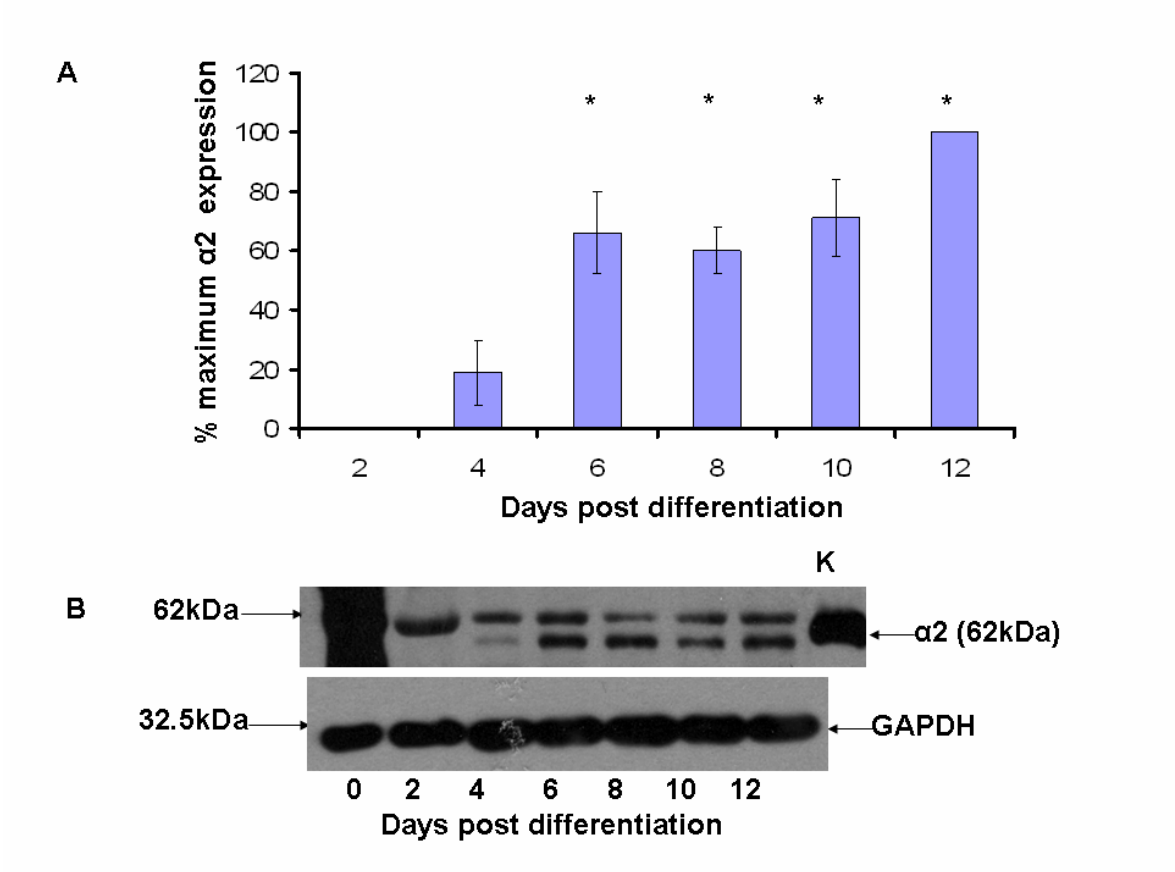

Figure 3-4: AMPK α2 subunit expression during adipogensis.
*Lysates (15 µg) obtained from cells at various time points post differentiation were resolved by 10% SDS-PAGE, transferred to nitrocellulose, and probed with anti-AMPK α2 and anti-GAPDH antibodies. K = purified rat liver AMPK (positive control). (A) Quantification of AMPK α2 expression was determined by comparison with total GAPDH using densitometric analysis, *p < 0.05 (one-way ANOVA), compared to 2 days post differentiation. Data shown represents the mean % maximum +/- S.E.M of three independent experiments. (B) Representative blots from three independent experiments. The position of the molecular weight markers are shown to the left of the gel.*

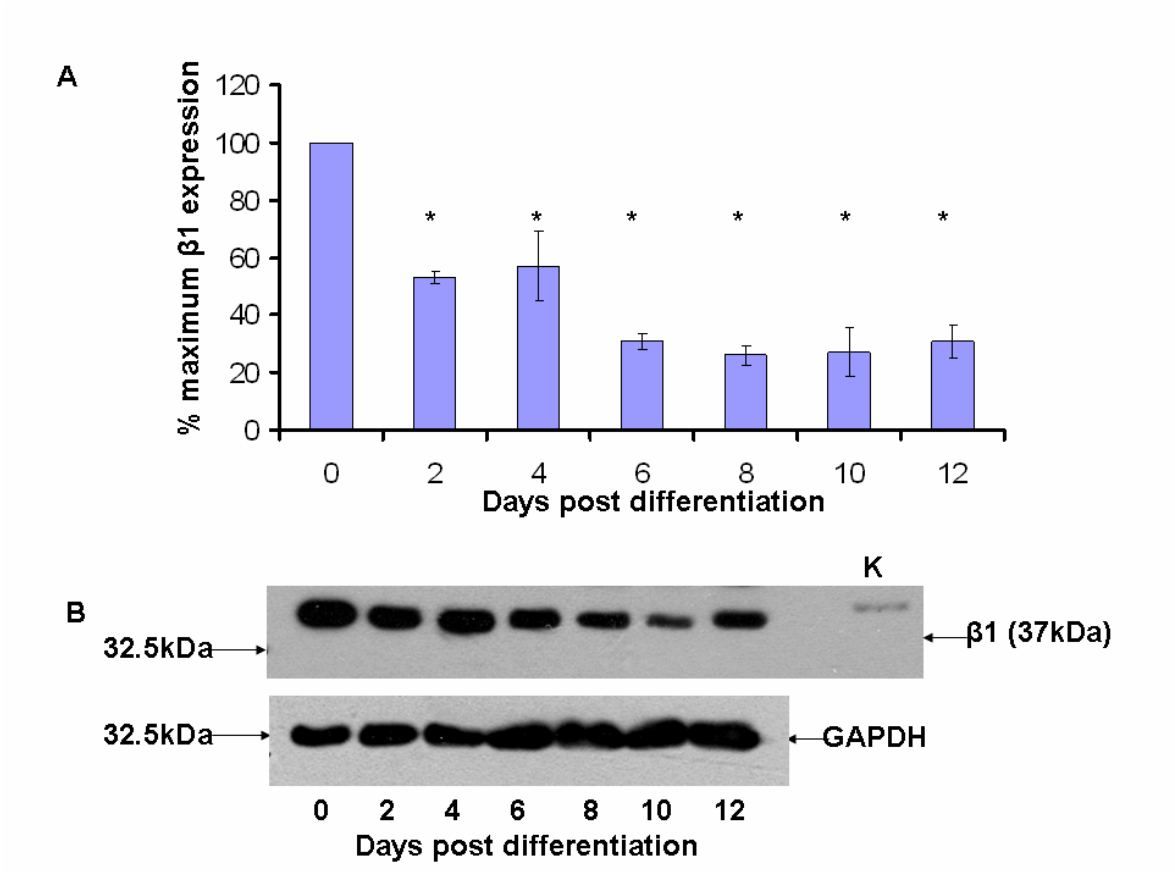

Figure 3-5: AMPK β1 subunit expression during adipogenesis

*Lysates (15 µg) obtained from cells at various time points post differentiation were resolved by 10% SDS-PAGE, transferred to nitrocellulose, and probed with anti-AMPK β1 and anti-GAPDH antibodies. K = purified rat liver AMPK (positive control). (A) Quantification of AMPK β1 expression was determined by comparison with total GAPDH using densitometric analysis, *p < 0.05 (one-way ANOVA), compared to 0 days post differentiation. Data shown represents the mean % maximum +/- S.E.M of three independent experiments. (B) Representative blots from three independent experiments. The position of the molecular weight markers are shown to the left of the gel.*

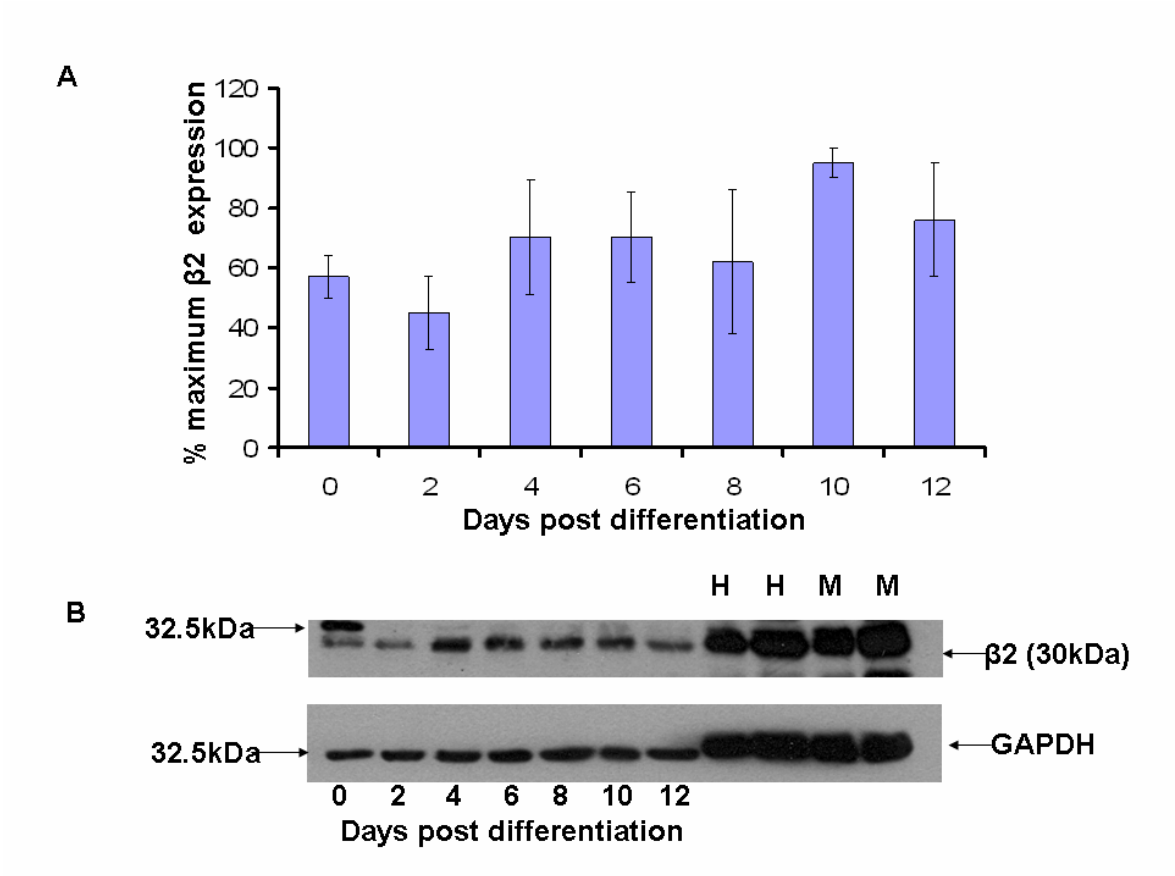

Figure 3-6: AMPK β2 subunit expression during adipogenesis.
Lysates (15 µg) obtained from cells at various time points post differentiation were resolved by 10% SDS-PAGE, transferred to nitrocellulose, and probed with anti-AMPK β2 and anti-GAPDH antibodies. H = rat heart extract, M = rat muscle extract (positive controls). (A) Quantification of AMPK β2 expression was determined by comparison with total GAPDH using densitometric analysis. Data shown represents the mean % maximum +/- S.E.M, of three independent experiments. (B) Representative blots from three independent experiments. The position of the molecular weight markers are shown to the left of the gel.

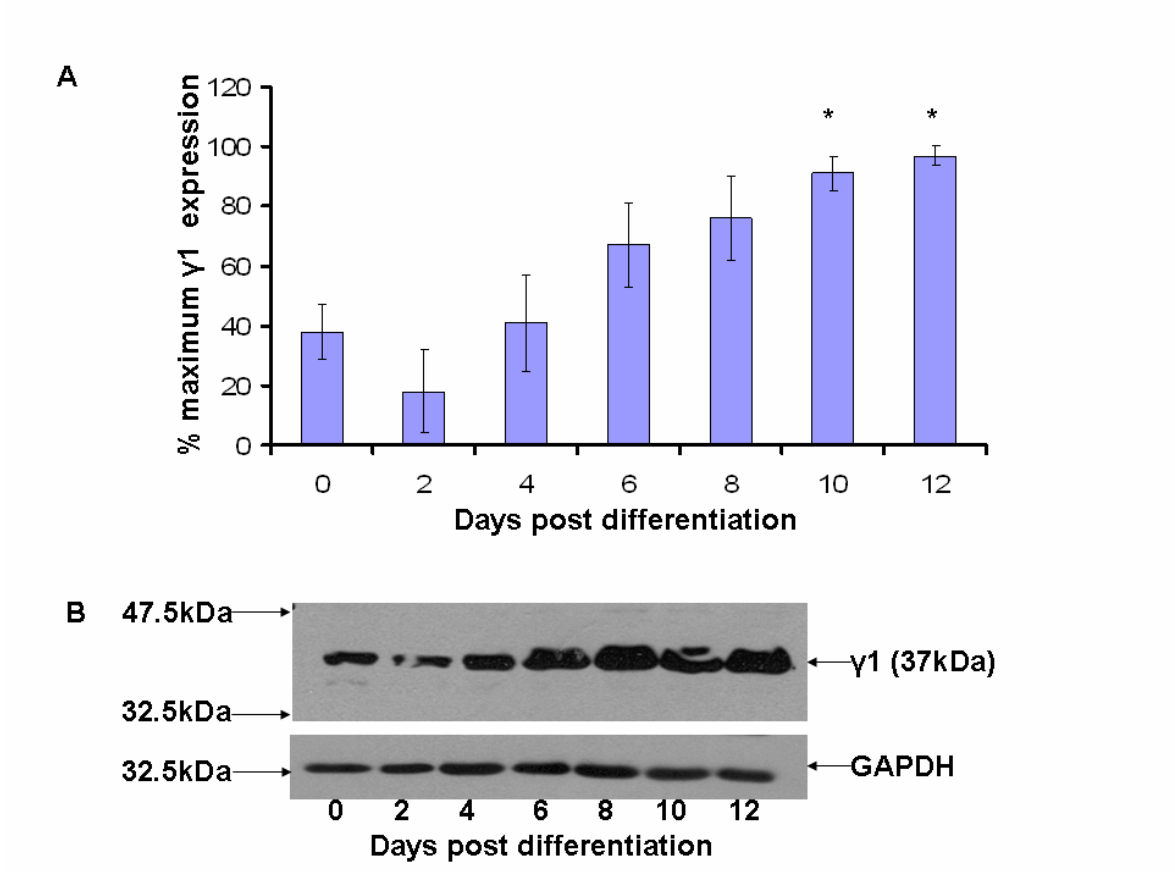

Figure 3-7: AMPK γ1 subunit expression during adipogenesis.
*Lysates (15 µg) obtained from cells at various time points post differentiation were resolved by 10% SDS-PAGE, transferred to nitrocellulose, and probed with anti-AMPK γ1 and anti-GAPDH antibodies. (A) Quantification of AMPK γ1 expression was determined by comparison with total GAPDH using densitometric analysis, *p < 0.05 (one-way ANOVA), compared to 0 days post differentiation. Data shown represents the mean % maximum +/- S.E.M of three independent experiments. (B) Representative blots from three independent experiments. The position of the molecular weight markers are shown to the left of the gel.*

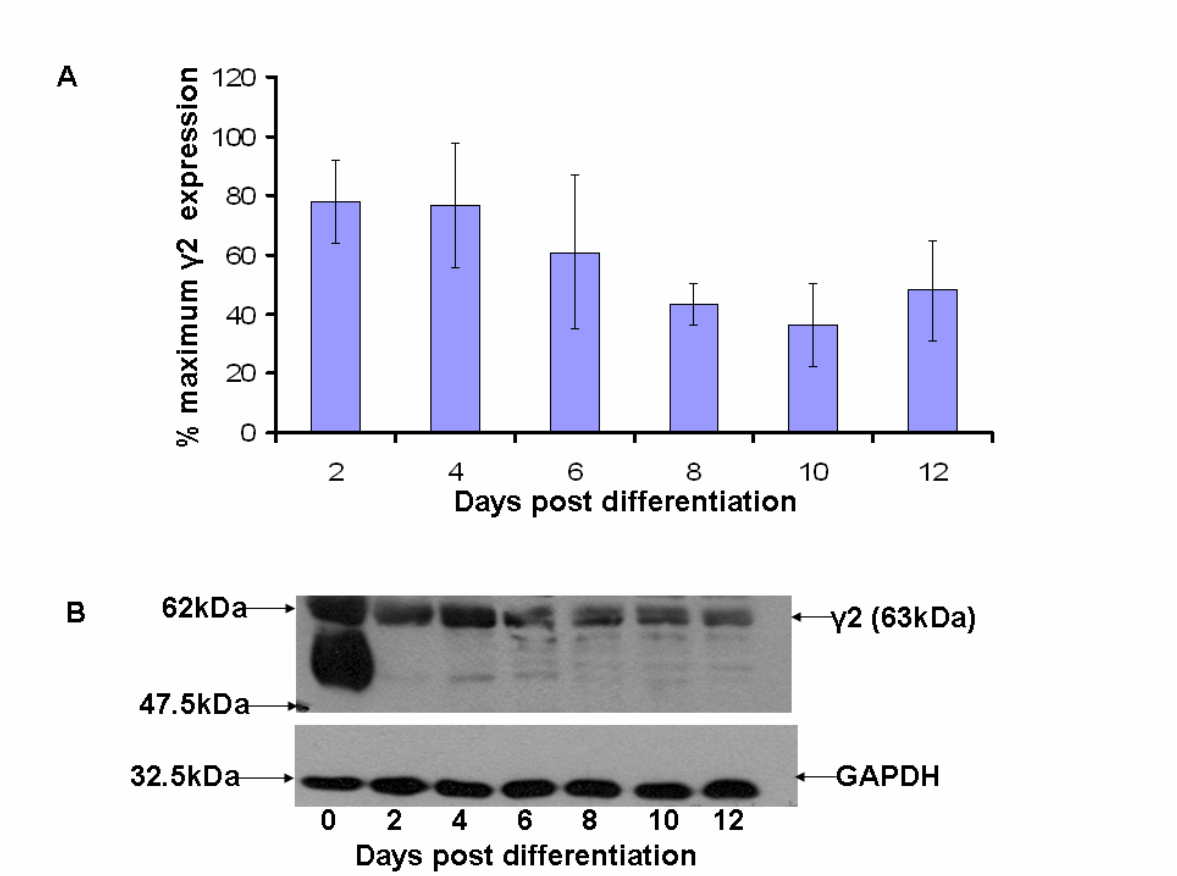

Figure 3-8: AMPK γ2 subunit expression during adipogenesis.
Lysates (15 µg) obtained from cells at various time points post differentiation were resolved by 10% SDS-PAGE, transferred to nitrocellulose, and probed with anti-AMPK γ2 and anti-GAPDH antibodies. (A) Quantification of AMPK γ2 expression was determined by comparison with total GAPDH using densitometric analysis. Data shown represents the mean % maximum +/- S.E.M of three independent experiments. (B) Representative blots from three independent experiments. The position of the molecular weight markers are shown to the left of the gel.

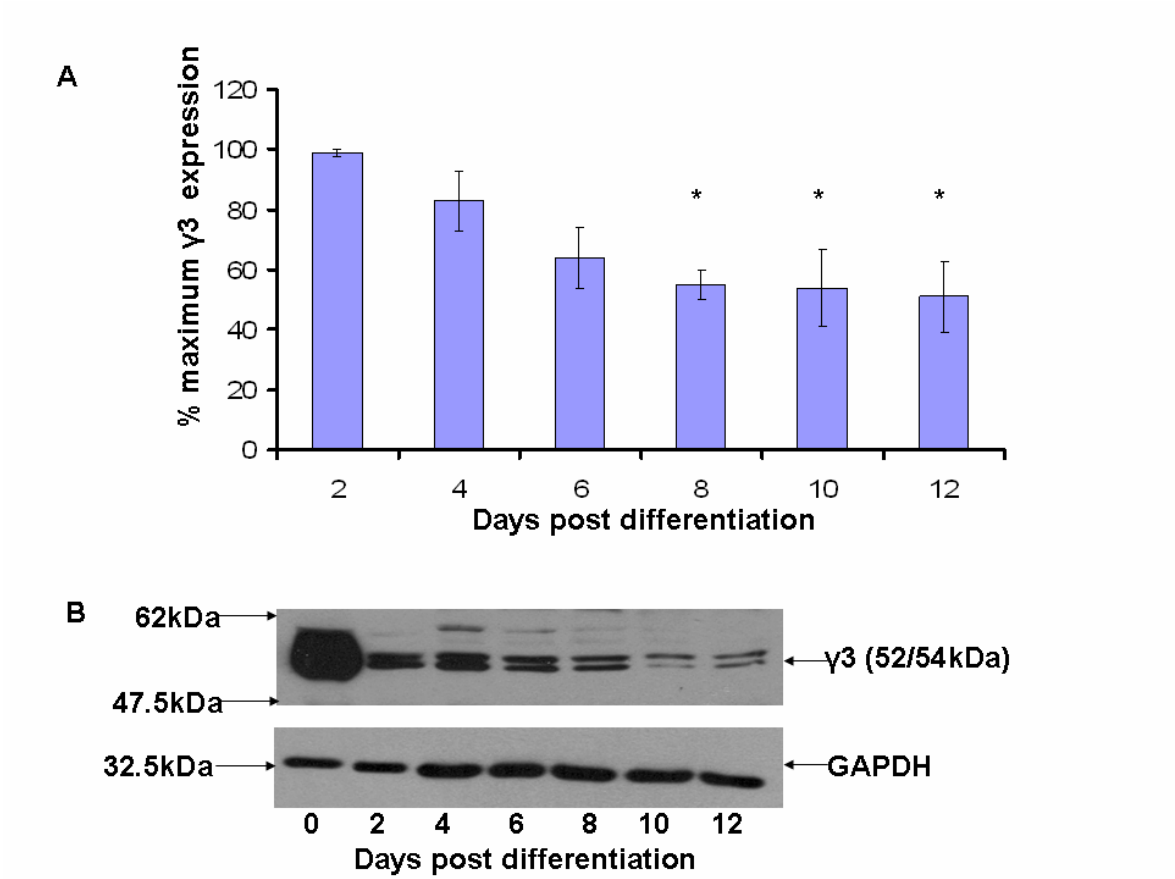

Figure 3-9: AMPK γ3 subunit expression during adipogenesis.
*Lysates (15 µg) obtained from cells at various time points post differentiation were resolved by 10% SDS-PAGE, transferred to nitrocellulose, and probed with anti-AMPK γ3 and anti-GAPDH antibodies. (A) Quantification of AMPK γ3 expression was determined by comparison with total GAPDH using densitometric analysis, *p < 0.05 (one-way ANOVA), compared to 2 days post differentiation. Data shown represents the mean % maximum +/- S.E.M of three independent experiments. (B) Representative blots from three independent experiments. The position of the molecular weight markers are shown to the left of the gel.*

3.2.3 Investigating catalytic α-subunit isoform specific AMPK activity during adipogenesis

AMPK was immunoprecipitated from fibroblasts and 3T3-L1 adipocytes in order to determine the contribution of the two catalytic AMPK subunits to total AMPK activity throughout adipogenesis. As shown below (Fig. 3.10A), the α1 subunit was found to contribute almost all of the total basal AMPK activity in both fibroblasts and adipocytes. In addition there was no significant change in total AMPK activity observed between fibroblasts and adipocytes throughout adipogenesis. To ensure that the α2 AMPK subunit was successfully immunoprecipitated from the 3T3-L1 lysates, α2 immunoprecipitates were subjected to western blotting. As shown in figure 3.10B the α2 AMPK subunit was successfully immunoprecipitated. Western blotting of the α2 AMPK subunit immunoprecipitates also clearly shows (Fig. 3.10B) that α2 AMPK subunit expression is increased throughout adipogenesis, which is in support of a previous observation (Fig. 3.4).

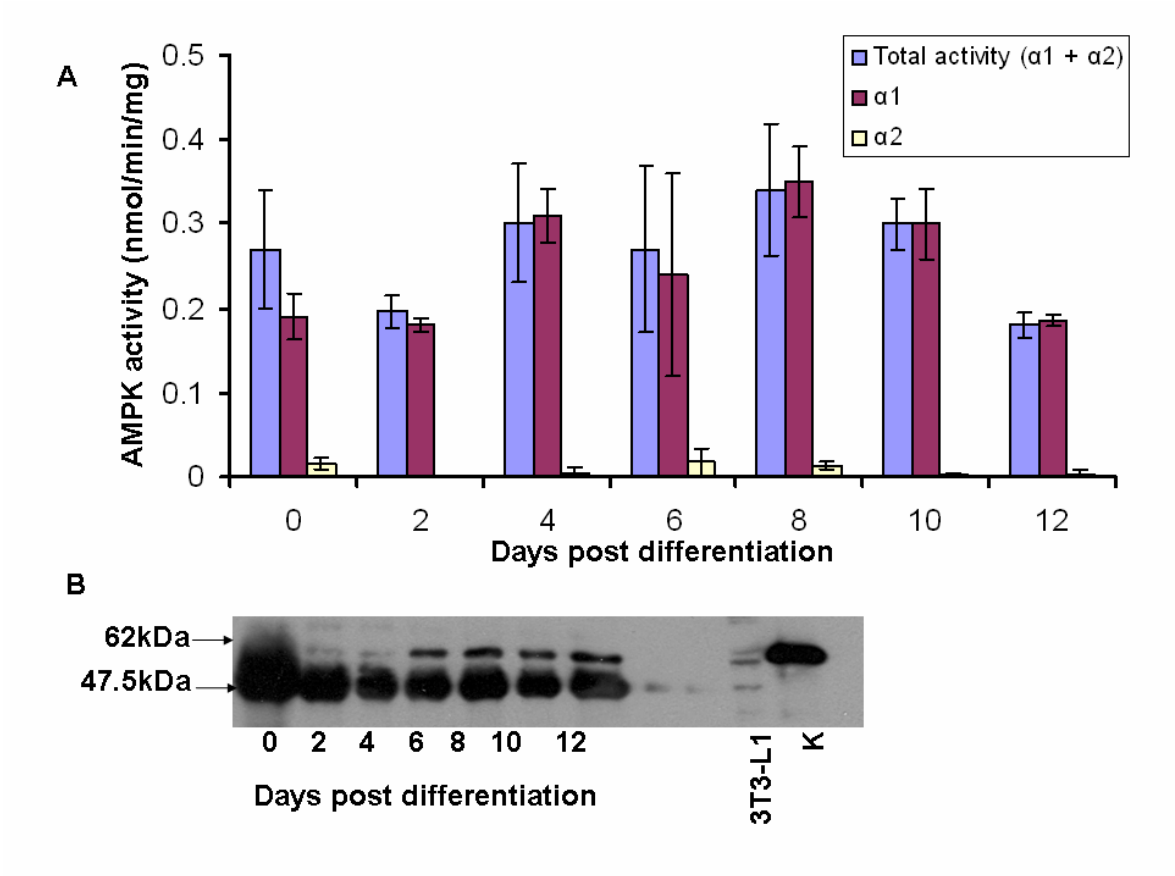

Figure 3-10: Contribution of the AMPK α1 and AMPK α2 subunits to total AMPK activity throughout adipogenesis.

Fibroblast and 3T3-L1 adipocyte lysates were prepared at the indicated time points throughout adipogenesis. Anti-α1 and anti-α2 antibodies were used to immunoprecipitate α1 containing AMPK complexes, α2 containing AMPK complexes and total AMPK complexes (α1 and α2) from 3T3-L1 lysates (100 µg). (A) Immunoprecipitates were then assayed for AMPK activity. Data shown represents the mean % basal +/- S.E.M of three independent experiments. The remaining 5 µl from the AMPK α2 immunoprecipitates were resolved on 10% SDS-PAGE, transferred to nitrocellulose and probed with anti-AMPK α2 antibody. (B) Representative blot from the three independent experiments. K=purified rat liver kinase, 3T3-L1 = adipocyte lysate (3 µg) from 12 days post differentiation. The position of the molecular weight markers are shown to the left of the gel.

3.2.4 Investigating AMPK activation parameters by various stimuli in 3T3-L1 adipocytes

Using a mixture of anti-AMPKα1 and anti-AMPKα2 antibodies, AMPK was immunoprecipitated from 3T3-L1 lysates prepared from cells incubated for various durations with different stimuli and assayed for AMPK activity. In addition, phosphorylation of AMPK at Thr172 in these lysates was also assessed by western blotting.

The AMPK activation parameters and the extent of Thr172 phosphorylation after incubation of 3T3-L1 adipocytes with 0.6 M sorbitol, 2 mM AICAR, 100 µM arsenite, 5 µM A23187, 100 µM rosiglitazone, 1 mM metformin, 1 µM isopreterenol, 5 mM sodium azide, 1 mM H_2O_2 0.1 µM leptin and 300 µM A769662, are shown below (Figs. 3.11 – 3.21).

Sorbitol

Incubation of 3T3-L1 adipocytes with sorbitol (Fig. 3.11) caused a significant ($p < 0.05$) increase, compared to the basal level, in AMPK activity after 5 min, 15 min, 30 min and 60 min. A significant ($p < 0.05$) maximum 3.71 +/- 0.54 fold increase in AMPK activity occurred after 30 min and was sustained for a further 30 min. In parallel, AMPK Thr172 phosphorylation was also increased, compared to the basal level. Statistically significant ($p < 0.05$) increases in Thr172 phosphorylation were observed after 5 min, 15 min, 30 min and 60 min, with a significant ($p < 0.05$) maximum 3.5 +/- 0.6 fold increase in Thr172 phosphorylation, occurring after 30 min.

AICAR

AICAR (Fig. 3.12) displayed a tendency to increase AMPK activity. A maximum 2.05 +/- 0.55 fold increase, compared to the basal level, in AMPK activity, occurred after 30 min, although this did not reach statistical significance ($p < 0.05$), and was sustained for a further 30 min. A maximum 1.38 +/- 0.24 fold increase, compared to the basal level, in AMPK Thr172 phosphorylation, was observed after 15 min.

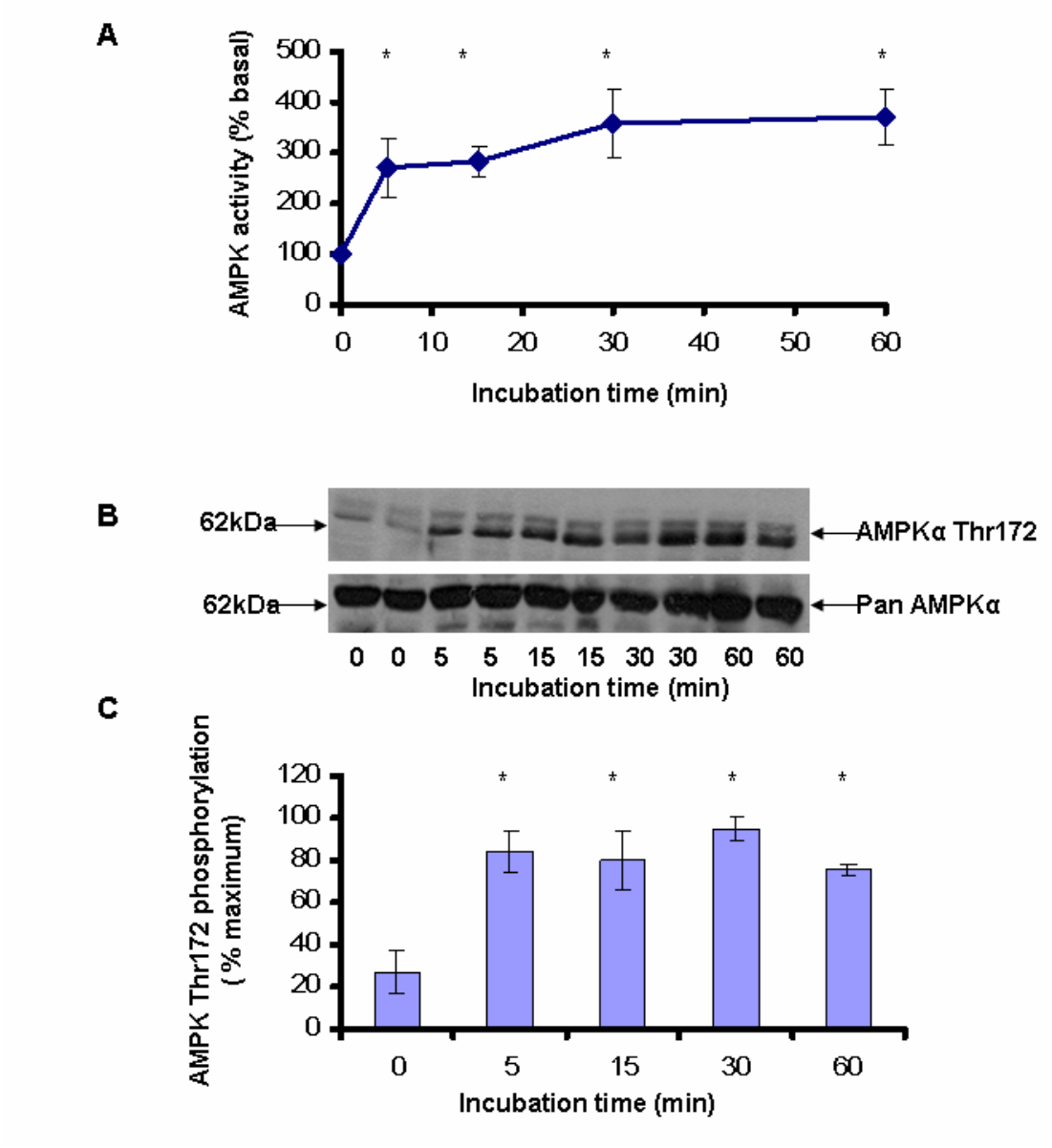

Figure 3-11: Effect of 0.6 M sorbitol on AMPK activity and Thr172 phosphorylation.
*3T3-L1 cells were incubated in 0.6 M sorbitol for various times and lysates prepared. (A) Total AMPK was immunoprecipitated from 3T3-L1 lysates (200 µg) with a mixture of anti-AMPK α1 and α2 antibodies and assayed for AMPK activity. Data shown represents the mean % basal +/- S.E.M of three independent experiments performed in duplicate, *p < 0.05 (1-tail t-test). Basal AMPK activity (nmol ^{32}P incorporated into the SAMS substrate peptide/min/mg protein) is 0.15 +/- 0.03 (mean +/- S.E.M). Lysates (30 µg) were resolved by 7% SDS-PAGE, transferred to nitrocellulose, and probed with anti-AMPKα Thr172 and anti-Pan AMPKα antibodies. (B) Representative blots are shown, from three independent experiments in duplicate. (C) Quantification of AMPKα Thr172 phosphorylation was determined by comparison with total AMPK using densitometric analysis. Data shown represents the mean % maximum +/- S.E.M of three independent experiments performed in duplicate, *p < 0.05 (one-way ANOVA).*

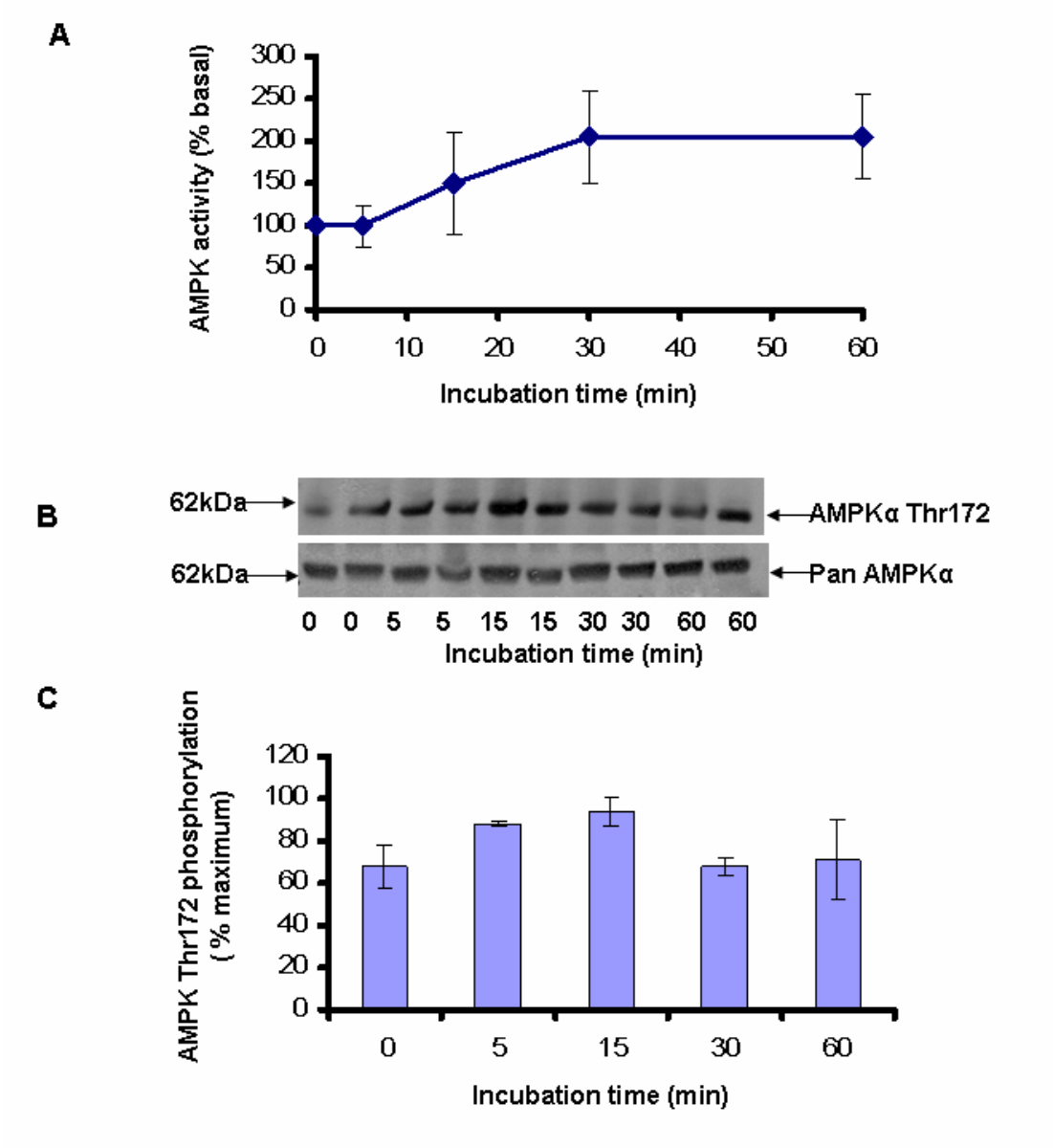

Figure 3-12: Effect of 2 mM AICAR on AMPK activity and Thr172 phosphorylation.
3T3-L1 cells were incubated in 2 mM AICAR for various times and lysates prepared. (A) Total AMPK was immunoprecipitated from 3T3-L1 lysates (200 µg) with a mixture of anti- AMPK α1 and α2 antibodies and assayed for AMPK activity. Data shown represents the mean % basal +/- S.E.M of three independent experiments performed in duplicate. Basal AMPK activity (nmol ^{32}P incorporated into the SAMS substrate peptide/min/mg protein) is 0.28 +/- 0.06 (mean +/- S.E.M). Lysates (30 µg) were resolved by 7% SDS-PAGE, transferred to nitrocellulose, and probed with anti-AMPKα Thr172 and anti-Pan AMPKα antibodies. (B) Representative blots are shown, from three independent experiments in duplicate. (C) Quantification of AMPKα Thr172 phosphorylation was determined by comparison with total AMPK using densitometric analysis. Data shown represents the mean % maximum +/- S.E.M of three independent experiments performed in duplicate.

Arsenite

There was no significant ($p < 0.05$) increase, compared to the basal level, in AMPK activity in 3T3-L1 adipocytes incubated with arsenite for various durations. However, a modest maximum 1.76 +/- 0.8 fold increase, compared to the basal level, in AMPK activity, was obtained after incubation of 3T3-L1 adipocytes with arsenite (Fig. 3.13) for 15 min. In addition, there was no significant increase, compared to the basal level, in AMPK Thr172 phosphorylation. However, a maximum 1.81 +/- 0.66 fold increase in Thr172 phosphorylation occurred after 15 min.

A23187

Incubation of 3T3-L1 adipocytes with A23187 (Fig. 3.14) displayed a modest 1.4 increase, compared to the basal level, in AMPK activity after 5 min. A significant ($p < 0.05$) maximum 1.61 +/- 0.25 fold increase in AMPK activity occurred at 60 min. There was no significant increase, compared to the basal level, in AMPK Thr172 phosphorylation. However, a maximum 1.54 +/- 0.73 fold increase in AMPK Thr172 phosphorylation occurred at 60 min.

Rosiglitazone

A significant ($p < 0.05$) increase, compared to the basal level, in AMPK activity was obtained after incubation of 3T3-L1 adipocytes in rosiglitazone (Fig. 3.15) for 5 min, 15 min and 60 min. A maximum 2.27 +/- 0.75 fold increase in AMPK activity occurred after 30 min, although this did not reach statistical significance. There was no significant increase, compared to the basal level, in AMPK Thr172 phosphorylation. However, rosiglitazone displayed a tendency to increase Thr172 phosphorylation after 15 min, and reached a maximum 1.53 +/- 0.41 fold increase after 30 min.

Metformin

Metformin (Fig. 3.16) stimulated a subtle significant ($p < 0.05$) 1.30 +/- 0.07 fold increase, compared to the basal level, in AMPK activity after 5 min in 3T3-L1 adipocytes. A maximum 1.35 +/- 0.35 fold increase was observed after 30 min, although this did not reach statistical significance ($p < 0.05$). There was no significant increase, compared to the basal level, in AMPK Thr172 phosphorylation. However, a maximum 1.79 +/- 0.51 fold increase in Thr172 phosphorylation was obtained after 5 min.

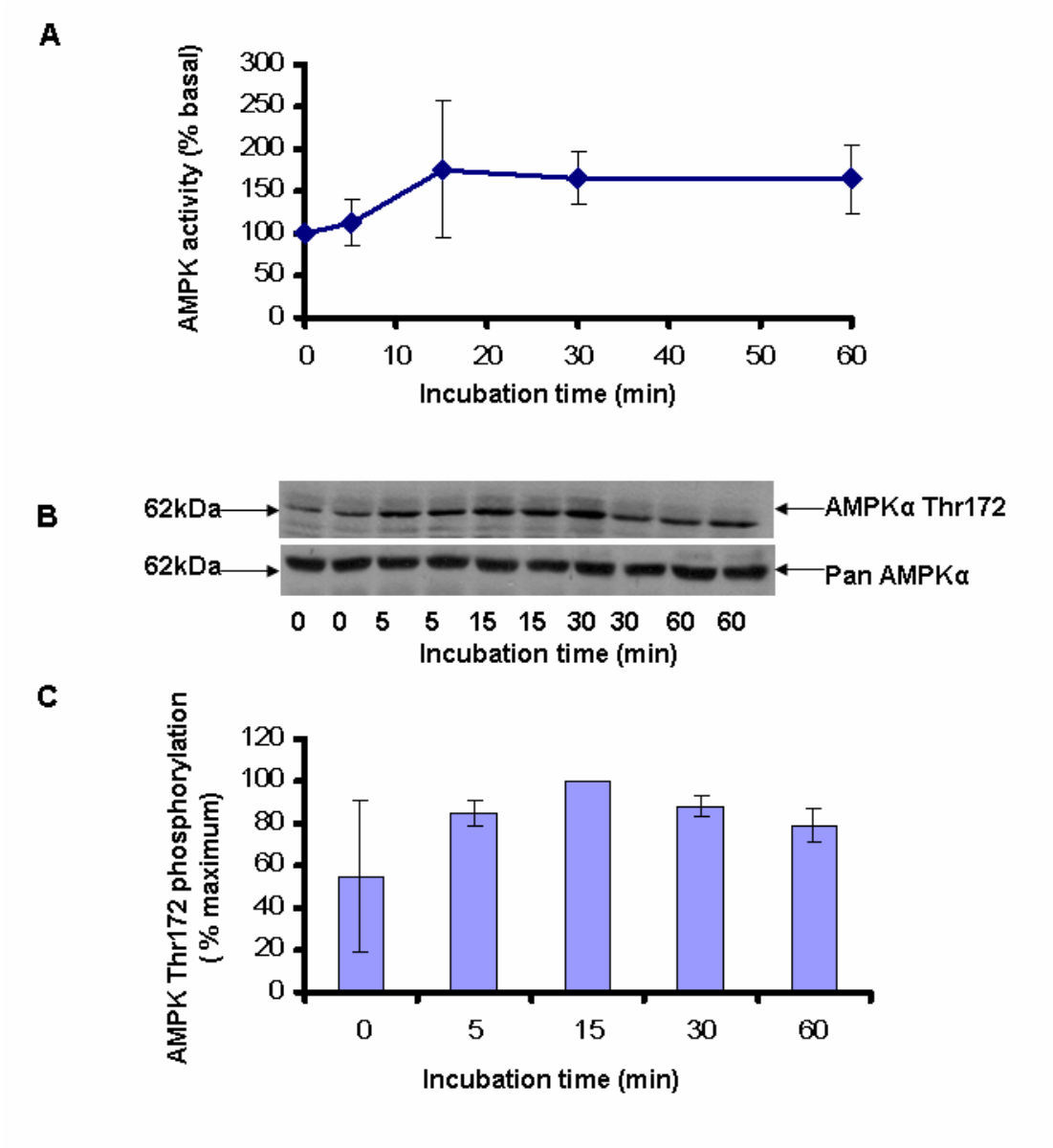

Figure 3-13: Effect of 100 µM arsenite on AMPK activity and Thr172 phosphorylation.
3T3-L1 cells were incubated in 100 µM arsenite for various times and lysates prepared. (A) Total AMPK was immunoprecipitated from 3T3-L1 lysates (200 µg) with a mixture of anti- AMPK α1 and α2 antibodies and assayed for AMPK activity. Data shown represents the mean % maximum +/- S.E.M of three independent experiments performed in duplicate. Basal AMPK activity (nmol ^{32}P incorporated into the SAMS substrate peptide/min/mg protein) is 0.14 +/- 0.01 (mean +/- S.E.M). Lysates (30 µg) were resolved by 7% SDS-PAGE, transferred to nitrocellulose, and probed with anti-AMPKα Thr172 and anti-Pan AMPKα antibodies. (B) Representative blots are shown, from three independent experiments in duplicate. (C) Quantification of AMPKα Thr172 phosphorylation was determined by comparison with total AMPK using densitometric analysis. Data shown represents the mean % maximum +/- S.E.M of three independent experiments performed in duplicate.

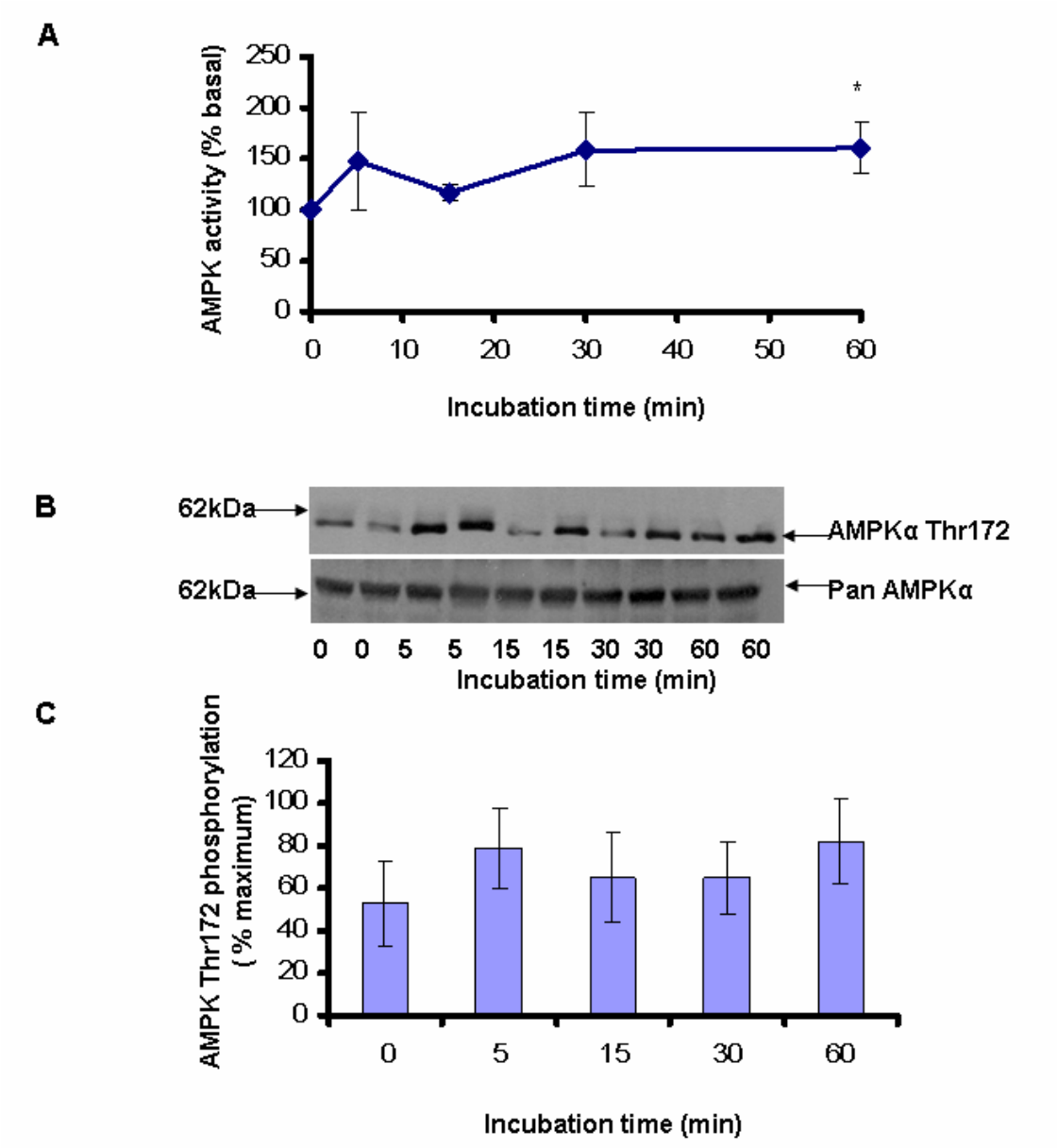

Figure 3-14: Effect of 5 µM A23187 on AMPK activity and phosphorylation.
*3T3-L1 cells were incubated in 5 µM A23187 for various times and lysates prepared. (A) Total AMPK was immunoprecipitated from 3T3-L1 lysates (200 µg) with a mixture of anti-AMPK α1 and α2 antibodies and assayed for AMPK activity. . Data shown represents the mean % maximum +/- S.E.M of three independent experiments performed in duplicate, *p < 0.05 (1-tail t-test). Basal AMPK activity (nmol ^{32}P incorporated into the SAMS substrate peptide/min/mg protein) is 0.30 +/- 0.13 (mean +/- S.E.M). Lysates (30 µg) were resolved by 7% SDS-PAGE, transferred to nitrocellulose, and probed with anti-AMPKα Thr172 and anti-Pan AMPKα antibodies. (B) Representative blots are shown, from three independent experiments in duplicate. (C) Quantification of AMPKα Thr172 phosphorylation was determined by comparison with total AMPK using densitometric analysis. Data shown represents the mean % maximum +/- S.E.M of three independent experiments performed in duplicate.*

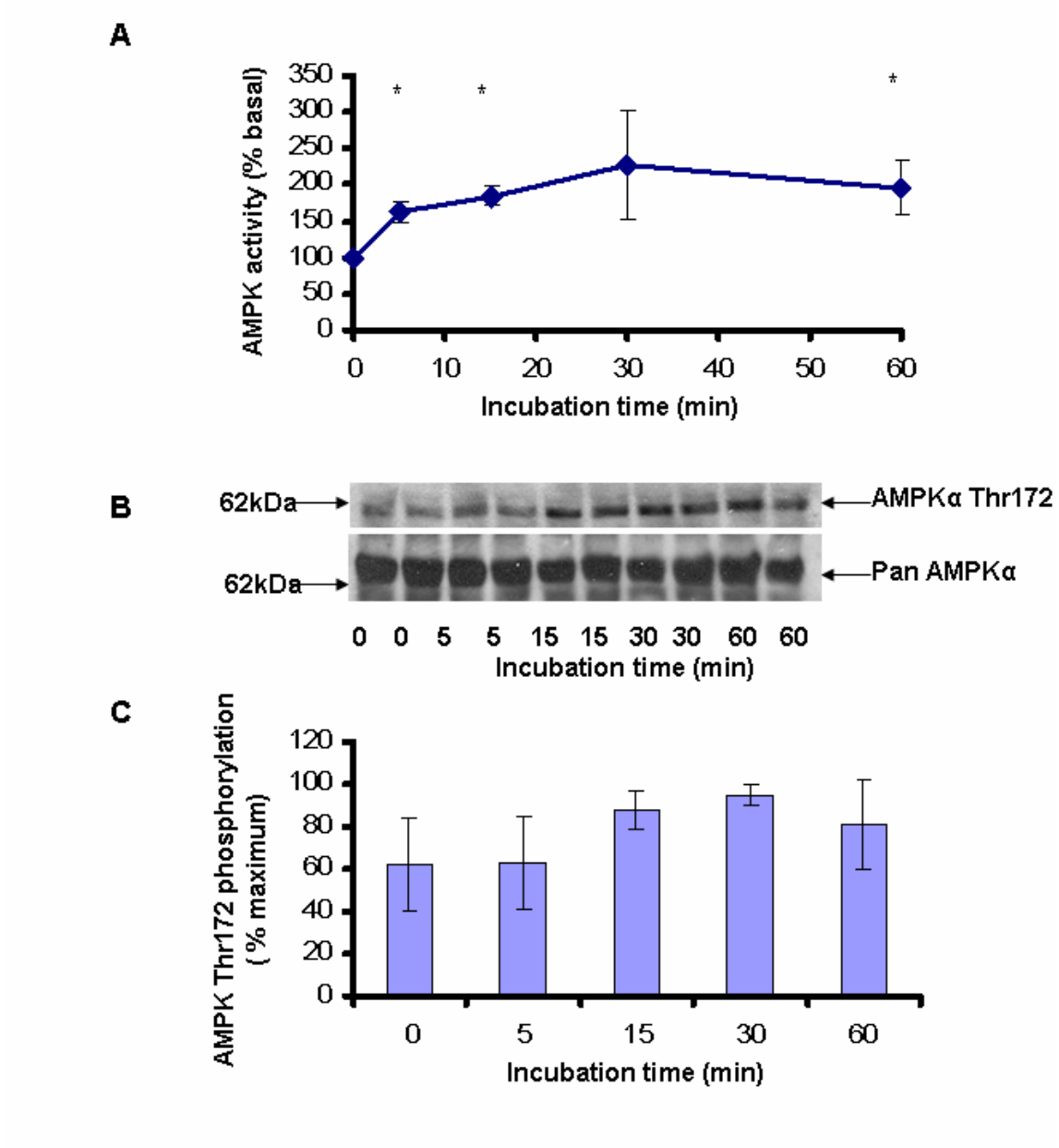

Figure 3-15: Effect of 100 µM rosiglitazone on AMPK activity and phosphorylation.
*3T3-L1 cells were incubated in 100 µM rosiglitazone for various times and lysates prepared. (A) Total AMPK was immunoprecipitated from 3T3-L1 lysates (200 µg) with a mixture of anti-AMPK α1 and α2 antibodies and assayed for AMPK activity. Data shown represents the mean % maximum +/- S.E.M of three independent experiments performed in duplicate, *p < 0.05 (1-tail t-test). Basal AMPK activity (nmol ^{32}P incorporated into the SAMS substrate peptide/min/mg protein) is 0.32 +/- 0.04 (mean +/- S.E.M). Lysates (30 µg) were resolved by 7% SDS-PAGE, transferred to nitrocellulose, and probed with anti- AMPKα Thr172 and anti-Pan AMPKα antibodies. (B) Representative blots are shown, from three independent experiments in duplicate. (C) Quantification of AMPKα Thr172 phosphorylation was determined by comparison with total AMPK using densitometric analysis. Data shown represents the mean % maximum +/- S.E.M of three independent experiments performed in duplicate.*

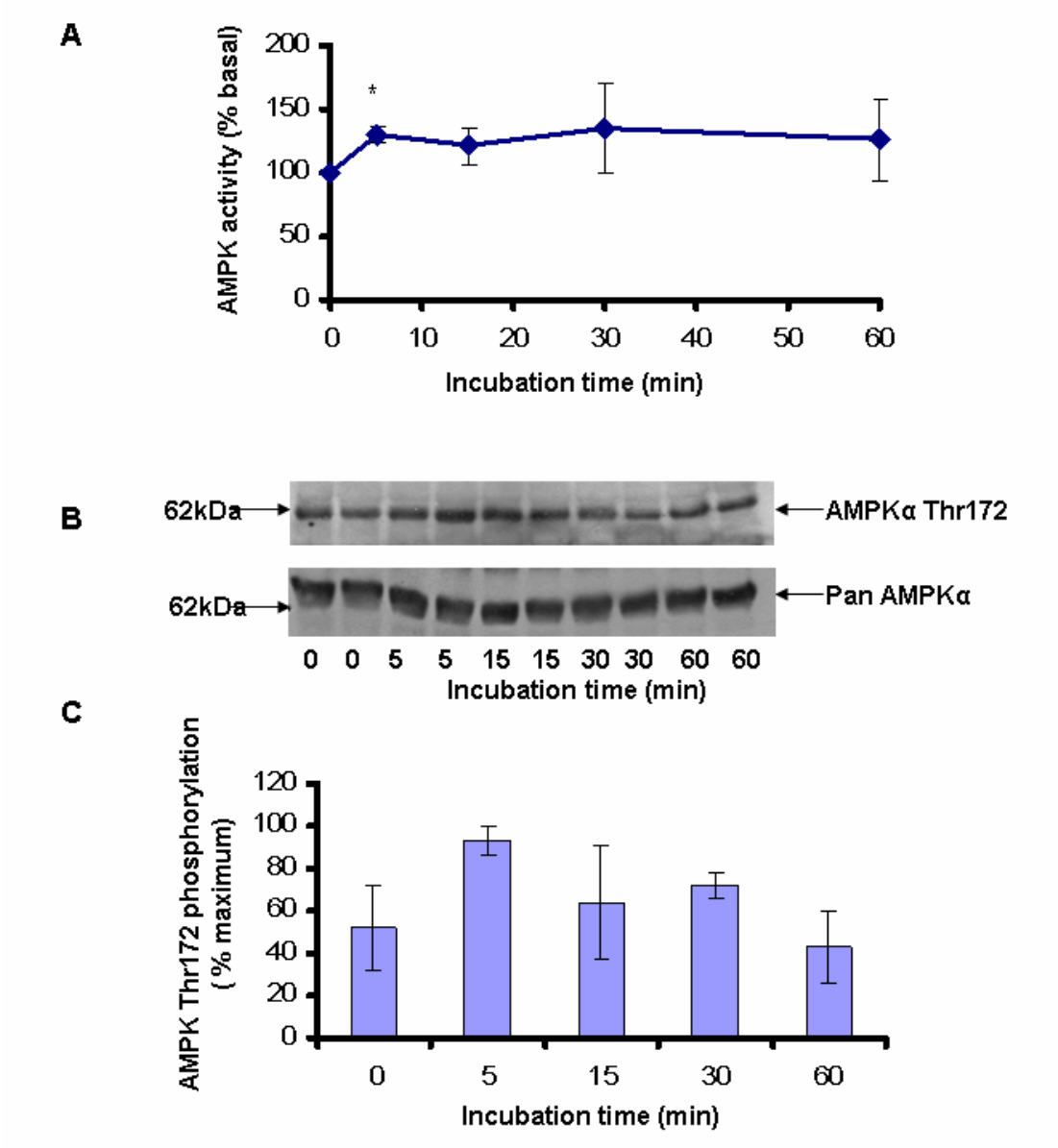

Figure 3-16: Effect of 1 mM metformin on AMPK activity and phosphorylation.
*3T3-L1 cells were incubated in 1 mM metformin for various times and lysates prepared. (A) Total AMPK was immunoprecipitated from 3T3-L1 lysates (200 µg) with a mixture of anti-AMPK α1 and α2 antibodies and assayed for AMPK activity. Data shown represents the mean % maximum +/- S.E.M of three independent experiments performed in duplicate, *p < 0.05 (1-tail t-test). Basal AMPK activity (nmol ^{32}P incorporated into the SAMS substrate peptide/min/mg protein) is 0.27 +/- 0.02 (mean +/- S.E.M). Lysates (30 µg) were resolved by 7% SDS-PAGE, transferred to nitrocellulose, and probed with anti-AMPKα Thr172 and anti-Pan AMPKα antibodies. (B) Representative blots are shown, from three independent experiments in duplicate. (C) Quantification of AMPKα Thr172 phosphorylation was determined by comparison with total AMPK using densitometric analysis. Data shown represents the mean % maximum +/- S.E.M of three independent experiments performed in duplicate.*

Isoproterenol

A significant ($p < 0.05$) (Fig. 3.17) increase, compared to the basal level, in AMPK activity was observed after incubation of 3T3-L1 adipocytes with isoproterenol for 15 min. A maximum 1.99 +/- 0.78 fold increase in AMPK activity was obtained after 30 min, although this did not reach statistical significance. There was no significant increase, compared to the basal level, in AMPK Thr172 phosphorylation. However, a maximum subtle 1.18 +/- 0.40 fold increase in Thr172 phosphorylation did occur after 15 min.

Sodium azide

Incubation of 3T3-L1 adipocytes with sodium azide (Fig. 3.18) displayed a tendency to increase AMPK activity, compared to the basal level. A maximum 3.01 +/- 0.79 fold increase was obtained after 30 min, although this did not reach statistical significance. A maximum 2.3 +/- 0.37 fold increase, compared to the basal level, in AMPK Thr172 phoshorylation was observed after incubation of the 3T3-L1 adipocytes with azide for 15 min.

Hydrogen peroxide

Incubation of 3T3-L1 adipocytes with hydrogen peroxide (Fig. 3.19) caused a significant increase, compared to the basal level, in AMPK activity after 15 min, 30 min and 60 min. A maximum 1.92 +/- 0.17 fold increase in AMPK activity occurred after 30 min, and was sustained for a further 30 min. In parallel, hydrogen peroxide displayed a significant increase, compared to the basal level, in Thr172 phosphorylation after 5 min, 15 min, 30 min and 60 min, with a maximum 3.32 +/- 0.33 fold increase in Thr172 phosphorylation occurring after 60 min.

Leptin

Incubation of 3T3-L1 adipocytes with leptin (Fig. 3.20) displayed a tendency to increase AMPK activity, compared to the basal level. A maximum 2.3 +/- 0.72 fold increase in AMPK activity occurred after 30 min, although it did not reach statistical significance. There was no significant increase, compared to the basal level, in AMPK Thr172 phosphorylation. However, a maximum 1.55 +/- 0.66 fold increase in Thr172 phosphorylation was observed at 30 min.

A769662

Incubation of 3T3-L1 adipocytes with the novel direct AMPK activator, A769662, (Fig. 3.21) caused a significant ($p < 0.05$) increase, compared to the basal level, in AMPK activity after 30 min and 60 min. A maximum 1.9 +/- 0.29 fold increase in AMPK activity was observed after 60 min. In parallel, A769662 caused an increase, compared to the basal level, in Thr172 phosphorylation after 15 min, 30 min and 60 min, with a maximum significant ($p < 0.05$) 1.92 +/- 0.10 fold increase in Thr172 phosphorylation, occurring after 60 min.

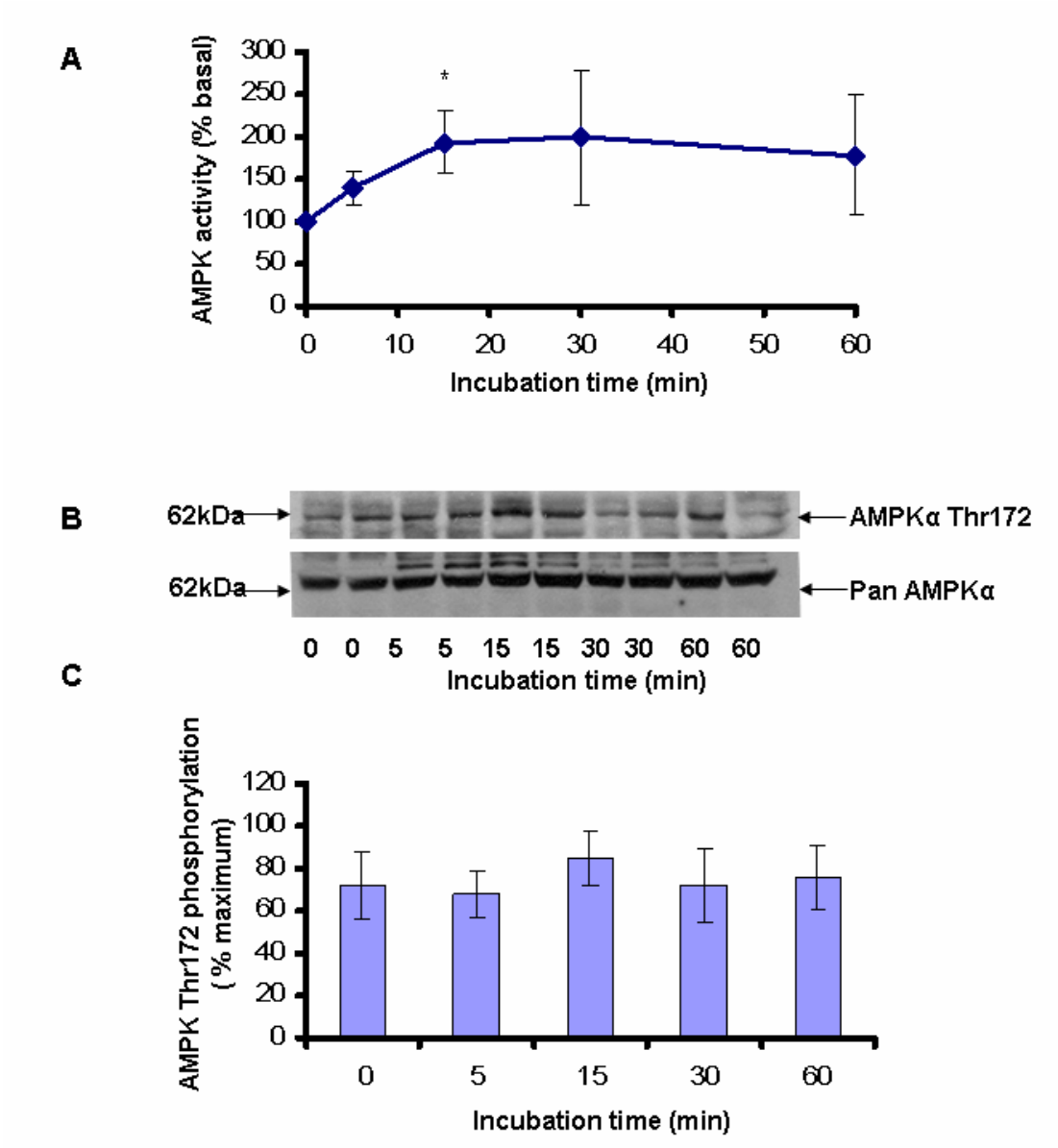

Figure 3-17: Effect of 1 µM isoproterenol on AMPK activity in 3T3-L1 adipocytes
*3T3-L1 cells were incubated in 1 µM isoproterenol for various times and lysates prepared. (A) Total AMPK was immunoprecipitated from 3T3-L1 lysates (200 µg) with a mixture of anti-AMPK α1 and α2 antibodies and assayed for AMPK activity. Data shown represents the mean % maximum +/- S.E.M of three independent experiments performed in duplicate, *p < 0.05 (1-tail t-test). Basal AMPK activity (nmol ^{32}P incorporated into the SAMS substrate peptide/min/mg protein) is 0.36 +/- 0.16 (mean +/- S.E.M). Lysates (30 µg) were resolved by 7% SDS-PAGE, transferred to nitrocellulose, and probed with anti-AMPKα Thr172 and anti-Pan AMPKα antibodies. (B) Representative blots are shown, from three independent experiments in duplicate. (C) Quantification of AMPKα Thr172 phosphorylation was determined by comparison with total AMPK using densitometric analysis. Data shown represents the mean % maximum +/- S.E.M of three independent experiments performed in duplicate.*

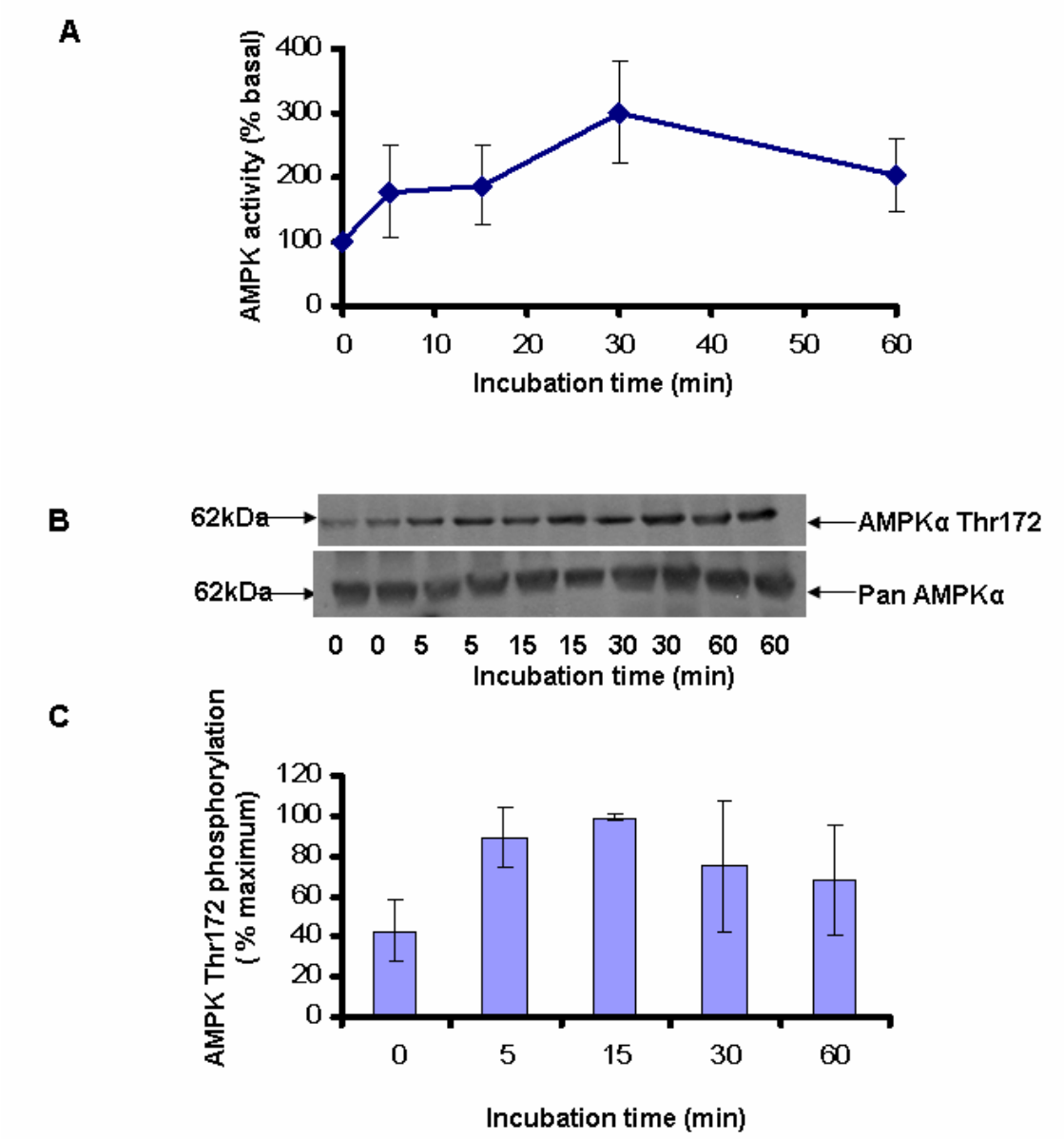

Figure 3-18: Effect of 5 mM sodium azide on AMPK activity and phosphorylation.
3T3-L1 cells were incubated in 5 mM sodium azide for various times and lysates prepared. (A) Total AMPK was immunoprecipitated from 3T3-L1 lysates (200 µg) with a mixture of anti-AMPK α1 and α2 antibodies and assayed for AMPK activity. Data shown represents the mean % maximum +/- S.E.M of three independent experiments performed in duplicate. Basal AMPK activity (nmol ^{32}P incorporated into the SAMS substrate peptide/min/mg protein) is 0.40 +/- 0.04 (mean +/- S.E.M). Lysates (30 µg) were resolved by 7% SDS-PAGE, transferred to nitrocellulose, and probed with anti-AMPKα Thr172 and anti-Pan AMPKα antibodies. (B) Representative blots are shown, from three independent experiments in duplicate. (C) Quantification of AMPKα Thr172 phosphorylation was determined by comparison with total AMPK using densitometric analysis. Data shown represents the mean % maximum +/- S.E.M of two independent experiments performed in duplicate.

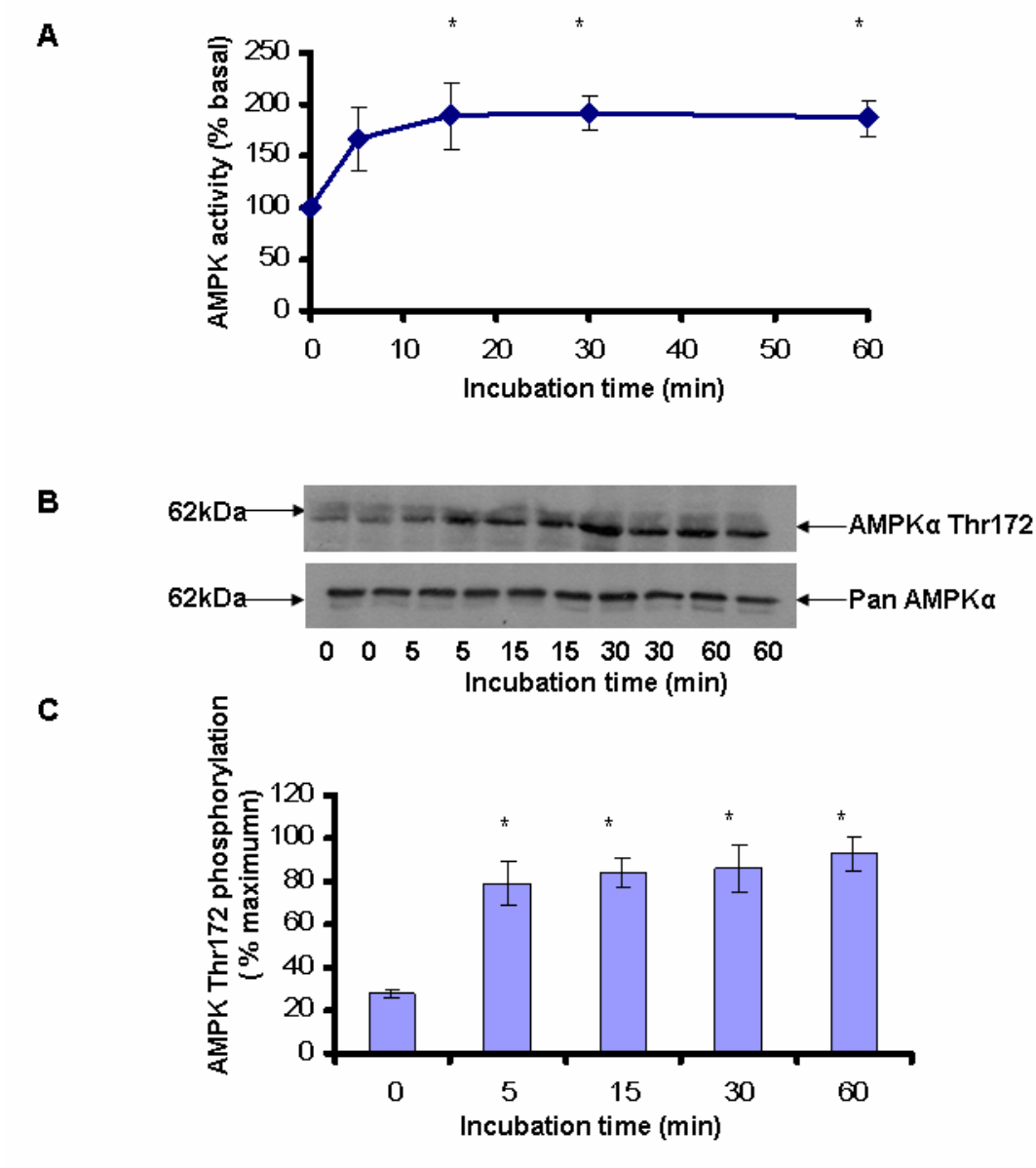

Figure 3-19: Effect of 1 mM hydrogen peroxide on AMPK activity and phosphorylation.
*3T3-L1 cells were incubated in 1 mM hydrogen peroxide for various times and lysates prepared. (A) Total AMPK was immunoprecipitated from 3T3-L1 lysates (200 µg) with a mixture of anti-AMPK α1 and α2 antibodies and assayed for AMPK activity. Data shown represents the mean % maximum +/- S.E.M of three independent experiments performed in duplicate, *p < 0.05 (1-tail t-test). Basal AMPK activity (nmol ^{32}P incorporated into the SAMS substrate peptide/min/mg protein) is 0.10 +/- 0.01 (mean +/- S.E.M). Lysates (30 µg) were resolved by 7% SDS-PAGE, transferred to nitrocellulose, and probed with anti-AMPKα Thr172 and anti-Pan AMPKα antibodies. (B) Representative blots are shown, from three independent experiments in duplicate. (C) Quantification of AMPKα Thr172 phosphorylation was determined by comparison with total AMPK using densitometric analysis. Data shown represents the mean % maximum +/- S.E.M of three independent experiments performed in duplicate, *p < 0.05 (one-way ANOVA).*

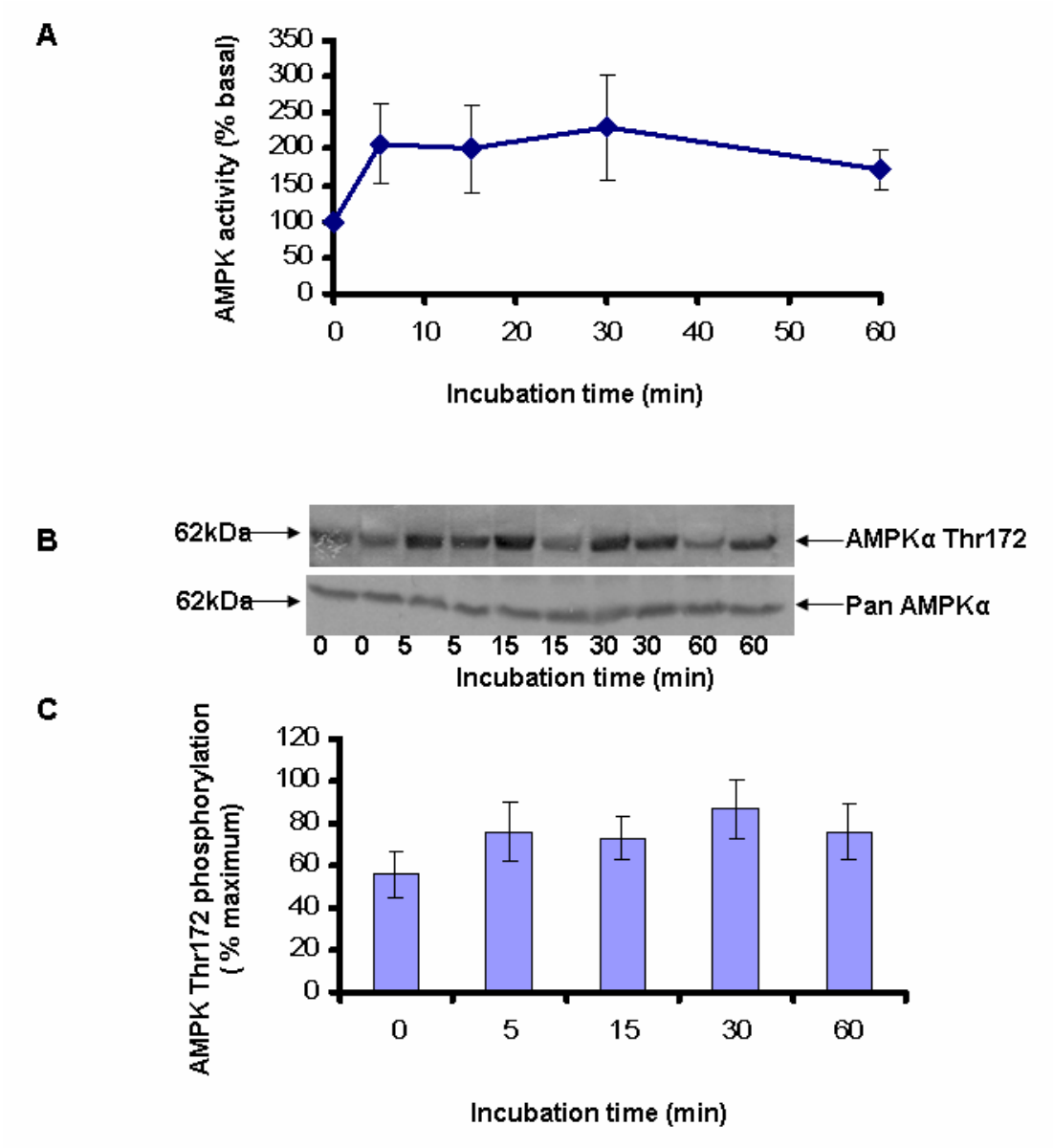

Figure 3-20: Effect of 0.1 µM leptin on AMPK activity and phosphorylation.
*3T3-L1 cells were incubated in 0.1 µM leptin for various times and lysates prepared. (A) Total AMPK was immunoprecipitated from 3T3-L1 lysates (200 µg) with a mixture of anti-AMPK α1 and α2 antibodies and assayed for AMPK activity. Data shown represents the mean % maximum +/- S.E.M of three independent experiments performed in duplicate, *p < 0.05 (1-tail). Basal AMPK activity (nmol ^{32}P incorporated into the SAMS substrate peptide/min/mg protein) is 0.28 +/- 0.14 (mean +/- S.E.M). Lysates (30 µg) were resolved by 7% SDS-PAGE, transferred to nitrocellulose, and probed with anti-AMPKα Thr172 and anti-Pan AMPKα antibodies. (B) Representative blots are shown, from three independent experiments in duplicate. (C) Quantification of AMPKα Thr172 phosphorylation was determined by comparison with total AMPK using densitometric analysis. . Data shown represents the mean % maximum +/- S.E.M of three independent experiments performed in duplicate.*

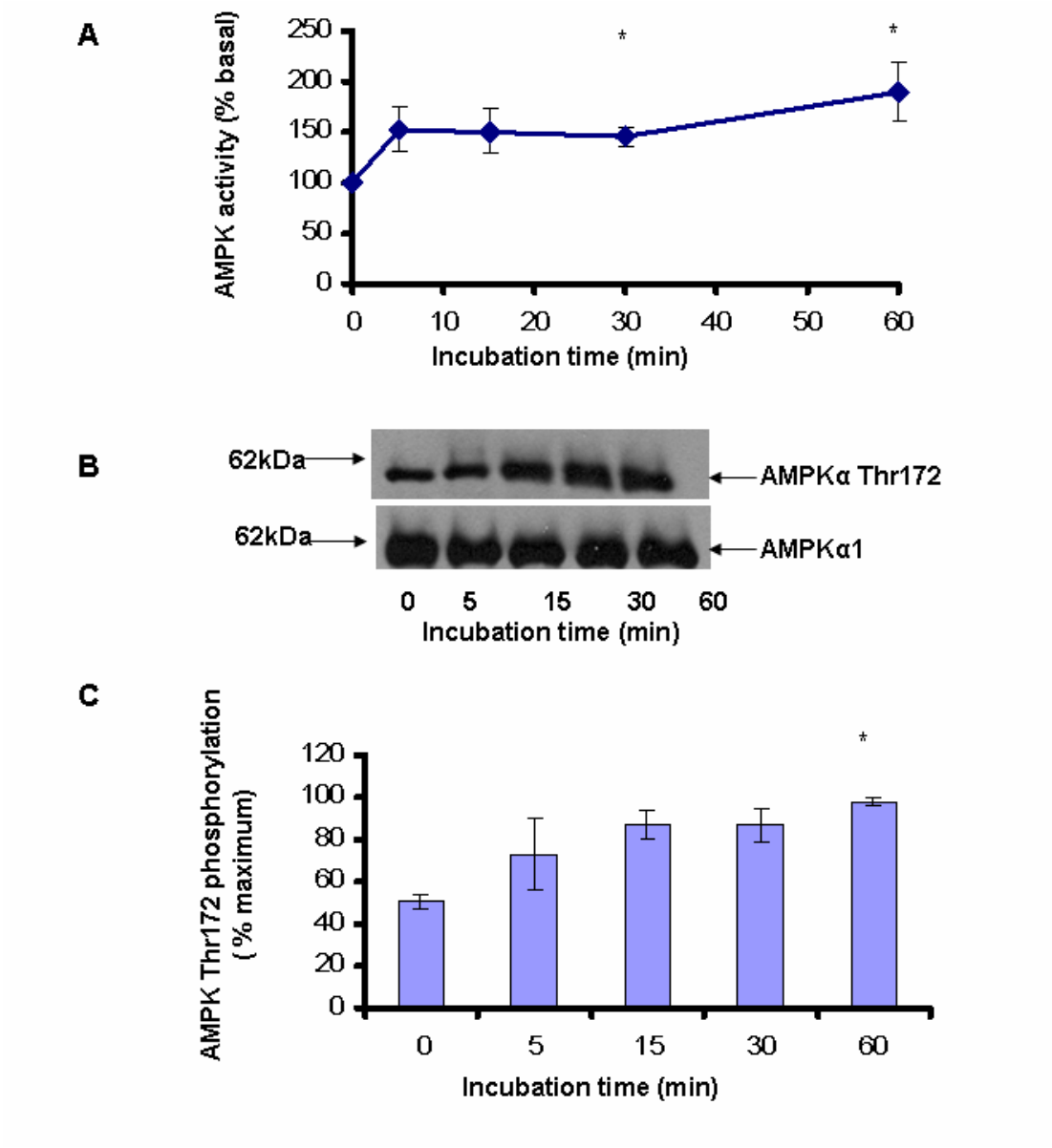

Figure 3-21: Effect of 300 µM A769662 on AMPK activity and phosphorylation.
*3T3-L1 cells were incubated in 300 µM A769662 for various times and lysates prepared. (A) Total AMPK was immunoprecipitated from 3T3-L1 lysates (200 µg) with a mixture of anti-AMPK α1 and α2 antibodies and assayed for AMPK activity. Data shown represents the mean % maximum +/- S.E.M of three independent experiments, *p < 0.05 (1-tail t-test). Basal AMPK activity (nmol ^{32}P incorporated into the SAMS substrate peptide/min/mg protein) is 0.25 +/- 0.025 (mean +/- S.E.M). Lysates (30 µg) were resolved by 7% SDS-PAGE, transferred to nitrocellulose, and probed with anti-AMPKα Thr172 and anti-AMPKα1 antibodies. (B) Representative blots are shown, from three independent experiments in duplicate. (C) Quantification of AMPKα Thr172 phosphorylation was determined by comparison with total AMPK using densitometric analysis. Data shown represents the mean % maximum +/- S.E.M of three independent experiments, *p < 0.05 (one-way ANOVA).*

3.2.5 Investigation of the molecular mechanism of AMPK activation by various stimuli in 3T3-L1 adipocytes

3.2.5.1 Effect of STO-609 on AMPK activity in response to various stimuli

To determine whether any of the stimuli activate AMPK via CaMKK in 3T3-L1 adipocytes, the cells were treated with the different stimuli, in the presence or absence of the CaMKK inhibitor STO-609 (Tokumitsu *et al* 2002). AMPK was immunoprecipitated with a mixture of anti-AMPKα1 and anti-AMPKα2 antibodies, and total AMPK activity assayed.

In the presence of STO-609, A23187-stimulated AMPK activity was significantly ($p < 0.05$) abrogated. A statistically significant ($p < 0.05$) increase in AMPK activity was obtained from AICAR, sorbitol and azide in the presence and absence of STO-609, isoproterenol, metformin, arsenite and A23187 in the absence of STO-609 and rosiglitazone in the presence of STO-609. AMPK stimulated activity by all these activators, apart from A23187, was not significantly altered in the presence of STO-609. Leptin and hydrogen peroxide, in the presence and absence of STO-609, did not cause a significant ($p < 0.05$) increase in AMPK activity compared to basal levels.

These results suggest these activators, apart from A23187, may activate AMPK via a CaMKK independent pathway (Fig. 3.22).

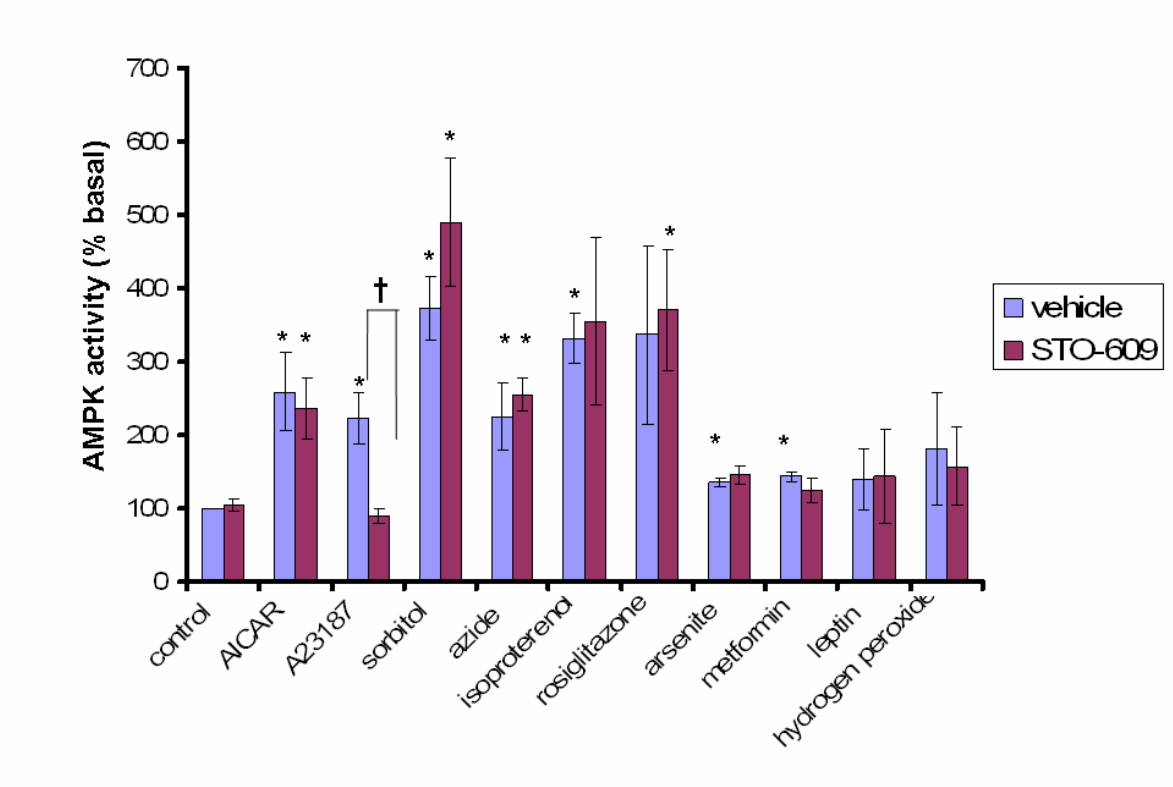

Figure 3-22: Effect of STO-609 on AMPK activity, stimulated by different AMPK activators. *Lysates were prepared from cells pre-incubated in the presence and absence of the CaMKK inhibitor STO-609 (25 μM) for 20 min, prior to the addition of 5 mM sodium azide, 0.6 M sorbitol, 2 mM AICAR, 5 μM A23187, 100 μM rosiglitazone, 1 mM metformin, 1 μM isopreterenol, 1 mM H_2O_2 and 0.1 μM leptin for 30 min or 100 μM arsenite for 15 min. Total AMPK activity was immunoprecipitated from the 3T3-L1 lysates (200 μg) with a mixture of anti-AMPK α1 and α2 antibodies and assayed for AMPK activity. Data shown represents the mean % basal +/- S.E.M of three independent experiments performed in duplicate, *p < 0.05 (1-tail t-test), increase in AMPK activity, relative to control. †p < 0.05 (2-tail t-test), compared to the presence of STO-609. Basal AMPK activity was 0.315 +/- 0.03 nmol/min/mg (SEM).*

3.2.5.2 Effect of various stimuli on the AMP/ATP and ADP/ATP ratios

HPLC was used to determine whether any of the AMPK activators caused a change in the cellular adenine nucleotide ratios (AMP/ATP or ADP/ATP).

The elution times of AMP, ADP, and ATP are shown below (Fig. 3.23).

To ensure that other common nucleosides/nucleotides did not have an elution time that would mask the AMP, ADP or ATP peaks, the elution times of the candidate molecules; adenosine, cAMP and ZMP were determined. It was established that these molecules had distinct elution times, as shown below (Fig. 3.24-3.26).

As AICAR is phosphorylated to the nucleotide ZMP in cells, nucleotide extracts from AICAR-treated cells were subjected to HPLC to ensure separation and identification of the ZMP/AMP peaks. Analysis (Figs. 3.27 and 3.28) of the chromatogram from the nucleotide extract of AICAR treated cells, suggested that the peaks occurring at 4.4 min and 5.4 min are ZMP and AICAR respectively.

3T3-L1 adipocytes were incubated in the presence of various stimuli, prior to nucleotide extraction and analysis using HPLC. A significant ($p < 0.05$) 4.14 +/- 0.38, 4.14 +/- 0.96 and 2.71 +/- 0.38 fold increase in the ADP/ATP ratio, compared to basal level, was observed in cells incubated in the presence of isoproterenol, sodium azide, and rosiglitazone respectively (Fig. 3.29).

None of the AMPK stimuli produced a significant fold increase in the AMP/ATP ratio, compared to basal level. However, isoproterenol, sodium azide, rosiglitazone and AICAR all displayed a tendency to increase the AMP/ATP ratio compared to basal levels.

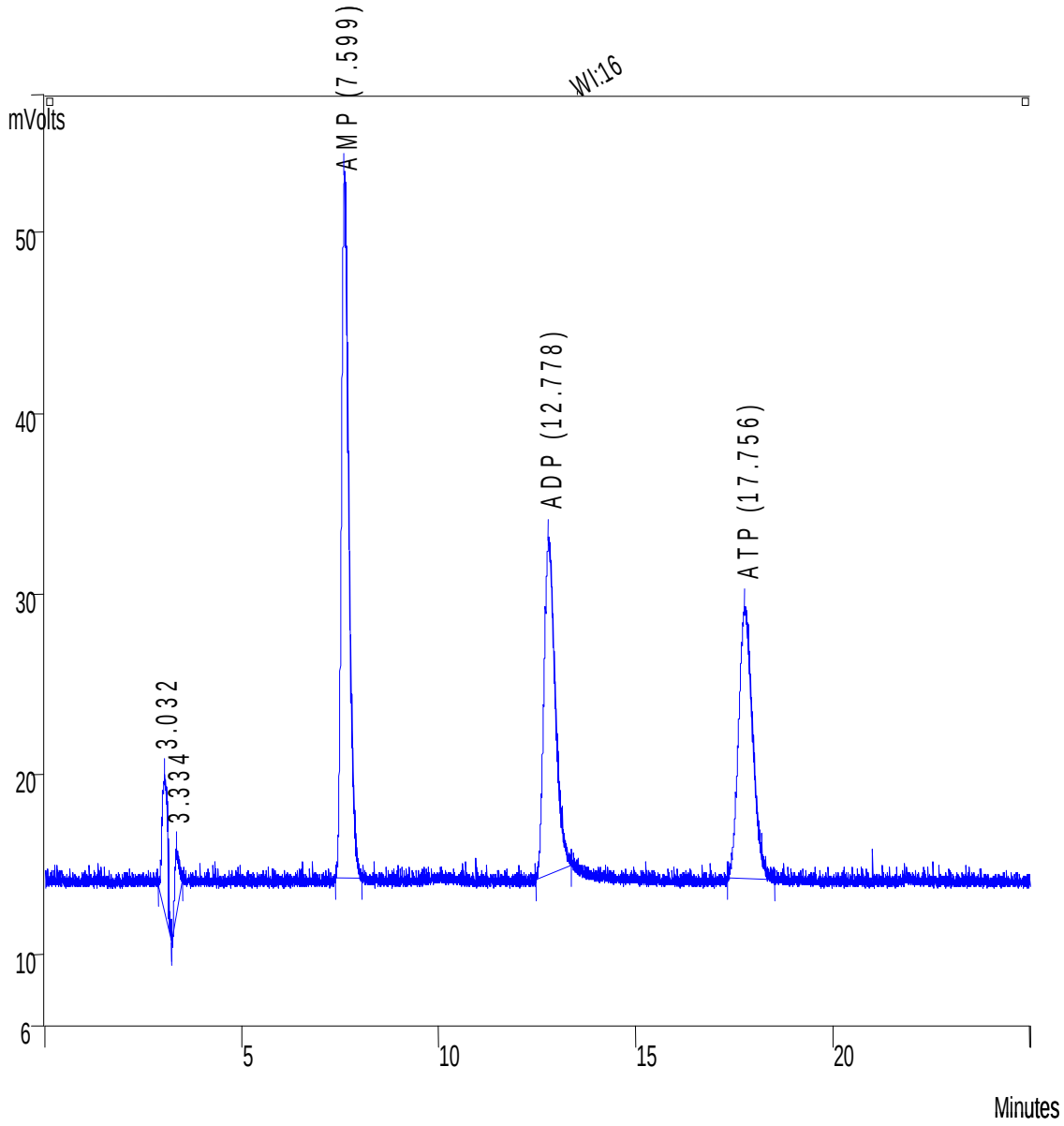

Figure 3-23: Elution times of AMP, ADP and ATP.
HPLC analysis, as described in section 2.2.9, of a mixture of 1 nmol each of AMP, ADP and ATP. Individual runs of each nucleotide were performed in order to identify the elution time for each molecule (data not shown).

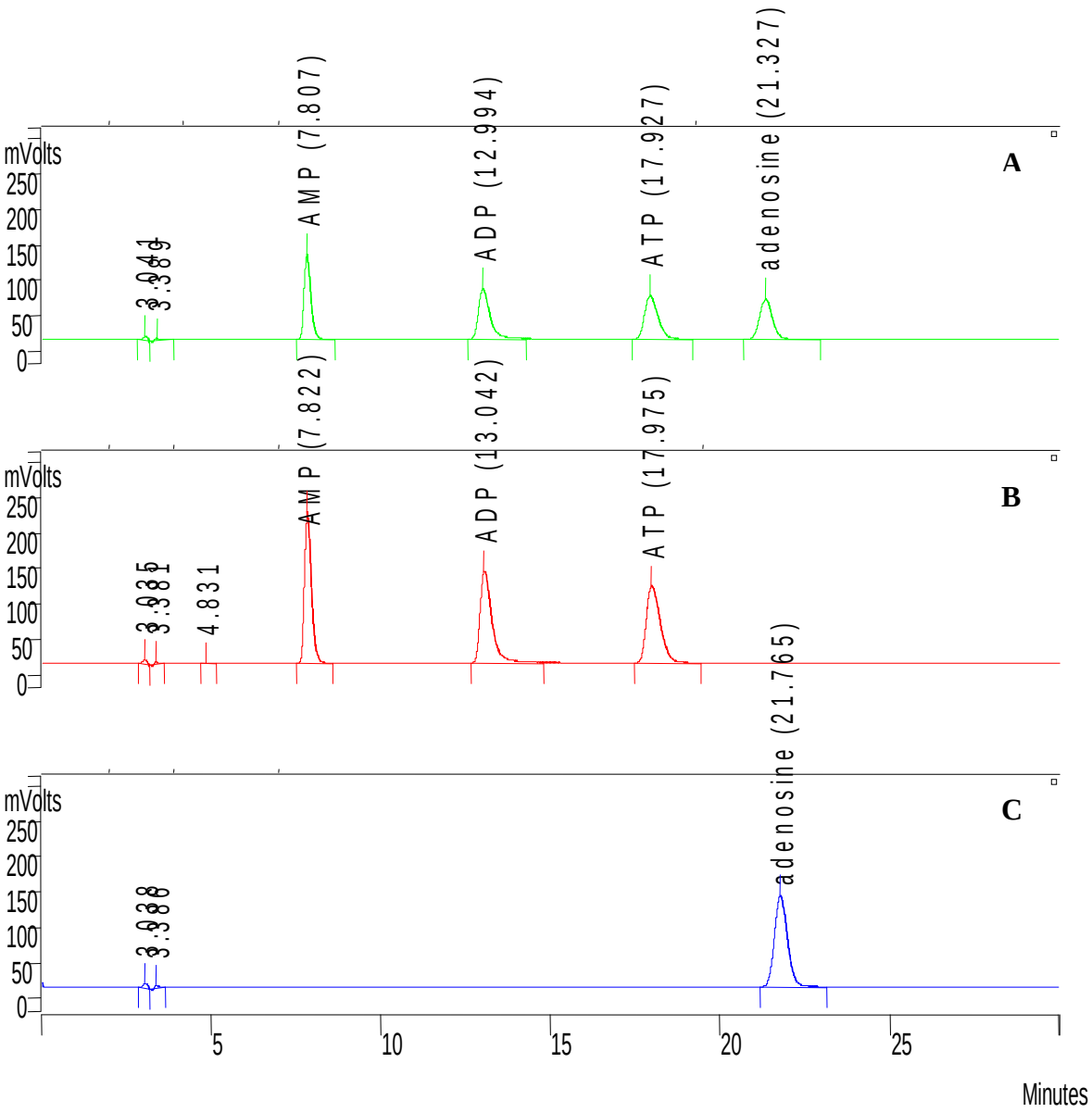

Figure 3-24: Elution time of adenosine.
HPLC analysis, as described in section 2.2.9, of (A) a mixture of 2.5 nmol each of AMP, ADP, ATP and adenosine, (B) a mixture of 5 nmol each of AMP, ADP and ATP, and (C) 5 nmol adenosine.

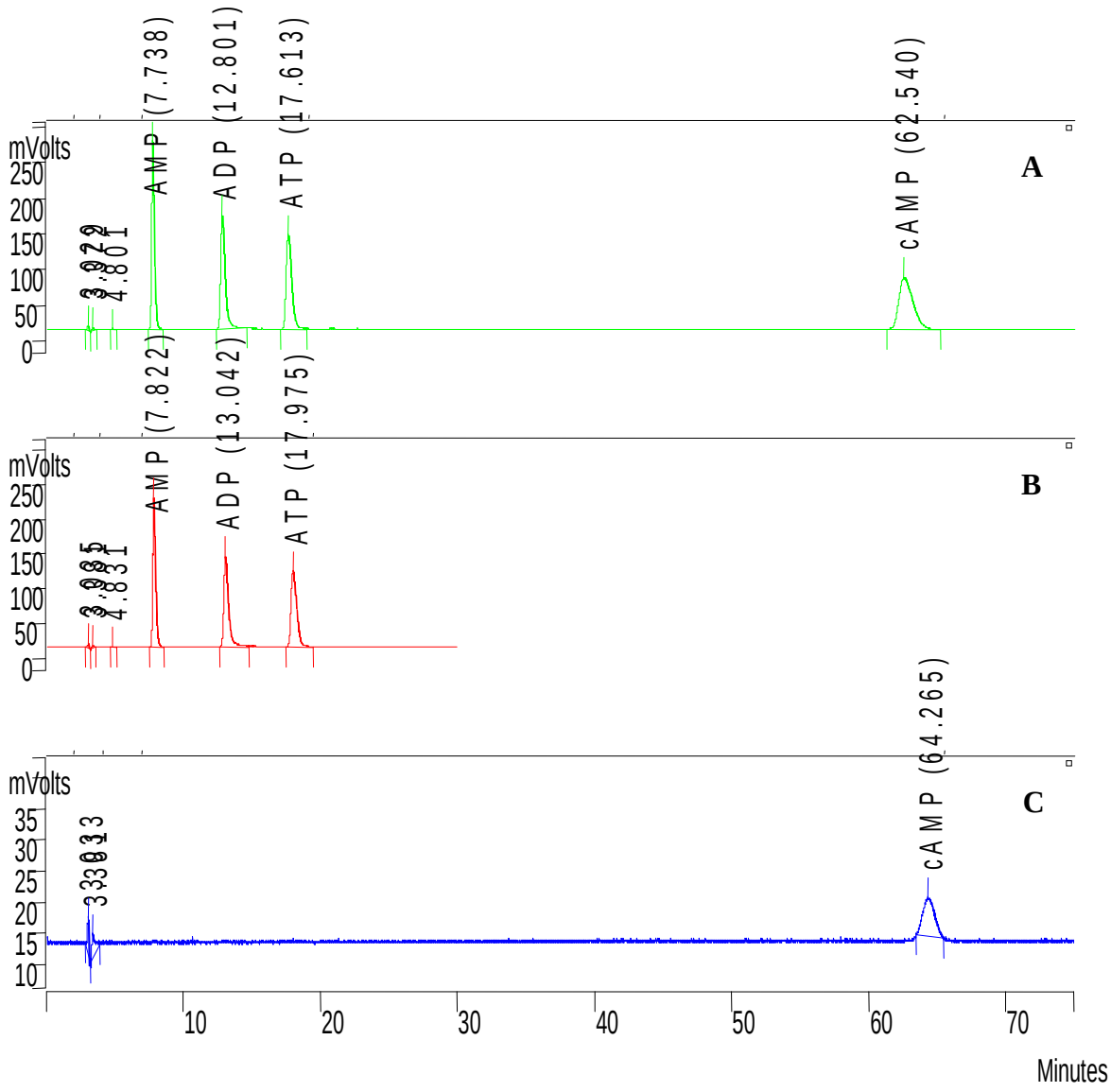

Figure 3-25: Elution time of cAMP.
HPLC analysis, as described in section 2.2.9, of (A) a mixture of 5 nmol each of AMP, ADP, ATP and cAMP, (B) a mixture of 5 nmol each of AMP, ADP and ATP, and (C) 1 nmol cAMP.

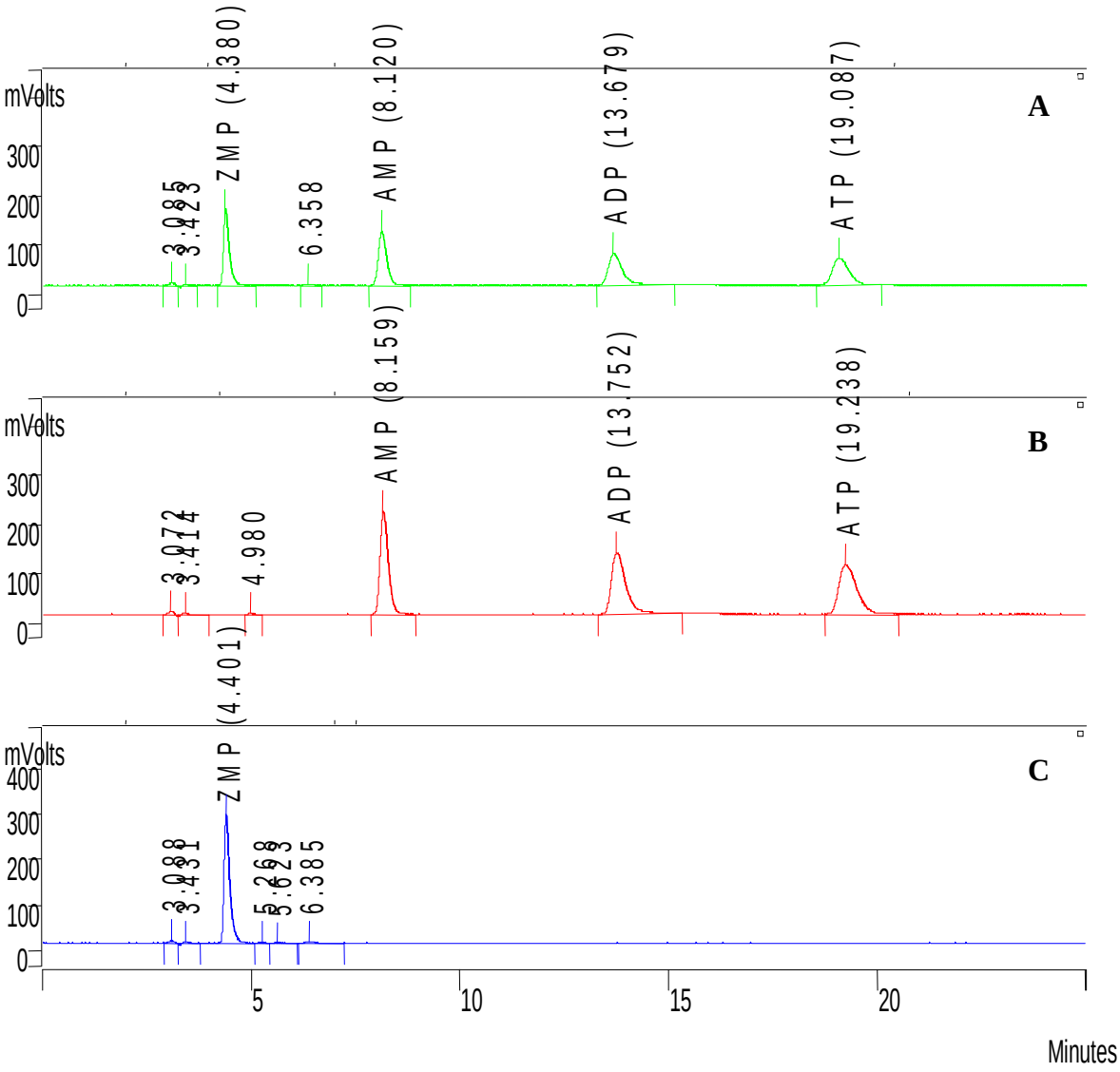

Figure 3-26: Elution time of ZMP.
HLPC analysis, as described in section 2.2.9 of (A) a mixture of 2.5 nmol each of AMP, ADP, ATP and ZMP, (B) a mixture of 5 nmol each of AMP, ADP and ATP, and (C) 5 nmol ZMP.

.

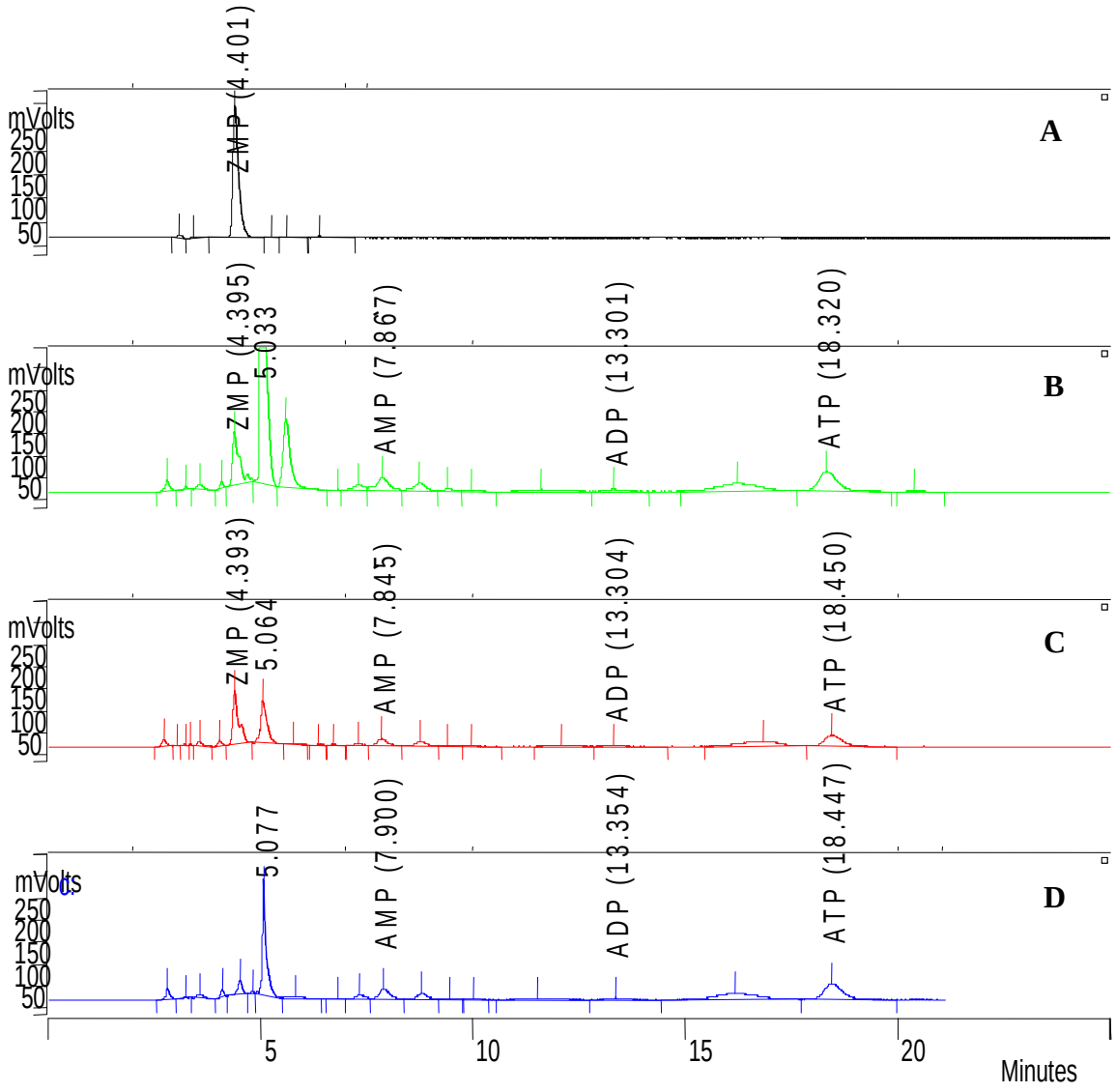

Figure 3-27: Identification of a ZMP peak in a nucleotide extract from AICAR treated cells using HPLC.

HPLC analysis, as described in section 2.2.9, of (A) 5 nmol ZMP, (B) a nucleotide extract obtained from AICAR treated cells, (C) a nucleotide extract obtained from control cells, spiked with 2.5 nmol ZMP and (D) a nucleotide extract obtained from control cells.

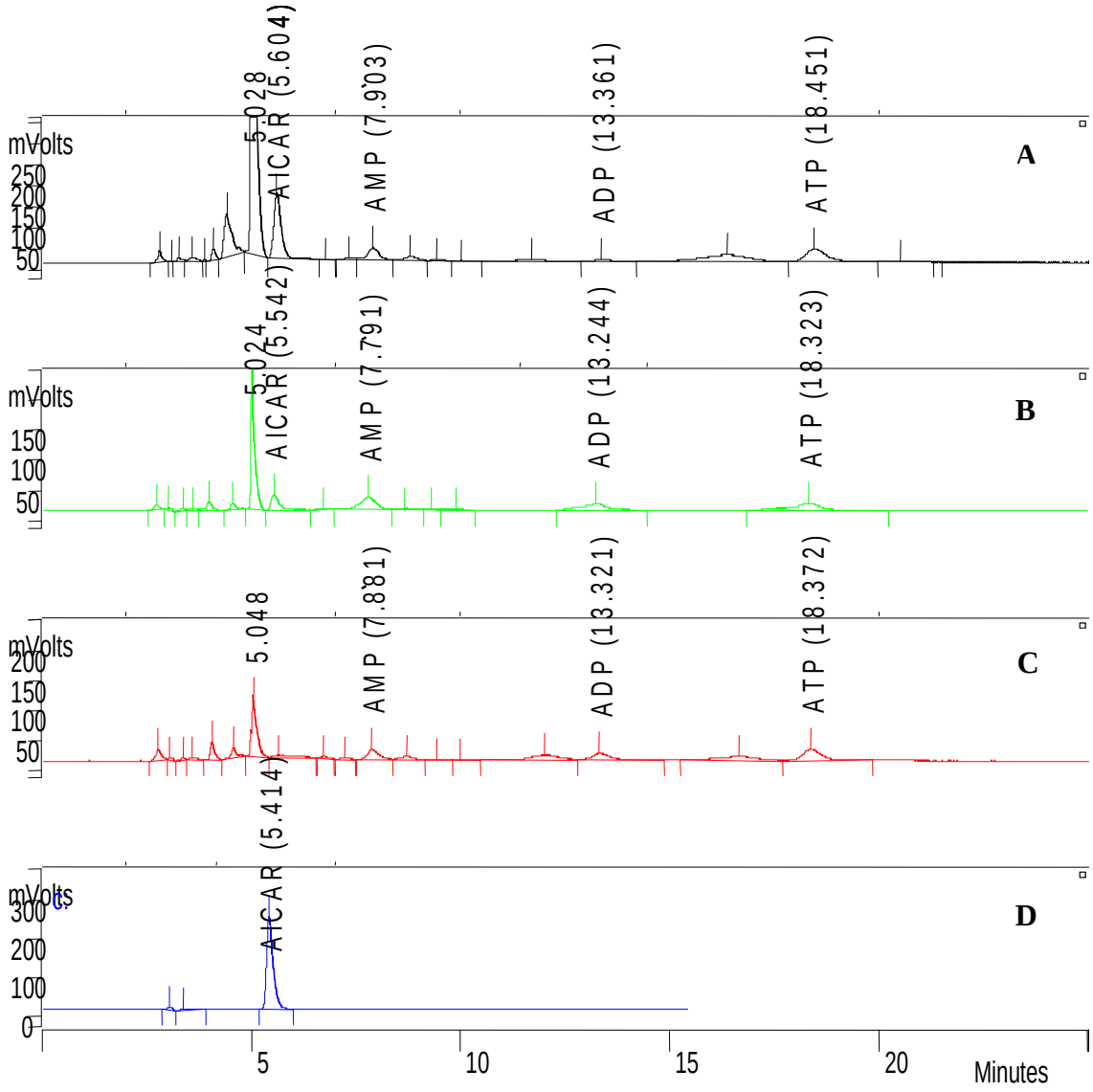

Figure 3-28: Identification of an AICAR peak in a nucleotide extract from AICAR treated cells using HPLC.

HPLC analysis, as described in section 2.2.9, of (A) a nucleotide extract obtained from AICAR treated cells, (B) a nucleotide extract obtained from control cells, spiked with 1 nmol AICAR, (C) a nucleotide extract obtained from control cells and (D)5 nmol AICAR.

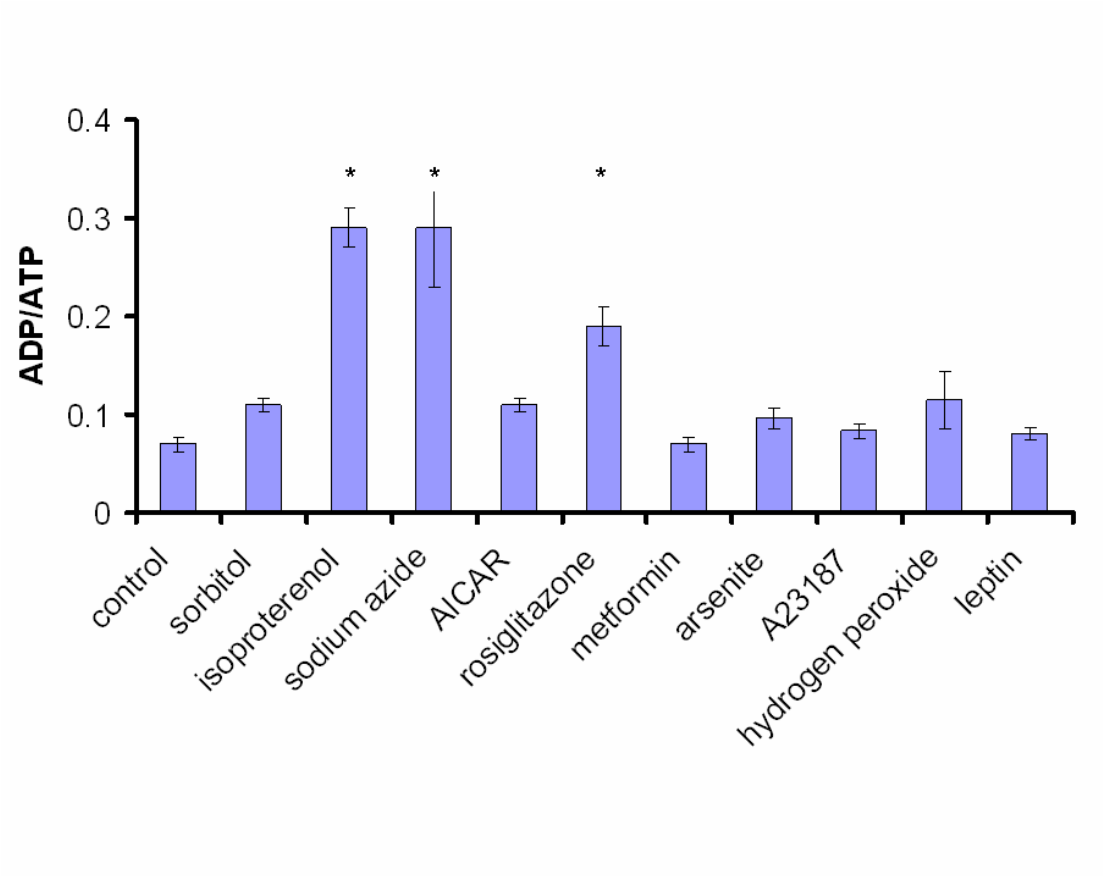

Figure 3-29: The effect of various AMPK activators on the ADP/ATP ratio.
*Nucleotide extracts were prepared from cells incubated for 15 min in 100 µM arsenite and 30 min in 5 mM sodium azide, 0.6 M sorbitol, 1 µM isoproterenol, 2 mM AICAR, 100 µM rosiglitazone, 1 mM metformin, 5 µM A23187, 0.1 µM leptin or 1 mM hydrogen peroxide. Analysis of nucleotide ratios (ADP/ATP) was performed using HPLC, as described in section 2.2.9. Data shown represents the mean ADP/ATP ratio +/- S.E.M of three independent experiments performed in duplicate, *p < 0.05 (one-way ANOVA). Basal ADP and ATP concentrations were 2.07 µM +/- 0.14 and 32 µM +/- 1.82 respectively.*

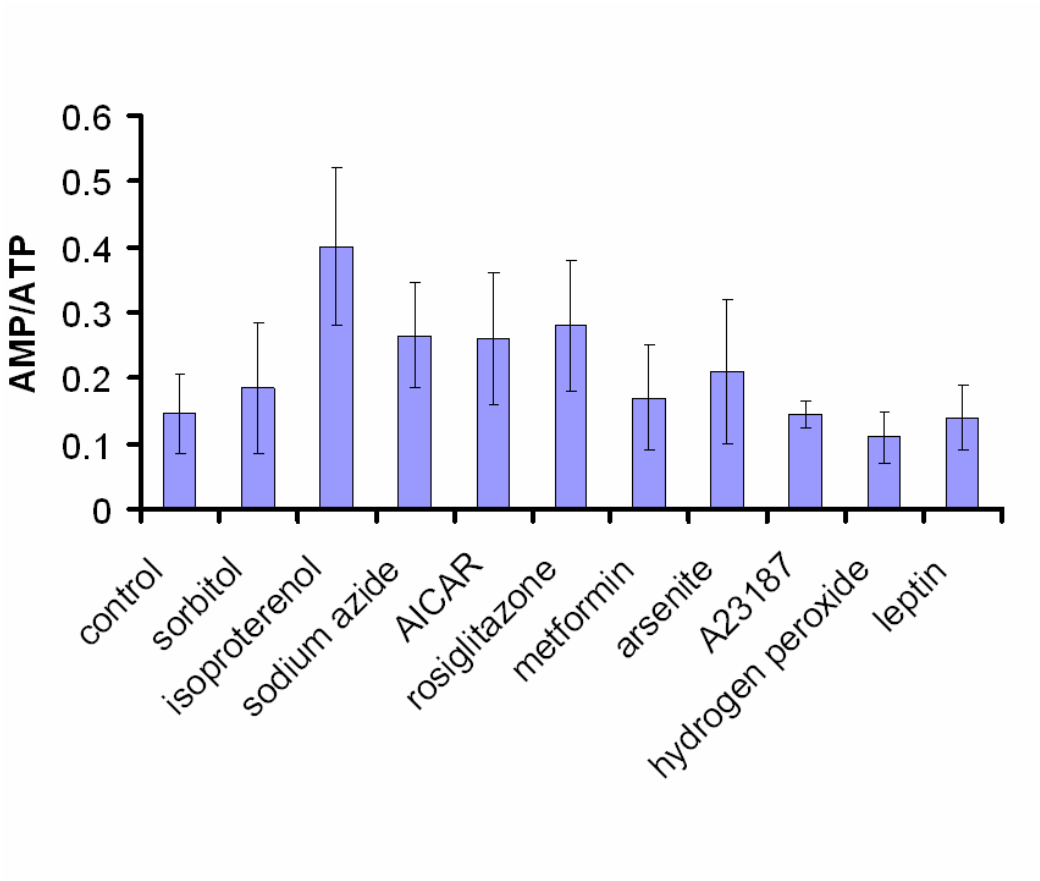

Figure 3-30: The effect of various AMPK activators on the AMP/ATP ratio
Nucleotide extracts were prepared from cells incubated for 15 min in 100 μM arsenite and 30 min in 5 mM sodium azide, 0.6 M sorbitol, 1 μM isoproterenol, 5 mM azide, 2 mM AICAR, 100 μM rosiglitazone, 1 mM metformin, 5 μM A23187, 0.1 μM leptin or 1 mM hydrogen peroxide. AMP and ATP were separated and quantified by HPLC, as described in section 2.2.9. Data shown represents the mean AMP/ATP ratio +/- S.E.M of three independent experiments performed in duplicate. Basal AMP and ATP concentrations were 3.7 μM +/- 0.21 and 32 μM +/- 1.82 respectively.

3.3 Discussion

The initial studies reported here investigated the expression of molecules both upstream and downstream of AMPK in the AMPK signalling cascade.

3T3-L1 adipocytes expressed LKB1, CaMKKα and CaMKKβ at the protein level. Tumour cell lines have been shown to lack the tumour suppressor LKB1 (Tiainen *et al* 1999). As shown in figure 3.1A LKB1 is expressed in 3T3-L1 adipocytes, which is as expected since only tumour cells lack the tumour suppressor LKB1.

CaMKKα/β are both expressed in brain tissue (Sakagami *et al* 1998) and in mouse skeletal muscle (Witczak *et al* 2007, Jensen *et al* 2007, McGee *et al* 2008). In addition CaMKKα has been shown to be expressed in mouse liver and adipose tissue (McGee *et al* 2008). Previous work in 3T3-L1 adipocytes has shown the expression of CaMKKβ at the mRNA level (Yamauchi *et al* 2008) however this study is, to our knowledge, the first to show the expression at the protein level of both CaMKK isoforms in 3T3-L1 adipocytes (Fig. 3.1B/C).

Downstream of AMPK, ACC catalyses the conversion of acetyl CoA to malonyl CoA. The relative levels of expression of the two isoforms of ACC, termed ACC1 and ACC2 are tissue specific. ACC1 is primarily expressed in liver and adipose, where as ACC2 is primarily expressed in cardiac and skeletal muscle (Ha *et al* 1996).

As malonyl-CoA is the substrate for fatty acid synthesis, ACC1 which is predominantly expressed in liver and adipose, regulates the biosynthesis of long-chain fatty acids**.** Thus, expression of the lipogenic enzyme ACC1 in 3T3-L1 adipocytes (Fig. 3.2A) is also not surprising as 3T3-L1 adipocytes undergo significant lipogenesis. In addition previous work has shown the expression of ACC1 in 3T3-L1 adipocytes at the mRNA level (Mizuarai *et al* 2005, Kim *et al* 2004).

In contrast, ACC2 which is primarily expressed in cardiac and skeletal muscle (Ha *et al* 1996), is reported to primarily regulate fatty acid oxidation, whereby malonyl-CoA inhibits CPT1, the rate-limiting step in fatty acid uptake and oxidation by mitochondria. The identification of the band in the 3T3-L1 lysate (Fig. 3.2B) corresponding to ACC2 remains uncertain. Rat and mouse ACC2 are known to differ from each other by 8 amino acid residues, whereby rat ACC2 has 2456 amino acid residues and mouse ACC2 has 2448

amino acid residues. This would suggest that mouse ACC2 may run at a slightly lower molecular weight than rat muscle ACC2. Thus perhaps the intense lower molecular weight band, from the doublet, in the 3T3-L1 lysate lane corresponds to ACC2. However, the difference of 8 amino acid residues, approximately 800Da, is probably too small to observe any difference in migration between rat and mouse ACC2. Previous work in 3T3-L1 adipocytes has shown the expression of ACC2 at the mRNA level (Du *et al* 2008). Thus in summary, it is likely that the ACC2 protein is expressed in 3T3-L1 adipocytes, however as the antibody appears not to be particularly specific, the band corresponding to mouse ACC2 in 3T3-L1 adipocytes remains unclear.

Investigation of AMPK subunit isoform expression (Fig. 3.3-3.9) revealed changes in all subunit isoform expression levels throughout adipogenesis, apart from AMPKα1 subunit expression which remained at a constant level throughout adipogenesis. An increase in expression throughout development from fibroblasts to adipocytes was observed with the α2, β2 and γ1 subunits. In contrast β1, γ2 and γ3 subunit expression decreased throughout adipogenesis. As the differentiation process involves treatment of fibroblasts with insulin, dexamethasone and IBMX on day 0 and insulin on day 2 it is possible that insulin and / or IMBX and / or dexamethasone may suppress or promote the expression levels of the different subunit isoforms.

Both α1 and α2 subunits recognise the *(X,β)XXS/TXXX* motif (where * represents a hydrophobic residue and β a basic residue). However, it appears that the subunits exhibit differences with respect to preferences for the hydrophobic residues as the P-5 and P+4 positions (Woods *et al* 1996b). These subtle differences may confer substrate specificity of the two isoforms within the cell. Thus increased expression of the α2 subunit throughout adipogenesis may allow phosphorylation of specific substrates, such as lipogeneic proteins, which may not be phosphorylated by α1.

Previous work using recombinant AMPK heterotrimeric complexes (Scott *et al* 2004) and native rat complexes (Cheung *et al* 2000) found that the different γ isoform complexes differed in their degree of stimulation by AMP. γ2 displayed the greatest stimulation by AMP, while γ1 displayed an intermediate stimulation by AMP and γ3 the lowest stimulation by AMP. In this study during adipogenesis the γ1 subunit expression is increased, where as the γ2 and γ3 subunit expression is decreased. There was no significant ($p < 0.05$) difference in total AMPK activity (Fig. 3.10), as determined under a saturating AMP concentration (200μM), between fibroblasts and adipocytes. Thus it would be

interesting to investigate the sensitivity to AMP, of AMPK complexes immunoprecipitated, from both fibroblasts and adipocytes, given that the expression levels of the γ subunit isoforms are altered during adipogenesis.

Previous work in human adipose tissue (Lihn *et al* 2004) and rat adipocytes (Daval *et al* 2005) found that the α1 catalytic subunit accounts for the major part of basal AMPK activity. Interestingly, the α1 subunit was found to account for almost all total basal AMPK activity in both fibroblasts and adipocytes throughout adipogenesis, while the α2 subunit displayed negligible contribution to total basal AMPK activity (Fig. 3.10). Salt and co-workers also found that the α1 subunit accounts for the majority of the basal AMPK activity in 3T3-L1 adipocytes (Salt *et al* 2000). However, in contrast to this study, Salt and co-workers (Salt *et al* 2000), also found that the α2 subunit contributed about 20% to the total basal AMPK activity. Thus in this current study it was initially thought that the lack of α2-specific AMPK activity might be due to the failure of the anti-α2 antibody to successfully immunoprecipitate the AMPK complexes containing α2 subunits. However, this seems unlikely as α2 is detected in the α2 immunoprecipitates as shown in figure 3.10 The relative contribution of the α1 and α2 isoforms to total AMPK activity in rat liver is approximately equal (Woods *et al* 1996b). Equal volumes of the rat liver kinase (K) were used as a positive control for α1 and α2 subunit expression blots (Fig. 3.3 and 3.4). Comparable intensities of the rat liver kinase (K) with expression levels of the α1 and α2 isoforms suggests there is indeed far less α2 subunit expression in fibroblasts and adipocytes compared to α1 i.e the intensity of the α2 band in the purified rat liver kinase detected by the anti-α2 antibody is more intense compared to the 3T3-L1 lysate, whereas the α1 band detected by the anti-α1 antibody in the purified liver kinase is less intense compared to the 3T3-L1 lysates suggesting that α1 expression is far more abundant than α2 throughout adipogenesis. Thus, in conclusion, it is likely that α1 may account for almost all total AMPK activity in this study, due to its predominant expression level. Thus the only other possible explanation for the discrepancy is that the 3T3-L1 cell passage number and initial source were different in this work compared to the work by Salt and co-workers (Salt *et al* 2000), and that either of these differences altered the contribution of the α2 subunit to the total basal AMPK activity.

In this study the kinetics of AMPK activity in response to various activators was assessed, in order to determine whether there is a correlation between AMPK activation and various downstream effects such as glucose transport. The extent of AMPK activation and Thr172 phosphorylation in the 3T3-L1 adipocytes varied for each of the different stimuli, as shown

in (Figs. 3.11-21). In 3T3-L1 adipocytes sorbitol produced the greatest fold increase in AMPK activity compared to basal levels. It should be noted that the direct AMPK activator A769662 has been shown to activate only β1 containing AMPK complexes **(**Scott *et al* 2008), whereas it is probable that the other stimuli can activate both β1 and β2 containing AMPK complexes. Thus potentially this may account for the very modest increase in AMPK activity observed with the direct AMPK activator A769662.

These results support previous studies reporting the stimulation of AMPK activity by various AMPK activators in various tissues; arsenite in rat hepatocytes (Corton *et al* 1994), azide in fao hepatoma cells (Witters *et al* 1991), rosiglitazone in mouse muscle cells (Fryer *et al* 2002b) and *in vivo* in rat adipose tissue (Ye *et al* 2004), metformin in rat hepatocytes (Zhou *et al* 2001) and adipocytes (Huypens *et al* 2005), sorbitol in mouse muscle cells (Fryer *et al* 2002b), AICAR in rat hepatocytes (Corton *et al* 1995) and adipocytes (Corton *et al* 1995), hydrogen peroxide in NIH-3T3 cells (Choi *et al* 2001), leptin in skeletal muscle (Minokoshi *et al* 2002) and adipose tissue (Orci *et al* 2004), adiponectin in muscle and liver (Yamauchi *et al* 2002) and adipose (Wu *et al* 2003) and isoproterenol in isolated rat epididymal fat cells (Moule and Denton 1998) and in 3T3-L1 adipocytes (Yin *et al* 2003).

Subsequently, this study investigated the molecular mechanisms by which AMPK is activated by each test substance in 3T3-L1 adipocytes. This included using the CaMKK inhibitor STO-609 and determining whether there was a change in the nucleotide ADP/ATP ratio and AMP/ATP ratio by HPLC.

As mentioned AICAR is converted into ZMP in the cell which functions as a cellular mimetic of AMP. Thus like AMP, ZMP causes allosteric activation of AMPK and protects phosphorylation of Thr172, by the constitutively active AMPK kinase LKB1, from dephosphorylation. Thus, it was not surprising that STO-609 did not inhibit AICAR stimulated AMPK activity (Fig. 3.22), and that AICAR did not significantly alter the ADP/ATP ratio (Fig. 3.29) and AMP/ATP (Fig. 3.30) ratio. In contrast, the calcium ionophore A23187 stimulates AMPK activity via CaMKK. Therefore in the presence of STO-609, A23187 stimulated AMPK activity is significantly ($p < 0.05$) attenuated (Fig. 3.22). Thus, this study shows that 3T3-L1 adipocytes express CaMKK and exhibit CaMKK-dependent AMPK activation upon A23187 stimulation. These results suggest a potential role for CaMKK as an upstream AMPK kinase in 3T3-L1 adipocytes. However, Hawley *et al* 2005 showed that CaMKKβ appears to activate AMPK much more rapidly

than CaMKKα in cell-free assays. Further work such as siRNA knockdown of CaMKKα/β, is required to determine which CaMKK isoform is most catalytically active in 3T3-L1 adipocytes.

This current study found that sorbitol did not significantly increase the ADP/ATP ratio (Fig. 3.29) and AMP/ATP ratio (Fig. 3.30). Indeed, previous observations in a mouse skeletal muscle cell line (Fryer *et al* 2002b) have concluded that sorbitol can activate AMPK without altering the cellular energy level. Sorbitol has been shown to be able to increase intracellular calcium levels in the chicken B cell line DT40 (Qin *et al* 1997) and was recently suggested to stimulate AMPK activity in LKB1 deficient HeLa cells via CaMKKβ (Woods *et al* 2005). However this current study suggests that in 3T3-L1 adipocytes sorbitol appears to be able to activate AMPK in a CaMKK independent and nucleotide independent manner (Fig. 3.22). Thus, sorbitol may stimulate AMPK activity in adipocytes via an alternative AMPK kinase. A recent study has suggested that TAK1 (Momcilovic *et al* 2006) may function as a novel mammalian AMPK kinase. Furthermore it should be noted that there is still residual basal AMPK activity in CaMKKβ knockout studies in HeLa cells, which lack LKB1 (Woods *et al* 2005). This could be explained in part by the incomplete knockdown of CaMKKβ protein expression in these cells, however the possibility still remains that another unidentified upstream kinase is contributing to AMPK activity in these cells. This supports the idea that there may be as yet unidentified mammalian AMPK kinases, which may exhibit differential tissue expression.

The β adrenoreceptor agonist isoproterenol has previously been shown to activate AMPK in rat epididymal fat cells (Moule and Denton 1998) and 3T3-L1 adipocytes (Yin *et al* 2003, Gauthier *et al* 2008). In addition incubation of isolated adipocytes with the β adrenoreceptor agonists, adrenaline and forskolin, also increased AMPK activity and the AMP/ATP ratio (Koh *et al* 2007) (Gauthier *et al* 2008). This study showed that ST0-609 does not perturb the ability of isoproterenol (Fig. 3.22) to stimulate AMPK activity in 3T3-L1 adipocytes, and that it stimulates a statistically significant ($p < 0.05$) increase in the ADP/ATP ratio (Fig. 3.29), and displays a tendency to increase the AMP/ATP ratio (Fig. 3.30). This suggests that isoproterenol activates AMPK by a mechanism which is independent of CaMKK, and dependent on a decrease in the cellular energy level. Thus, in 3T3-L1 adipocytes, isoproterenol potentially activates AMPK via LKB1.

A recent study (Gauthier *et al* 2008) concluded that the activation of AMPK, and subsequent inhibition of lipolysis, in 3T3-L1 adipocytes, by agents (isoproterenol, IBMX

and forskoline) that increase cAMP appears to be secondary to an increase in the AMP/ATP ratio that accompanies lipolysis and not the direct result of increases in cAMP levels and PKA activity, as treatment of cells with orlistat partially inhibited isoproterenol induced lipolysis and AMPK activity, yet did not alter cAMP levels or PKA activity. The re-esterification of NEFAs back into TG requires their acylation, which is catalysed by acyl-CoA synthetase. This process is energy dependent consequently reducing ATP levels and increasing AMP levels. Gauthier and co-workers concluded that reduced energy levels are possibly due in part to acylation of fatty acids produced during lipolysis, as Triacsin C, an acyl-CoA synthetase inhibitor, blunted isoproterenol induced increases in AMPK activity and the AMP/ATP ratio.

Other events may contribute to the reduced energy state which accompanies lipolysis. NEFAs cause uncoupling of oxidative phosphorylation which depletes energy levels, (Wojtczak *et al* 1993) and the formation of glycerol-3-phosphate used for the re-esterification of NEFAs into TG is also energy dependent.

In addition, NEFAs have been shown to activate AMPK in rat islets, the MIN6 β cell line (Wang *et al* 2007) and rat L6 skeletal muscle cells (Fediuc *et al* 2006). Thus, it is possible that NEFAs accumulating in adipose tissue following isoproterenol induced lipolysis activate AMPK via an AMP/ATP dependent pathway.

In contrast it has also been shown that activation of AMPK in 3T3-L1 adipocytes by isoproterenol stimulates lipolysis (Yin *et al* 2003). Interestingly, Yin *et al* 2003, showed that cAMP analogues also stimulated AMPK phosphorylation. Furthermore, they showed that insulin, which inhibits lipolysis via the activation of PDE3B which breaks down cAMP to AMP, antagonized the activation of AMPK by forskolin. Therefore Yin and co-workers suggested that isoproterenol is activating AMPK via an intermediary rise in cAMP levels and not via an increase in AMP levels resulting from degradation by PDE3B (Yin *et al* 2003).

In this current study the source of this decrease in cellular energy level was not investigated. As maximum AMPK activity was observed after 30 min, it is perhaps more likely that NEFAs or re-esterification of NEFAs and glycerol to TG may play a role in the AMP/ATP dependent stimulation of AMPK activity, rather than elevated AMP levels resulting from the degradation of cAMP to AMP by PDE3. To confirm this, a PDE3B inhibitor could be used to determine whether isoproterenol is activating AMPK via

elevating AMP levels resulting from degradation of cAMP into AMP, or indeed whether re-esterification of NEFAs is playing a role in the AMP/ATP dependent stimulation of AMPK activity.

In cells treated with metformin, hydrogen peroxide, leptin and arsenite there was no observed increase in the ADP/ATP or AMP/ATP ratio (Fig. 3.29, 3.30). In addition, these stimuli did not appear to stimulate AMPK activity in a CAMKK dependent manner (Fig. 3.22). These results suggest that metformin, hydrogen peroxide, leptin and arsenite all activate AMPK via a nucleotide and CAMKK independent manner. However, in general, the effect of these activators on AMPK activity is very subtle in 3T3-L1 adipocytes, thus potentially masking any alterations in nucleotide levels and effects of STO-609. Leptin, hydrogen peroxide and arsenite have previously been shown to activate AMPK, in skeletal muscle, NIH-3T3-L1 cells, and rat hepatocytes respectively, and cause an increase in the AMP/ATP ratio (Minokoshi *et al* 2002, Chou *et al* 2001, Corton *et al* 1994). Previous studies in CHO cells, the rat hepatoma cell line H4IIE and the skeletal muscle cell line H-2K^b have also reported that metformin activates AMPK without altering the cellular energy level (Hawley *et al* 2002, Fryer *et al* 2002b). Interestingly, Huypens and co-workers showed that prolonged stimulation of 3T3-L1 adipocytes with metformin stimulated AMPK activity, as shown by an increase in AMPK Thr172 phosphorylation (Huypens *et al* 2005). It has been demonstrated that metformin is transported into liver cells via the organic cation transporter 1 (OCT1), stimulating AMPK phosphorylation (Shu *et al 2*007). The same study found that acute treatment of 3T3-L1 adipocytes with metformin did not stimulate AMPK Thr172 phosphorylation, and that 3T3-L1 adipocytes exhibited little OCT-activity (Shu *et al 2*007). Thus, it has been suggested (Shu *et al 2*007) that perhaps prolonged metformin treatment results in passive diffusion of metformin into 3T3-L1 adipocytes which consequently causes an increase in AMPK activity.

In this study azide and rosiglitazone were both shown to cause a significant ($p < 0.05$) increase in the ADP/ATP ratio (Fig. 3.29), and displayed a tendency to increase the AMP/ATP ratio (Fig. 3.30). This supports previous work by Witters and co-workers (Witters *et al* 1991) in fao hepatoma cells and Fryer and co-workers (Fryer *et al* 2002b) in mouse muscle cells that azide and rosiglitazone can both decrease the cellular energy level. In addition, in this study these activators did not appear to stimulate AMPK activity in a CAMKK dependent manner (Fig. 3.22). Thus, it is possible that both azide and rosiglitazone stimulate AMPK activity in 3T3-L1 adipocytes in a LKB1 dependent manner.

It should be noted that in this study the basal AMP concentration appeared to be greater than the basal ADP concentration, which differs from the studies by Fryer and co-workers (Fryer *et al* 2002b) and Luo and co-workers (Luo *et al* 2007) which reported that the ADP concentration was greater than the AMP concentration under basal conditions in muscle cells and 3T3-L1 adipocytes respectively. Also, the AMP/ATP ratio in the muscle cells under basal conditions was 0.05 and in the 3T3-L1 cells, 0.04, which is lower than the AMP/ATP ratio of 0.14 under basal condition in this study. It is possible that another molecule not tested in this study such as guanosine monophosphate (GMP), inosine monophosphate (IMP), or uridine monophosphate (UMP) may have a similar elution time as AMP in this system, which could mask the real AMP peak and account for the apparently elevated AMP concentrations. Thus further work is required to determine the elution time of other candidates including GMP, IMP and UMP. Furthermore, the equilibrium between adenine nucleotides (2ADP ↔ AMP + ATP) refers to free AMP in the cell**.** This study measured the adenine nucleotide ratio using total cellular nucleotide concentrations, i.e including AMP bound to proteins. Thus in general these results should be taken with caution, given that AMPK is only regulated by the cytosolic AMP/ATP ratio.

As shown in figure 3.31, there was no simple linear relationship between the fold increase in AMPK activity and the ADP/ATP ratio for each stimuli in 3T3-L1 adipocytes.

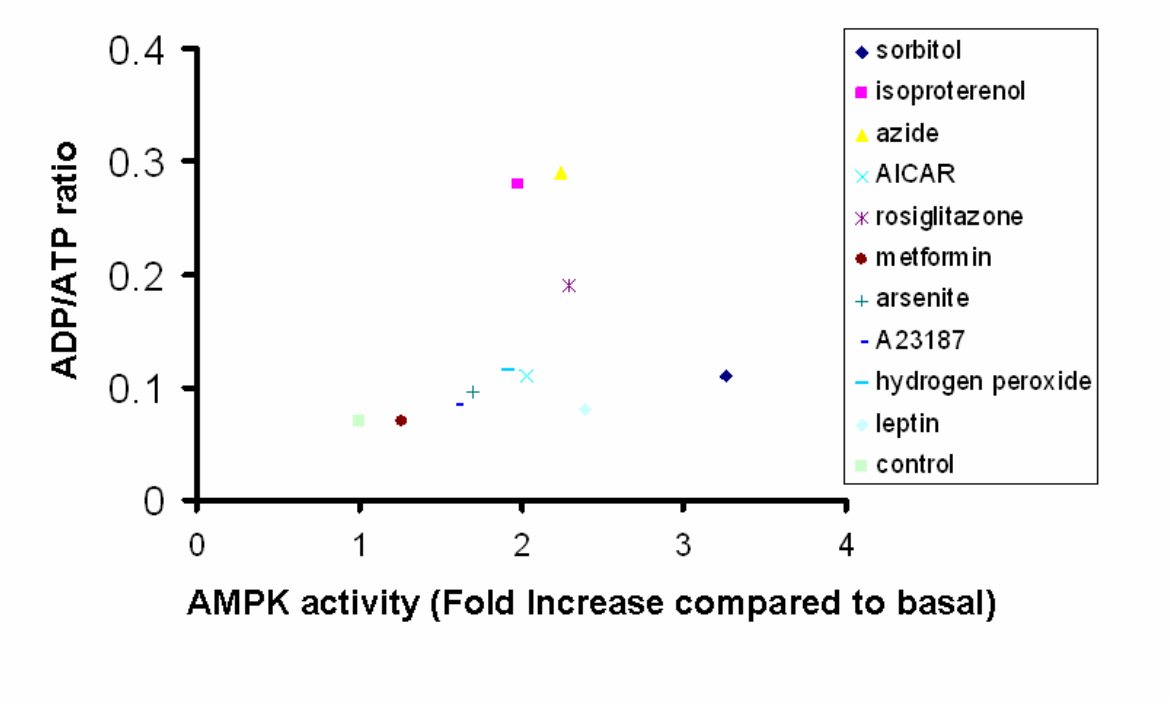

Figure 3-31: Effects of various stimuli on AMPK activity versus ADP/ATP ratio.

Figure 3.32 summarises the proposed mechanisms of AMPK activation in 3T3-L1 adipocytes. AICAR is converted into ZMP in the cell which functions as a cellular mimetic of AMP i.e ZMP causes allosteric activation of AMPK and protects phosphorylation of Thr172, by the constitutively active AMPK kinase LKB1, from dephosphorylation. The novel direct AMPK activator A769662 activates AMPK by mimicking the effects of AMP. The calcium ionophore A23187 is thought to stimulate AMPK activity through CaMKK, as A23187 stimulated AMPK activity is perturbed by STO-609. AMPK activation by isoproterenol, azide and rosiglitazone caused a significant ($p < 0.05$) increase in the ADP/ATP ratio and displayed a tendency to increase the AMP/ATP ratio. In addition AMPK stimulated activity by these activators was not significantly altered in the presence of STO-609. Therefore it is possible that these activators are stimulating AMPK via an LKB1 dependent pathway. Sorbitol, metformin, arsenite, hydrogen peroxide and leptin were found to have no significant ($p < 0.05$) effect on the nucleotide ratios, and AMPK stimulated activity by these activators was not significantly altered in the presence of STO-609. In summary, these results suggest a role for both LKB1 and CaMKK as AMPK kinases in 3T3-L1 adipocytes. However, potentially there exists other as yet unidentified AMPK kinases in 3T3-L1 adipocytes, which are both nucleotide and calcium independent.

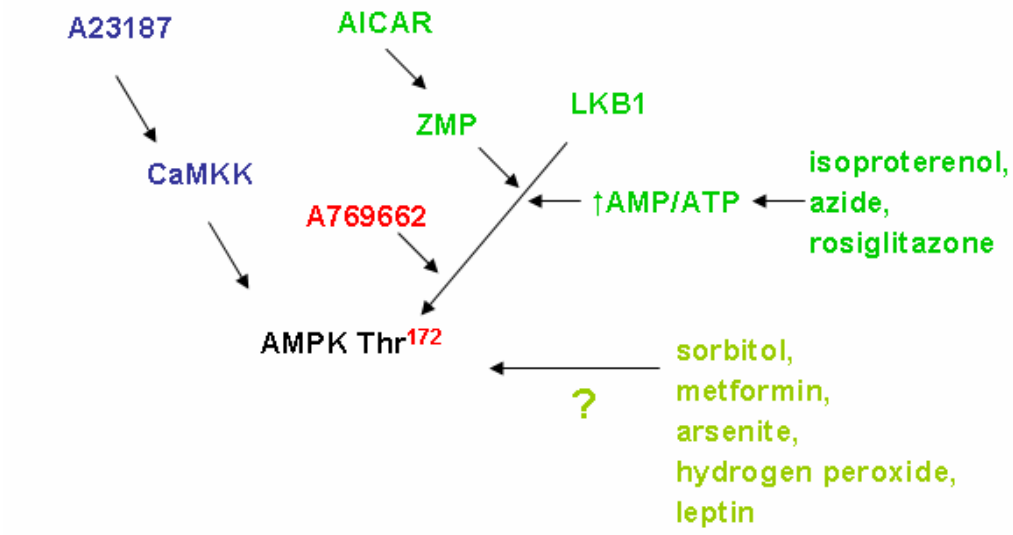

Figure 3-32: Mechanism of acute AMPK activation in 3T3-L1 adipocytes.

Chapter 4 - Role of acute AMPK activation in adipocyte insulin action

4.1 Introduction

4.1.1 Insulin-stimulated glucose uptake

Insulin is a polypeptide hormone which is produced in the Islets of Langerhans in the pancreas. After feeding, elevated blood glucose levels trigger exocytosis of the insulin secretary vesicles and release of insulin into the bloodstream (see 1.2.2).

Upon insulin signalling (see 1.2.2) in target tissues, glucose transporters which facilitate the uptake of glucose into target cells, are transported to the plasma membrane in vesicles. In muscle and fat cells the glucose transporter, GLUT4, is responsible for the uptake of glucose into the cells where it is stored as glycogen and TG respectively (Saltiel *et al* 2001).

4.1.2 Insulin indepedent glucose uptake

In muscle, exercise has been reported to stimulate AMPK activity (Winder and Hardie 1996) and increase glucose transport in an insulin-independent manner, resulting in increased translocation of GLUT4 to the plasma membrane from intracellular stores (Hayashi *et al* 1997, Douen *et al* 1990, Douen *et al* 1989, Goodyear *et al* 1991). In addition, contraction of isolated rat epitrochlearis muscles via electrical stimulation has also been shown to increase AMPK activity and glucose transport in an insulin-independent manner (Hayashi *et al* 1998). Like physical exercise, contraction has also been reported to increase GLUT4 translocation to the plasma membrane (Goodyear *et al* 1990, Lund *et al* 1995).

The AMPK activator AICAR has also been reported to increase glucose transport in L6 myocytes (Chen *et al* 2002), isolated rat epitrochlearis muscles (Hayashi *et al* 1998**,** Hayashi *et al* 2000, Bergeron *et al* 1999), perfused rat hindlimbs (Merrill *et al* 1997) and in skeletal muscle of conscious rats (Bergeron *et al* 1999). In addition, AICAR has been shown to potentiate insulin-stimulated glucose transport (Bergeron *et al* 1999, Hayashi *et*

al 1998) in isolated rat epitrochlearis muscles, and stimulate GLUT4 translocation to the plasma membrane in perfused rat hindlimbs **(**Kurth-Kraczek *et al* 1999).

Since exercise, contraction and AICAR all activate AMPK activity and stimulate glucose uptake into skeletal muscle independently of insulin-stimulated glucose transport, it has been hypothesised that AMPK mediates this effect (Hayashi *et al* 1998). However currently there exists a great deal of confusion as to whether AMPK mediates contraction-stimulated glucose uptake into muscle due to conflicting studies. Experiments using genetically manipulated mice with knockout catalytic (Jørgensen *et al* 2004) or regulatory (Barnes *et al* 2004) AMPK subunits in skeletal muscles have reported that contraction-stimulated glucose transport was unaffected. Although AMPK activity was only partially reduced in these studies, the AMPK knockouts did inhibit the effect of AICAR on muscle glucose transport (Jørgensen *et al* 2004, Barnes *et al* 2004). In contrast, another study using genetically manipulated mice where AMPK was completely knocked down in skeletal muscle by overexpression of functionally inactive AMPK (Mu *et al* 2001) reported that there was a significant reduction in contraction-stimulated glucose transport in fast and slow twitch muscles. Interestingly, another study in perfused rat hindlimbs (Derave *et al* 2000) showed that there was a significant correlation between AMPK activity and glucose transport in contracting fast-twitch muscles, however in slow-twitch muscles glucose transport was increased during contraction whereas AMPK activity did not increase. This suggests that the role of AMPK may differ between muscle fibre type.

Interestingly, in adipocytes AICAR was shown to modestly stimulate basal glucose transport while demonstrating an inhibitory effect on insulin-stimulated glucose transport and GLUT4 translocation to the plasma membrane (Salt *et al* 2000). Thus the effect of AICAR in adipocytes contrasts with the effect of AICAR in skeletal muscle.

4.1.3 The role of AS160 and TBC1D1 in glucose transport

AS160 has been identified as a potential target of PKB and AMPK which both mediate GLUT4 translocation in response to insulin and AICAR respectively in muscle cells (Bruss *et al* 2005, Thong *et al* 2007).

AS160 is a 160kDa Rab GAP which was first discovered using the PAS antibody to immunoprecipitate proteins harbouring phosphorylated PKB substrate motifs from insulin-stimulated adipocytes (Kane *et al* 2002). In addition to a GAP domain at the C-terminus,

AS160 also contains two phospho-tyrosine binding domains and six potential phosphorylation sites (Ser318, Ser341, Ser570, Ser588, Thr642, Ser751) that match the criteria for a PKB consensus motif (RXRXXS*/T*) (Sano *et al* 2003)**.** Quantification of the relative amount of phosphopeptides derived from extracts of 3T3-L1 adipocytes in the presence or absence of insulin revealed that levels of phosphorylation at five of these phosphorylation sites (Ser318, Ser570, Ser588, Thr642, and Thr751) was increased with insulin (Sano *et al* 2003)**.** More recently, in HEK 293 cells, Geraghty and co-workers identified two novel AS160 sites Thr568 and Ser666, which lie within a motif which is not a consensus sequence for PKB (Geraghty *et al* 2007).

AS160 has been implicated in insulin-stimulated GLUT4 trafficking of vesicles to the plasma membrane. It has been demonstrated in 3T3-L1 cells that AS160 can retain GLUT4 vesicles intracellularly by the activity of its GAP domain under basal conditions (Eguez *et al* 2005, Larance *et al* 2005). It has been proposed that AS160 phosphorylation at PAS sites in response to insulin promotes exocytosis of GLUT4 vesicles by reducing the GAP activity of the protein towards Rab proteins associated with GLUT4 vesicles, as transfection of 3T3-L1 adipocytes and L6 GLUT4-myc myoblasts with a constitutively active AS160 incapable of being phosphorylated at PAS regulatory motifs displayed reduced insulin-induced GLUT4 translocation (Sano *et al* 2003, Thong *et al* 2005).

Despite the finding that AS160 is thought to integrate signals from both PKB and AMPK in muscle cells (Bruss *et al* 2005, Thong *et al* 2007), it is possible that this is not the case in adipocytes due to the opposing action of AICAR on insulin-stimulated glucose transport (Salt *et al* 2000). In addition, it is thought that the inhibitory effect of AICAR on insulin-stimulated glucose transport in adipocytes is at a site downstream of PKB in the insulin signalling cascade, as AICAR appears to have no effect on IRS-1 tyrosine phosphorylation, PI3K recruitment to IRS-1 or PKB activity (Salt *et al* 2000).

TBC1D1 is a paralogue of AS160, with a predicted molecular mass of 133kDa (Chen *et al* 2008). TBC1D1 and AS160 both contain GAP domains which are highly conserved, but display sequence variation at the N-terminus and within the two distinct clusters of phosphorylated sites that are located either side of the second phospho-tyrosine binding domain. TBC1D1 contains predicted PKB phosphorylation sites at Thr596 and Ser507 corresponding to Thr642 and Ser570 on AS160, respectively (Roach *et al* 2007). Mass spectrometer analysis of TBC1D1 isolated from HEK 293 cells incubated in medium containing serum identified Thr596, Ser507, Ser237, Ser263, Ser565, Ser566 and Ser585

as phosphorylation sites on TBC1D1 (Chen *et al* 2008). Interestingly it has been established that Ser237 on TBC1D1 becomes phosphorylated in response to treatments that elevate levels of active and phosphorylated AMPK in 3T3-L1 adipocytes, HEK 293 cells and rat L6 myotubes (Chavez *et al* 2008, Chen *et al* 2008). During the course of this work TBC1D1 emerged as a Rab GAP also involved in regulating glucose transport.

TBC1D1 is expressed in 3T3-L1 adipocytes (Chavez *et al* 2008), however it appears to be only 1/20 as abundant as AS160. Insulin treatment of 3T3-L1 adipocytes has been shown to cause phosphorylation of TBC1D1 on Thr596 in the PKB phosphorylation motif RRRANTL (Roach *et al* 2007). TBC1D1 is thought not to be as important as AS160 in 3T3-L1 cells as TBC1D1 did not contribute significantly to the total GAP activity towards the Rab(s) involved in GLUT4 translocation. This was shown by knockdown of TBC1D1 which did not increase the amount of GLUT4 at the cell surface in the absence of insulin (Chavez *et al* 2008), whereas knockdown of AS160 did (Eguez *et al* 2005). Interestingly, overexpression of TBC1D1 was shown to markedly inhibit insulin-stimulated GLUT4 translocation (Roach *et al* 2007) in 3T3-L1 adipocytes, whereas overexpression of AS160 did not (Sano *et al* 2003). It was initially thought that perhaps the endogenous PKB was insufficient to phosphorylate ectopic TBC1D1 to the extent required. However, in a subsequent study overexpressed TBC1D1 was also shown to inhibit GLUT4 translocation elicited by ectopic activated PKB which suggests that the GAP activity of TBC1D1 is not suppressed by PKB phosphorylation (Chavez *et al* 2008), whereas the GAP activity of AS160 is suppressed by PKB phosphorylation. Thus, although TBC1D1 is expressed in 3T3-L1 adipocytes, it is considered unlikely to participate significantly in insulin-stimulated GLUT4 translocation. Hence, in adipocytes it is thought that insulin signals GLUT4 translocation primarily through AS160 and not TBC1D1.

TBC1D1 is highly expressed in skeletal muscle (Chavez *et al* 2008, Taylor *et al* 2008) and was shown to be phosphorylated at PAS sites in mouse skeletal muscle *in vivo* by insulin, AICAR and contraction (Taylor *et al* 2008). However AMPK is thought to be the more important regulator as semi-quantitative analysis of spectra suggested that AICAR caused greater overall phosphorylation of TBC1D1 sites compared to insulin (Taylor *et al* 2008). Recent work by Chavez and co-workers, showed that AICAR partially reversed the inhibition of insulin-stimulated GLUT4 translocation by overexpressed TBC1D1 in 3T3-L1 cells (Chavez *et al* 2008). These findings have led to the proposal that TBC1D1 may participate in the regulation of GLUT4 translocation in response to contraction and/or AMPK activation.

Insulin-stimulated GLUT4 translocation in 3T3-L1 adipocytes is thought to require insulin-stimulated association of 14-3-3 proteins with phosphorylated AS160 (Ramm *et al* 2006). In rat L6 myotubes, insulin was shown to promote the phosphorylation of Thr596 on TBC1D1 but not the binding of 14-3-3 proteins, whereas AMPK activation by AICAR, phenformin and A-769662 was shown to promote the phosphorylation of Ser237 on TBC1D1 and binding of 14-3-3 proteins. In contrast, AS160 was shown to be phosphorylated on its 14-3-3 binding sites (Ser341 and Thr642) and to bind 14-3-3 proteins in response to insulin, but not the AMPK activator A-769662 in rat L6 myotubes (Chen *et al* 2008). These findings further support the proposal that TBC1D1 and AS160 may have complementary roles in regulating vesicle trafficking in response to insulin and AMPK activation in skeletal muscle.

The mechanism by which AS160/TBC1D1/Rabs mediate exocytosis of GLUT4 vesicles remains undefined. However, the v-SNARE VAMP2 and the t-SNAREs syntaxin4 and SNAP23 have been shown to be involved in GLUT4 exocytosis (Bryant et al 2002, Hou and Pessin 2007). In addition, the syntaxin 4-binding proteins, Munc18c, tomosyn and synip have also been proposed to regulate SNARE complex assembly and GLUT4 translocation (Kanda *et al* 2005, Widberg *et al* 2003, Yamada *et al* 2005).

4.1.4 Rab proteins

Rabs are small G-proteins that in their GTP-bound form participate in vesicle movement and membrane fusion (Zerial *et al* 2001). Rabs are activated by replacement of GDP with GTP catalysed by GEFs (guanine nucleotide exchange factors). Active Rabs can interact with Rab effector proteins on target membranes, which allows tethering of the vesicle to its target membrane and other membrane proteins, including the SNARE proteins, to interact, facilitating docking of the vesicle to the plasma membrane. SNARE proteins can be classified as either v-SNARES, (SNARES associated with the vesicle) and, t-SNARES, (SNARES associated with the target membrane) (Bryant *et al* 2002). GAP degrades GTP to GDP which allows the Rabs to be recycled. GDP dissociation inhibitor (GDI) binds the Rab inhibiting the exchange of GDP for GTP, and a Rab escort protein escorts the Rab back to its original membrane (Fig. 4.1).

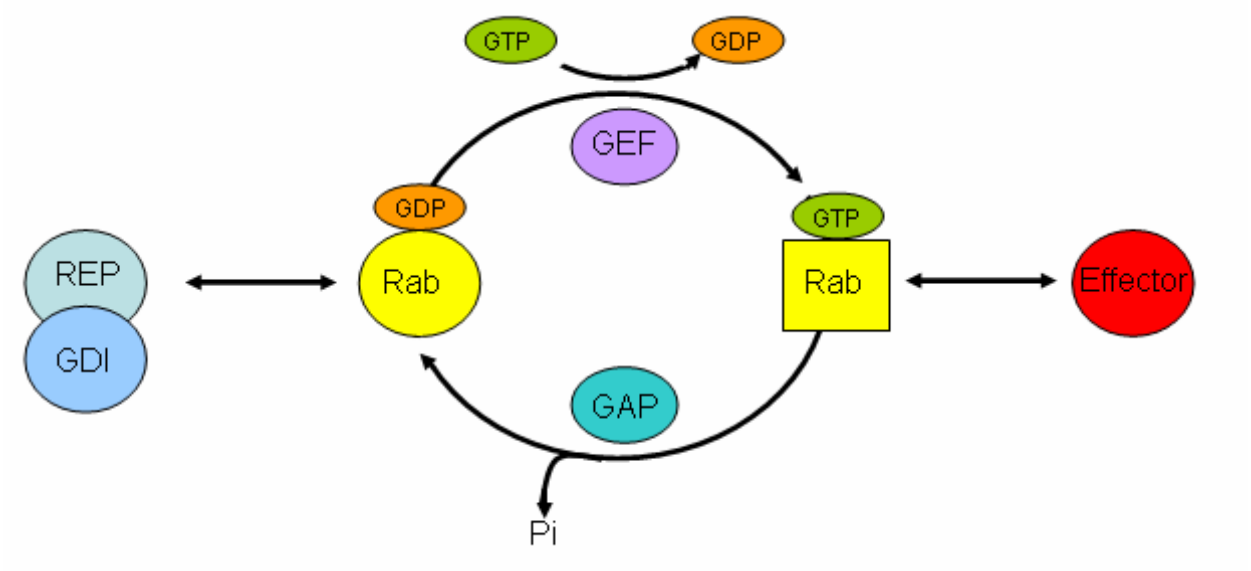

Figure 4-1: The Rab GTPase cycle.
The Rab GTPase switches between GDP- and GTP-bound forms, which have different conformations. Conversion from the GDP- to the GTP-bound form is caused by nucleotide exchange, catalyzed by a GDP/GTP exchange factor (GEF). Conversion from the GTP-to the GDP-bound form occurs by GTP hydrolysis, facilitated by a GTPase-activating protein (GAP). The GTP-bound form interacts with effector molecules, whereas the GDP-bound form interacts with Rab escort protein (REP) and GDP dissociation inhibitor (GDI). Pi, inorganic phosphate.

Miinea and co-workers identified specific Rab isoforms (Rab1A, 1B, 2A, 3A, or 3D; Rab 4B, 5A, 5B, 5C, 6A, or 6B; Rab7, 8A, or 8B; Rab10, 11B, 14, 18, and 35) associated with GLUT4 vesicles in 3T3-L1 cells by immunoprecipitation (Miinea *et al* 2005). Also in 3T3-L1 adipocytes, Larance and co-workers found that GLUT4 vesicles were associated with Rab 10, 11 and 14 (Larance *et al* 2005). In addition RNAi knockdown of Rab10 was found to result in an approximately 80% reduction in GLUT4 translocation in 3T3-L1 adipocytes (Sano *et al* 2007). Thus, Rab 10 is currently thought to be the most likely Rab involved in GLUT4 vesicle translocation in 3T3-L1 adipocytes.

4.1.5 Aims

Previous work (Salt *et al* 2000) showed that AICAR inhibits insulin-stimulated glucose transport in 3T3-L1 adipocytes, which is in contrast to the effect of AICAR in muscle. In order to further characterise the role of AMPK in the inhibition of insulin-stimulated glucose transport, this study investigated the effect of various AMPK activators, including the direct AMPK activator A769662, on insulin-stimulated glucose transport in 3T3-L1 adipocytes. The effect of AMPK inhibition and knockdown, on AICAR stimulated basal

glucose transport and inhibition of insulin-stimulated glucose transport was also assessed to determine whether the effects of AICAR on glucose transport were dependent on AMPK activation.

Previous work by Salt and co-workers showed that AICAR did not alter IRS-1 phosphorylation, association of PI3K with IRS-1 or PKB activity in 3T3-L1 adipocytes (Salt *et al* 2000). During the course of this project AS160 and TBC1D1 have both emerged as Rab GAPs involved in the regulation of glucose transport. Therefore, in this study the mechanism by which AICAR inhibits insulin-stimulated glucose transport in adipocytes was further investigated, with particular attention being paid to the effect of AICAR on basal and insulin-stimulated AS160/TBC1D1 phosphorylation at PAS sites.

4.2 Results

4.2.1 Effect of various AMPK activators on basal and insulin-stimulated glucose transport

The effect of various AMPK activators on basal and insulin-stimulated glucose transport was investigated using 2-[^{3}H] deoxy-D-glucose. A significant ($p < 0.05$) 39.7 +/- 2.28 %, 49 +/- 10.7 %, 73.6 +/- 5.7 %, 38.7 +/- 3.5 % and 67.5 +/- 7.8 % inhibition of insulin-stimulated glucose transport (Fig. 4.2) was observed in cells pre-treated with AICAR, sorbitol, rosiglitazone, isoproterenol and A769662 respectively. A23187 did display an apparent tendency to inhibit insulin-stimulated glucose transport, however this effect was not statistically significant (Fig. 4.2). In addition, sorbitol produced a significant ($p < 0.05$) 5.74 +/- 0.55 fold increase in basal glucose transport, whereas the other stimuli did not significantly alter basal glucose transport.

4.2.2 Investigating whether the inhibition of insulin-stimulated glucose transport by AICAR is dependent on AMPK activation

4.2.2.1 Effect of Compound C on AICAR mediated inhibition of insulin-stimulated glucose uptake

The AMPK inhibitor, Compound C, was utilized to determine the effect of AMPK inhibition on the inhibition of insulin-stimulated glucose transport by AICAR. Western blotting assessing phosphorylation of the AMPK target protein ACC, at Ser79, was performed to determine whether AMPK activity was inhibited by Compound C. As shown in figure 4.3B/C, AICAR caused a significant ($p < 0.05$) 2.18 +/- 0.69 and 2.54 +/- 0.49 fold increase in ACC Ser79 phosphorylation, in non-insulin-stimulated cells and insulin-stimulated cells respectively. In comparison, AICAR was not found to significantly increase ACC Ser79 phosphorylation, under non-insulin-stimulated and insulin-stimulated conditions, in 3T3-L1 adipocytes incubated in the presence of Compound C. Incubation of 3T3-L1 adipocytes in AICAR caused a significant ($p < 0.05$) 28.4 +/- 3.5 % inhibition of insulin-stimulated glucose transport (Fig. 4.3A). However, in the presence of Compound C, AICAR did not inhibit insulin-stimulated glucose transport in 3T3-L1 adipocytes (Fig. 4.3A). In addition, a significant ($p < 0.05$) 32 +/- 1.2 % reduction in insulin-stimulated

glucose transport was observed in 3T3-L1 adipocytes incubated in the presence of Compound C.

4.2.2.2 Effect of a DN AMPK mutant on AICAR mediated inhibition of insulin-stimulated glucose transport

Adenovirus-mediated gene transfer was used to overexpress a dominant negative AMPK mutant (Ad.α1DN) in 3T3-L1 adipocytes, in order to further investigate the effect of down-regulation of AMPK on AICAR mediated inhibition of insulin-stimulated glucose transport.

The α1DN mutant protein is based on the entire α1 subunit sequence and contains an N-terminal myc tag. The expression of α1DN is shown by the presence of a band detected by the myc antibody at about 62kDa (Fig. 4.4A). In addition, AICAR stimulated ACC Ser79 phosphorylation was decreased in Ad.α1DN infected cells, compared to Ad.null infected cells.

AICAR caused a 22.4 +/- 9.2 % and 41 +/- 26.8 % inhibition of insulin-stimulated glucose transport in Ad.null and Ad.α1DN infected cells, respectively. In addition, this current work also found that both insulin-stimulated and basal glucose transport were exacerbated in Ad.α1DN infected cells, compared to Ad.null infected cells (Figure 4.4B). In Ad.null infected cells the fold increase in glucose transport upon insulin-stimulation was 8 +/- 0.62 and 4.38 +/- 0.8 in non-AICAR treated cells and AICAR treated cells respectively. However, in Ad.α1DN infected cells the fold increase in glucose transport upon insulin-stimulation was 4.54 +/- 1.42 and 2.27 +/- 0.8 in non-AICAR treated cells and AICAR treated cells respectively. This implies that suppression of AMPK increases basal glucose transport, while reducing the extent by which insulin activates glucose transport.

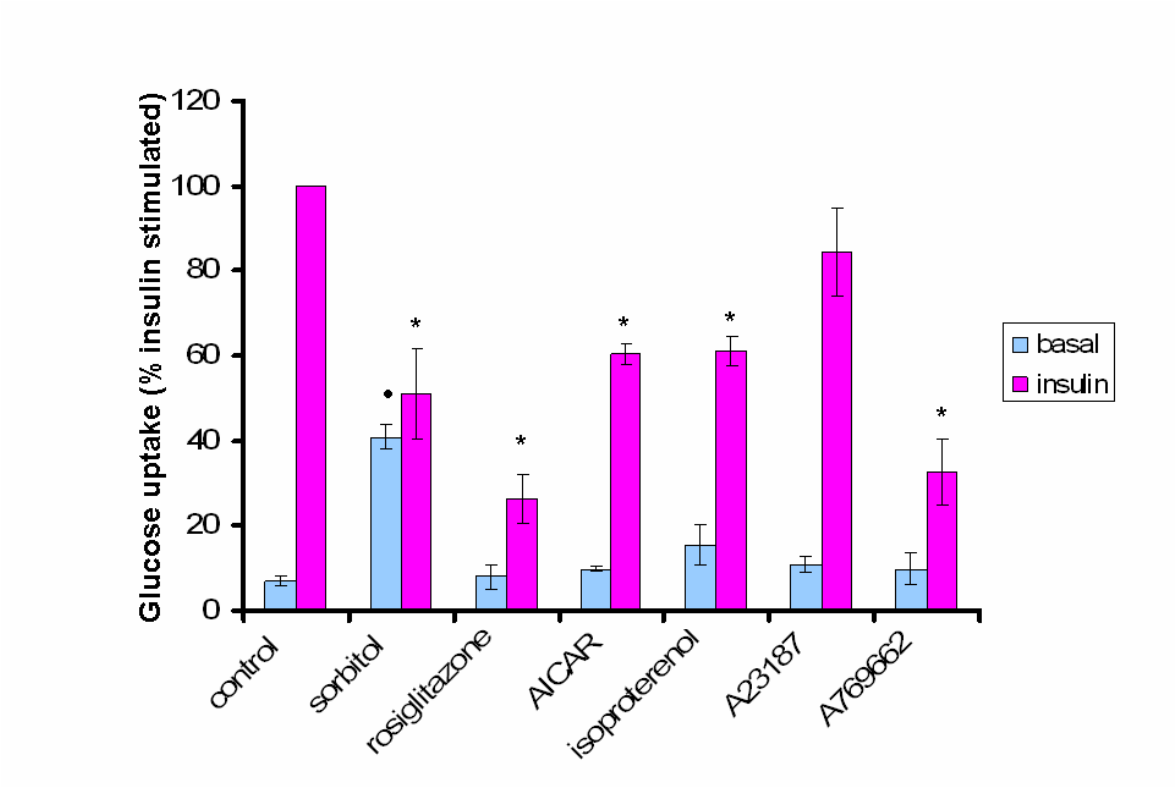

Figure 4-2: Effect of various AMPK activators on basal and insulin-stimulated glucose transport.

*3T3-L1 adipocytes were pre-incubated for 30 min in the presence of 2 mM AICAR, 0.6 M sorbitol, 100 µM rosiglitazone, 1 µM isoproterenol, 5 µM A23187or 300 µM A-769662 prior to stimulation with 10 nM insulin for 15 min. Glucose transport was initiated by the addition of 2-[^{3}H]-deoxy-D-glucose, and terminated after 3 min. Data shown represents the mean % insulin-stimulated +/- S.E.M of three independent experiments, *p < 0.05 (2-tail t-test), compared to insulin-stimulated, •p < 0.05 (2-tail t-test), compared to control. Insulin-stimulated glucose transport was 644 +/- 34 (mean +/- SEM) pmol glucose transported / min / mg protein.*

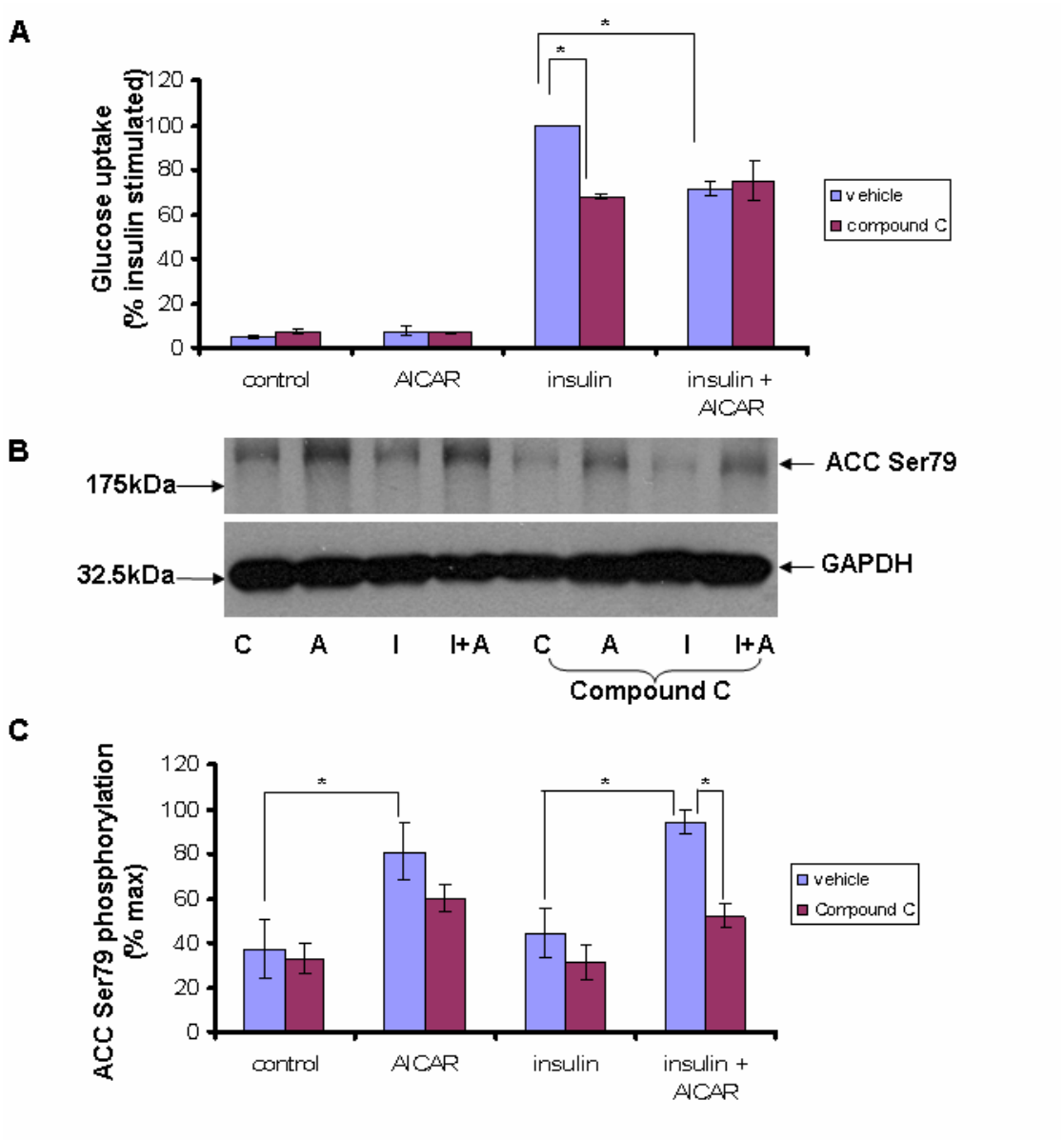

Figure 4-3: Effect of Compound C on AICAR mediated inhibition of insulin-stimulated glucose transport.

*3T3-L1 adipocytes were pre-incubated for 30 min in the presence of 60 µM Compound C, prior to the addition of 2 mM AICAR for 30 min. The cells were then stimulated with 10 nM insulin for 15 min. (A) Glucose transport was initiated by the addition of 2-[^{3}H]-deoxy-D-glucose, and terminated after 3 min. Data shown represents the mean % insulin-stimulated +/- S.E.M of three independent experiments, *p < 0.05 (one-way ANOVA). Insulin-stimulated glucose transport was 940 +/- 378 (mean +/- SEM) pmol glucose transported / min / mg protein. 3T3-L1 lysates (10 µg) were resolved on 10% polyacrylamide gels, transferred to nitrocellulose and probed with anti-ACC Ser79 and anti-GAPDH antibodies. (B) Representative blots from three independent experiments. (C) Quantification of ACC Ser79 phosphorylation was determined by comparison with total GAPDH using densitometric analysis. Data shown represents the mean % maximum +/- S.E.M of three independent experiments, *p < 0.05 (one-way ANOVA). The position of the molecular weight markers are shown to the left of the gel.*

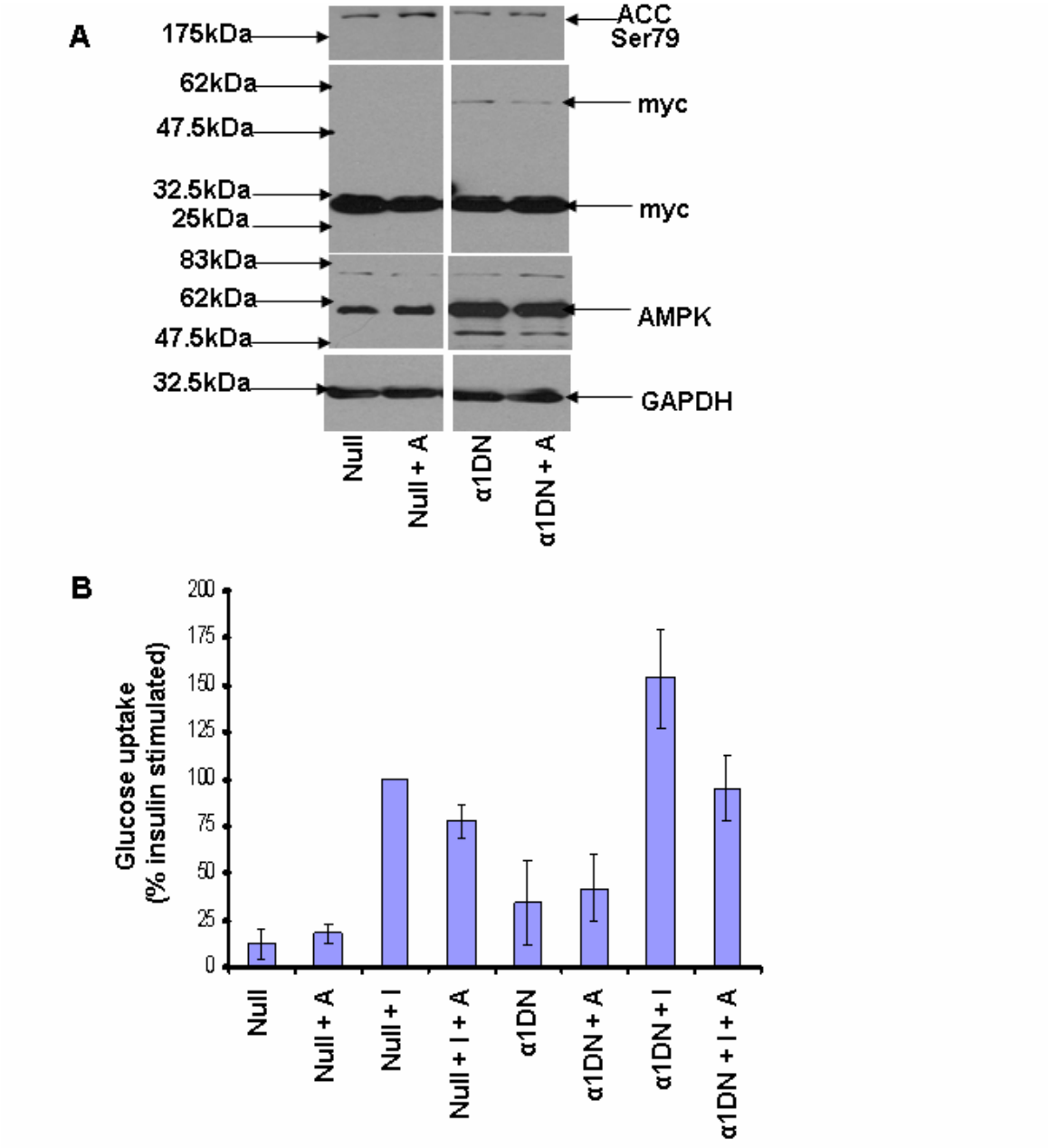

Figure 4-4: Effect of overexpression of a dominant negative AMPK mutant on AICAR mediated inhibition of insulin stimulated glucose transport in 3T3-L1 adipocytes
(A) 3T3-L1 adipocytes were infected (600 ifu/cell) for 48 hr with Ad.α1DN or Ad.null prior to stimulation for 30 min with 2 mM AICAR. Cell lysates (25 µg) were resolved by SDS-PAGE, transferred to nitrocellulose and probed with anti-ACC Ser79, anti-AMPKα1, anti-c-myc and anti-GAPDH antibodies. The position of the molecular weight markers are shown to the left of the gel. (B) 3T3-L1 adipocytes cultured on 12 well plates were infected (600 ifu/cell) with Ad.α1DN or Ad.null. After 48 hr 3T3-L1 adipocytes were pre-incubated for 30 min in the presence of 2 mM AICAR prior to stimulation with 10 nM insulin for 15 min. Glucose transport was initiated by the addition of 2-[^{3}H]-deoxy-D-glucose, and terminated after 3 min. Data shown represents the mean % insulin-stimulated +/- S.E.M of three independent experiments. Insulin-stimulated glucose transport in Ad.null cells was 540 +/- 126 (mean +/- SEM) pmol glucose transported / min / mg protein. A = AICAR, I = insulin.

4.2.3 Investigating the mechanism of AICAR mediated inhibition of insulin-stimulated glucose uptake in 3T3-L1 adipocytes.

4.2.3.1 Specificity of anti-AS160 and anti-TBC1D1 antibodies

AS160 and TBC1D1 are highly related Rab GAPs. To investigate the specificity of the anti-AS160 and anti-TBC1D1 antibodies, AS160 and TBC1D1 were immunprecipitated from 3T3-L1 lysates using anti-TBC1D1 and anti-AS160 antibodies. The immunoprecipitates and respective supernatants were analysed by western blotting using anti-TBC1D1 and anti-AS160 antibodies. As shown in figure 4.5A TBC1D1 is detected in the TBC1D1 immunoprecipitate and the supernatants from both TBC1D1 and AS160 immunoprecipitates. However, it would appear that the anti-AS160 antibody does not immunoprecipitate TBC1D1 since TBC1D1 is not detected in the AS160 immunoprecipitate. Conversely, as shown in figure 4.5B, AS160 is detected only in the AS160 immunoprecipitate, suggesting that the anti-TBC1D1 antibody does not immunoprecipitate AS160.

4.2.3.2 Effect of AICAR on basal and insulin-stimulated AS160 phosphorylation at PAS sites and association of 14-3-3 proteins.

In order to determine the effect of AICAR on basal and insulin-stimulated AS160 phosphorylation at PAS sites and association of 14-3-3 proteins with phosphorylated AS160, AS160 was immunoprecipitated from 3T3-L1 lysates treated in the presence and absence of AICAR, prior to stimulation with insulin. Immunoprecipitates were then subjected to western blotting with anti-PAS and anti-14-3-3 antibodies.

As shown in figure 4.6, AICAR did not significantly alter basal or insulin stimulated phosphorylation of AS160 at PAS sites. Interestingly, the amount of proteins that co-immunoprecipited with AS160 with apparent molecular masses matching those of the 14-3-3 proteins, did not differ between basal and insulin-stimulated conditions.

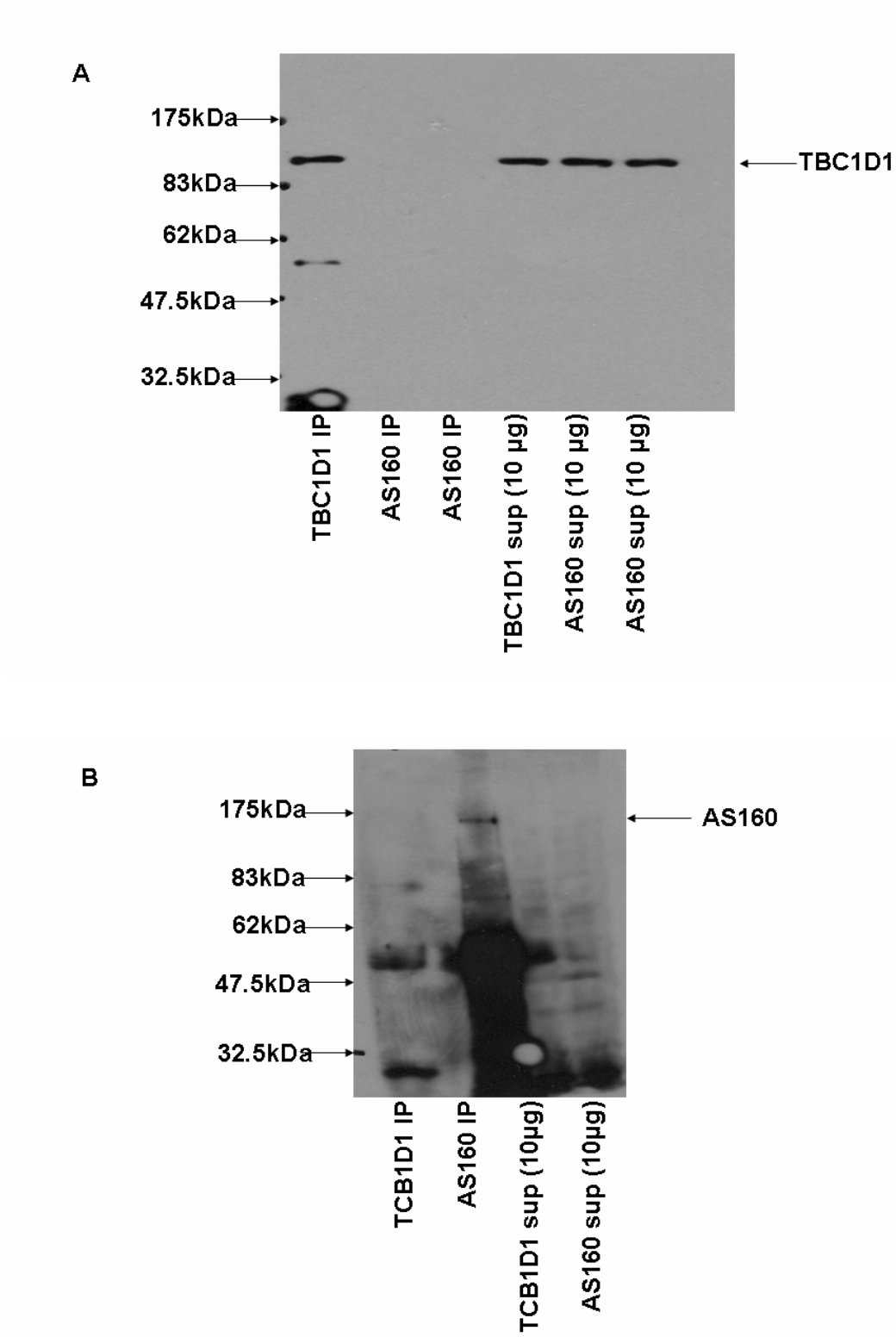

Figure 4-5: Specificity of anti-AS160 and anti-TBC1D1 antibodies.
(A) AS160 and TBC1D1 were immunoprecipitated from 3T3-L1 adipocyte lysates (200 µg) using anti-TBC1D1 and anti-AS160 antibodies. Immunoprecipitates and respective supernatants were then resolved on 10% SDS-PAGE, transferred to nitrocellulose and probed with (A) anti-TBC1D1 antibody, (B) anti-AS160 antibody. Representative blots from two independent experiments. The position of the molecular weight markers are shown to the left of the gel. IP = immunoprecipitate, sup = supernatant.

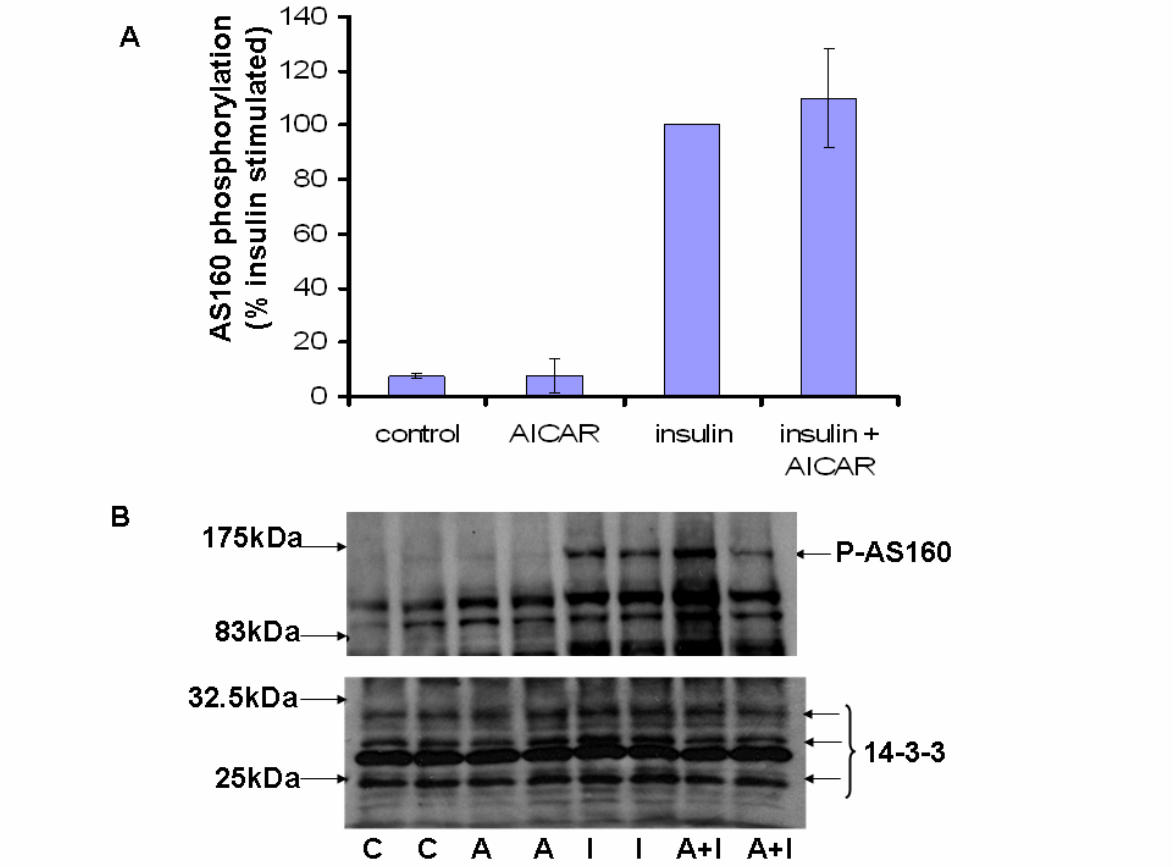

Figure 4-6: Effect of AICAR on basal and insulin-stimulated AS160 phosphorylation at PAS sites and association with 14-3-3 proteins.

AS160 was immunoprecipitated from 3T3-L1 lysates (250 µg) obtained from cells treated in the presence and absence of 2 mM AICAR for 30 min, prior to stimulation with 10 nM insulin for 30 min. Immunoprecipitates were resolved on 10% SDS-PAGE, transferred to nitrocellulose and probed with anti-PAS and anti-14-3-3 antibodies. (A) Quantative analysis of AS160 phosphorylation at PAS sites. Data shown represents the mean % insulin-stimulated +/- S.E.M of three independent experiments with duplicates in each. (B) Representative western blot, from three independent experiments with duplicates. C = control, A = AICAR, I = insulin. The position of the molecular weight markers are shown to the left of the gel.

4.2.3.3 Effect of AICAR on basal and insulin-stimulated TBC1D1 phosphorylation at PAS sites.

In order to determine the effect of AICAR on basal and insulin-stimulated TBC1D1 phosphorylation at PAS sites, TBC1D1 was immunoprecipitated from 3T3-L1 lysates treated in the presence and absence AICAR, prior to stimulation with insulin. Immunoprecipitates were then subjected to western blotting with anti-PAS antibody.

As shown below in figure 4.7, there was no detectable levels of PAS phosphorylated TBC1D1 in control or AICAR treated 3T3-L1 adipocytes. In addition, AICAR did not significantly alter insulin-stimulated TBC1D1 phosphorylation at PAS sites.

4.2.3.4 Effect of AICAR on PKB substrate phosphorylation

To determine whether AICAR alters the phosphorylation of any insulin-stimulated PKB substrate proteins, lysates from 3T3-L1 adipocytes pre-incubated for 30 min in the presence of 2 mM AICAR, prior to stimulation with 10 nM insulin for 15 min, were resolved by SDS-PAGE and western blotted with the anti-PAS antibody. As shown in figure 4.8, AICAR does not appear to perturb insulin-stimulated phosphorylation of any proteins. However, AICAR does appear to increase PAS phosphorylation, compared to basal levels, of two proteins * with molecular masses of about 40kDa and 48kDa.

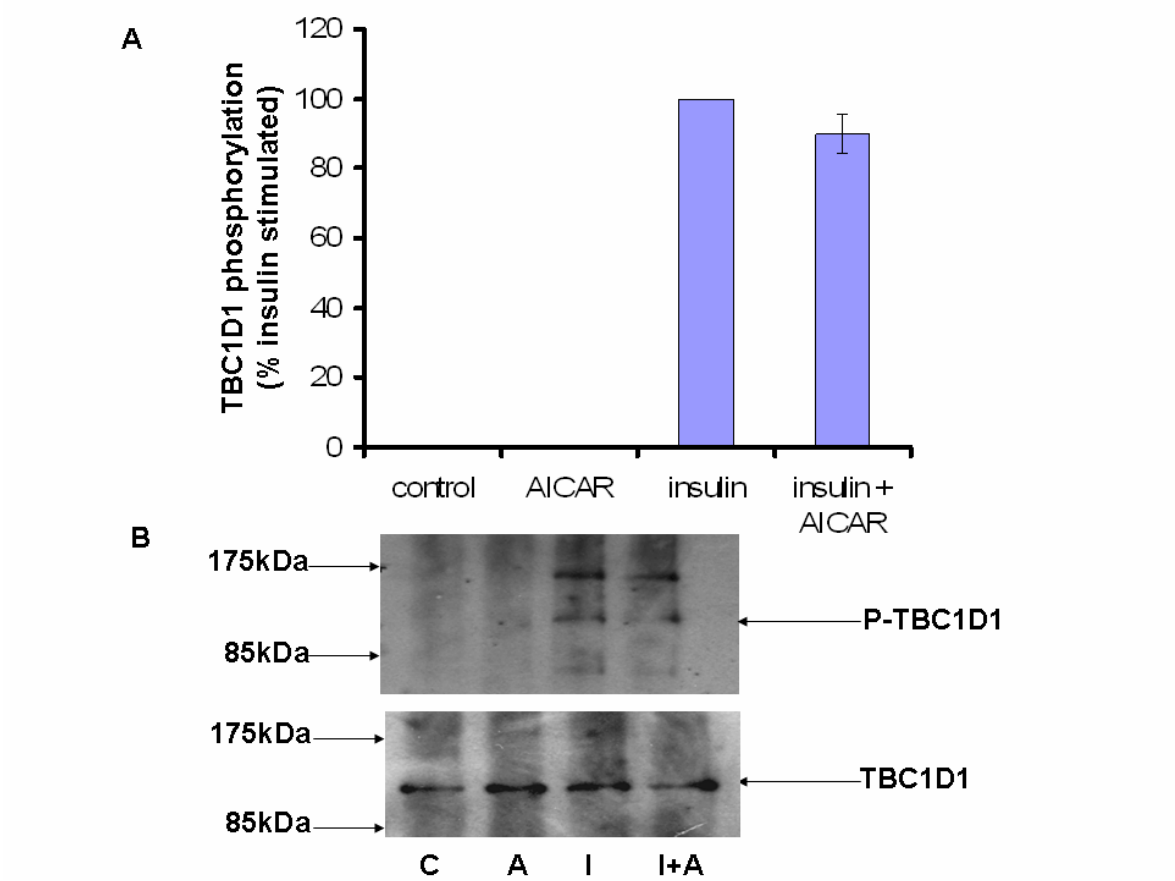

Figure 4-7: Effect of AICAR on basal and insulin-stimulated TBC1D1 phosphorylation at PAS sites.

TBC1D1 was immunoprecipitated from 3T3-L1 lysates (200 µg) obtained from cells treated in the presence and absence of 2 mM AICAR for 30 min, prior to stimulation with 10 nM insulin for 30 min. Immunoprecipitates were resolved on 10% SDS-PAGE, transferred to nitrocellulose and probed with anti-PAS and anti-TBC1D1 antibodies. (A) Quantification of TBC1D1 phosphorylation was determined by comparison with total TBC1D1 using densitometric analysis. Data shown represents the mean % insulin-stimulated +/- S.E.M of two independent experiments. (B) Representative western blot, from two independent experiments. C = control, A = AICAR, I = insulin. The position of the molecular weight markers are shown to the left of the gel.

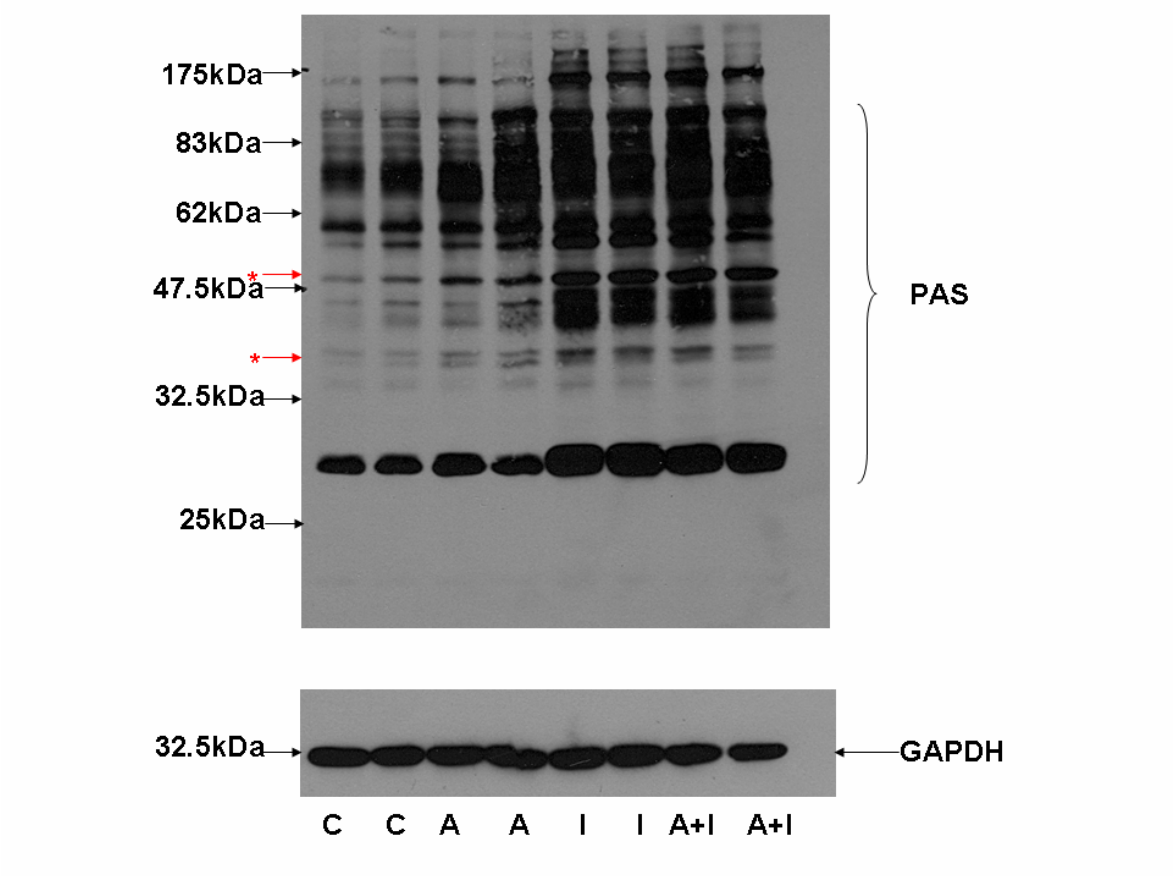

Figure 4-8: Effect of AICAR on PKB substrate phosphorylation.
*3T3-L1 adipocytes were pre-incubated for 30 min in the presence of 2 mM AICAR, prior to stimulation with 10 nM insulin for 15 min. Lysates (25 µg) were then resolved on 10% SDS-PAGE gels, transferred to nitrocellulose and probed with the anti-PAS antibody. Representative blot from four independent experiments with duplicates. C = control, A = AICAR, I = insulin. The position of the molecular weight markers are shown to the left of the gel. * = AICAR increases basal PAS phosphorylation of the indicated proteins.*

4.3 Discussion

The key findings of this chapter are that multiple AMPK stimuli inhibited insulin-stimulated glucose transport, that in the presence of the AMPK inhibitor Compound C the inhibitory effect of AICAR on insulin-stimulated glucose transport was no longer apparent, and that inhibition of insulin-stimulated glucose transport by AICAR was not associated with altered PKB-mediated phosphorylation of AS160/TBC1D1.

AMPK and glucose transport

AICAR

In muscle cells, AICAR stimulates basal glucose transport and potentiates insulin-stimulated glucose transport (Bergeron *et al* 1999). In contrast this study showed that AICAR significantly ($p < 0.05$) inhibits insulin-stimulated glucose uptake in 3T3-L1 adipocytes, which supports previous work by Salt and co-workers (Salt *et al* 2000). AICAR has also been shown to inhibit insulin-stimulated glucose transport in isolated rat adipocytes (Gaidhu *et al* 2006), and rat cardiomyocytes (Segalen *et al* 2008). Salt and co-workers also reported that AICAR inhibited insulin-stimulated GLUT4 translocation to the plasma membrane in 3T3-L1 adipocytes by assay of plasma membrane lawns (Salt *et al* 2000). In contrast, Chavez and co-workers measured the amount of GLUT4 at the cell surface by the quantitative single-cell fluorescence assay that employs the reporter construct of GLUT4 with a haemagglutinin (HA) tag in the amino-terminal extracellular loop and green fluorescent protein (GFP) fused to the carboxyl terminus (HA-GLUT4-GFP), and reported that AICAR did not alter insulin-stimulated GLUT4 translocation to the plasma membrane (Chavez *et al* 2008). Potentially the tagged GLUT4 construct may behave differently to endogenous GLUT4 in the 3T3-L1 adipocytes, which could explain the contrasting results. For example AICAR may increase the rate at which endogenous GLUT4 is trafficked from the plasma membrane into intracellular storage vesicles, which would deplete the amount of GLUT4 at the plasma membrane, whereas potentially the tagged GLUT4 maybe retained at the plasma membrane.

Sorbitol

This study found that sorbitol caused a significant ($p < 0.05$) 5 fold increase in basal glucose transport and significantly ($p < 0.05$) inhibited insulin-stimulated glucose uptake. Previous studies have also shown that sorbitol stimulates basal glucose transport in rat adipocytes, L6 myotubes and 3T3-L1 adipocytes (Sajan *et al* 2002, Chen *et al* 1997, Chen

et al 1999). In 3T3-L1 adipocytes, signalling pathways downstream of Grb2-associated binding protein 1 (Gab1), and specifically the Gab1 / CT10 sarcoma oncogene cellular homolog II (CrkII) / GTP binding protein TC10 (TC10) signalling pathway, are thought to play a crucial role in osmotic-stress induced glucose transport (Janez *et al* 2000, Gual *et al* 2002). It has also been reported that hyperosmotic stress activates the proline-rich tyrosine kinase 2 (PYK2) / extracellular signal-regulated kinase (ERK) / phospholipase D (PLD) / aPKC pathway in 3T3-L1 adipocytes and rat adipocytes, leading to GLUT4 translocation and glucose uptake (Sajan *et al* 2002).

In muscle overexpression of a dominant-negative form of AMPK blocked the stimulation of GLUT4 translocation by hyperosmotic stress (Fryer *et al* 2002a), suggesting a role for AMPK activation in hyperosmotic-induced glucose uptake. In skeletal muscle, hyperosmotic stress was shown to stimulate AMPK activity and increase insulin-stimulated glucose transport (Smith *et al* 2005). In addition, the increase in insulin-stimulated glucose transport caused by hyperosmotic stress was prevented by inclusion of the AMPK inhibitor Compound C, suggesting that AMPK activation may mediate the synergistic effect of hyperosmotic stress on insulin-stimulated glucose transport (Smith *et al* 2005). This is in stark contrast to the findings of this study and a previous study in 3T3-L1 adipocytes (Chen *et al* 1999), which found that hyperosmotic stress induced by sorbitol inhibited insulin-stimulated glucose transport in 3T3-L1 adipocytes. Similarly, in rat epididymal adipose cells, hyperosmotic stress was shown to markedly reduce insulin-induced glucose transport (Komjati *et al* 1998). The proposed modes of action of hyperosmotic stress induced inhibition of insulin-stimulated glucose transport in 3T3-L1 adipocytes include; inactivation of PKB (Chen *et al* 1999) serine phosphorylation of IRS1 (Gual *et al* 2003) and enhanced degradation of IRS proteins (Gual *et al* 2003).

Rosiglitazone

This study showed that acute treatment of 3T3-L1 adipocytes with the anti-diabetic drug, rosiglitazone, significantly ($p < 0.05$) inhibited insulin-stimulated glucose transport. It should be noted that using concentrations of 100µM rosiglitazone in this study was merely a tool to stimulate activation of AMPK, and that this acute inhibition of insulin-stimulated glucose transport with 100µM rosiglitazone has no clinical significance as the maximum concentration of rosiglitazone reached in patients is approximately 1µM. Indeed previous work, showed that chronic (48hr) treatment of 3T3-L1 adipocytes with increasing concentrations (1nM-10µM) of rosiglitazone resulted in progressive increases in both basal and insulin-stimulated 2-deoxyglucose uptake (Standaert *et al* 2002). Interestingly, a recent

study showed that long-term TZD treatment enhanced AMPK-stimulated glucose uptake into muscle and adipose tissue in insulin-resistant states in rats (Ye *et al* 2006).

Isoproterenol

This current study showed that isoproterenol significantly ($p < 0.05$) inhibited insulin-stimulated glucose transport. Previously, isoproterenol was shown to induced a two fold increase in glucose transport (Smith *et al* 1984) and inhibit insulin-stimulated glucose uptake in rat adipose cells (Smith *et al* 1984, Joost *et al* 1986, Kirsch *et al* 1983, Kashiwagi *et al* 1983, Yang *et al* 2002).

A23187

It has been reported that calcium is involved in insulin signalling in muscle (Clausen *et al* 1974) and adipose (Clausen *et al* 1974, Draznin *et al* 1987, Yang *et al* 2000). Calcium is thought to be involved in at least two different steps of the insulin-dependent recruitment of GLUT4 to the plasma membrane. One involves the translocation step. The second involves the fusion of GLUT4 vesicles with the plasma membrane (Whitehead *et al* 2001). In this study the calcium ionophore A23187 displayed a modest tendency to inhibit insulin-stimulated glucose transport, however this was not statistically significant. Previous work by Draznin and co-workers also showed that another calcium ionophore, ionomycin, inhibited insulin-stimulated glucose transport in isolated rat adipocytes (Draznin *et al* 1987). Draznin and co-workers proposed that high and/or sustained levels of intracellular calcium may function as a postreceptor feedback sensor to diminish cellular responsiveness to insulin (Draznin *et al* 1987). Potentially elevated intracellular calcium levels by the two ionophores may activate AMPK via CaMKK, which in turn may mediate inhibition of insulin-stimulated glucose transport.

A769662

Interestingly, this current study also found that the novel, direct AMPK activator, A769662, significantly ($p < 0.05$) inhibited insulin-stimulated glucose transport. Given that A769662 is a direct AMPK activator, these results provide the best evidence so far that activation of AMPK inhibits insulin-stimulated glucose transport in 3T3-L1 adipocytes.

As AICAR, sorbitol, rosiglitazone, isoproterenol and the direct AMPK activator, A769662, have all been shown to stimulate AMPK activity (Figs. 3.11-3.21), and inhibit insulin-stimulated glucose transport in 3T3-L1 adipocytes (Fig. 4.1), it is possible that activation

of AMPK inhibits insulin-stimulated glucose transport in 3T3-L1 adipocytes. In addition, there did appear to be a correlation between the % inhibition of insulin-stimulated glucose transport and fold increase in AMPK activity in 3T3-L1 adipocytes (Fig. 4.9) i.e rosiglitazone displayed a large % inhibition of insulin-stimulated glucose transport and stimulated a large fold increase in AMPK activity, isoproterenol and AICAR displayed a lower % inhibition of insulin-stimulated glucose transport and stimulated a lower fold increase in AMPK activity compared to rosiglitazone, and A23187 displayed the lowest % inhibition of insulin-stimulated glucose transport and stimulated the lowest fold increase in AMPK activity. The exceptions were the direct AMPK activator A769662, which displayed the second greatest % inhibition of insulin-stimulated glucose uptake, despite only modestly stimulating AMPK activity**,** and sorbitol which displayed the third highest % inhibition of insulin-stimulated glucose transport, despite stimulating the greatest fold increase in AMPK activity. The direct AMPK activator, A769662, has been reported to activate only β1 containing AMPK complexes **(**Scott *et al* 2008), which is likely to account for the modest increase in AMPK activity observed in cells incubated with A769662. Since sorbitol, is not a direct AMPK activator it is possible that through non-AMPK mediated pathways sorbitol is having additional effects on insulin-stimulated glucose transport.

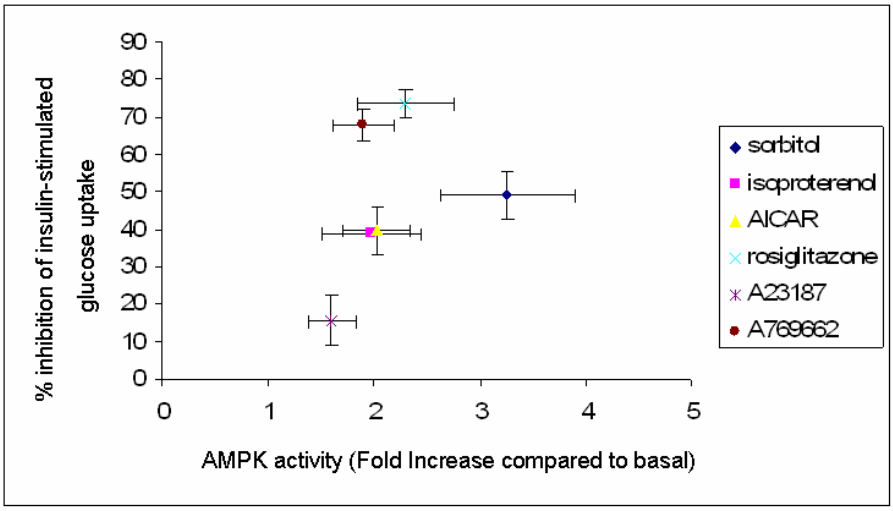

Figure 4-9: Fold increase in AMPK activity versus % inhibition of insulin-stimulated glucose transport.

It should also be noted that the most potent AMPK activator, sorbitol, displayed a highly significant ($p < 0.05$) five fold increase in basal glucose transport, whereas all the other stimuli did not significantly alter basal glucose transport. This suggests that the exceptionally high increase in basal glucose transport by sorbitol may be mediated by both AMPK-dependent and -independent mechanisms.

Interestingly in isolated hepatocytes and heart, insulin has been shown to inhibit AMPK activity (Witters and Kemp 1992, Gamble and 1997). However, in the liver cell line H4IIE insulin was found to have no effect on AMPK activity (Lochhead *et al* 2000). In this current work insulin did not significantly alter AMPK activity as assessed by ACC Ser79 phosphorylation (Fig. 4.3). In addition, previous work in our lab showed that insulin did not alter AMPK activity, as assessed by AMPK assays, in 3T3-L1 adipocytes (personal correspondence with Dr. I.P Salt).

In order to investigate whether the effect of AICAR on insulin-stimulated glucose transport is mediated by AMPK activation, the effect of AICAR on insulin-stimulated glucose transport was assessed in the presence of the AMPK inhibitor Compound C (Fig. 4.3). This study found that in the presence of Compound C, AICAR did not inhibit insulin-stimulated glucose transport. This suggests that AMPK activation in 3T3-L1 adipocytes inhibits insulin-stimulated glucose transport. However, it is difficult to conclude whether Compound C is rescuing the inhibition of insulin-stimulated glucose transport by AICAR, given the fact that Compound C itself significantly inhibits insulin-stimulated glucose transport.

In general the results obtained using Compound C should be interpreted with caution as Compound C is not a specific AMPK inhibitor. It has been shown to also inhibit a number of other protein kinases *in vitro* including; ERK 8, MAP kinase-interacting kinase 1 (MNK1), phosphorylase kinase (PHK), maternal embryonic leucine zipper kinase (MELK), dual specificity tyrosine phosphorylation and regulated kinase (DYRK) isoforms, homeodomain-interacting protein kinase2 (HIPK2), sarcoma kinase (Src) and lymphocyte cell-specific protein-tyrosine kinase (Lck) (Bain *et al* 2007). Bain and co-workers also found that the CaMKK inhibitor STO-609 was a more potent AMPK inhibitor than Compound C *in vitro* (Bain *et al* 2007). In the previous chapter, 25 μM STO-609 was used to inhibit CaMKK in 3T3-L1 adipocytes. However, 25 μM STO-609 did not appear to inhibit AMPK since AICAR stimulated AMPK activity was not perturbed in the presence of STO-609. Potentially a higher concentration of STO-609 could be used to inhibit

AMPK and assess the role of AMPK in AICAR mediated inhibition of insulin-stimulated glucose transport.

Interestingly, Fryer and co-workers, showed that Compound C can inhibit the adenosine transporter, which is the main transport system used by cells in the uptake of AICAR (Fryer *et al* 2002c). Thus, the reduction in AICAR stimulated ACC Ser79 phosphorylation in the presence of Compound C could have resulted from the inhibition of AMPK activation by AICAR and/or inhibition of AICAR uptake into the cell.

Adenoviral DN AMPK was also used to investigate whether the effect of AICAR on insulin-stimulated glucose transport is mediated by AMPK activation (Fig. 4.4). Although inhibition of insulin-stimulated glucose transport by AICAR did not reach statistical significance in Ad.null and Ad.α1DN infected cells, the results do suggest that the effect of AICAR on insulin-stimulated glucose transport is not dependent on AMPK activation. This is in contrast to results obtained using the AMPK inhibitor Compound C. However, perhaps in this current study Compound C inhibited a greater proportion of total AMPK in 3T3-L1 adipocytes compared to Ad.α1DN, which could explain the discrepancy between the results. In addition, this study found that both basal and insulin-stimulated glucose transport were exacerbated in Ad.α1DN infected cells, compared to Ad.null infected cells. However, the fold increase in glucose transport upon insulin-stimulation was reduced in Ad.α1DN infected cells compared to Ad.null infected cells. These results suggest that long term suppression of AMPK improves glucose transport while reducing the extent by which insulin increases glucose transport. The increase in glucose transport may be due to the inhibition of endogenous AMPK activity, which if the case, supports the possibility that AMPK activation may inhibit insulin-stimulated glucose transport. In addition, long-term treatment of adipocytes with Ad.α1DN maybe increasing glucose transport by altering the expression level of key insulin-signalling molecules such as SNARES, AS160 and PKB. Previous work in muscle showed that prolonged AMPK activation increased expression levels of GLUT4 (Holmes *et al* 1999). However, currently the effect of prolonged AMPK activation on GLUT4 expression in adipocytes has yet to be determined.

Interestingly, Sakoda and co-workers found that overexpression of α1DN abolishes AMPK activation, without affecting the increase in basal glucose uptake by AICAR, thereby suggesting that AICAR-induced glucose uptake in 3T3-L1 adipocytes is independent of AMPK activation (Sakoda *et al* 2002). However, in this current study AICAR did not significantly increase basal glucose transport in Ad.null infected cells.

Since the inhibition of insulin-stimulated glucose transport by AICAR is rescued in cells incubated in Compound C, but not in Ad.α1DN, further work is required to determine whether AMPK activation inhibits insulin-stimulated glucose transport. This might involve investigating the effect of Compound C and Ad.α1DN on the inhibition of insulin-stimulated glucose transport by other AMPK stimuli. In particular, sorbitol and rosiglitazone which both displayed a large % inhibition of insulin-stimulated glucose transport, and the novel AMPK activator A769662 which differs from the other AMPK stimuli including AICAR, in that it directly activates AMPK.

Mechanism of AICAR mediated inhibition of insulin-stimulated glucose transport

The mechanism by which AICAR inhibits insulin-stimulated glucose transport in 3T3-L1 adipocytes was explored. This study (Fig. 4.6) found that in 3T3-L1 adipocytes AICAR does not appear to alter AS160 phosphorylation at PAS sites compared to basal levels, which is in contrast to observed effects in skeletal muscle where AICAR has been shown to increase AS160 phosphorylation at PAS sites (Bruss *et al* 2005). Figure 4.6 also shows that concomitant incubation of AICAR with insulin does not alter insulin-stimulated AS160 phosphorylation at PAS sites, thus it is unlikely that AMPK inhibits insulin-stimulated glucose transport by inhibiting insulin-stimulated AS160 phosphorylation.

In addition, this study found that the anti-AS160 antibody did not appear to immunoprecipitate TBC1D1, which has an apparent molecular weight of 130kDa (Fig. 4.5). Thus the intense dark band present at approximately 140kDa in the AS160 IP's (Fig. 4.6) detected with the PAS antibody is most likely to be a short splice variant of AS160 or another PKB substrate molecule which co-immunoprecipitates with AS160, and not TBC1D1.

Ramm and co-workers previously showed that in 3T3-L1 adipocytes, insulin-stimulated a 4 fold increase in the amount of 14-3-3 associated with AS160 (Ramm *et al* 2006). This current study also looked at whether AICAR altered insulin-stimulated AS160 binding to 14-3-3 proteins. The several protein bands detected by the anti-14-3-3 antibody with apparent molecular masses matching those of the 14-3-3 proteins were thought to correspond to the various 14-3-3 protein isoforms (Fig. 4.6). However, the intense band, recognised by the anti-14-3-3 antibody, which resolves at about approximately 27kDa is most likely to correspond to the AS160 antibody light chain (Fig 4.6). The identity of the 14-3-3 proteins and antibody light chain could be confirmed by comparison with a negative control i.e antibody and protein G beads, which is lacking in this experiment. In

contrast to the work by Ramm and co-workers, in this current study the amount of proteins that co-immunoprecipitated with AS160 with apparent molecular masses matching that of the 14-3-3 proteins, did not differ between basal and insulin-stimulated conditions. Chen and co-workers, used cross linking to stabilize the insulin-stimulated 14-3-3 interactions with TBC1D1 (Chen *et al* 2008), thus perhaps the interaction between 14-3-3 proteins and AS160 in this study were lost during the immunoprecipitation process.

TBC1D1 was shown to be phosphorylated at PAS sites in mouse skeletal muscle *in vivo* by insulin, AICAR and contraction (Taylor *et al* 2008). Although, insulin was shown to stimulate TBC1D1 phosphorylation at PAS sites, this current study could not detect any TBC1D1 phosphorylation at PAS sites in AICAR treated 3T3-L1 cells (Fig. 4.7). The current study also found that AICAR did not alter insulin-stimulated PAS phosphorylation of TBC1D1 (Fig. 4.7). Interestingly, anti-TBC1D1 appears to immunoprecipitate a protein with a molecular weight of about 160kDa, which is PAS phosphorylated. A likely candidate was thought to be AS160. However, western blotting of TBC1D1 and AS160 immunoprecipitates, with the anti-AS160 antibody, suggested that anti-TBC1D1 does not immunoprecipitate AS160. However, this experiment remains inconclusive, as unlike TBC1D1, AS160 was not detected in the immunoprecipitation supernatants, suggesting that the AS160 antibody is relatively weak. Thus potentially anti-TBC1D1 may immunoprecipitate small quantities of AS160 which are detected by the more sensitive anti-PAS antibody, but not by the anti-AS160 antibody.

It should be noted that AMPK may be altering insulin-stimulated AS160/TBC1D1 phosphorylation at PAS sites which are not primarily recognized by the anti-PAS antibody in 3T3-L1 adipocytes which may alter AS160/TBC1D1 activity. Indeed in HEK 293 cells the anti-PAS antibody was found to primarily detect phospho-Thr642 on AS160 (Geraghty *et al* 2007). Furthermore AMPK activation in 3T3-L1 adipocytes may result in phosphorylation of AS160/TBC1D1 at non-PAS sites, and such phosphorylations may have additional effects on AS160/TBC1D1 function and GLUT4 trafficking.

Antibodies against specific phosphorylation sites on AS160 and TBC1D1 could be used in order to determine whether AICAR alters phosphorylation of these Rab GAP proteins at PAS sites not primarily detected by the anti-PAS antibody and/or stimulates phosphorylation at non-PAS sites. Site directed mutagenesis of any such sites could be used to investigate whether AICAR inhibits insulin-stimulated glucose transport, by altering phosphorylation of AS160 /TBC1D1 at a specific site.

Finally this study found that AICAR did not appear to perturb insulin-stimulated phosphorylation of any PKB target proteins. However, interestingly it appears that AICAR stimulates phosphorylation at PAS sites, compared to basal levels, of two proteins with molecular weights of approximately 37kDa and 50kDa. However, the identity of these bands remains unknown. Potentially, mass spectrometry could be used to identify the proteins.

Interestingly, intracellular acidification shown to be induced by the AMPK stimuli AICAR and isoproterenol, has been proposed to mediate the inhibition of insulin-stimulated glucose transport by these reagents (Segalen *et al* 2008, Yang *et al* 2002, Civelek *et al* 1996).

Exposure of cells to insulin has been shown to cause an increase in intracellular pH in rat adipocytes (Civelek *et al* 1996), 3T3-L1 cells (Klip *et al* 1988), muscle (Fidelman *et al* 1982, Klip *et al* 1986), and liver (Peak *et al* 1992). This alkalinization of cells by insulin is reported to be required for optimal glucose transport.

Inhibition of insulin-induced glucose uptake by AICAR in rat cardiomyocytes is reported to occur via the inhibition of the Na^+/H^+ exchanger-1 (NHE-1), which subsequently decreases the insulin mediated increase in intracellular pH (Segalen *et al* 2008). In addition AICAR is thought to exert these effects independently of AMPK activation (Segalen *et al* 2008). Although the Na^+/H^+ exchanger 1 is ubiquitously expressed (Fliegel 2005), it is possible that this is a cell type specific mechanism of inhibition by AICAR, and that the mechanism of inhibition of insulin-stimulated glucose transport by AICAR in 3T3-L1 adipocytes is different. This may well be the case given that the effect of AICAR on basal glucose transport differs between the two cell types i.e AICAR inhibits basal glucose transport in rat cardiomyocytes, while modestly stimulating basal glucose transport in 3T3-L1 adipocytes (Salt *et al* 2000).

Civelek and co-workers have suggested that treatment of adipocytes with isoproterenol induces acidification in adipocytes due to the lipolytic release of free fatty acids **(**Civelek *et al* 1996). Thus it has been proposed that the inhibition of insulin-stimulated glucose transport by isoproterenol may occur through cytosol acidification, which essentially reverses the alkalinizing effects of insulin required for optimum glucose transport (Yang *et al* 2002)**.**

Overall this current work suggests that acute AMPK activation by AICAR in adipocytes inhibits insulin-stimulated glucose uptake, yet this is not associated with altered PKB-mediated phosphorylation of AS160/TBC1D1. As discussed (1.1.2) glucose is taken up into adipocytes in the fed state and stored as TG. Therefore inhibition of glucose uptake into adipocytes would subsequently reduce fatty acid and TG synthesis. Thus, it could be reasoned that AMPK activation inhibits insulin-stimulated glucose uptake in adipocytes in order to reduce the ATP-dependent synthesis of fatty acids and TG in adipocytes. Furthermore, the inhibition of glucose transport would allow glucose to be used by other tissues as a source of energy, rather than adipocytes, which would start using the stored triglyceride.

Chapter 5 - Effect of sustained AMPK activation on adipocyte insulin action

5.1 Introduction

In chapter 4 it was reported that acute treatment of 3T3-L1 adipocytes with various AMPK stimuli inhibited insulin-stimulated glucose transport. Furthermore, in the presence of the AMPK inhibitor, Compound C, the inhibitory effect of AICAR on insulin-stimulated glucose transport was no longer apparent. However, AICAR still displayed a tendency to inhibit insulin-stimulated glucose transport in Ad.α1DN infected cells. In addition, sustained AMPK knockdown in Ad.α1-DN infected cells appeared to enhance both basal and insulin-stimulated glucose transport. Currently, the effect of sustained AMPK activation on insulin-stimulated glucose transport in adipocytes has still to be determined.

As discussed in section 1.4.12, previous studies have reported that sustained AMPK activation by AICAR inhibits differentiation of 3T3-L1 preadipocytes (Habinowski and Witters 2001, Giri *et al* 2006, Tong *et al* 2008). In contrast other studies suggest that AMPK may not play a role in regulating adipocyte differentiation *in vivo* (Villena *et al* 2004, Giri *et al* 2006). Huypens and co-workers showed that long term treatment with the AMPK activators metformin and AICAR reduced adiponectin protein expression and release in 3T3-L1 adipocytes (Huypens *et al* 2005). A recent study by Gaidhu and co-workers showed that prolonged AICAR-induced AMPK activation promotes energy dissipation in white adipocytes by preventing TG storage and by activating pathways that promote energy dissipation within the adipocyte, such as fatty acid oxidation (Gaidhu *et al* 2008). Interestingly, Gaidhu and co-workers also reported that lipolysis was first suppressed, but then increased both *in vitro* and *in vivo* with prolonged AICAR treatment in rat epididymal adipocytes (Gaidhu *et al* 2008). However, in general the effect of prolonged AMPK activation in mature adipocytes remains poorly characterized, particularly with respect to glucose transport and insulin signalling.

5.1.1 Aims

The principal aim of this study was, therefore, to investigate the effect of sustained AMPK activation on glucose transport and insulin signaling in 3T3-L1 adipocytes. In addition, the

effects of sustained AMPK activation on insulin signaling in human adipose tissue was investigated.

5.2 Results

5.2.1 Effect of sustained AMPK activation on basal and insulin-stimulated glucose transport in 3T3-L1 adipocytes.

5.2.1.1 Effect of 24 hr and 48 hr incubation of 3T3-L1 adipocytes with AICAR on AMPK expression, ACC expression, AMPK Thr12 phosphorylation and ACC Ser79 phosphorylation

As shown in figure 5.1 a significant ($p < 0.05$) 2.02 +/- 0.36 and 2.08 +/- 0.57 fold increase in AMPK Thr172 phosphorylation was obtained in 3T3-L1 adipocytes incubated with AICAR for 24 hr and 48 hr, respectively, in insulin-stimulated cells. These significant ($p < 0.05$) increases in Thr172 phsophoryaltion were not associated with altered AMPK α1 protein expression. In addition, a significant ($p < 0.05$) 3.1 +/- 0.69 and 2.84 +/- 0.73 fold increase in phosphorylation of the AMPK downstream target ACC at Ser79 was obtained in 3T3-L1 adipocytes incubated with AICAR for 24 hr and 48 hr respectively, in insulin-stimulated cells. These significant increases were also not associated with altered ACC protein expression (Fig. 5.1).

5.2.1.2 Effect of 24 hr and 48 hr incubation of 3T3-L1 adipocytes with metformin on AMPK expression, ACC expression, AMPK Thr12 phosphorylation and ACC Ser79 phosphorylation

As shown in figure 5.2, AMPK Thr172 phosphorylation, ACC Ser79 phosphorylation, AMPK protein expression and ACC protein expression were not significantly altered in non-insulin-stimulated and insulin-stimulated 3T3-L1 adipocytes incubated with metformin for 24 hr and 48 hr.

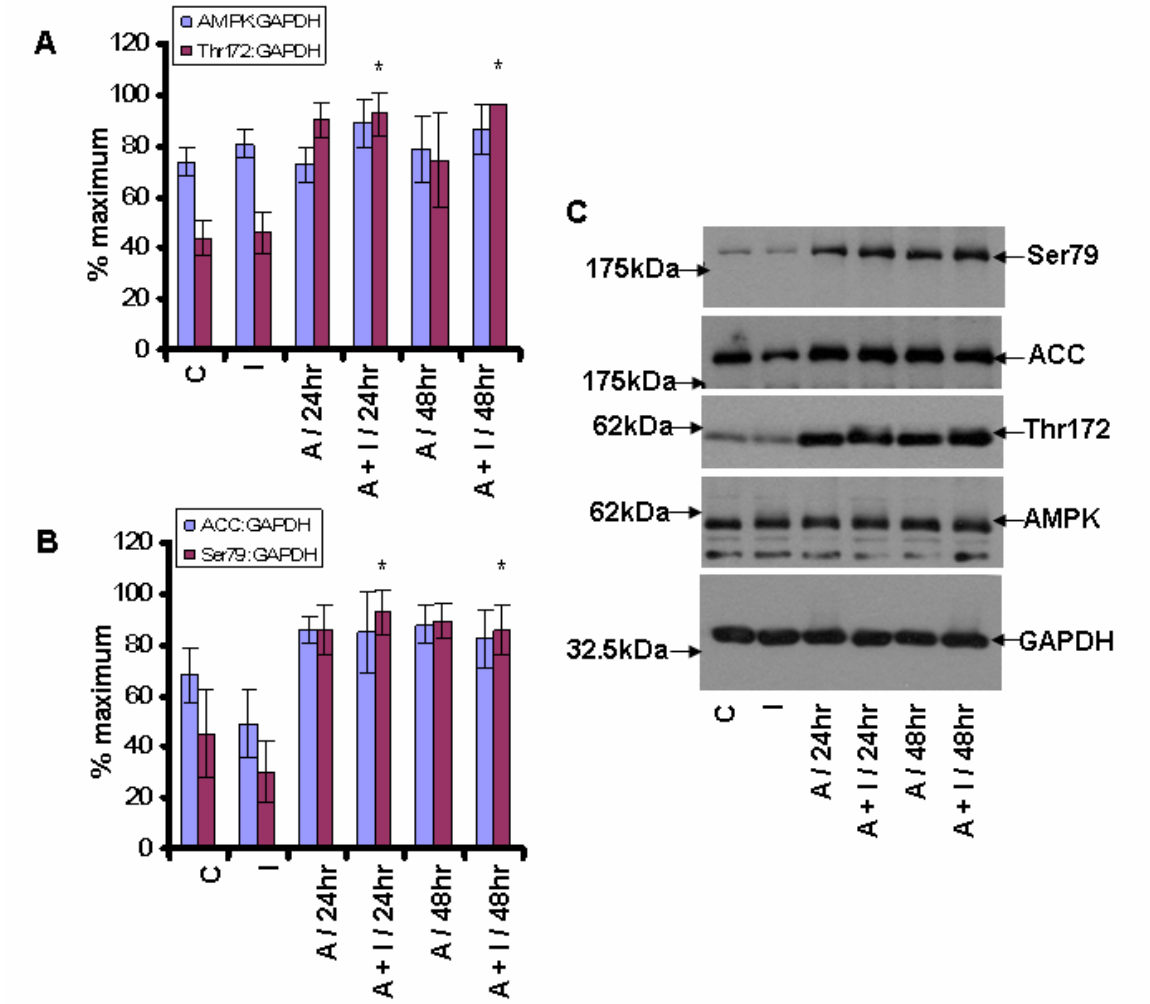

Figure 5-1: Effect of 24 hr and 48 hr incubation of 3T3-L1 adipocytes with AICAR on AMPK expression, ACC expression, AMPK Thr172 phosphorylation and ACC Ser79 phosphorylation.

*3T3-L1 lysates (15 µg) obtained from cells incubated for 24 hr and 48 hr with 1mM AICAR were resolved by 10% SDS-PAGE, transferred to nitrocellulose, and probed with anti-AMPK α1, anti-AMPK Thr172, anti-ACC Ser79, anti-ACC1 and anti-GAPDH antibodies. (A) Quantification of AMPK Thr172 phosphorylation and AMPK α1 expression were determined by comparison with GAPDH by densitometric analysis. Data shown represents the mean % maximum +/- S.E.M of three independent experiments, *p < 0.05 (one-way ANOVA). (B) Quantification of ACC Ser79 phosphorylation and ACC1 expression were determined by comparison with GAPDH by densitometric analysis. Data shown represents the mean % maximum +/- S.E.M of three independent experiments, *p < 0.05 (one-way ANOVA). (C) Representative blots from three independent experiments. The position of the molecular weight markers are shown to the left of the gel. A = AICAR, I = insulin.*

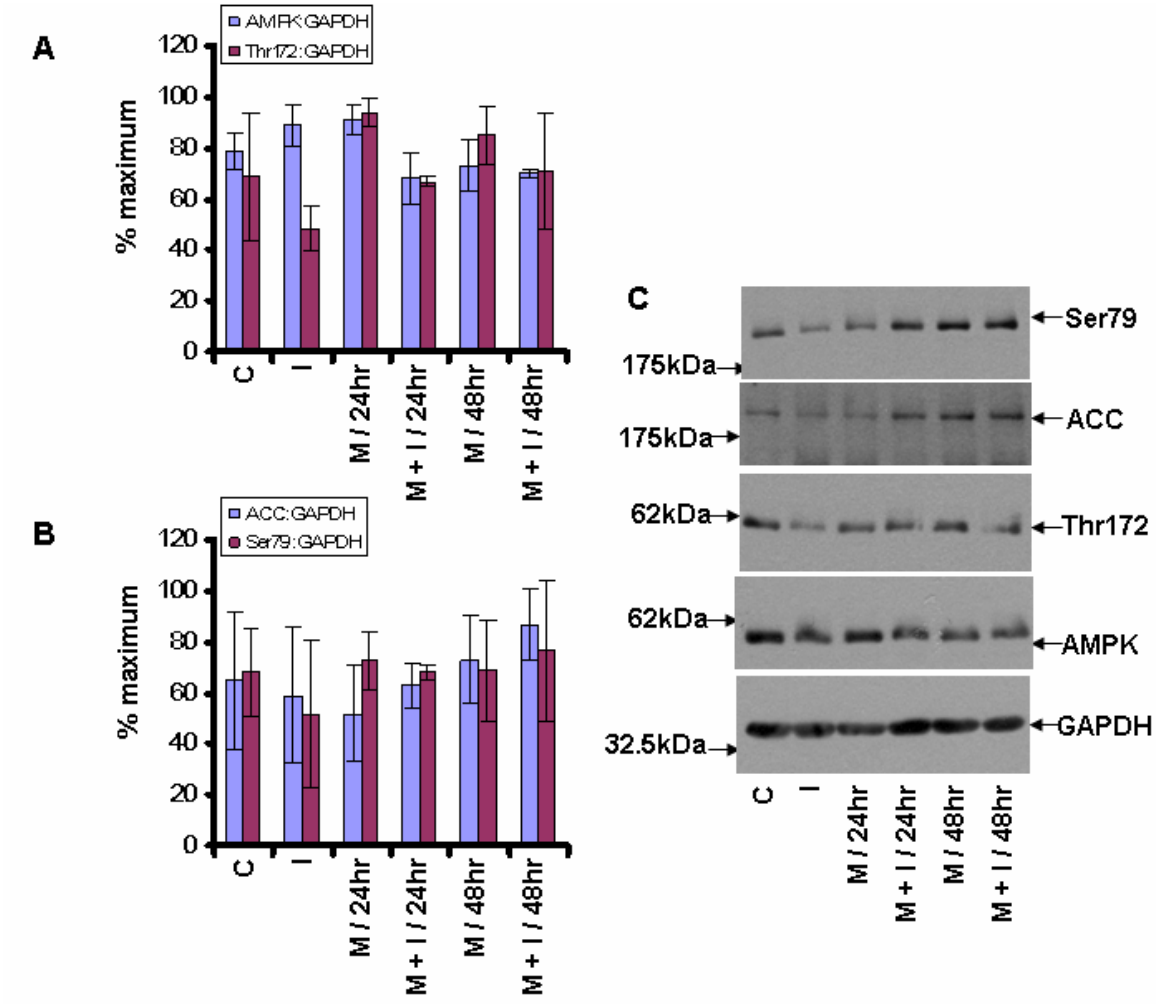

Figure 5-2: Effect of 24 hr and 48 hr incubation of 3T3-L1 adipocytes with metformin on AMPK expression, ACC expression, AMPK Thr172 phosphorylation and ACC Ser79 phosphorylation.

3T3-L1 lysates (15 µg) obtained from cells incubated for 24 hr and 48 hr with 1mM metformin were resolved by 10% SDS-PAGE, transferred to nitrocellulose, and probed with anti-AMPK α1, anti-AMPK Thr172, anti-ACC Ser79, anti-ACC1 and anti-GAPDH antibodies. (A) Quantification of AMPK Thr172 phosphorylation and AMPK α1 expression. Data shown represents the mean % maximum +/- S.E.M of three independent experiments. (B) Quantification of ACC Ser79 phosphorylation and ACC1 expression were determined by comparison with GAPDH by densitometric analysis. Data shown represents the mean % maximum +/- S.E.M of three independent experiments. (C) Representative blots from three independent experiments. The position of the molecular weight markers are shown to the left of the gel. M = metformin, I = insulin

.

5.2.1.3 Effect of 24 hr and 48 hr incubation of 3T3-L1 adipocytes with AICAR on insulin-stimulated glucose transport

The effect of sustained incubation of 3T3-L1 adipocytes with AICAR, on basal and insulin-stimulated glucose transport was investigated. As shown in figure 5.3 a significant ($p < 0.05$) 73 +/- 11.3 % and 67 +/- 27 % inhibition of insulin-stimulated glucose transport was observed in cells incubated with AICAR for 24 hr and 48 hr respectively. However, 24 hr and 48 hr treatment of 3T3-L1 adipocytes with AICAR did not significantly alter basal glucose transport.

5.2.1.4 Effect of 24 hr and 48 hr incubation of 3T3-L1 adipocytes with metformin on insulin-stimulated glucose transport

As shown in figure 5.4, basal and insulin-stimulated glucose transport were not significantly altered in 3T3-L1 adipocytes incubated with metformin for 24 hr and 48 hr.

5.2.1.5 Effect of overexpression of a constitutively active AMPK mutant on basal and insulin-stimulated glucose transport in 3T3-L1 adipocytes.

Adenovirus-mediated gene transfer was used to overexpress a constitutively active (CA) AMPK mutant ($\alpha1^{312}$) in 3T3-L1 adipocytes in order to investigate the effects of sustained AMPK activation on basal and insulin-stimulated glucose transport.

The $\alpha1^{312}$ mutant protein is based on the first 312 amino acid residues of the AMPK α1 subunit and contains an N-terminal myc tag. Therefore the expression of the $\alpha1^{312}$ mutant in 3T3-L1 adipocytes was confirmed by the presence of a band detected by the myc antibody at about 35kDa (Fig. 5.5A). As expected the AMPK activator sorbitol increased ACC Ser79 phosphorylation in control infected cells (Ad.null). In addition, basal ACC Ser79 phosphorylation was increased in Ad.$\alpha1^{312}$ infected cells, compared to Ad.null infected cells.

Interestingly, in Ad.$\alpha1^{312}$ infected cells there appears to be a reduction in insulin-stimulated glucose transport compared to Ad.null infected cells (Fig. 5.5B).

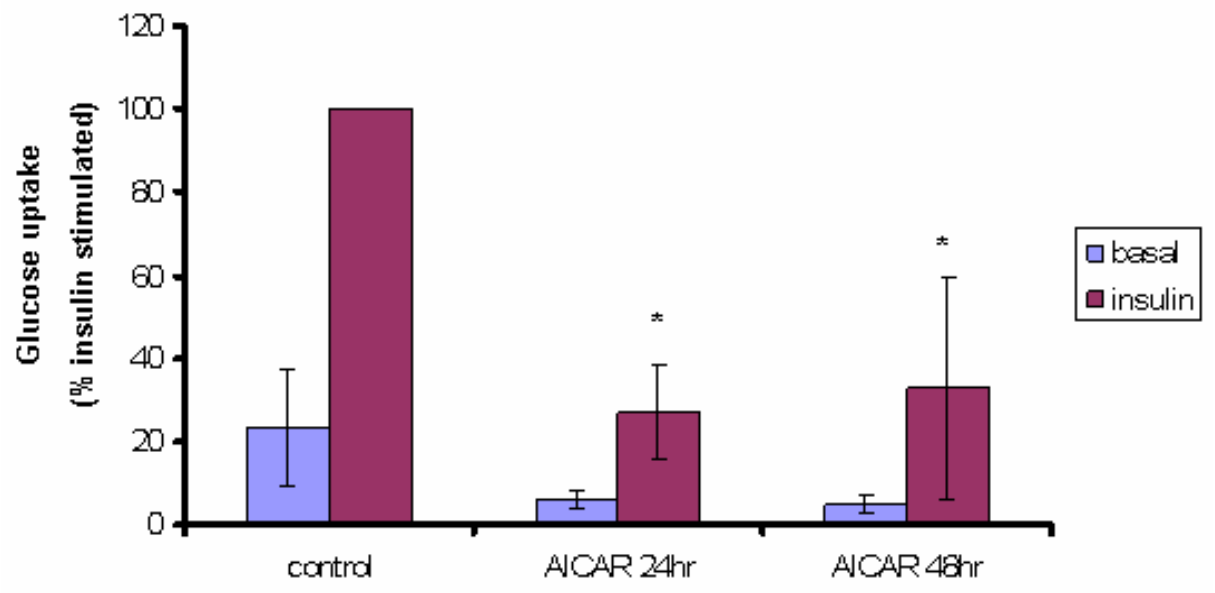

Figure 5-3: Effect of 24 hr and 48 hr incubation of 3T3-L1 adipocytes with AICAR on basal and insulin-stimulated glucose transport.

*3T3-L1 adipocytes were incubated for 24 hr and 48 hr in the presence of 1 mM AICAR prior to stimulation with 10 nM insulin for 15 min. Glucose transport was initiated by the addition of 2-[^{3}H]-deoxy-D-glucose, and terminated after 3 min. Data shown represents the mean % insulin-stimulated +/- S.E.M of three independent experiments, *p < 0.05 (2-tail), compared to insulin-stimulated. Insulin-stimulated glucose transport was 3366 +/- 3173 (S.E.M) pmol transported / min / mg protein.*

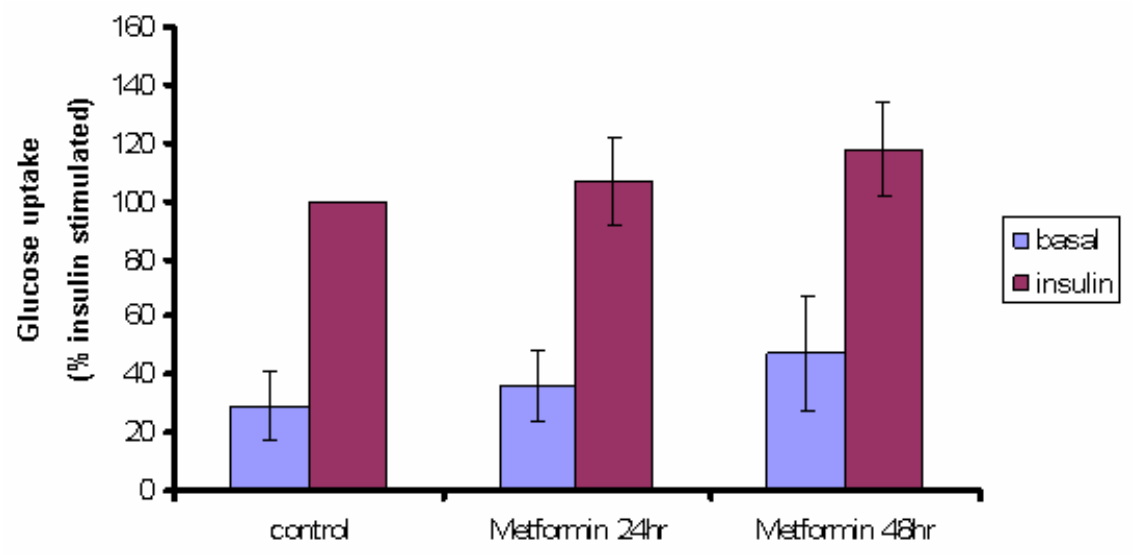

Figure 5-4: Effect of 24 hr and 48 hr incubation of 3T3-L1 adipocytes with metformin on basal and insulin-stimulated glucose transport.

3T3-L1 adipocytes were incubated for 24 hr and 48 hr in the presence of 1 mM metformin prior to stimulation with 10 nM insulin for 15 min. Glucose transport was initiated by the addition of 2-[^{3}H]-deoxy-D-glucose, and terminated after 3 min. Data shown represents the mean % insulin-stimulated +/- S.E.M of three independent experiments. Insulin-stimulated glucose transport was 519 +/- 357 (S.E.M) pmol transported / min / mg protein. This work was performed by Dr.I.Salt (FBLS, University of Glasgow).

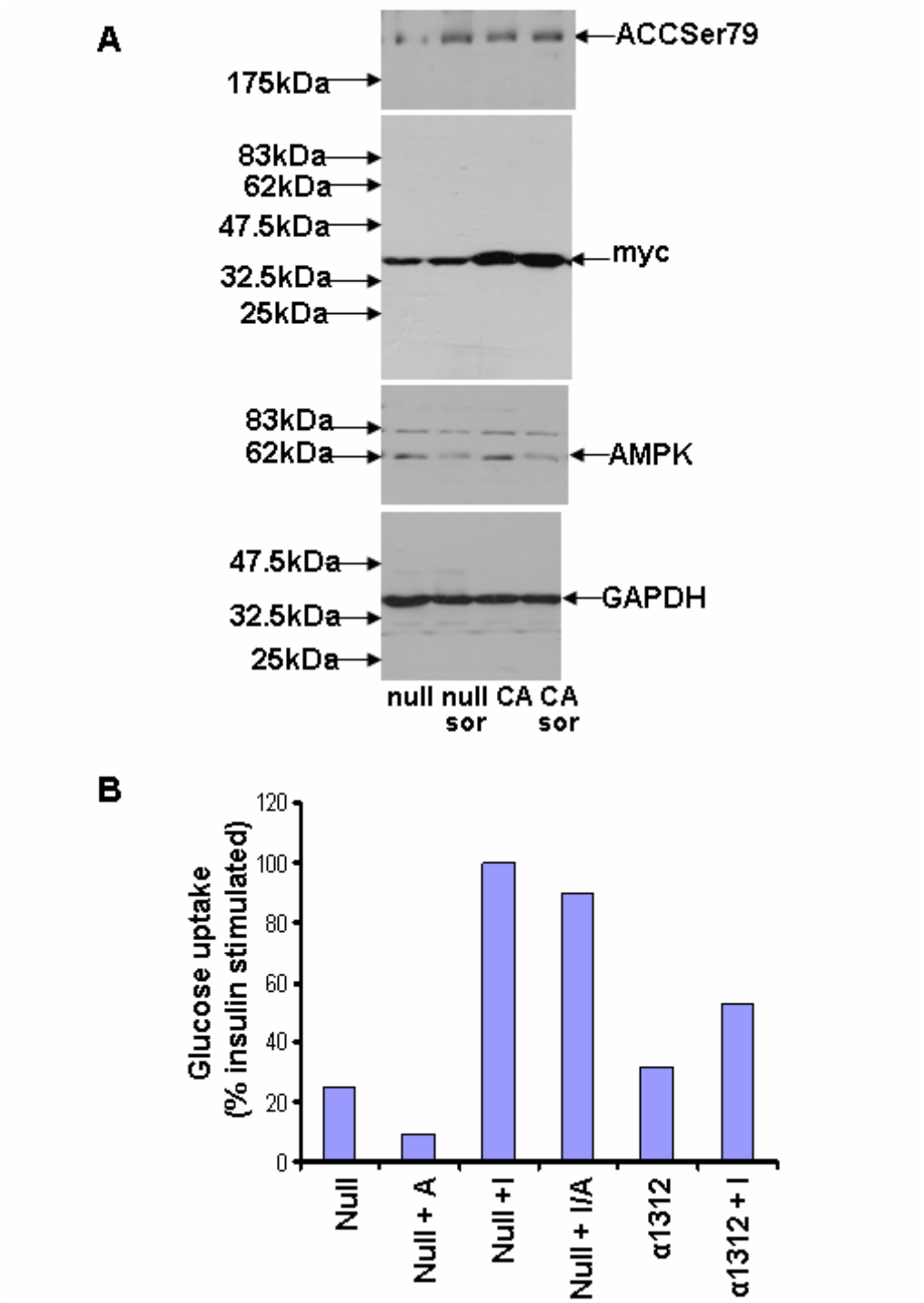

Figure 5-5: Effect of overexpression of a constitutively active AMPK mutant on basal and insulin stimulated glucose transport in 3T3-L1 adipocytes.
(A) 3T3-L1 adipocytes were infected (600 ifu/cell) for 48 hr with Ad. α1^{312} or Ad.null prior to stimulation for 30 min with 0.6M sorbitol. Cell lysates (25 µg) were resolved by SDS-PAGE, transferred to nitrocellulose and probed with anti-ACC Ser79, anti-AMPKα1, anti-c-myc and anti-GAPDH antibodies. The position of the molecular weight markers are shown to the left of the gel. (B) 3T3-L1 adipocytes cultured on 12 well plates were infected (600 ifu/cell) with Ad. α1^{312} or Ad.null. After 48 hr 3T3-L1 adipocytes were incubated for 30 min in the presence of 2 mM AICAR prior to stimulation with 10 nM insulin for 15 min. Glucose transport was initiated by the addition of 2-[^{3}H]-deoxy-D-glucose, and terminated after 3 min. Data compiled from one experiment. A = AICAR, I = insulin.

5.2.1.6 Effect of 24 hr and 48 hr incubation of 3T3-L1 adipocytes with AICAR on PKB expression and insulin-stimulated PKB phosphorylation

Stimulation of 3T3-L1 adipocytes with insulin caused a significant ($p < 0.05$) 13.38 +/- 3.16, 12.46 +/- 2.73 and 13.8 +/- 2.59 fold increase in PKB Ser473 phosphorylation under control conditions and incubation of adipocytes with AICAR for 24 hr and 48 hr respectively (Fig. 5.6). Insulin-stimulated PKB Ser473 phosphorylation was not altered in 3T3-L1 adipocytes incubated in AICAR for 24 hr and 48 hr. In addition, in non-insulin-stimulated cells and insulin-stimulated cells PKB protein expression was not significantly altered in 3T3-L1 adipocytes incubated with AICAR for 24 hr or 48 hr.

5.2.1.7 Effect of 24 hr and 48 hr incubation of 3T3-L1 adipocytes with metformin on PKB expression and insulin-stimulated PKB phosphorylation

Stimulation of 3T3-L1 adipocytes with insulin caused a significant ($p < 0.05$) 6.35 +/- 1.07, 6.28 +/- 0.64 and 5.64 +/- 1.06 fold increase in PKB Ser473 phosphorylation under control conditions and pre-treatment of adipocytes with metformin for 24 hr and 48 hr respectively (Fig. 5.7). Insulin-stimulated PKB Ser473 phosphorylation was not altered in 3T3-L1 adipocytes incubated in metformin for 24 hr and 48 hr. In addition, in non-insulin-stimulated cells and insulin-stimulated cells PKB protein expression was not significantly altered in 3T3-L1 adipocytes incubated with metformin for 24 hr or 48 hr.

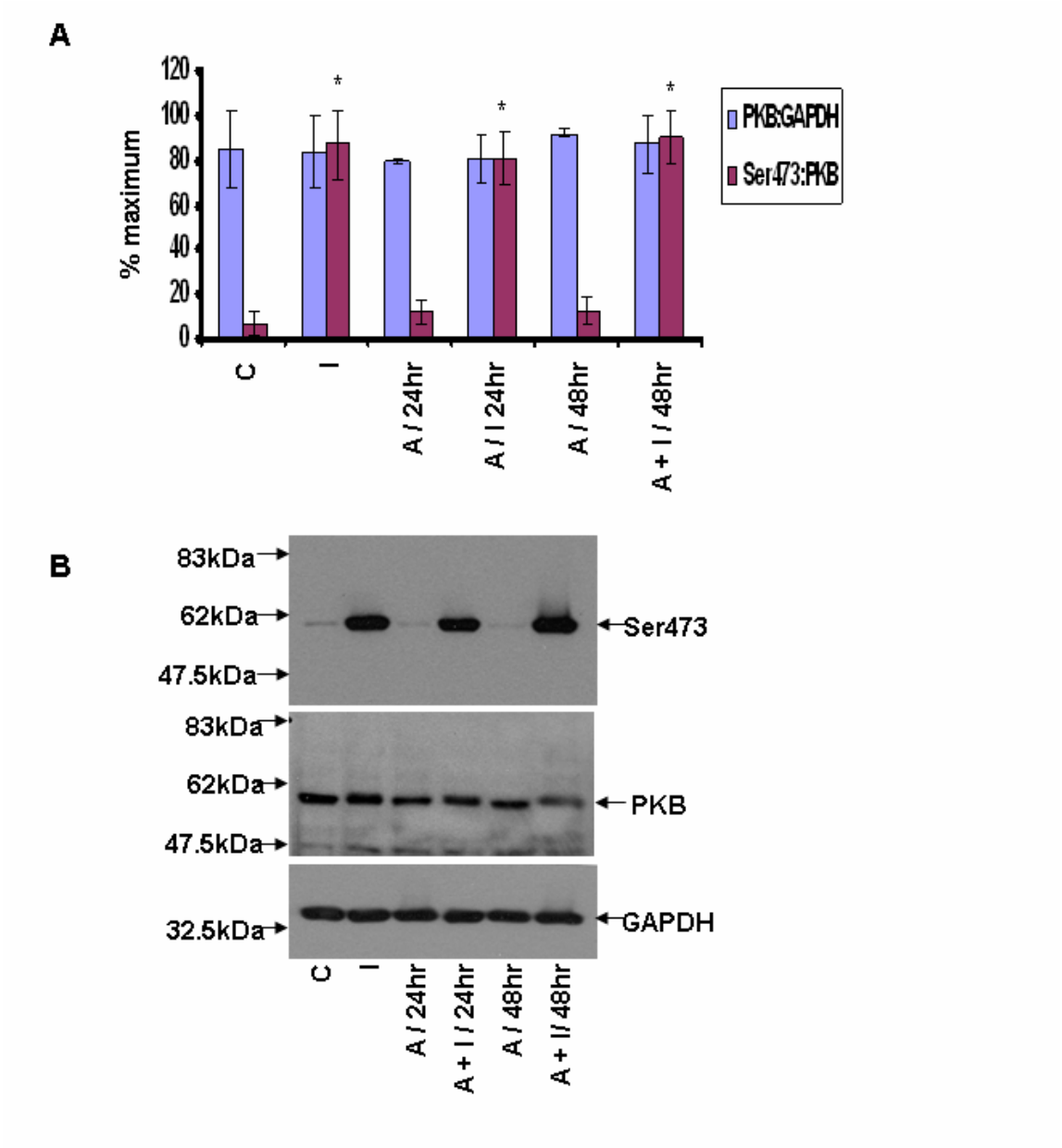

Figure 5-6: Effect of 24 hr and 48 hr incubation of 3T3-L1 adipocytes with AICAR on PKB expression and insulin-stimulated PKB phosphorylation.
*3T3-L1 lysates (15 µg) obtained from cells incubated for 24 hr and 48 hr with 1mM AICAR prior to stimulation for 15 min with 10nM insulin were resolved by 10% SDS-PAGE, transferred to nitrocellulose, and probed with anti-PKB, anti-PKB Ser473 and anti-GAPDH antibodies. (A) Quantification of PKB expression was determined by comparison with GAPDH, and quantification of PKB phosphorylation was determined by comparison with PKB by densitometric analysis. Data shown represents the mean % maximum +/- S.E.M of three independent experiments, *p < 0.05 (one-way ANOVA) compared to non-insulin stimulated cells. (B) Representative blots from three independent experiments. The position of the molecular weight markers are shown to the left of the gel. A = AICAR, I = insulin.*

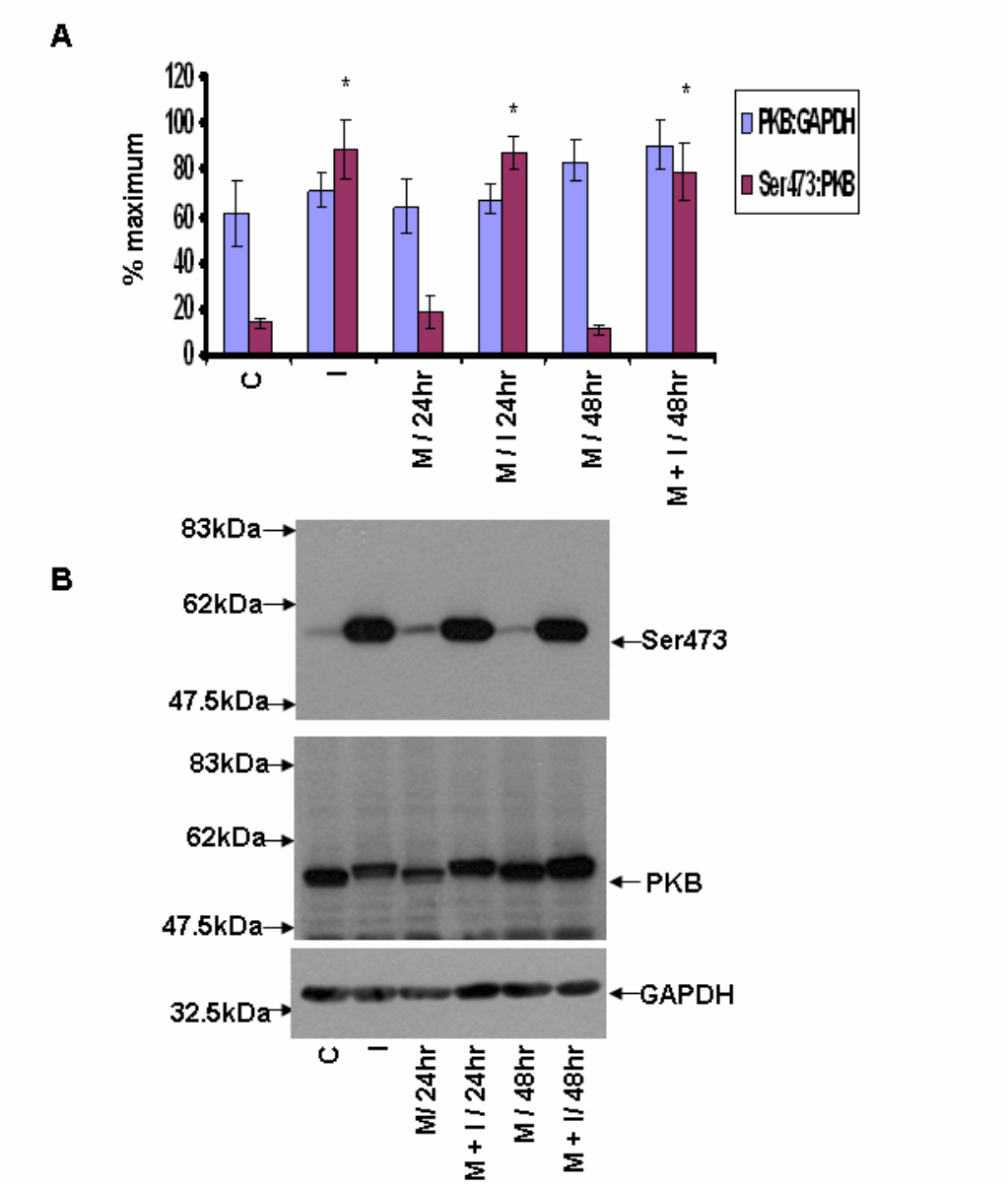

Figure 5-7: Effect of 24 hr and 48 hr incubation of 3T3-L1 adipocytes with metformin on PKB expression and insulin-stimulated PKB phosphorylation.
*3T3-L1 lysates (15 µg) obtained from cells incubated for 24 hr and 48 hr with 1mM metformin prior to stimulation for 15 min with 10nM insulin were resolved by 10% SDS-PAGE, transferred to nitrocellulose, and probed with anti-PKB, anti-PKB Ser473 and anti-GAPDH antibodies. (A) Quantification of PKB expression was determined by comparison with GAPDH, and quantification of PKB phosphorylation was determined by comparison with PKB by densitometric analysis. Data shown represents the mean % maximum +/- S.E.M of three independent experiments, *p < 0.05 (one-way ANOVA) compared to non-insulin-stimulated cells. (B) Representative blots from three independent experiments. The position of the molecular weight markers are shown to the left of the gel. M = metformin, I = insulin.*

5.2.2 Effect of chronic AMPK activation in human adipose tissue

5.2.2.1 Effect of prolonged treatment of type 2 diabetic subjects with metformin on AMPK activity in human adipose tissue.

In a separate study undertaken by others in the laboratory, the effect of metformin on adipose tissue AMPK activity was assessed in subjects with type 2 diabetes. 20 men (aged 50-70, BMI 27-33) with type 2 diabetes, treated with diet or monotherapy were recruited for the study. The study was a double-blinded crossover design, randomised to gliclazide (80 mg twice a day) or metformin (500 mg once a day) for 10 weeks with a 6 week washout period. Subjects were treated with gliclazide in order to try to match glycaemic control at the end of each treatment phase. The clinical and metabolic parameters of test subjects after each treatment phase are shown below (Table 5.1). There was no significant difference in BMI, total serum adiponectin concentration, total cholesterol concentration, HDL cholesterol concentration or triglyceride concentration after each phase of therapy. However, gliclazide therapy was more effective at lowering HbA1c than metformin (7.8 +/- 1.73 % versus 8.3 +/- 1.7 %, $p < 0.001$). This was complemented by significantly lower fasting blood glucose with gliclazide versus metformin therapy (10.3 +/- 3.2 mM versus 12.1 +/- 4.7 mM). Furthermore LDL cholesterol concentration was significantly lower after gliclazide therapy compared with metformin therapy (2.42 +/- 0.74 mM versus 2.79 +/- 0.74 mM, $p = 0.022$).

	Metformin mean (SD)	**Gliclazide mean (SD)**	***p*-value**
BMI (Kg/m^2)	31.0 (4.3)	31.0 (4.5)	0.80
Adiponectin (ng/ml)	4193 (2670)	4648 (3291)	0.054
HbA1c (%)	8.34 (1.70)	7.82 (1.74)	<0.001
Fasting blood glucose (mM)	12.1 (4.7)	10.3 (3.2)	0.005
Insulin (U/L)	15.6 (13.8)	14.3 (6.0)	0.69
Cholesterol (mM)	5.16 (1.16)	4.75 (1.59)	0.054
HDL-C (mM)	1.25 (0.24)	1.20 (0.24)	0.13
LDL-C (mM)	2.79 (0.74)	2.42 (0.73)	0.022
Triglycerides (mM)	2.78 (3.76)	2.94 (4.80)	0.58

Table 5-1: Clinical and metabolic parameters of test subjects

As shown in figure 5.8, metformin did not alter AMPK expression levels, but did cause an approximate 2 fold significant ($p < 0.01$) increase in AMPK activity in adipose tissue in type 2 diabetic subjects.

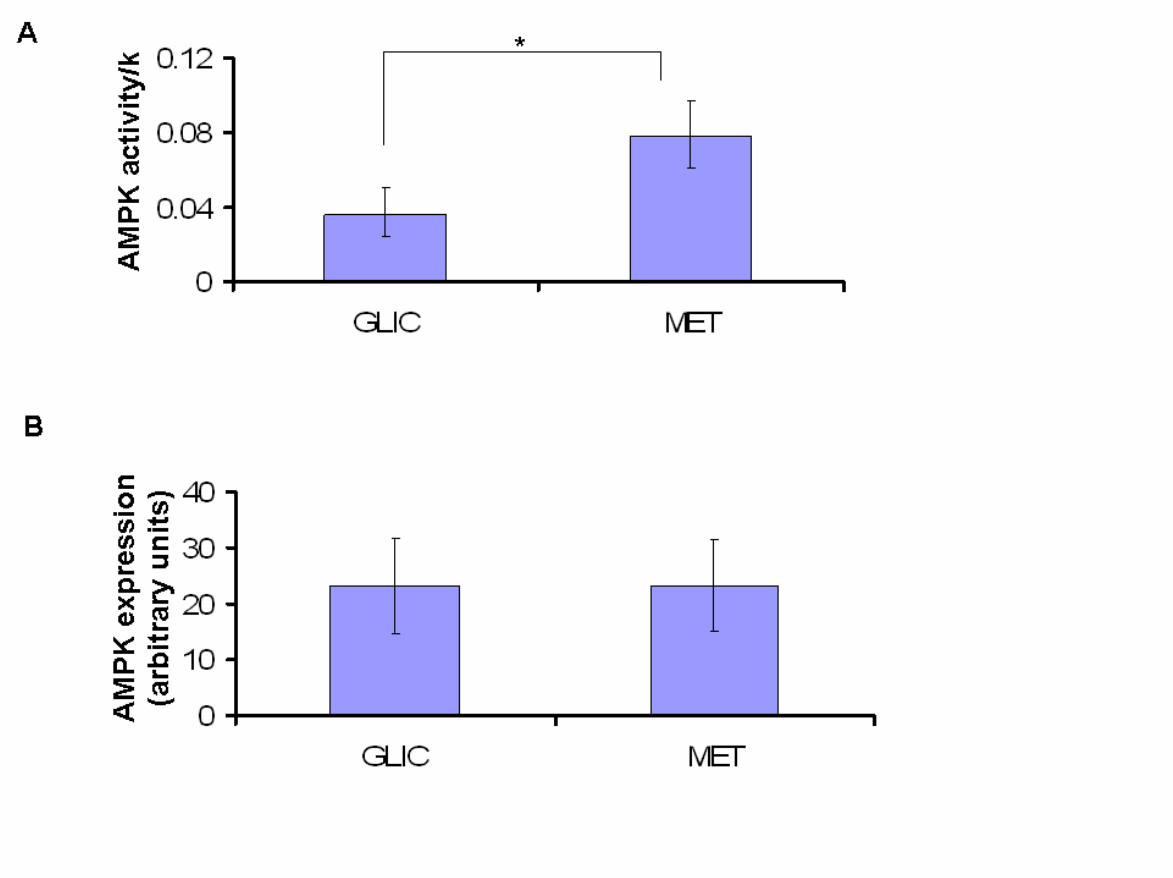

Figure 5-8: Effect of prolonged treatment of type 2 diabetic subjects with metformin on AMPK activity and expression in human adipose tissue.
*Total AMPK was immunoprecipitated from the adipose biopsies (100 µg) with a mixture of anti-AMPK α1 and α2 antibodies and assayed for AMPK activity. (A) AMPK activity in each experiment was standardized against the activity of purified rat liver AMPK kinase (K). Data shown represents the mean +/- 95% confidence intervals of the mean, of 20 subjects, each treated for 10 weeks with gliclazide (80 mg) and 10 weeks with metformin (500 mg), *p < 0.01. The values given for the means and 95% confidence intervals were calculated using logarithmic transformed data, and back transformed for purposes of presentation. Adipose tissue (80 µg) was resolved on 10% SDS-PAGE, transferred to nitrocellulose and probed with anti-Pan AMPKα antibody. (B) Quantification of AMPK expression. Data shown represents the mean +/- 95% confidence intervals of the mean, of 19 subjects, each treated for 10 weeks with gliclazide (80 mg) and 10 weeks with metformin (500 mg).This work was performed by Dr Jim Boyle (FBLS, University of Glasgow).*

5.2.2.2 Effect of prolonged treatment of type 2 diabetic subjects with metformin on the expression of GAPDH in human adipose tissue

As the human adipose tissue lysates used in the study described in 5.2.2.1 represent sustained activation of AMPK by metformin *in vivo*, the expression of several key insulin signalling molecules was assessed. As shown below in figure 5.9, prolonged treatment of type 2 diabetic subjects with metformin did not significantly alter the expression of GAPDH in adipose tissue. Thus, GAPDH was used as a loading control in subsequent blotting which assessed the expression of the PI3K p85 subunit, PKB, IRS-1 and FAS.

5.2.2.3 Effect of prolonged treatment of type 2 diabetic subjects with metformin on the expression of PI3K in human adipose tissue.

As shown below in figure 5.10, prolonged treatment of type 2 diabtic subjects with metformin did not significantly alter the expression of the PI3K subunit p85 in adipose tissue.

5.2.2.4 Depletion of albumin from human adipose tissue samples.

Subsequent western blotting of the adipose tissue samples with anti-PKB antibody, anti-IRS-1 antibody and anti-FAS antibody was problematic, as they produced unclear data even after numerous high salt washes. Albumin is an abundant protein in these samples. Thus in an attempt to improve the quality of the western blots, an albumin depletion kit was used to remove albumin from the adipose tissue samples. As shown below in figure 5.11, the kit was efficient at removing most of the albumin (albumin depletion column). Elution of the unbound proteins, which included proteins of interest, did cause elution of some bound albumin, however the amount of albumin in this elution fraction was an improvement compared to the amount in the initial starting material.

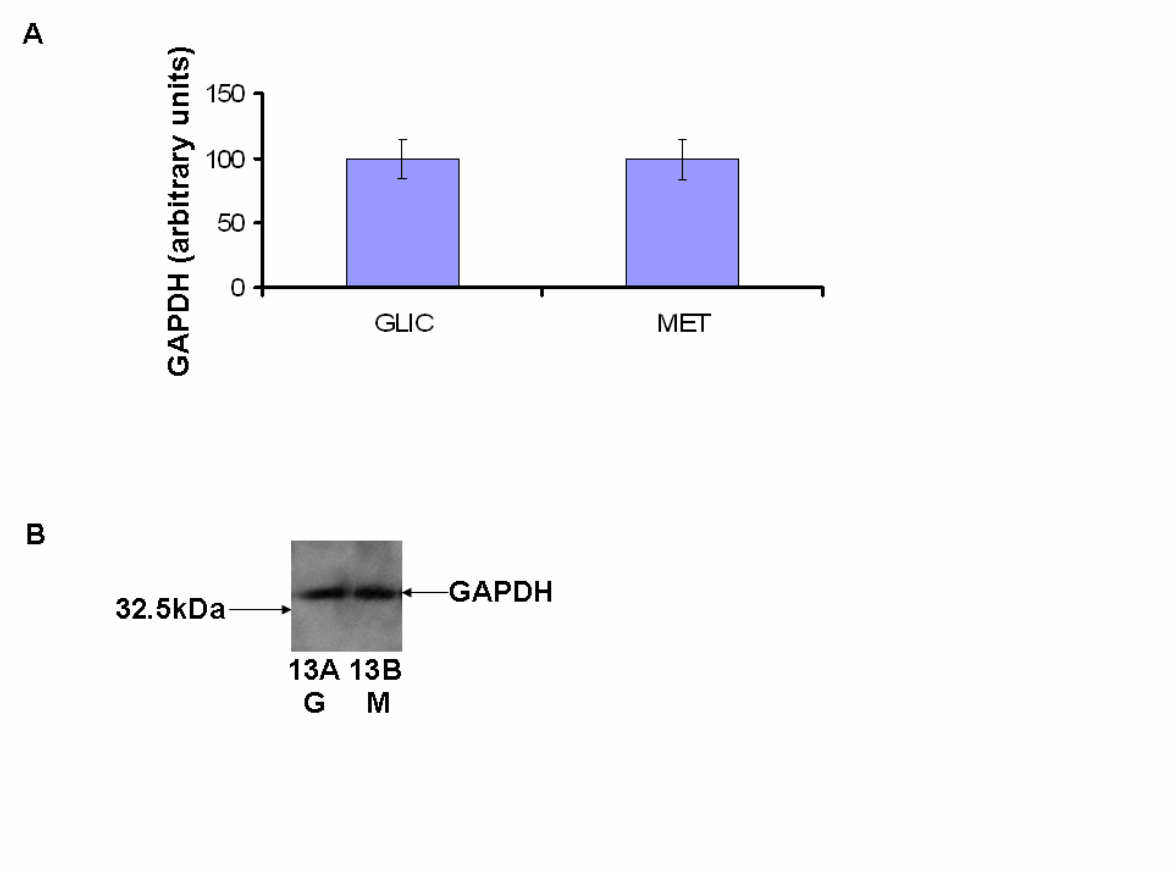

Figure 5-9: Effect of prolonged treatment of type 2 diabetic subjects with metformin on GAPDH expression in human adipose tissue.
Adipose tissue (80 µg) was resolved on 10% SDS-PAGE, transferred to nitrocellulose and probed with anti-GAPDH antibody. (A) Quantification of GAPDH expression, relative to an internal control (subject 14). Data shown represents the mean +/- 95% confidence intervals of the mean, of 19 subjects, each treated for 10 weeks with gliclazide (80 mg) and 10 weeks with metformin (500 mg). (C) Representative western blot (subject 13). The position of the molecular weight markers are shown to the left of the gel. G = gliclazide, M = metformin.

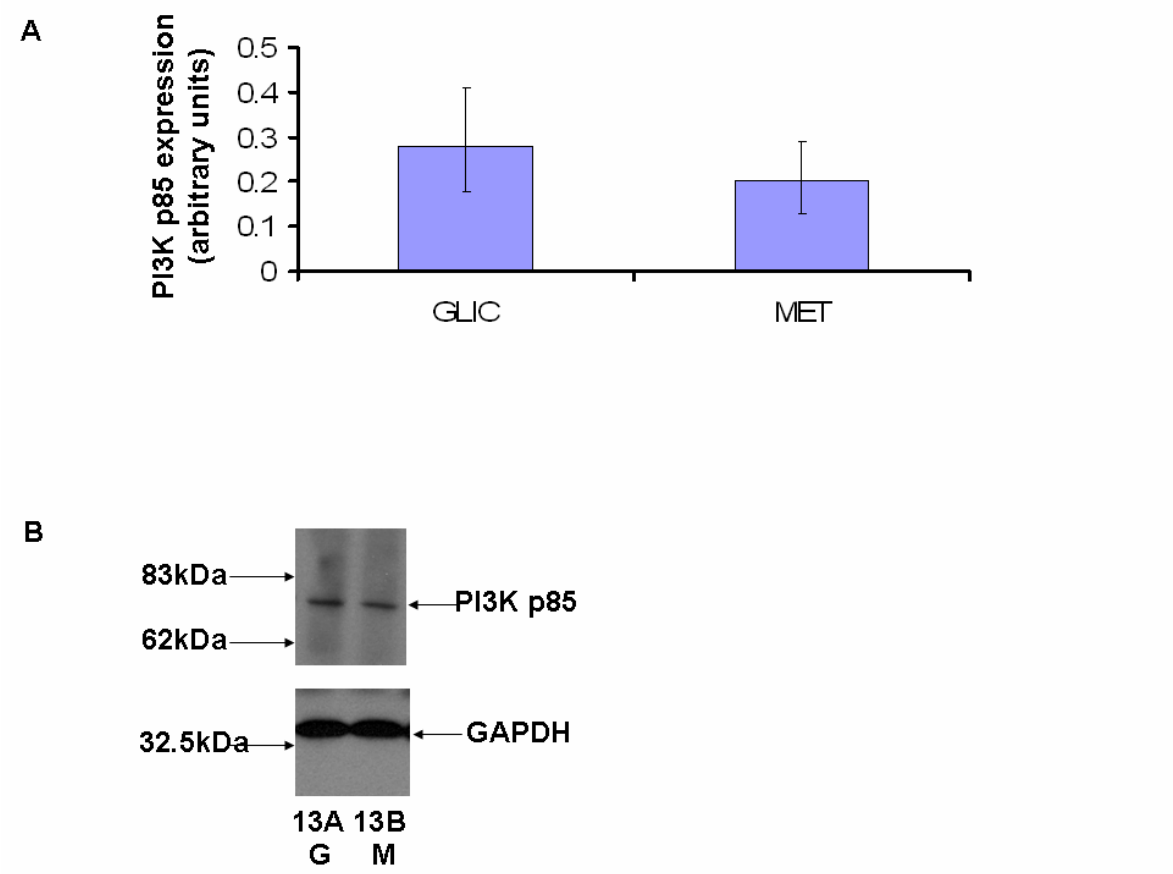

Figure 5-10: Effect of prolonged treatment of type 2 diabetic subjects with metformin on the expression of the PI3K p85 subunit in adipose tissue.

Adipose tissue (80 µg) was resolved on 10% SDS-PAGE, transferred to nitrocellulose and probed with anti-PI3K p85 antibody. (A) Quantification of PI3K p85 subunit expression, relative to an internal standard (subject 14) and GAPDH. Data shown represents the mean +/- 95% confidence intervals of the mean, of 19 subjects, each treated for 10 weeks with gliclazide (80 mg) and 10 weeks with metformin (500 mg). The values given for the means and 95% confidence intervals were calculated using square root transformed data, and back transformed for purposes of presentation. (C) Representative western blot (subject 13). The position of the molecular weight markers are shown to the left of the gel. G = gliclazide, M = metformin.

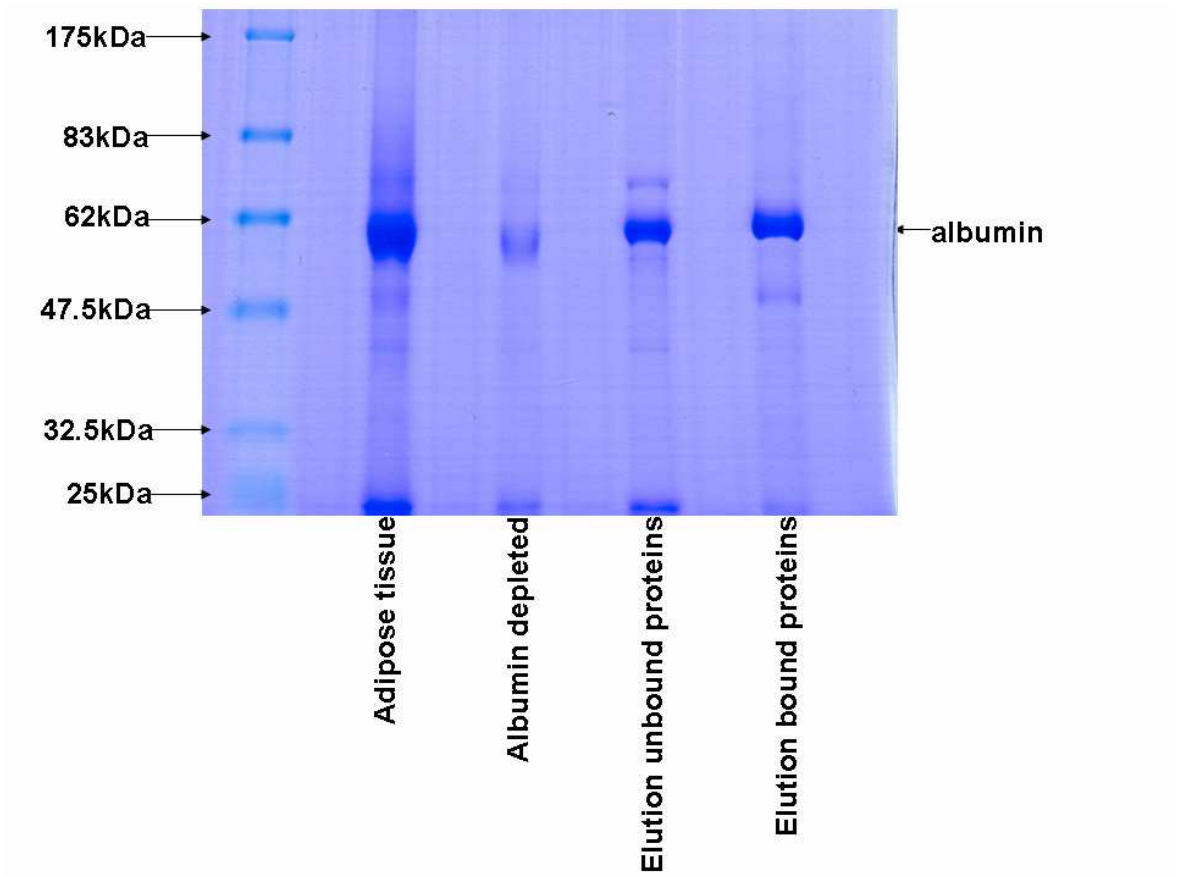

Figure 5-11: Albumin depletion from adipose tissue sample.
Equal equivalent volumes from samples obtained at various points throughout the albumin depletion process, from one adipose tissue sample (subject 13), were resolved by 10% SDS-PAGE. Proteins were visualized by Coomassie stain.

5.2.2.5 Effect of prolonged treatment of type 2 diabetic subjects with metformin on the expression of IRS-1 and PKB in human adipose tissue.

The albumin depleted samples were then subjected to western blotting to investigate the effect of prolonged treatment of type 2 diabetic subjects with metformin on IRS-1 and PKB expression in adipose tissue. As shown below in figure 5.12 and 5.13, IRS-1 expression and PKB expression, respectively, were not significantly altered by metformin.

5.2.2.6 Effect of prolonged treatment of type 2 diabetic subjects with metformin on FAS expression in human adipose tissue.

As the AMPK assays were performed on adipose biopsies obtained from subjects treated with metformin which contain other cells such as endothelial and fibroblasts, it is possible that AMPK activation is occuring in another cell type different from that of adipocytes.

To determine whether AMPK activation was occurring in adipocytes within adipose tissue the effect of metformin on the expression of the late adipogenic marker FAS, whose expression has previously been shown to be reduced during differentiation of 3T3-L1 preadipocytes by AMPK activation (Habinowski and Witters 2001), was investigated. As shown in figure 5.14 prolonged treatment of type 2 diabetic subjects with metformin did not appear to significantly alter the expression of FAS in adipose.

The expression of the transcription factors C/EBPα and PPARγ have also previously been shown to be reduced by AMPK activation during differentiation of 3T3-L1 preadipocytes (Habinowski and Witters 2001, Giri *et al* 2006, Tong *et al* 2008) and in fully differentiated 3T3-F442A adipocytes (Dagon *et al* 2006). In addition AMPK activation in muscle has been shown to increase the expression level of GLUT4 (Holmes *et al* 1999). Thus the effect of metformin on the expression of C/EBPα, PPARγ and GLUT4 were also investigated. Unfortunately it was not possible to reliably determine expression by western blotting (data not shown).

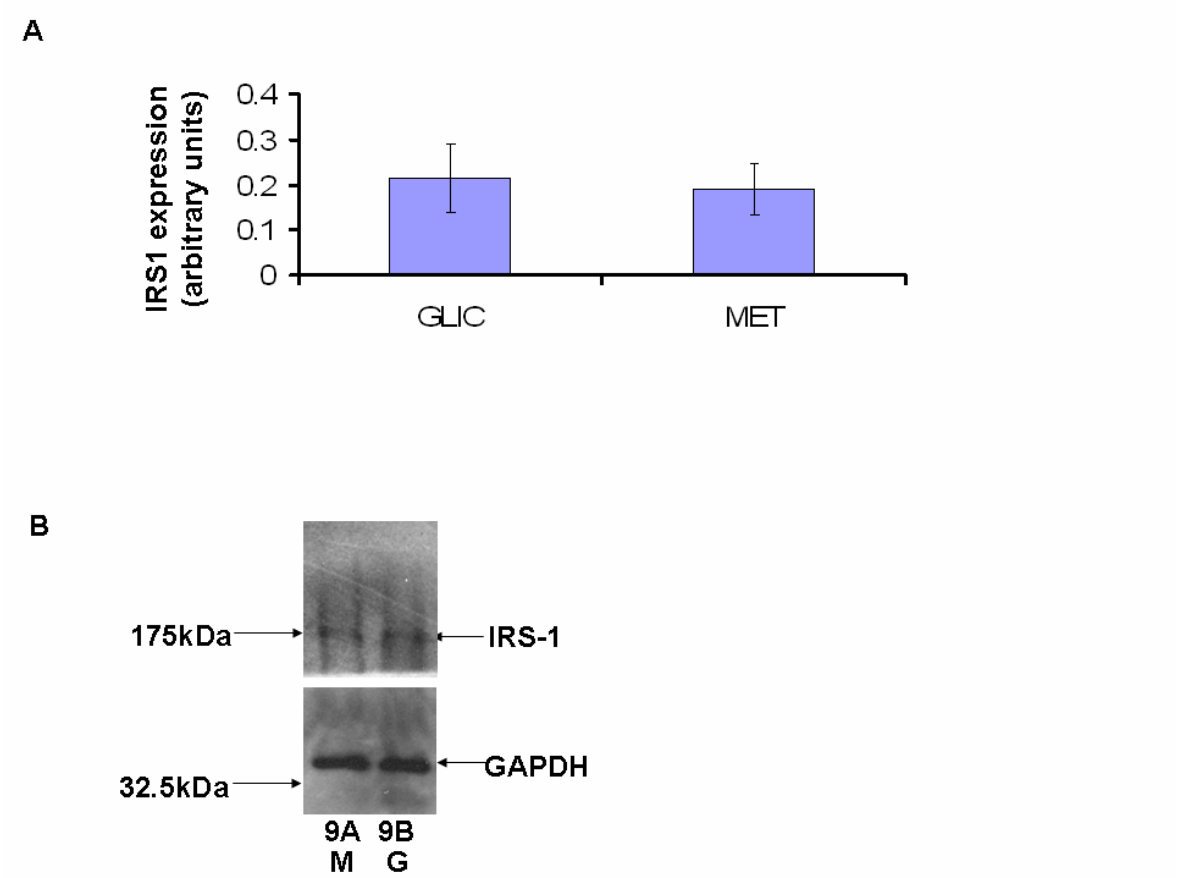

Figure 5-12: Effect of prolonged treatment of type 2 diabetic subjects with metformin on the expression of IRS-1 in adipose tissue.

Albumin depleted adipose tissue (80 µg) was resolved on 10% SDS-PAGE, transferred to nitrocellulose and probed with anti-IRS-1 antibody. (A) Quantification of IRS-1 expression, relative to an internal standard (subject 14) and GAPDH. Data shown represents the mean +/- 95% confidence intervals of the mean, of 19 subjects, each treated for 10 weeks with gliclazide (80 mg) and 10 weeks with metformin (500 mg). (B) Representative western blot (subject 9). The position of the molecular weight markers are shown to the left of the gel. G = gliclazide, M = metformin.

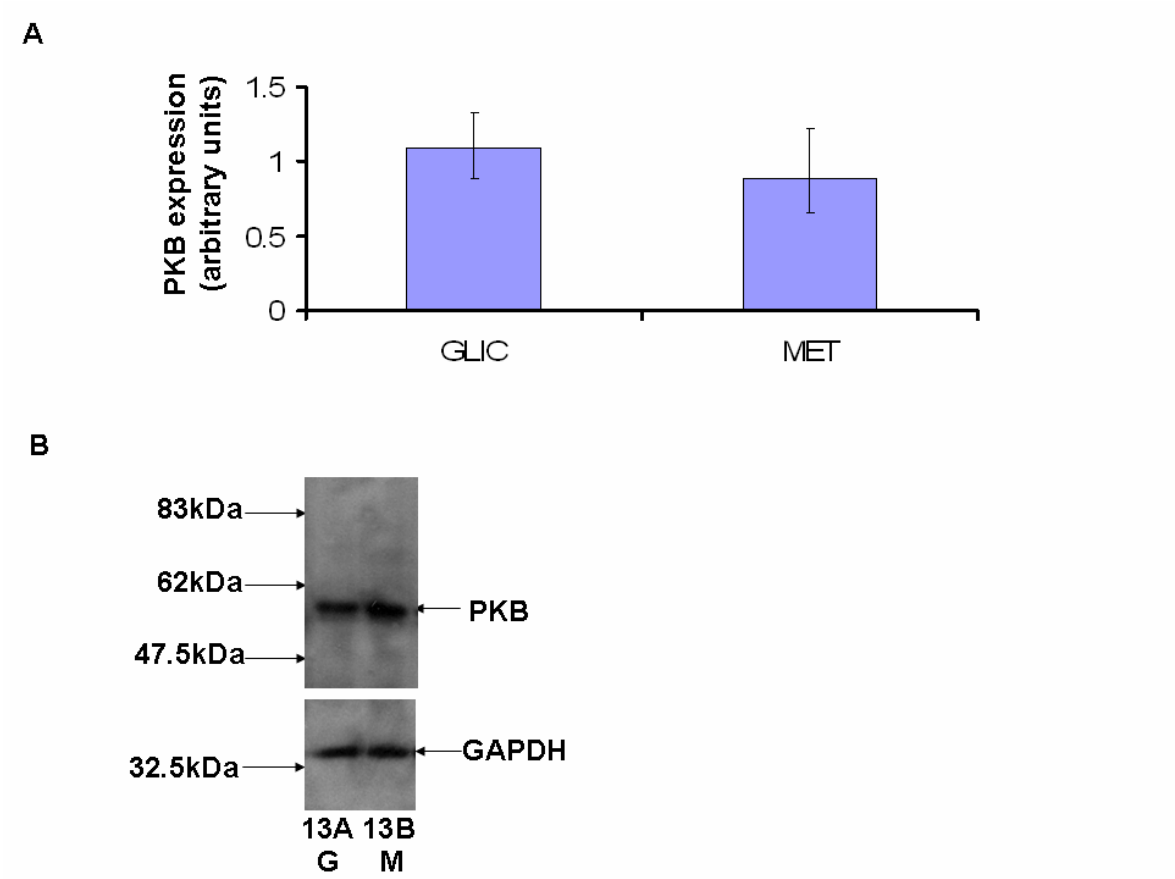

Figure 5-13: Effect of prolonged treatment of type 2 diabetic subjects with metformin on the expression of PKB in adipose tissue.

Albumin depleted adipose tissue (80 µg) was resolved on 10% SDS-PAGE, transferred to nitrocellulose and probed with anti-PKB antibody. (A) Quantification of PKB expression, relative to an internal standard (subject 14) and GAPDH. Data shown represents the mean +/- 95% confidence intervals of the mean, of 19 subjects, each treated for 10 weeks with gliclazide (80 mg) and 10 weeks with metformin (500 mg). The values given for the means and 95% confidence intervals were calculated using logarithmic transformed data, and back transformed for purposes of presentation. (B) Representative western blot (subject 13). The position of the molecular weight markers are shown to the left of the gel. G = gliclazide, M = metformin.

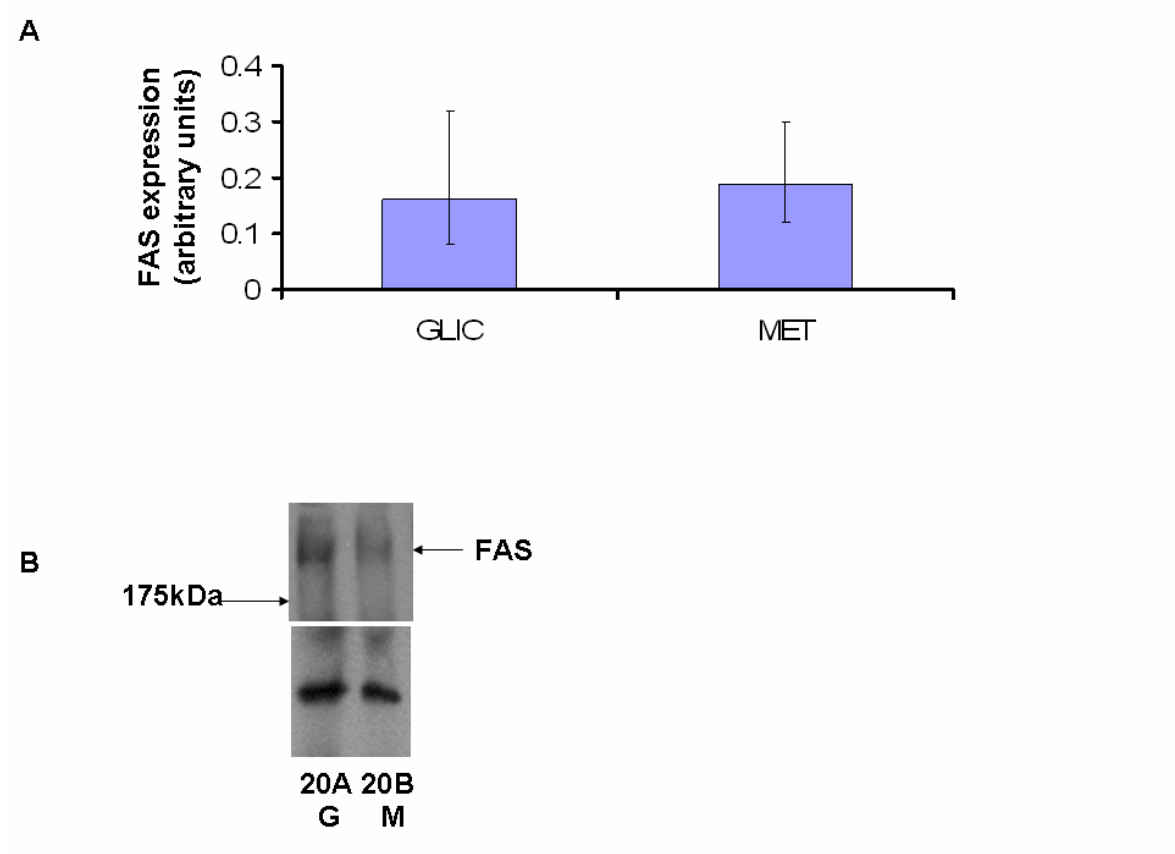

Figure 5-14: Effect of prolonged treatment of type 2 diabetic subjects with metformin on the expression of FAS in adipose tissue.
Albumin depleted adipose tissue (80 µg) was resolved on 10% SDS-PAGE, transferred to nitrocellulose and probed with anti-FAS antibody. (A) Quantification of FAS expression, relative to an internal standard (subject 14) and GAPDH. Data shown represents the mean +/- 95% confidence intervals of the mean, of 13 subjects, each treated for 10 weeks with gliclazide (80 mg) and 10 weeks with metformin (500 mg). The values given for the means and 95% confidence intervals were calculated using logarithmic transformed data, and back transformed for purposes of presentation. (B) Representative western blot (subject 13). The position of the molecular weight markers are shown to the left of the gel. G = gliclazide, M = metformin.

5.3 Discussion

The principal findings of this study are that prolonged treatment of 3T3-L1 adipocytes with AICAR, but not metformin, increased AMPK Thr172 phosphorylation and inhibited insulin-stimulated glucose transport. Inhibition of insulin-stimulated glucose transport by AICAR in 3T3-L1 adipocytes was not associated with altered PKB protein expression or insulin-stimulated PKB Ser473 phosphorylation. Chronic AMPK activation in adipose tissue was observed in metformin treated type 2 diabetic subjects, and was not associated with altered expression of three key insulin signalling molecules; PKB, the PI3K p85 subunit and IRS-1.

Incubation of 3T3-L1 adipocytes with AICAR for 24 hr and 48 hr was shown to significantly ($p < 0.05$) increase AMPK Thr172 phosphorylation in insulin-stimulated cells (Fig. 5.1), and significantly ($p < 0.05$) inhibit insulin-stimulated glucose transport (Fig. 5.3). Total AMPK expression was not altered in 3T3-L1 adipocytes incubated with AICAR for 24 hr and 48 hr (Fig. 5.1), suggesting that it is the specific activity of AMPK that is increasing rather than an increase in AMPK protein expression. However it should be noted that only AMPK α1 protein expression levels were assessed. Thus, it is possible that incubation of 3T3-L1 adipocytes with AICAR for 24 hr and 48 hr may increase AMPK α2 protein expression which could account for the increase in AMPK Thr172 phosphorylation. In addition, this study also found that incubation of 3T3-L1 adipocytes with AICAR for 24 hr and 48 hr displayed a significant increase in phosphorylation of the AMPK downstream target ACC at Ser79 in insulin-stimulated cells (Fig. 5.1). Habinowski and Witters, previously showed that prolonged AMPK activation by AICAR during differentiation of 3T3-L1 preadipocytes decreased the expression level of ACC (Habinowski and Witters 2001). However, in contrast this current study found that prolonged treatment of 3T3-L1 adipocytes with AICAR did not significantly alter ACC1 expression (Fig. 5.1). Thus, perhaps the effect of AICAR on ACC expression differs between fibroblasts and fully differentiated adipocytes. In addition to assessing ACC1 protein expression it would have been interesting to have also investigated the effect of AICAR on ACC2 protein expression, as it is possible that the effect of AICAR on ACC expression observed by Habinowski and Witters was ACC2 specific.

In contrast, incubation of 3T3-L1 adipocytes with metformin for 24 hr and 48 hr did not significantly alter AMPK Thr172 phosphorylation (Fig. 5.2), nor alter insulin-stimulated glucose transport (Fig. 5.4). It should be noted that this work is in contrast to a previous

study (Huypens *et al* 2005) which showed that treatment of 3T3-L1 adipocytes with 1mM metformin for 48 hr did not alter AMPK protein expression levels, but did increase AMPK Thr172 phosphorylation. Since this current study found that treatment of 3T3-L1 adipocytes with metformin for 24 hr and 48 hr did not significantly alter AMPK Thr172 phosphorylation, it was not surprising that phosphorylation of the AMPK downstream target ACC at Ser 79 was also not found to be significantly altered (Fig. 5.2). In addition, ACC1 protein expression was also found not to be significantly altered (Fig. 5.2).

In hepatocytes and intestinal cells metformin is transported into the cell by the organic cation transporter1 (OCT1) (McKinney and Hosford 1992, Wang *et al* 2002). However, there was no detectable level of OCT1 mRNA expression in 3T3-L1 adipocytes (Helen M McLeod, University of Glasgow personal communication). However, as mentioned previously, Huypens and co-workers (Huypens *et al* 2005) have suggested that metformin may be taken up into 3T3-L1 adipocytes via another transporter or by diffusion, although this does not appear to be the case in this current study.

A preliminary experiment showed that in Ad.α1^{312} infected cells there appeared to be a reduction in insulin-stimulated glucose transport compared to Ad.null infected cells (Fig. 5.5). This suggests that prolonged AMPK activation in 3T3-L1 adipocytes does indeed inhibit insulin-stimulated glucose transport. However, it is important to stress that this was a preliminary experiment (n=1), thus further repetitions are required in order to confirm this observation.

Collectively, these results suggest that prolonged AMPK activation in adipocytes inhibits insulin-stimulated glucose transport. This is in stark contrast to the effect of chronic AMPK activation by AICAR in skeletal muscle. Long-term activation of AMPK with AICAR increases glycogen content, hexokinase activity, and total GLUT4 protein content in rat skeletal muscle (Holmes *et al* 1999, Ojuka *et al* 2000). In addition, long term treatment of rats with AICAR was shown to induce a pronounced increase in insulin-stimulated glucose uptake and GLUT4 cell surface content in rat skeletal muscle (Buhl *et al* 2001).

This current work showed that long-term AMPK activation by AICAR in 3T3-L1 adipocytes did not alter PKB protein expression levels, nor alter insulin-stimulated PKB phosphorylation at Ser473 (Fig. 5.6). However, it is highly possible that prolonged AMPK activation in 3T3-L1 adipocytes may inhibit insulin-stimulated glucose transport by

altering the expression level of other key insulin-signalling molecules, as prolonged AMPK activation has previously been demonstrated to alter protein expression. Activation of AMPK by AICAR during differentiation of 3T3-L1 preadipocytes has been shown to reduce the expression of the early adipogenic transcription factors C/EBPα, C/EBPβ and PPARγ (Habinowski and Witters 2001, Giri *et al* 2006, Tong *et al* 2008), and the late adipogenic markers FAS and ACC (Habinowski and Witters 2001). Incubation of rat hepatocytes with AICAR was also found to inhibit glucose activated FAS gene expression (Foretz *et al* 1998). In addition the expression of the genes for the gluconeogenic enzyme phosphoenolpyruvate carboxy kinase and glucose-6-phosphatase were also shown to be reduced in hepatoma cells by activating AMPK using AICAR (Lochhead *et al* 2000). In muscle, AMPK activation by AICAR, was shown to increase both GLUT4 and hexokinase gene transcription (Holmes *et al* 1999, Zheng *et al* 2001, Ojuka *et al* 2000). AMPK has been proposed to regulate gene expression by directly phosphorylating certain transcription factors and co-activators including; p53, p300, TRIP6, and TORC2 (Leff 2003, Imamura *et al* 2001, Solaz-Fuster *et al* 2006, Shaw *et al* 2005).

The biguanide metformin, used in the treatment of type 2 diabetes, works primarily by reducing hepatic glucose release from hepatic glycogen stores (Kirpichnikov *et al* 2002). Metformin is thought to mediate its effects on hepatic glucose production via AMPK activation in cultured primary rat and human hepatocytes (Zhou *et al* 2001). This AMPK dependent mechanism has been further investigated and recent work suggests that metformin increases the expression of the nuclear receptor gene, SHP, via AMPK activation and that this in turn inhibits the expression of the hepatic gluconeogenic genes PEPCK and G6Pase (Kim *et al* 2008). Metformin has also been shown to increase AMPK activity in human muscle of subjects with Type 2 diabetes (Musi *et al* 2002). Furthermore this metformin-induced increase in AMPK activity in muscle is associated with higher rates of glucose disposal (Musi *et al* 2002). Prolonged treatment of 3T3-L1 adipocytes with metformin has previously been reported to stimulate AMPK activity (Huypens *et al* 2005), in contrast to the data presented here, yet metformin increases adipose AMPK activity *in vivo* in adipose tissue of subjects with type 2 diabetes compared with gliclazide (Fig. 5.8). The increase in adipose AMPK activity was not associated with an increase in AMPK protein expression. This suggests that the change in AMPK activity is due to an increase in the specific activity of AMPK rather than simply a difference in the total amount of AMPK between phases. The study design aimed to match glycaemic control at the end of each phase but this, in the event, proved not to be possible. Metformin increased AMPK activity

when compared to gliclazide despite better glycaemic control with the latter, supporting a glucose-independent mechanism for this metformin effect.

Prolonged AMPK activation *in vivo* in adipose tissue could occur under other conditions. The β adrenoreceptor agonists isoproterenol and adrenaline have both previously been shown to stimulate acute AMPK activity in adipocytes (Moule and Denton 1998, Yin *et al* 2003, Koh *et al* 2007). Thus it is feasible that sustained isoproterenol or adrenaline levels could result in prolonged AMPK activation *in vivo* in human adipose tissue. Leptin (Orci *et al* 2004) has been shown to acutely activate AMPK in adipose tissue. Given that leptin secretion increases with adipose tissue mass (Maffei *et al* 1995), it is possible that prolonged AMPK activation may occur *in vivo* in adipose tissue in obese individuals. Hypoxia/ischaemia has previously been shown to stimulate AMPK activity (Marsin *et al* 2000, Kudo *et al* 1995) in rat hearts. Thus, sustained ischemia *in vivo* in adipose tissue may also cause prolonged AMPK activation given that it is well established that adipose tissue is highly susceptible to ischemia (Kovach *et al* 1976**,** Coban *et al* 2005).

The TZD's are another class of drugs used in the treatment of type 2 diabetes. They stimulate PPARγ mediated adipocyte differentiation and increase the number of small adipocytes (Okuno *et al* 1998). This is associated with reduced serum NEFAs and reduced TNFα expression, which increases insulin sensitivity in liver and skeletal muscle (Quinn *et al* 2008). In addition, TZDs can also elevate levels of adiponectin. This is achieved in part via the generation of the small adipocytes which abundantly express and secrete adiponectin (Yamauchi *et al* 2001) and by the up-regulation of adiponectin via direct effects of TZDs on adiponectin gene transcription (Iwaki *et al* 2003). Adiponectin has previously been demonstrated to activate AMPK in muscle, liver and adipocytes (Yamauchi *et al* 2002, Wu *et al* 2003). In addition, Yamauchi and co-workers have shown that adiponectin stimulates glucose utilization and fatty-acid oxidation by activating AMP-activated protein kinase in liver and muscle (Yamauchi *et al* 2002). Thus TZDs are able to activate AMPK indirectly via adiponectin. In addition, the TZD, rosiglitazone has been shown to stimulate AMPK activity after 30 min in H-2K^{b} muscle cells suggesting an adiponectin independent effect (Fryer *et al* 2002b). Saha and co-workers showed that prolonged treatment of rats with pioglitazone increased the activity of AMPK in rat adipose and liver tissue, however, it is unclear whether it does so by a direct effect and/or by increasing plasma levels of adiponectin (Saha *et al* 2004). Therefore rosiglitazone may directly or indirectly, via adiponectin, cause sustained AMPK activation *in vivo* in human adipose tissue.

Metformin has also been shown to reduce the expression of various genes involved in the endocrine system in adipocytes; i.e inhibition of resistin (Rea and Donnelly 2006) leptin (Klein *et al* 2004) and adiponectin (Huypens *et al* 2005). The study by Huypens and co-workers is one of the few that effectively links metformin's suppression of gene expression with AMPK activation. In this current study the effect of chronic AMPK activation by metformin on the expression of key insulin signalling molecules in the human adipose biopsies was investigated. In summary, this study found that chronic AMPK activation by metformin in human adipose tissue did not appear to significantly alter the expression of IRS-1 (Fig. 5.12), the PI3K p85 subunit (Fig. 5.10) and PKB (Fig. 5.13). However, it still remains to be determined whether metformin alters the insulin sensitivity of these molecules in adipose tissue of type 2 diabetic subjects.

It should be noted that potentially metformin may not be having a direct effect on adipose tissue *in vivo*. Perhaps another molecule secreted from the liver, the primary site of metformin action, may be activating AMPK *in vivo* in human adipose tissue.

Adiponectin is secreted exclusively from adipocytes and has been shown to activate AMPK in isolated rat adipocytes (Wu *et al* 2003). Thus potentially metformin, via a direct or indirect effect on adipose tissue, could increase the adiponectin expression level in plasma and/or locally in adipose tissue in type 2 diabetic subjects which could subsequently result in adiponectin-mediated AMPK activation in adipose tissue. However, this seems unlikely since the data (Table 5.1) presented in this study shows that the increase in adipose AMPK activity after metformin treatment was not associated with any difference in the serum adiponectin level. This is in agreement with other previous studies which also found that metformin did not alter serum adiponectin concentration in type 2 diabetic subjects (Phillips *et al* 2003, Tiikkainen *et al* 2004). In addition it has also been reported that treatment of type 2 diabetic subjects with metformin does not alter adiponectin mRNA concentration in adipose tissue or the adipocyte adiponectin protein content (Tiikkainen *et al* 2004, Phillips *et al* 2003). However it should also be noted that measuring the total serum adiponectin level does not discriminate between adiponectin trimeric, hexameric and higher order polymeric structures which all exist in plasma (Pajvani *et al* 2003). The biological activity of adiponectin depends on its structure, with different oligomeric complexes activating different pathways. For example only globular and trimeric adiponectin were found to activate AMPK in myocytes (Tasao *et al* 2003, Tomas *et al* 2002).

Adipose tissue is constructed of different components including; adipocytes, connective tissue matrix, nerve tissue, stromovascular cells and immune cells. Thus potentially metformin may not be directly or indirectly activating AMPK in adipocytes within human adipose tissue. This current study found that the expression of FAS, whose expression has previously been shown to be reduced by AMPK activation during differentiation of 3T3-L1 preadipocytes (Habinowski and Witters 2001) was not significantly altered (Fig. 5.14) in adipose tissue from type 2 diabetic subjects treated with metformin. This suggests that metformin, either directly or indirectly, may be stimulating an increase in AMPK activity in non-adipocyte cells within adipose tissue. Prolonged AMPK activation by AICAR during differentiation of 3T3-L1 preadipocytes has also been reported to block the expression of the early adipogenic transcription factors C/EBPα, C/EBPβ and PPARγ, and of the late adipogenic marker ACC (Habinowski and Witters 2001, Giri *et al* 2006, Tong *et al* 2008). In addition, 24 hr AICAR treatment has also been shown to inhibit the expression of C/EBPα and PPARγ in fully differentiated 3T3-F442A cells (Dagon *et al* 2006). Therefore it would be useful to determine whether the expression of these adipogenic transcription factors and adipogenic markers in metformin treated type 2 diabetic subjects is altered in order to establish whether chronic AMPK activation by metformin in type 2 diabetic subjects activates AMPK in adipocytes within adipose tissue. However it is possible that the effect of AMPK activation on the expression of the adipogenic transcription factors and adipogenic markers may differ in mature adipocytes. In addition, adipocytes could be isolated from the adipose tissue biopsies and AMPK activity assessed. However, this would take several hours which may result in any non-genomic effects of metformin on the AMPK activity being lost.

Overall the findings of this study suggest that prolonged AMPK activation in 3T3-L1 adipocytes inhibits insulin-stimulated glucose transport and that this is not associated with altered PKB protein expression or insulin-stimulated PKB Ser473 phosphorylation. This study also reported that prolonged treatment of type 2 diabetic subjects with metformin increased AMPK activity in adipose tissue and that this was not associated with altered expression of three key insulin signalling molecules; PKB, the PI3K subunit p85 and IRS-1. The very modest effect of acute metformin treatment on AMPK activity in 3T3-L1 adipocytes, the lack of effect of prolonged metformin treatment on AMPK activity in 3T3-L1 adipocytes and the lack of effect of metformin on FAS expression in human adipose tissue suggests metformin's effects in adipose may not represent direct effects on the adipocytes within that tissue.

Chapter 6 – Final discussion

The principal findings of this study were that AMPK activity in 3T3-L1 adipocytes is sensitive to multiple stimuli that act via different mechanisms, did not alter substantially during adipogenesis and is associated with reduced insulin-stimulated glucose transport.

AMPK has been proposed to be a therapeutic target for patients with type 2 diabetes and the metabolic syndrome due to its beneficial effects on metabolic parameters. In skeletal muscle AMPK stimulates glucose uptake and fatty acid oxidation, whereas in liver it inhibits gluconeogenesis, fatty acid synthesis and cholesterol synthesis (Hardie 2004a). Overall the beneficial metabolic effects of AMPK activation in muscle and liver have been well-studied. However, despite the importance of adipose tissue in energy homeostasis the potential role of AMPK in the regulation of adipocyte biology was poorly characterised prior to this study.

Work in this current study showed that AMPK can be acutely activated in 3T3-L1 adipocytes by a variety of different stimuli; sorbitol, AICAR, arsenite, A23187, rosiglitazone, metformin, isopreterenol, sodium azide, H_2O_2, leptin and A769662. The mechanism of AMPK activation differs for the different stimuli (Fig. 6.1). AICAR is converted into ZMP in the cell which functions as a cellular mimetic of AMP i.e ZMP causes allosteric activation of AMPK and protects phosphorylation of Thr172, by the constitutively active AMPK kinase LKB1, from dephosphorylation. The novel direct AMPK activator A769662 activates AMPK by mimicking the effects of AMP. The calcium ionophore A23187 elevates intracellular calcium concentrations, thereby stimulating AMPK activity via a CaMKK dependent pathway. AMPK activation by isoproterenol, azide and rosiglitazone was not significantly altered in the presence of the CaMKK inhibitor STO-609. In addition these stimuli caused a significant increase in the ADP/ATP ratio which suggests that these stimuli activate AMPK via an LKB1-dependent pathway. Sorbitol, metformin, arsenite, hydrogen peroxide and leptin were found to have no significant effect on the nucleotide ratios, and AMPK stimulated activity by these activators was not significantly altered in the presence of STO-609. This suggests that these stimuli may be activating AMPK via novel AMPK kinases which are both nucleotide and calcium independent. One potential candidate is TAK1, which has recently been identified as a possible novel AMPK kinase in mammalian cells (Momcilovic *et al* 2006), however there may also exist other currently unidentified AMPK kinases.

Previous work by Salt and co-workers reported that stimulation of AMPK is associated with reduced insulin-stimulated glucose transport in 3T3-L1 adipocytes (Salt *et al* 2000), which is in contrast to the effect in muscle.

Acute stimulation of AMPK activity by sorbitol, rosiglitazone, isoproterenol, AICAR and A769662 in 3T3-L1 adipocytes significantly ($p < 0.05$) inhibited insulin-stimulated glucose transport. Although AICAR still displayed a tendency to inhibit insulin-stimulated glucose transport in Ad.α1DN infected cells, in the presence of the most effective AMPK inhibitor available, compound C, the inhibitory effect of AICAR on insulin-stimulated glucose transport was no longer apparent. Taken together these results provide strong evidence that acute AMPK activation does inhibit insulin-stimulated glucose transport. Results from this current study also showed that AMPK activation does not impair insulin-stimulated phosphorylation of AS160 or TBC1D1 at PAS sites. Thus, the molecular mechanism by which AMPK elicits the inhibition of insulin-stimulated glucose uptake still remains to be determined, but may potentially occur at a site downstream of AS160/TBC1D1 in the insulin signalling cascade. These findings are summarized below (Fig. 6.1).

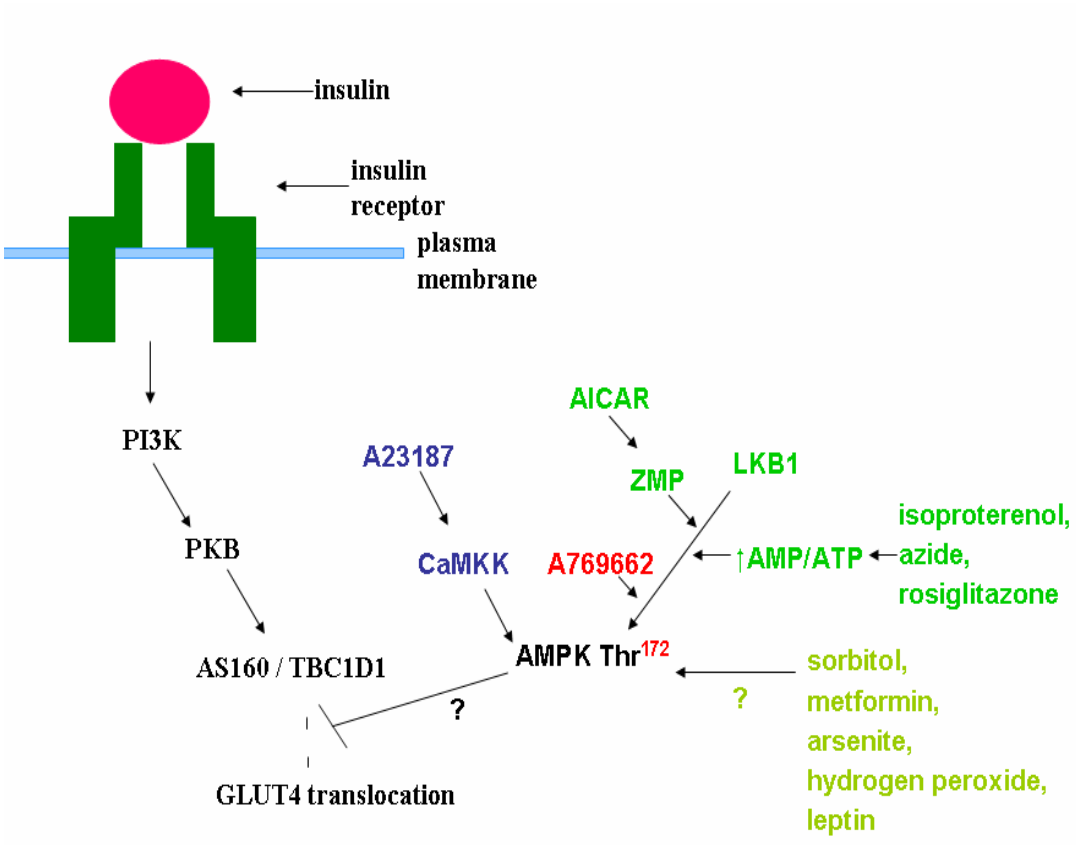

Figure 6-1: Proposed mechanism of acute AMPK activation and subsequent inhibition of insulin-stimulated glucose transport in 3T3-L1 adipocytes.

This current work also investigated the long-term effects of AMPK activation on insulin-stimulated glucose transport. Prolonged treatment of 3T3-L1 adipocytes with AICAR was found to activate AMPK activity and dramatically inhibit insulin-stimulated glucose transport. In addition a preliminary experiment showed that infection of 3T3-L1 adipocytes with Ad.$\alpha 1^{312}$ also inhibited insulin-stimulated glucose transport. Collectively, these results suggest that prolonged AMPK activation also inhibits-insulin-stimulated glucose transport in 3T3-L1 adipocytes. The mechanism of inhibition of insulin-stimulated glucose transport by prolonged AMPK activation in adipocytes was also investigated in this current study. However prolonged treatment of 3T3-L1 adipocytes was not associated with altered PKB expression or insulin-stimulated PKB phosphorylation. Furthermore chronic AMPK activation by metformin in adipose tissue of type 2 diabetic subjects was not associated with altered expression of three key insulin signalling molecules; PKB, the PI3K p85 subunit and IRS-1.

Overall this study suggests that both acute and prolonged AMPK activation in adipocytes inhibits insulin-stimulated glucose uptake. As discussed (1.1.2) glucose is taken up into adipocytes in the fed state and is stored as TG. Therefore inhibition of glucose uptake into adipocytes would subsequently reduce fatty acid and TG synthesis. The synthesis of fatty acids and TG from glucose is an energy dependent process. Thus, it could be reasoned that AMPK activation inhibits insulin-stimulated glucose uptake in adipocytes in order to reduce the ATP-dependent synthesis of fatty acids and TG in adipocytes. Furthermore, the inhibition of glucose transport would allow glucose to be used as an energy source by other tissues, rather than adipocytes, which would start using the stored triglyceride.

Although this current work reported that there was no change in total AMPK activity, as determined under a saturating AMP concentration (200μM), between fibroblasts and adipocytes throughout adipogenesis, there was an observed change in the expression levels of the γ subunit isoforms throughout adipogenesis i.e there was an increase in the γ1 isoform expression level and a reduction in the expression level of the γ2 and γ3 isoforms. Previous studies using native rat complexes and recombinant AMPK heterotrimeric complexes (Cheung *et al* 2000, Scott *et al* 2004) reported that different γ isoform complexes differed in their degree of stimulation by AMP i.e γ2 displayed the greatest stimulation by AMP, while γ1 displayed an intermediate stimulation by AMP and γ3 the lowest stimulation by AMP. Since the expression level of the different γ isoforms is altered during adipogenesis it would be interesting to investigate the sensitivity of AMPK complexes immunoprecipitated from fibroblasts and adipocytes to AMP, as it is possible

that during adipogenesis the sensitivity of adipocytes to energy balance changes may be altered.

Currently the mechanism by which AMPK activation in 3T3-L1 adipocytes inhibits insulin-stimulated glucose transport remains to be elucidated. This current work reported that AMPK activation did not impair insulin-stimulated phosphorylation of AS160/TBC1D1 at PAS sites. AS160 contains six potential PKB phosphorylation sites (Ser318, Ser341, Ser570, Ser588, Thr642, Ser751) (Sano *et al* 2003), and TBC1D1 contains two potential PKB phosphorylation sites (Thr596 and Ser507) (Roach *et al* 2007). The anti-PAS antibody only gives a measure of total phosphorylated AS160/TBC1D. Thus although the total PAS phosphorylation is unaltered, the actual extent of phosphorylation at each PAS site may be altered, with consequent effects on AS160/TBC1D1 activity. Since AMPK (*(*X*β)*XX*(S/T)*XXX**); *= Met, Val, Leu, Ile, or Phe, and β = Arg, Lys, or His) (Dale *et al* 1995) and PKB (R*X*R*XX*(S/T) (Yaffe *et al* 2001) have subtly different substrate specificities it is feasible that AICAR would preferentially cause phosphorylation of some PAS sites, and insulin (via PKB) of different ones. This could result in a different phosphorylation pattern on AS160/TBC1D1 with the same phosphorylation stoichiometry. It is not known precisely which PAS sites are important for regulating activity *in vivo*, thus it is possible that AICAR/PKB may cause phosphorylation at different PAS sites with corresponding changes in AS160/TBC1D1 activity, without altering total AS160/TBC1D1 PAS phosphorylation.

In HEK 293 cells the anti-PAS antibody was found to primarily detect phospho-Thr642 on AS160 (Geraghty *et al* 2007). Thus potentially AMPK may be altering insulin-stimulated AS160/TBC1D1 phosphorylation at PAS sites which may not be primarily recognized by the anti-PAS antibody in 3T3-L1 adipocytes.

In addition activation of AMPK in 3T3-L1 adipocytes may result in phosphorylation of AS160/TBC1D1 at non-PAS sites which may subsequently alter the activity of AS160/TBC1D1. Since the AMPK phosphorylation sites on AS160 lie within the PAS sites, and are thus detected by the PAS antibody, it is more likely that AMPK activation may result in the subsequent activation of a downstream kinase which may then phosphorylate AS160 at non-PAS sites, rather than AMPK directly phosphorylating AS160 at non-PAS sites. Thr568 and Ser666 have previously been identified as phosphorylation sites on AS160 which do not lie within a PKB consensus phosphorylation motif, and have been shown to be phosphorylated by RSK1 and SGK1 *in vivo* in HEK

cells (Geraghty *et al* 2007). Thus it is feasible that AMPK activation in adipocytes may result in activation of downstream kinases which may subsequently phosphorylate Thr568/Ser666 or novel sites on AS160.

Ser237, which lies within an AMPK consensus phosphorylation motif on TBC1D1, has been shown to be phosphorylated in response to treatments that elevate levels of active and phosphorylated AMPK in HEK 293 cells and rat L6 myotubes (Chen *et al* 2008). As previously mentioned overexpression of TBC1D1 was shown to markedly inhibit insulin-stimulated GLUT4 translocation in 3T3-L1 adipocytes (Roach *et al* 2007). Furthermore, this inhibition was reported to be partially reversed by AICAR (Chavez *et al* 2008). Interestingly, phosphorylation at Ser237 did not appear to underlie the effect of AICAR to relieve in part TBC1D1 inhibition of the insulin-stimulated increase in cell surface GLUT4 in 3T3-L1 adipocytes (Chavez *et al* 2008). In addition to Ser237, human TBC1D1 contains three other Ser/Thr residues that conform to the AMPK consensus phosphorylation sequence at amino acid residues 69, 372, and 565 (Chavez *et al* 2008). Thus in 3T3-L1 adipocytes it is possible that AMPK may phosphorylate TBC1D1 at non-PAS sites, which may subsequently alter the activity of TBC1D1.

Mass spectrometer analysis of TBC1D1 isolated from HEK 293 cells incubated in medium containing serum also identified Ser263, Ser566 and Ser585 as phosphorylation sites on TBC1D1 (Chen *et al* 2008). Thus, as discussed with regards to AS160, AMPK activation in 3T3-L1 adipocytes may result in the activation of downstream kinases which may subsequently phosphorylate TBC1D1 at non-PAS sites and alter its activity.

Although antibodies against specific phosphorylation sites could be used to further investigate the effect of AMPK activation on AS160/TBC1D1 phosphorylation, it is currently not possible to directly assess endogenous AS160/TBC1D1 Rab-GAP activity or Rab activation in adipocytes.

It is also possible that AICAR inhibits insulin-stimulated glucose transport at a site downstream of AS160/TBC1D1. It has been established that the SNARE complex VAMP2/SNAP23/syntaxin4 is involved in insulin-stimulated GLUT4 translocation to the plasma membrane (Bryant *et al* 2002). In addition, the accessory proteins, munc18c, synip and tomosyn, have also been proposed to regulate SNARE complex assembly and GLUT4 translocation (Kanda *et al* 2005**,** Widberg *et al* 2003**,** Yamada *et al* 2005).

Since the known molecular machinery (VAMP2/SNAP23/syntaxin4, munc18c, synip, tomosyn) that regulates GLUT4 exocytosis, downstream of AS160/TBC1D1, is common to muscle and adipocytes (Foster and Klip 2000, Randhawa *et al* 2000, Olson *et al* 1997, Widberg *et al* 2003, Yang *et al* 2001, Kanda *et al* 2005, Spurlin *et al* 2003, Yamada *et al* 2005, Min *et al* 1999), it is possible that the inhibition of insulin-stimulated glucose transport by AMPK activation in adipocytes is mediated by an effector specific to adipocytes that is absent or not functioning in muscle.

Thus the aim of future experiments would be to determine the molecular mechanism by which AMPK suppresses insulin-stimulated glucose transport in adipocytes. There a few potential mechanisms by which AMPK may be mediating inhibition of insulin-stimulated glucose transport in adipocytes; 1. AMPK may alter the subcellular location of key components of the insulin-stimulated GLUT4 trafficking pathway, subsequently altering their function, 2. AMPK may phosphorylate a currently unidentified protein which may inhibit insulin-stimulated glucose transport at a site downstream of AS160/TBC1D1, 3. AMPK may increase the rate at which GLUT4 is trafficked from the plasma membrane into intracellular storage vesicles, thus effectively reducing the amount of GLUT4 at the plasma membrane under insulin-stimulated conditions, 4. AMPK could potentially be altering the Cbl-TC10 pathway which is required for insulin-stimulated glucose transport.

In order to determine the effect of AMPK activation on the subcellular localization of key insulin-signalling molecules, cell lysates obtained from 3T3-L1 adipocytes incubated in the presence or absence of insulin and AMPK activators, could be subjected to subcellular fractionation. Proteins from the cytosolic, plasma membrane and microsomal fractions could then be subjected to immunoblotting with specific antibodies to insulin signalling and GLUT4 trafficking proteins.

In order to try to identify the AMPK effector proteins that inhibit insulin-stimulated glucose transport, 3T3-L1 adipocytes would be labelled with $^{33}PO_4^{3-}$ and incubated in the presence or absence of insulin and AMPK activators. Incorporation of $^{33}PO_4^{3-}$ into any proteins in the presence of AMPK activators could be detected by autoradiography, with target protein bands being subsequently excised and identified by sequencing. The effect of knockdown of the potential AMPK effector proteins in 3T3-L1 adipocytes, using siRNA, on AMPK mediated inhibition of insulin-stimulated glucose transport would help identify the AMPK effector mediating inhibition of insulin-stimulated glucose transport.

In the absence of insulin, GLUT4 is sequestered away from the cell surface plasma membrane, and stored in GLUT4 storage vesicles, available for rapid mobilisation upon insulin binding (Bryant *et al* 2002). To determine whether AMPK activation in 3T3-L1 adipocytes accelerates internalization and sequestration of GLUT4 from the plasma membrane under insulin-stimulated conditions, the rate of reversal of insulin-stimulated glucose transport could be determined by washing away insulin, as previously described (Proctor *et al* 2006), in the presence and absence of AMPK activators. If a change in trafficking was observed, 3T3-L1 adipocytes transfected with a GLUT4 tagged with an HA on the extracellular loop (HA-GLUT4) could be utilized to permit the precise determination of GLUT4 internalisation under basal and insulin-stimulated conditions.

The Cbl-TC10 pathway is a parallel insulin-signalling pathway which has been reported to contribute to GLUT4 translocation. Insulin-stimulated phosphorylation of Cbl activates the small GTP-binding protein TC10, which functions to stimulate trafficking of GLUT4 vesicles due to actin rearrangement (Saltiel and Pessin 2002). To determine the effect of AMPK activation on the Cbl-TC10 pathway, Cbl phosphorylation could be assessed by western blotting using phospho-specific antibodies in lysates obtained from 3T3-L1 adipopcytes incubated in the presence or absence of insulin and AMPK activators. In addition, analysis of TC10 activity (GTP-loading) could also be determined in cell lysates.

Impaired insulin-stimulated glucose transport in muscle and adipose contributes to hyperglycaemia in patients with diabetes. Thus elucidation of the molecular mechanisms which mediate the regulation of insulin-stimulated glucose transport in adipocytes, may uncover potential novel therapeutic targets, which may lead to the development of novel therapies for treating type 2 diabetes.

List of References

2000. Type 2 diabetes in children and adolescents. American Diabetes Association. *Diabetes Care*. 23:381-9.

Abu-Elheiga, L., A. Jayakumar, A. Baldini, S.S. Chirala, and S.J. Wakil. 1995. Human acetyl-CoA carboxylase: characterization, molecular cloning, and evidence for two isoforms. *Proc Natl Acad Sci U S A*. 92:4011-5.

Adan, R.A., R.D. Cone, J.P. Burbach, and W.H. Gispen. 1994. Differential effects of melanocortin peptides on neural melanocortin receptors. *Mol Pharmacol*. 46:1182-90.

Agati, J.M., D. Yeagley, and P.G. Quinn. 1998. Assessment of the roles of mitogen-activated protein kinase, phosphatidylinositol 3-kinase, protein kinase B, and protein kinase C in insulin inhibition of cAMP-induced phosphoenolpyruvate carboxykinase gene transcription. *J Biol Chem*. 273:18751-9.

Aguirre, V., T. Uchida, L. Yenush, R. Davis, and M.F. White. 2000. The c-Jun NH(2)-terminal kinase promotes insulin resistance during association with insulin receptor substrate-1 and phosphorylation of Ser(307). *J Biol Chem*. 275:9047-54.

Aguirre, V., E.D. Werner, J. Giraud, Y.H. Lee, S.E. Shoelson, and M.F. White. 2002. Phosphorylation of Ser307 in insulin receptor substrate-1 blocks interactions with the insulin receptor and inhibits insulin action. *J Biol Chem*. 277:1531-7.

Ahima, R.S., J. Dushay, S.N. Flier, D. Prabakaran, and J.S. Flier. 1997. Leptin accelerates the onset of puberty in normal female mice. *J Clin Invest*. 99:391-5.

Alessi, D.R., S.R. James, C.P. Downes, A.B. Holmes, P.R. Gaffney, C.B. Reese, and P. Cohen. 1997. Characterization of a 3-phosphoinositide-dependent protein kinase which phosphorylates and activates protein kinase Balpha. *Curr Biol*. 7:261-9.

Alonso, A., J. Sasin, N. Bottini, I. Friedberg, A. Osterman, A. Godzik, T. Hunter, J. Dixon, and T. Mustelin. 2004. Protein tyrosine phosphatases in the human genome. *Cell*. 117:699-711.

Anthonsen, M.W., L. Ronnstrand, C. Wernstedt, E. Degerman, and C. Holm. 1998. Identification of novel phosphorylation sites in hormone-sensitive lipase that are phosphorylated in response to isoproterenol and govern activation properties in vitro. *J Biol Chem*. 273:215-21.

Arad, M., D.W. Benson, A.R. Perez-Atayde, W.J. McKenna, E.A. Sparks, R.J. Kanter, K. McGarry, J.G. Seidman, and C.E. Seidman. 2002. Constitutively active AMP kinase mutations cause glycogen storage disease mimicking hypertrophic cardiomyopathy. *J Clin Invest*. 109:357-62.

Arad, M., C.E. Seidman, and J.G. Seidman. 2007. AMP-activated protein kinase in the heart: role during health and disease. *Circ Res*. 100:474-88.

Arena, S., S. Benvenuti, and A. Bardelli. 2005. Genetic analysis of the kinome and phosphatome in cancer. *Cell Mol Life Sci*. 62:2092-9.

Assimacopoulos-Jeannet, F., S. Brichard, F. Rencurel, I. Cusin, and B. Jeanrenaud. 1995. In vivo effects of hyperinsulinemia on lipogenic enzymes and glucose transporter expression in rat liver and adipose tissues. *Metabolism*. 44:228-33.

Bailey, C.J. 1992. Biguanides and NIDDM. *Diabetes Care*. 15:755-72.

Bailey, C.J., and R.C. Turner. 1996. Metformin. *N Engl J Med*. 334:574-9.

Bain, J., L. Plater, M. Elliott, N. Shpiro, C.J. Hastie, H. McLauchlan, I. Klevernic, J.S. Arthur, D.R. Alessi, and P. Cohen. 2007. The selectivity of protein kinase inhibitors: a further update. *Biochem J*. 408:297-315.

Barnes, B.R., S. Marklund, T.L. Steiler, M. Walter, G. Hjalm, V. Amarger, M. Mahlapuu, Y. Leng, C. Johansson, D. Galuska, K. Lindgren, M. Abrink, D. Stapleton, J.R. Zierath, and L. Andersson. 2004. The 5'-AMP-activated protein kinase gamma3 isoform has a key role in carbohydrate and lipid metabolism in glycolytic skeletal muscle. *J Biol Chem*. 279:38441-7.

Bateman, A. 1997. The structure of a domain common to archaebacteria and the homocystinuria disease protein. *Trends Biochem Sci*. 22:12-3.

Bayascas, J.R., N.R. Leslie, R. Parsons, S. Fleming, and D.R. Alessi. 2005. Hypomorphic mutation of PDK1 suppresses tumorigenesis in PTEN(+/-) mice. *Curr Biol*. 15:1839-46.

Beg, Z.H., J.A. Stonik, and H.B. Brewer, Jr. 1978. 3-Hydroxy-3-methylglutaryl coenzyme A reductase: regulation of enzymatic activity by phosphorylation and dephosphorylation. *Proc Natl Acad Sci U S A*. 75:3678-82.

Bergeron, R., J.M. Ren, K.S. Cadman, I.K. Moore, P. Perret, M. Pypaert, L.H. Young, C.F. Semenkovich, and G.I. Shulman. 2001. Chronic activation of AMP kinase results in NRF-1 activation and mitochondrial biogenesis. *Am J Physiol Endocrinol Metab*. 281:E1340-6.

Bergeron, R., R.R. Russell, 3rd, L.H. Young, J.M. Ren, M. Marcucci, A. Lee, and G.I. Shulman. 1999. Effect of AMPK activation on muscle glucose metabolism in conscious rats. *Am J Physiol*. 276:E938-44.

Bernal, D., K. Almind, L. Yenush, M. Ayoub, Y. Zhang, L. Rosshani, C. Larsson, O. Pedersen, and M.F. White. 1998. Insulin receptor substrate-2 amino acid polymorphisms are not associated with random type 2 diabetes among Caucasians. *Diabetes*. 47:976-9.

Bjorbaek, C., and B.B. Kahn. 2004. Leptin signaling in the central nervous system and the periphery. *Recent Prog Horm Res*. 59:305-31.

Blair, E., C. Redwood, H. Ashrafian, M. Oliveira, J. Broxholme, B. Kerr, A. Salmon, I. Ostman-Smith, and H. Watkins. 2001. Mutations in the gamma(2) subunit of AMP-activated protein kinase cause familial hypertrophic cardiomyopathy: evidence for the central role of energy compromise in disease pathogenesis. *Hum Mol Genet*. 10:1215-20.

Bontemps, F., G. Van den Berghe, and H.G. Hers. 1986. Pathways of adenine nucleotide catabolism in erythrocytes. *J Clin Invest*. 77:824-30.

Borthwick, A.C., A.M. Wells, J.J. Rochford, S.J. Hurel, D.M. Turnbull, and S.J. Yeaman. 1995. Inhibition of glycogen synthase kinase-3 by insulin in cultured human skeletal muscle myoblasts. *Biochem Biophys Res Commun*. 210:738-45.

Bozaoglu, K., K. Bolton, J. McMillan, P. Zimmet, J. Jowett, G. Collier, K. Walder, and D. Segal. 2007. Chemerin is a novel adipokine associated with obesity and metabolic syndrome. *Endocrinology*. 148:4687-94.

Brazil, D.P., Z.Z. Yang, and B.A. Hemmings. 2004. Advances in protein kinase B signalling: AKTion on multiple fronts. *Trends Biochem Sci*. 29:233-42.

Brunmair, B., K. Staniek, F. Gras, N. Scharf, A. Althaym, R. Clara, M. Roden, E. Gnaiger, H. Nohl, W. Waldhausl, and C. Furnsinn. 2004. Thiazolidinediones, like metformin, inhibit respiratory complex I: a common mechanism contributing to their antidiabetic actions? *Diabetes*. 53:1052-9.

Bruss, M.D., E.B. Arias, G.E. Lienhard, and G.D. Cartee. 2005. Increased phosphorylation of Akt substrate of 160 kDa (AS160) in rat skeletal muscle in response to insulin or contractile activity. *Diabetes*. 54:41-50.

Bruun, J.M., S.B. Pedersen, and B. Richelsen. 2001. Regulation of interleukin 8 production and gene expression in human adipose tissue in vitro. *J Clin Endocrinol Metab*. 86:1267-73.

Bryant, N.J., R. Govers, and D.E. James. 2002. Regulated transport of the glucose transporter GLUT4. *Nat Rev Mol Cell Biol*. 3:267-77.

Buhl, E.S., N. Jessen, O. Schmitz, S.B. Pedersen, O. Pedersen, G.D. Holman, and S. Lund. 2001. Chronic treatment with 5-aminoimidazole-4-carboxamide-1-beta-D-ribofuranoside increases insulin-stimulated glucose uptake and GLUT4 translocation in rat skeletal muscles in a fiber type-specific manner. *Diabetes*. 50:12-7.

Burks, D.J., S. Pons, H. Towery, J. Smith-Hall, M.G. Myers, Jr., L. Yenush, and M.F. White. 1997. Heterologous pleckstrin homology domains do not couple IRS-1 to the insulin receptor. *J Biol Chem*. 272:27716-21.

Burwinkel, B., J.W. Scott, C. Buhrer, F.K. van Landeghem, G.F. Cox, C.J. Wilson, D. Grahame Hardie, and M.W. Kilimann. 2005. Fatal congenital heart glycogenosis caused by a recurrent activating R531Q mutation in the gamma 2-subunit of AMP-activated protein kinase (PRKAG2), not by phosphorylase kinase deficiency. *Am J Hum Genet*. 76:1034-49.

Calleja, V., D. Alcor, M. Laguerre, J. Park, B. Vojnovic, B.A. Hemmings, J. Downward, P.J. Parker, and B. Larijani. 2007. Intramolecular and intermolecular interactions of protein kinase B define its activation in vivo. *PLoS Biol*. 5:e95.

Campbell, P.J., M.G. Carlson, and N. Nurjhan. 1994. Fat metabolism in human obesity. *Am J Physiol*. 266:E600-5.

Campfield, L.A., F.J. Smith, Y. Guisez, R. Devos, and P. Burn. 1995. Recombinant mouse OB protein: evidence for a peripheral signal linking adiposity and central neural networks. *Science*. 269:546-9.

Carling, D. 2004. The AMP-activated protein kinase cascade--a unifying system for energy control. *Trends Biochem Sci*. 29:18-24.

Carling, D., and D.G. Hardie. 1989. The substrate and sequence specificity of the AMP-activated protein kinase. Phosphorylation of glycogen synthase and phosphorylase kinase. *Biochim Biophys Acta*. 1012:81-6.

Carling, D., V.A. Zammit, and D.G. Hardie. 1987. A common bicyclic protein kinase cascade inactivates the regulatory enzymes of fatty acid and cholesterol biosynthesis. *FEBS Lett*. 223:217-22.

Carlson, C.A., and K.H. Kim. 1973. Regulation of hepatic acetyl coenzyme A carboxylase by phosphorylation and dephosphorylation. *J Biol Chem*. 248:378-80.

Carpenter, G. 2000. The EGF receptor: a nexus for trafficking and signaling. *Bioessays*. 22:697-707.

Castan-Laurell, I., J. Boucher, C. Dray, D. Daviaud, C. Guigne, and P. Valet. 2005. Apelin, a novel adipokine over-produced in obesity: friend or foe? *Mol Cell Endocrinol*. 245:7-9.

Chadt, A., K. Leicht, A. Deshmukh, L.Q. Jiang, S. Scherneck, U. Bernhardt, T. Dreja, H. Vogel, K. Schmolz, R. Kluge, J.R. Zierath, C. Hultschig, R.C. Hoeben, A. Schurmann, H.G. Joost, and H. Al-Hasani. 2008. Tbc1d1 mutation in lean mouse strain confers leanness and protects from diet-induced obesity. *Nat Genet*. 40:1354-9.

Chavez, J.A., T.A. Knotts, L.P. Wang, G. Li, R.T. Dobrowsky, G.L. Florant, and S.A. Summers. 2003. A role for ceramide, but not diacylglycerol, in the antagonism of insulin signal transduction by saturated fatty acids. *J Biol Chem*. 278:10297-303.

Chavez, J.A., W.G. Roach, S.R. Keller, W.S. Lane, and G.E. Lienhard. 2008. Inhibition of GLUT4 translocation by Tbc1d1, a Rab GTPase-activating protein abundant in skeletal

muscle, is partially relieved by AMP-activated protein kinase activation. *J Biol Chem*. 283:9187-95.

Chehab, F.F., M.E. Lim, and R. Lu. 1996. Correction of the sterility defect in homozygous obese female mice by treatment with the human recombinant leptin. *Nat Genet*. 12:318-20.

Chehab, F.F., K. Mounzih, R. Lu, and M.E. Lim. 1997. Early onset of reproductive function in normal female mice treated with leptin. *Science*. 275:88-90.

Chen, D., J.S. Elmendorf, A.L. Olson, X. Li, H.S. Earp, and J.E. Pessin. 1997. Osmotic shock stimulates GLUT4 translocation in 3T3L1 adipocytes by a novel tyrosine kinase pathway. *J Biol Chem*. 272:27401-10.

Chen, D., R.V. Fucini, A.L. Olson, B.A. Hemmings, and J.E. Pessin. 1999. Osmotic shock inhibits insulin signaling by maintaining Akt/protein kinase B in an inactive dephosphorylated state. *Mol Cell Biol*. 19:4684-94.

Chen, H., O. Charlat, L.A. Tartaglia, E.A. Woolf, X. Weng, S.J. Ellis, N.D. Lakey, J. Culpepper, K.J. Moore, R.E. Breitbart, G.M. Duyk, R.I. Tepper, and J.P. Morgenstern. 1996. Evidence that the diabetes gene encodes the leptin receptor: identification of a mutation in the leptin receptor gene in db/db mice. *Cell*. 84:491-5.

Chen, H.C., G. Bandyopadhyay, M.P. Sajan, Y. Kanoh, M. Standaert, R.V. Farese, Jr., and R.V. Farese. 2002. Activation of the ERK pathway and atypical protein kinase C isoforms in exercise- and aminoimidazole-4-carboxamide-1-beta-D-riboside (AICAR)-stimulated glucose transport. *J Biol Chem*. 277:23554-62.

Chen, S., J. Murphy, R. Toth, D.G. Campbell, N.A. Morrice, and C. Mackintosh. 2008. Complementary regulation of TBC1D1 and AS160 by growth factors, insulin and AMPK activators. *Biochem J*. 409:449-59.

Chien, D., D. Dean, A.K. Saha, J.P. Flatt, and N.B. Ruderman. 2000. Malonyl-CoA content and fatty acid oxidation in rat muscle and liver in vivo. *Am J Physiol Endocrinol Metab*. 279:E259-65.

Cho, H., J. Mu, J.K. Kim, J.L. Thorvaldsen, Q. Chu, E.B. Crenshaw, 3rd, K.H. Kaestner, M.S. Bartolomei, G.I. Shulman, and M.J. Birnbaum. 2001. Insulin resistance and a

diabetes mellitus-like syndrome in mice lacking the protein kinase Akt2 (PKB beta). *Science*. 292:1728-31.

Choi, S.L., S.J. Kim, K.T. Lee, J. Kim, J. Mu, M.J. Birnbaum, S. Soo Kim, and J. Ha. 2001. The regulation of AMP-activated protein kinase by H(2)O(2). *Biochem Biophys Res Commun*. 287:92-7.

Christ-Crain, M., B. Kola, F. Lolli, C. Fekete, D. Seboek, G. Wittmann, D. Feltrin, S.C. Igreja, S. Ajodha, J. Harvey-White, G. Kunos, B. Muller, F. Pralong, G. Aubert, G. Arnaldi, G. Giacchetti, M. Boscaro, A.B. Grossman, and M. Korbonits. 2008. AMP-activated protein kinase mediates glucocorticoid-induced metabolic changes: a novel mechanism in Cushing's syndrome. *Faseb J*. 22:1672-83.

Ciaraldi, T.P., A.P. Kong, N.V. Chu, D.D. Kim, S. Baxi, M. Loviscach, R. Plodkowski, R. Reitz, M. Caulfield, S. Mudaliar, and R.R. Henry. 2002. Regulation of glucose transport and insulin signaling by troglitazone or metformin in adipose tissue of type 2 diabetic subjects. *Diabetes*. 51:30-6.

Cigolini, M., O. Bosello, C. Zancanaro, P.G. Orlandi, O. Fezzi, and U. Smith. 1984. Influence of metformin on metabolic effect of insulin in human adipose tissue in vitro. *Diabete Metab*. 10:311-5.

Civelek, V.N., J.A. Hamilton, K. Tornheim, K.L. Kelly, and B.E. Corkey. 1996. Intracellular pH in adipocytes: effects of free fatty acid diffusion across the plasma membrane, lipolytic agonists, and insulin. *Proc Natl Acad Sci U S A*. 93:10139-44.

Clausen, T., J. Elbrink, and B.R. Martin. 1974. Insulin controlling calcium distribution in muscle and fat cells. *Acta Endocrinol Suppl (Copenh)*. 191:137-43.

Clement, K., C. Vaisse, N. Lahlou, S. Cabrol, V. Pelloux, D. Cassuto, M. Gourmelen, C. Dina, J. Chambaz, J.M. Lacorte, A. Basdevant, P. Bougneres, Y. Lebouc, P. Froguel, and B. Guy-Grand. 1998. A mutation in the human leptin receptor gene causes obesity and pituitary dysfunction. *Nature*. 392:398-401.

Cohen, P. 2000. The regulation of protein function by multisite phosphorylation--a 25 year update. *Trends Biochem Sci*. 25:596-601.

Cohen, P.T. 2002. Protein phosphatase 1--targeted in many directions. *J Cell Sci*. 115:241-56.

Coleman, R.A., and D.P. Lee. 2004. Enzymes of triacylglycerol synthesis and their regulation. *Prog Lipid Res*. 43:134-76.

Collins, S., W. Cao, and J. Robidoux. 2004. Learning new tricks from old dogs: beta-adrenergic receptors teach new lessons on firing up adipose tissue metabolism. *Mol Endocrinol*. 18:2123-31.

Collison, M., D.J. James, D. Graham, G.D. Holman, J.M. Connell, A.F. Dominiczak, G.W. Gould, and I.P. Salt. 2005. Reduced insulin-stimulated GLUT4 bioavailability in stroke-prone spontaneously hypertensive rats. *Diabetologia*. 48:539-46.

Combs, T.P., U.B. Pajvani, A.H. Berg, Y. Lin, L.A. Jelicks, M. Laplante, A.R. Nawrocki, M.W. Rajala, A.F. Parlow, L. Cheeseboro, Y.Y. Ding, R.G. Russell, D. Lindemann, A. Hartley, G.R. Baker, S. Obici, Y. Deshaies, M. Ludgate, L. Rossetti, and P.E. Scherer. 2004. A transgenic mouse with a deletion in the collagenous domain of adiponectin displays elevated circulating adiponectin and improved insulin sensitivity. *Endocrinology*. 145:367-83.

Considine, R.V., M.K. Sinha, M.L. Heiman, A. Kriauciunas, T.W. Stephens, M.R. Nyce, J.P. Ohannesian, C.C. Marco, L.J. McKee, T.L. Bauer, and et al. 1996. Serum immunoreactive-leptin concentrations in normal-weight and obese humans. *N Engl J Med*. 334:292-5.

Cook, D.L., and C.N. Hales. 1984. Intracellular ATP directly blocks K+ channels in pancreatic B-cells. *Nature*. 311:271-3.

Cook, K.S., D.L. Groves, H.Y. Min, and B.M. Spiegelman. 1985. A developmentally regulated mRNA from 3T3 adipocytes encodes a novel serine protease homologue. *Proc Natl Acad Sci U S A*. 82:6480-4.

Cool, B., B. Zinker, W. Chiou, L. Kifle, N. Cao, M. Perham, R. Dickinson, A. Adler, G. Gagne, R. Iyengar, G. Zhao, K. Marsh, P. Kym, P. Jung, H.S. Camp, and E. Frevert. 2006. Identification and characterization of a small molecule AMPK activator that treats key components of type 2 diabetes and the metabolic syndrome. *Cell Metab*. 3:403-16.

Corton, J.M., J.G. Gillespie, and D.G. Hardie. 1994. Role of the AMP-activated protein kinase in the cellular stress response. *Curr Biol*. 4:315-24.

Corton, J.M., J.G. Gillespie, S.A. Hawley, and D.G. Hardie. 1995. 5-aminoimidazole-4-carboxamide ribonucleoside. A specific method for activating AMP-activated protein kinase in intact cells? *Eur J Biochem*. 229:558-65.

Cozzone, A.J. 1988. Protein phosphorylation in prokaryotes. *Annu Rev Microbiol*. 42:97-125.

Cross, D.A., D.R. Alessi, P. Cohen, M. Andjelkovich, and B.A. Hemmings. 1995. Inhibition of glycogen synthase kinase-3 by insulin mediated by protein kinase B. *Nature*. 378:785-9.

Crute, B.E., K. Seefeld, J. Gamble, B.E. Kemp, and L.A. Witters. 1998. Functional domains of the alpha1 catalytic subunit of the AMP-activated protein kinase. *J Biol Chem*. 273:35347-54.

Currie, R.A., K.S. Walker, A. Gray, M. Deak, A. Casamayor, C.P. Downes, P. Cohen, D.R. Alessi, and J. Lucocq. 1999. Role of phosphatidylinositol 3,4,5-trisphosphate in regulating the activity and localization of 3-phosphoinositide-dependent protein kinase-1. *Biochem J*. 337 (Pt 3):575-83.

Czech, M.P., and S. Corvera. 1999. Signaling mechanisms that regulate glucose transport. *J Biol Chem*. 274:1865-8.

Dagon, Y., Y. Avraham, and E.M. Berry. 2006. AMPK activation regulates apoptosis, adipogenesis, and lipolysis by eIF2alpha in adipocytes. *Biochem Biophys Res Commun*. 340:43-7.

Dale, S., W.A. Wilson, A.M. Edelman, and D.G. Hardie. 1995. Similar substrate recognition motifs for mammalian AMP-activated protein kinase, higher plant HMG-CoA reductase kinase-A, yeast SNF1, and mammalian calmodulin-dependent protein kinase I. *FEBS Lett*. 361:191-5.

Daniel, T., and D. Carling. 2002. Functional analysis of mutations in the gamma 2 subunit of AMP-activated protein kinase associated with cardiac hypertrophy and Wolff-Parkinson-White syndrome. *J Biol Chem*. 277:51017-24.

Daval, M., F. Diot-Dupuy, R. Bazin, I. Hainault, B. Viollet, S. Vaulont, E. Hajduch, P. Ferre, and F. Foufelle. 2005. Anti-lipolytic action of AMP-activated protein kinase in rodent adipocytes. *J Biol Chem*. 280:25250-7.

Davies, S.P., N.R. Helps, P.T. Cohen, and D.G. Hardie. 1995. 5'-AMP inhibits dephosphorylation, as well as promoting phosphorylation, of the AMP-activated protein kinase. Studies using bacterially expressed human protein phosphatase-2C alpha and native bovine protein phosphatase-2AC. *FEBS Lett*. 377:421-5.

Davies, S.P., A.T. Sim, and D.G. Hardie. 1990. Location and function of three sites phosphorylated on rat acetyl-CoA carboxylase by the AMP-activated protein kinase. *Eur J Biochem*. 187:183-90.

Derave, W., H. Ai, J. Ihlemann, L.A. Witters, S. Kristiansen, E.A. Richter, and T. Ploug. 2000. Dissociation of AMP-activated protein kinase activation and glucose transport in contracting slow-twitch muscle. *Diabetes*. 49:1281-7.

Dhanasekaran, N., and E. Premkumar Reddy. 1998. Signaling by dual specificity kinases. *Oncogene*. 17:1447-55.

Dickens, M., C.A. Svitek, A.A. Culbert, R.M. O'Brien, and J.M. Tavare. 1998. Central role for phosphatidylinositide 3-kinase in the repression of glucose-6-phosphatase gene transcription by insulin. *J Biol Chem*. 273:20144-9.

Douen, A.G., T. Ramlal, G.D. Cartee, and A. Klip. 1990. Exercise modulates the insulin-induced translocation of glucose transporters in rat skeletal muscle. *FEBS Lett*. 261:256-60.

Douen, A.G., T. Ramlal, A. Klip, D.A. Young, G.D. Cartee, and J.O. Holloszy. 1989. Exercise-induced increase in glucose transporters in plasma membranes of rat skeletal muscle. *Endocrinology*. 124:449-54.

Draznin, B., K. Sussman, M. Kao, D. Lewis, and N. Sherman. 1987. The existence of an optimal range of cytosolic free calcium for insulin-stimulated glucose transport in rat adipocytes. *J Biol Chem*. 262:14385-8.

Du, J., Q. Chen, H. Takemori, and H. Xu. 2008. SIK2 can be activated by deprivation of nutrition and it inhibits expression of lipogenic genes in adipocytes. *Obesity (Silver Spring)*. 16:531-8.

Ducy, P., M. Amling, S. Takeda, M. Priemel, A.F. Schilling, F.T. Beil, J. Shen, C. Vinson, J.M. Rueger, and G. Karsenty. 2000. Leptin inhibits bone formation through a hypothalamic relay: a central control of bone mass. *Cell*. 100:197-207.

Eguez, L., A. Lee, J.A. Chavez, C.P. Miinea, S. Kane, G.E. Lienhard, and T.E. McGraw. 2005. Full intracellular retention of GLUT4 requires AS160 Rab GTPase activating protein. *Cell Metab*. 2:263-72.

El-Haschimi, K., D.D. Pierroz, S.M. Hileman, C. Bjorbaek, and J.S. Flier. 2000. Two defects contribute to hypothalamic leptin resistance in mice with diet-induced obesity. *J Clin Invest*. 105:1827-32.

El-Mir, M.Y., V. Nogueira, E. Fontaine, N. Averet, M. Rigoulet, and X. Leverve. 2000. Dimethylbiguanide inhibits cell respiration via an indirect effect targeted on the respiratory chain complex I. *J Biol Chem*. 275:223-8.

Fajas, L., K. Schoonjans, L. Gelman, J.B. Kim, J. Najib, G. Martin, J.C. Fruchart, M. Briggs, B.M. Spiegelman, and J. Auwerx. 1999. Regulation of peroxisome proliferator-activated receptor gamma expression by adipocyte differentiation and determination factor 1/sterol regulatory element binding protein 1: implications for adipocyte differentiation and metabolism. *Mol Cell Biol*. 19:5495-503.

Farooqi, I.S., S.A. Jebb, G. Langmack, E. Lawrence, C.H. Cheetham, A.M. Prentice, I.A. Hughes, M.A. McCamish, and S. O'Rahilly. 1999. Effects of recombinant leptin therapy in a child with congenital leptin deficiency. *N Engl J Med*. 341:879-84.

Febbraio, M., N.A. Abumrad, D.P. Hajjar, K. Sharma, W. Cheng, S.F. Pearce, and R.L. Silverstein. 1999. A null mutation in murine CD36 reveals an important role in fatty acid and lipoprotein metabolism. *J Biol Chem*. 274:19055-62.

Fediuc, S., M.P. Gaidhu, and R.B. Ceddia. 2006. Regulation of AMP-activated protein kinase and acetyl-CoA carboxylase phosphorylation by palmitate in skeletal muscle cells. *J Lipid Res*. 47:412-20.

Fernandez-Real, J.M., and W. Ricart. 2003. Insulin resistance and chronic cardiovascular inflammatory syndrome. *Endocr Rev*. 24:278-301.

Ferrer, A., C. Caelles, N. Massot, and F.G. Hegardt. 1985. Activation of rat liver cytosolic 3-hydroxy-3-methylglutaryl coenzyme A reductase kinase by adenosine 5'-monophosphate. *Biochem Biophys Res Commun*. 132:497-504.

Fidelman, M.L., S.H. Seeholzer, K.B. Walsh, and R.D. Moore. 1982. Intracellular pH mediates action of insulin on glycolysis in frog skeletal muscle. *Am J Physiol*. 242:C87-93.

Filippa, N., C.L. Sable, C. Filloux, B. Hemmings, and E. Van Obberghen. 1999. Mechanism of protein kinase B activation by cyclic AMP-dependent protein kinase. *Mol Cell Biol*. 19:4989-5000.

Fliegel, L. 2005. The Na+/H+ exchanger isoform 1. *Int J Biochem Cell Biol*. 37:33-7.

Flier, J.S. 1998. Clinical review 94: What's in a name? In search of leptin's physiologic role. *J Clin Endocrinol Metab*. 83:1407-13.

Foretz, M., D. Carling, C. Guichard, P. Ferre, and F. Foufelle. 1998. AMP-activated protein kinase inhibits the glucose-activated expression of fatty acid synthase gene in rat hepatocytes. *J Biol Chem*. 273:14767-71.

Foster, L.J., and A. Klip. 2000. Mechanism and regulation of GLUT-4 vesicle fusion in muscle and fat cells. *Am J Physiol Cell Physiol*. 279:C877-90.

Fredrikson, G., H. Tornqvist, and P. Belfrage. 1986. Hormone-sensitive lipase and monoacylglycerol lipase are both required for complete degradation of adipocyte triacylglycerol. *Biochim Biophys Acta*. 876:288-93.

Fryer, L.G., F. Foufelle, K. Barnes, S.A. Baldwin, A. Woods, and D. Carling. 2002a. Characterization of the role of the AMP-activated protein kinase in the stimulation of glucose transport in skeletal muscle cells. *Biochem J*. 363:167-74.

Fryer, L.G., E. Hajduch, F. Rencurel, I.P. Salt, H.S. Hundal, D.G. Hardie, and D. Carling. 2000. Activation of glucose transport by AMP-activated protein kinase via stimulation of nitric oxide synthase. *Diabetes*. 49:1978-85.

Fryer, L.G., A. Parbu-Patel, and D. Carling. 2002b. The Anti-diabetic drugs rosiglitazone and metformin stimulate AMP-activated protein kinase through distinct signaling pathways. *J Biol Chem*. 277:25226-32.

Fryer, L.G., A. Parbu-Patel, and D. Carling. 2002c. Protein kinase inhibitors block the stimulation of the AMP-activated protein kinase by 5-amino-4-imidazolecarboxamide riboside. *FEBS Lett*. 531:189-92.

Fukuhara, A., M. Matsuda, M. Nishizawa, K. Segawa, M. Tanaka, K. Kishimoto, Y. Matsuki, M. Murakami, T. Ichisaka, H. Murakami, E. Watanabe, T. Takagi, M. Akiyoshi, T. Ohtsubo, S. Kihara, S. Yamashita, M. Makishima, T. Funahashi, S. Yamanaka, R. Hiramatsu, Y. Matsuzawa, and I. Shimomura. 2005. Visfatin: a protein secreted by visceral fat that mimics the effects of insulin. *Science*. 307:426-30.

Gaidhu, M.P., S. Fediuc, N.M. Anthony, M. So, M. Mirpourian, R.L. Perry, and R.B. Ceddia. 2009. Prolonged aicar-induced amp-kinase activation promotes energy dissipation in white adipocytes: Novel mechanisms integrating HSL and ATGL. *J Lipid Res*. 50:704-15.

Gaidhu, M.P., S. Fediuc, and R.B. Ceddia. 2006. Aicar-induced AMPK phosphorylation inhibits basal and insulin-stimulated glucose uptake, lipid synthesis, and fatty acid oxidation in isolated rat adipocytes. *J Biol Chem*. 281:25956-64.

Gainsford, T., T.A. Willson, D. Metcalf, E. Handman, C. McFarlane, A. Ng, N.A. Nicola, W.S. Alexander, and D.J. Hilton. 1996. Leptin can induce proliferation, differentiation, and functional activation of hemopoietic cells. *Proc Natl Acad Sci U S A*. 93:14564-8.

Galuska, D., J. Zierath, A. Thorne, T. Sonnenfeld, and H. Wallberg-Henriksson. 1991. Metformin increases insulin-stimulated glucose transport in insulin-resistant human skeletal muscle. *Diabete Metab*. 17:159-63.

Gamble, J., and G.D. Lopaschuk. 1997. Insulin inhibition of 5' adenosine monophosphate-activated protein kinase in the heart results in activation of acetyl coenzyme A carboxylase and inhibition of fatty acid oxidation. *Metabolism*. 46:1270-4.

Gao, X., and D. Pan. 2001. TSC1 and TSC2 tumor suppressors antagonize insulin signaling in cell growth. *Genes Dev*. 15:1383-92.

Gao, X., Y. Zhang, P. Arrazola, O. Hino, T. Kobayashi, R.S. Yeung, B. Ru, and D. Pan. 2002. Tsc tumour suppressor proteins antagonize amino-acid-TOR signalling. *Nat Cell Biol*. 4:699-704.

Gauthier, M.S., H. Miyoshi, S.C. Souza, J.M. Cacicedo, A.K. Saha, A.S. Greenberg, and N.B. Ruderman. 2008. AMP-activated protein kinase is activated as a consequence of lipolysis in the adipocyte: potential mechanism and physiological relevance. *J Biol Chem*. 283:16514-24.

George, S., J.J. Rochford, C. Wolfrum, S.L. Gray, S. Schinner, J.C. Wilson, M.A. Soos, P.R. Murgatroyd, R.M. Williams, C.L. Acerini, D.B. Dunger, D. Barford, A.M. Umpleby, N.J. Wareham, H.A. Davies, A.J. Schafer, M. Stoffel, S. O'Rahilly, and I. Barroso. 2004. A family with severe insulin resistance and diabetes due to a mutation in AKT2. *Science*. 304:1325-8.

Geraghty, K.M., S. Chen, J.E. Harthill, A.F. Ibrahim, R. Toth, N.A. Morrice, F. Vandermoere, G.B. Moorhead, D.G. Hardie, and C. MacKintosh. 2007. Regulation of multisite phosphorylation and 14-3-3 binding of AS160 in response to IGF-1, EGF, PMA and AICAR. *Biochem J*. 407:231-41.

Gimeno, R.E., and J. Cao. 2008. Thematic review series: glycerolipids. Mammalian glycerol-3-phosphate acyltransferases: new genes for an old activity. *J Lipid Res*. 49:2079-88.

Giri, S., R. Rattan, E. Haq, M. Khan, R. Yasmin, J.S. Won, L. Key, A.K. Singh, and I. Singh. 2006. AICAR inhibits adipocyte differentiation in 3T3L1 and restores metabolic alterations in diet-induced obesity mice model. *Nutr Metab (Lond)*. 3:31.

Gollob, M.H., M.S. Green, A.S. Tang, T. Gollob, A. Karibe, A.S. Ali Hassan, F. Ahmad, R. Lozado, G. Shah, L. Fananapazir, L.L. Bachinski, and R. Roberts. 2001. Identification of a gene responsible for familial Wolff-Parkinson-White syndrome. *N Engl J Med*. 344:1823-31.

Gollob, M.H., M.S. Green, A.S. Tang, and R. Roberts. 2002. PRKAG2 cardiac syndrome: familial ventricular preexcitation, conduction system disease, and cardiac hypertrophy. *Curr Opin Cardiol*. 17:229-34.

Goodyear, L.J., M.F. Hirshman, and E.S. Horton. 1991. Exercise-induced translocation of skeletal muscle glucose transporters. *Am J Physiol*. 261:E795-9.

Goodyear, L.J., P.A. King, M.F. Hirshman, C.M. Thompson, E.D. Horton, and E.S. Horton. 1990. Contractile activity increases plasma membrane glucose transporters in absence of insulin. *Am J Physiol*. 258:E667-72.

Goransson, O., A. McBride, S.A. Hawley, F.A. Ross, N. Shpiro, M. Foretz, B. Viollet, D.G. Hardie, and K. Sakamoto. 2007. Mechanism of action of A-769662, a valuable tool for activation of AMP-activated protein kinase. *J Biol Chem*. 282:32549-60.

Grau, G.E., and J. Lou. 1993. TNF in vascular pathology: the importance of platelet-endothelium interactions. *Res Immunol*. 144:355-63.

Green, E.D., M. Maffei, V.V. Braden, R. Proenca, U. DeSilva, Y. Zhang, S.C. Chua, Jr., R.L. Leibel, J. Weissenbach, and J.M. Friedman. 1995. The human obese (OB) gene: RNA expression pattern and mapping on the physical, cytogenetic, and genetic maps of chromosome 7. *Genome Res*. 5:5-12.

Green, H., and O. Kehinde. 1975. An established preadipose cell line and its differentiation in culture. II. Factors affecting the adipose conversion. *Cell*. 5:19-27.

Green, H., and O. Kehinde. 1976. Spontaneous heritable changes leading to increased adipose conversion in 3T3 cells. *Cell*. 7:105-13.

Green, H., and M. Meuth. 1974. An established pre-adipose cell line and its differentiation in culture. *Cell*. 3:127-33.

Griffin, M.E., M.J. Marcucci, G.W. Cline, K. Bell, N. Barucci, D. Lee, L.J. Goodyear, E.W. Kraegen, M.F. White, and G.I. Shulman. 1999. Free fatty acid-induced insulin resistance is associated with activation of protein kinase C theta and alterations in the insulin signaling cascade. *Diabetes*. 48:1270-4.

Grunfeld, C., and K.R. Feingold. 1991. The metabolic effects of tumor necrosis factor and other cytokines. *Biotherapy*. 3:143-58.

Gual, P., T. Gonzalez, T. Gremeaux, R. Barres, Y. Le Marchand-Brustel, and J.F. Tanti. 2003. Hyperosmotic stress inhibits insulin receptor substrate-1 function by distinct mechanisms in 3T3-L1 adipocytes. *J Biol Chem*. 278:26550-7.

Gual, P., S. Shigematsu, M. Kanzaki, T. Gremeaux, T. Gonzalez, J.E. Pessin, Y. Le Marchand-Brustel, and J.F. Tanti. 2002. A Crk-II/TC10 signaling pathway is required for osmotic shock-stimulated glucose transport. *J Biol Chem*. 277:43980-6.

Gunton, J.E., P.J. Delhanty, S. Takahashi, and R.C. Baxter. 2003. Metformin rapidly increases insulin receptor activation in human liver and signals preferentially through insulin-receptor substrate-2. *J Clin Endocrinol Metab*. 88:1323-32.

Ha, J., J.K. Lee, K.S. Kim, L.A. Witters, and K.H. Kim. 1996. Cloning of human acetyl-CoA carboxylase-beta and its unique features. *Proc Natl Acad Sci U S A*. 93:11466-70.

Habinowski, S.A., and L.A. Witters. 2001. The effects of AICAR on adipocyte differentiation of 3T3-L1 cells. *Biochem Biophys Res Commun*. 286:852-6.

Hanks, S.K., A.M. Quinn, and T. Hunter. 1988. The protein kinase family: conserved features and deduced phylogeny of the catalytic domains. *Science*. 241:42-52.

Hardie, D.G. 2004a. The AMP-activated protein kinase pathway--new players upstream and downstream. *J Cell Sci*. 117:5479-87.

Hardie, D.G. 2004b. AMP-activated protein kinase: the guardian of cardiac energy status. *J Clin Invest*. 114:465-8.

Hardie, D.G., D. Carling, and M. Carlson. 1998. The AMP-activated/SNF1 protein kinase subfamily: metabolic sensors of the eukaryotic cell? *Annu Rev Biochem*. 67:821-55.

Hardie, D.G., and S.A. Hawley. 2001. AMP-activated protein kinase: the energy charge hypothesis revisited. *Bioessays*. 23:1112-9.

Hardie, D.G., I.P. Salt, S.A. Hawley, and S.P. Davies. 1999. AMP-activated protein kinase: an ultrasensitive system for monitoring cellular energy charge. *Biochem J*. 338 (Pt 3):717-22.

Hardie, D.G., J.W. Scott, D.A. Pan, and E.R. Hudson. 2003. Management of cellular energy by the AMP-activated protein kinase system. *FEBS Lett*. 546:113-20.

Hawley, S.A., J. Boudeau, J.L. Reid, K.J. Mustard, L. Udd, T.P. Makela, D.R. Alessi, and D.G. Hardie. 2003. Complexes between the LKB1 tumor suppressor, STRAD alpha/beta and MO25 alpha/beta are upstream kinases in the AMP-activated protein kinase cascade. *J Biol*. 2:28.

Hawley, S.A., M. Davison, A. Woods, S.P. Davies, R.K. Beri, D. Carling, and D.G. Hardie. 1996. Characterization of the AMP-activated protein kinase kinase from rat liver and identification of threonine 172 as the major site at which it phosphorylates AMP-activated protein kinase. *J Biol Chem*. 271:27879-87.

Hawley, S.A., A.E. Gadalla, G.S. Olsen, and D.G. Hardie. 2002. The antidiabetic drug metformin activates the AMP-activated protein kinase cascade via an adenine nucleotide-independent mechanism. *Diabetes*. 51:2420-5.

Hawley, S.A., D.A. Pan, K.J. Mustard, L. Ross, J. Bain, A.M. Edelman, B.G. Frenguelli, and D.G. Hardie. 2005. Calmodulin-dependent protein kinase kinase-beta is an alternative upstream kinase for AMP-activated protein kinase. *Cell Metab*. 2:9-19.

Hawley, S.A., M.A. Selbert, E.G. Goldstein, A.M. Edelman, D. Carling, and D.G. Hardie. 1995. 5'-AMP activates the AMP-activated protein kinase cascade, and Ca2+/calmodulin activates the calmodulin-dependent protein kinase I cascade, via three independent mechanisms. *J Biol Chem*. 270:27186-91.

Hayashi, T., M.F. Hirshman, N. Fujii, S.A. Habinowski, L.A. Witters, and L.J. Goodyear. 2000. Metabolic stress and altered glucose transport: activation of AMP-activated protein kinase as a unifying coupling mechanism. *Diabetes*. 49:527-31.

Hayashi, T., M.F. Hirshman, E.J. Kurth, W.W. Winder, and L.J. Goodyear. 1998. Evidence for 5' AMP-activated protein kinase mediation of the effect of muscle contraction on glucose transport. *Diabetes*. 47:1369-73.

Hayashi, T., J.F. Wojtaszewski, and L.J. Goodyear. 1997. Exercise regulation of glucose transport in skeletal muscle. *Am J Physiol*. 273:E1039-51.

Heid, H.W., R. Moll, I. Schwetlick, H.R. Rackwitz, and T.W. Keenan. 1998. Adipophilin is a specific marker of lipid accumulation in diverse cell types and diseases. *Cell Tissue Res*. 294:309-21.

Hemminki, A. 1999. The molecular basis and clinical aspects of Peutz-Jeghers syndrome. *Cell Mol Life Sci*. 55:735-50.

Holm, C. 2003. Molecular mechanisms regulating hormone-sensitive lipase and lipolysis. *Biochem Soc Trans*. 31:1120-4.

Holm, C., T. Osterlund, H. Laurell, and J.A. Contreras. 2000. Molecular mechanisms regulating hormone-sensitive lipase and lipolysis. *Annu Rev Nutr*. 20:365-93.

Holmes, B.F., E.J. Kurth-Kraczek, and W.W. Winder. 1999. Chronic activation of 5'-AMP-activated protein kinase increases GLUT-4, hexokinase, and glycogen in muscle. *J Appl Physiol*. 87:1990-5.

Hong, S.P., F.C. Leiper, A. Woods, D. Carling, and M. Carlson. 2003. Activation of yeast Snf1 and mammalian AMP-activated protein kinase by upstream kinases. *Proc Natl Acad Sci U S A*. 100:8839-43.

Horman, S., G. Browne, U. Krause, J. Patel, D. Vertommen, L. Bertrand, A. Lavoinne, L. Hue, C. Proud, and M. Rider. 2002. Activation of AMP-activated protein kinase leads to the phosphorylation of elongation factor 2 and an inhibition of protein synthesis. *Curr Biol*. 12:1419-23.

Horton, J.D., and I. Shimomura. 1999. Sterol regulatory element-binding proteins: activators of cholesterol and fatty acid biosynthesis. *Curr Opin Lipidol*. 10:143-50.

Hotamisligil, G.S. 1999. The role of TNFalpha and TNF receptors in obesity and insulin resistance. *J Intern Med*. 245:621-5.

Hotamisligil, G.S. 2003. Inflammatory pathways and insulin action. *Int J Obes Relat Metab Disord*. 27 Suppl 3:S53-5.

Hotamisligil, G.S., N.S. Shargill, and B.M. Spiegelman. 1993. Adipose expression of tumor necrosis factor-alpha: direct role in obesity-linked insulin resistance. *Science*. 259:87-91.

Hou, J.C., and J.E. Pessin. 2007. Ins (endocytosis) and outs (exocytosis) of GLUT4 trafficking. *Curr Opin Cell Biol*. 19:466-73.

Hresko, R.C., and M. Mueckler. 2005. mTOR.RICTOR is the Ser473 kinase for Akt/protein kinase B in 3T3-L1 adipocytes. *J Biol Chem*. 280:40406-16.

Hubbard, M.J., and P. Cohen. 1993. On target with a new mechanism for the regulation of protein phosphorylation. *Trends Biochem Sci*. 18:172-7.

Hudson, E.R., D.A. Pan, J. James, J.M. Lucocq, S.A. Hawley, K.A. Green, O. Baba, T. Terashima, and D.G. Hardie. 2003. A novel domain in AMP-activated protein kinase causes glycogen storage bodies similar to those seen in hereditary cardiac arrhythmias. *Curr Biol*. 13:861-6.

Hundal, H.S., T. Ramlal, R. Reyes, L.A. Leiter, and A. Klip. 1992. Cellular mechanism of metformin action involves glucose transporter translocation from an intracellular pool to the plasma membrane in L6 muscle cells. *Endocrinology*. 131:1165-73.

Hundal, R.S., M. Krssak, S. Dufour, D. Laurent, V. Lebon, V. Chandramouli, S.E. Inzucchi, W.C. Schumann, K.F. Petersen, B.R. Landau, and G.I. Shulman. 2000. Mechanism by which metformin reduces glucose production in type 2 diabetes. *Diabetes*. 49:2063-9.

Hurley R.L., K.A. Anderson, J.M Franzone, B.E Kemp, A.R Means, L.A Witters. 2005. The Ca2+/calmodulin-dependent protein kinase kinases are AMP-activated protein kinase kinases. *J Biol Chem*. 280:29060–66.

Hutber, C.A., D.G. Hardie, and W.W. Winder. 1997. Electrical stimulation inactivates muscle acetyl-CoA carboxylase and increases AMP-activated protein kinase. *Am J Physiol*. 272:E262-6.

Huypens, P., E. Quartier, D. Pipeleers, and M. Van de Casteele. 2005. Metformin reduces adiponectin protein expression and release in 3T3-L1 adipocytes involving activation of AMP activated protein kinase. *Eur J Pharmacol*. 518:90-5.

Hwa, J.J., L. Ghibaudi, J. Gao, and E.M. Parker. 2001. Central melanocortin system modulates energy intake and expenditure of obese and lean Zucker rats. *Am J Physiol Regul Integr Comp Physiol*. 281:R444-51.

Ibanez, L., K. Ong, C. Valls, M.V. Marcos, D.B. Dunger, and F. de Zegher. 2006. Metformin treatment to prevent early puberty in girls with precocious pubarche. *J Clin Endocrinol Metab*. 91:2888-91.

Imamura, K., T. Ogura, A. Kishimoto, M. Kaminishi, and H. Esumi. 2001. Cell cycle regulation via p53 phosphorylation by a 5'-AMP activated protein kinase activator, 5-aminoimidazole- 4-carboxamide-1-beta-D-ribofuranoside, in a human hepatocellular carcinoma cell line. *Biochem Biophys Res Commun*. 287:562-7.

Inoki, K., T. Zhu, and K.L. Guan. 2003. TSC2 mediates cellular energy response to control cell growth and survival. *Cell*. 115:577-90.

Iwaki, M., M. Matsuda, N. Maeda, T. Funahashi, Y. Matsuzawa, M. Makishima, and I. Shimomura. 2003. Induction of adiponectin, a fat-derived antidiabetic and antiatherogenic factor, by nuclear receptors. *Diabetes*. 52:1655-63.

Jakobsen, S.N., D.G. Hardie, N. Morrice, and H.E. Tornqvist. 2001. 5'-AMP-activated protein kinase phosphorylates IRS-1 on Ser-789 in mouse C2C12 myotubes in response to 5-aminoimidazole-4-carboxamide riboside. *J Biol Chem*. 276:46912-6.

James, D.J., F. Cairns, I.P. Salt, G.J. Murphy, A.F. Dominiczak, J.M. Connell, and G.W. Gould. 2001. Skeletal muscle of stroke-prone spontaneously hypertensive rats exhibits reduced insulin-stimulated glucose transport and elevated levels of caveolin and flotillin. *Diabetes*. 50:2148-56.

Janez, A., D.S. Worrall, T. Imamura, P.M. Sharma, and J.M. Olefsky. 2000. The osmotic shock-induced glucose transport pathway in 3T3-L1 adipocytes is mediated by gab-1 and requires Gab-1-associated phosphatidylinositol 3-kinase activity for full activation. *J Biol Chem*. 275:26870-6.

Jenne, D.E., H. Reimann, J. Nezu, W. Friedel, S. Loff, R. Jeschke, O. Muller, W. Back, and M. Zimmer. 1998. Peutz-Jeghers syndrome is caused by mutations in a novel serine threonine kinase. *Nat Genet*. 18:38-43.

Jensen, T.E., A.J. Rose, S.B. Jorgensen, N. Brandt, P. Schjerling, J.F. Wojtaszewski, and E.A. Richter. 2007. Possible CaMKK-dependent regulation of AMPK phosphorylation and

glucose uptake at the onset of mild tetanic skeletal muscle contraction. *Am J Physiol Endocrinol Metab*. 292:E1308-17.

Jiang, R., and M. Carlson. 1997. The Snf1 protein kinase and its activating subunit, Snf4, interact with distinct domains of the Sip1/Sip2/Gal83 component in the kinase complex. *Mol Cell Biol*. 17:2099-106.

Jiang, Z.Y., Q.L. Zhou, K.A. Coleman, M. Chouinard, Q. Boese, and M.P. Czech. 2003. Insulin signaling through Akt/protein kinase B analyzed by small interfering RNA-mediated gene silencing. *Proc Natl Acad Sci U S A*. 100:7569-74.

Jones, B.H., M.K. Standridge, J.W. Taylor, and N. Moustaid. 1997. Angiotensinogen gene expression in adipose tissue: analysis of obese models and hormonal and nutritional control. *Am J Physiol*. 273:R236-42.

Joost, H.G., T.M. Weber, S.W. Cushman, and I.A. Simpson. 1986. Insulin-stimulated glucose transport in rat adipose cells. Modulation of transporter intrinsic activity by isoproterenol and adenosine. *J Biol Chem*. 261:10033-6.

Jorgensen, S.B., B. Viollet, F. Andreelli, C. Frosig, J.B. Birk, P. Schjerling, S. Vaulont, E.A. Richter, and J.F. Wojtaszewski. 2004. Knockout of the alpha2 but not alpha1 5'-AMP-activated protein kinase isoform abolishes 5-aminoimidazole-4-carboxamide-1-beta-4-ribofuranosidebut not contraction-induced glucose uptake in skeletal muscle. *J Biol Chem*. 279:1070-9.

Kanda, H., Y. Tamori, H. Shinoda, M. Yoshikawa, M. Sakaue, J. Udagawa, H. Otani, F. Tashiro, J. Miyazaki, and M. Kasuga. 2005. Adipocytes from Munc18c-null mice show increased sensitivity to insulin-stimulated GLUT4 externalization. *J Clin Invest*. 115:291-301.

Kane, S., H. Sano, S.C. Liu, J.M. Asara, W.S. Lane, C.C. Garner, and G.E. Lienhard. 2002. A method to identify serine kinase substrates. Akt phosphorylates a novel adipocyte protein with a Rab GTPase-activating protein (GAP) domain. *J Biol Chem*. 277:22115-8.

Kashiwagi, A., T.P. Huecksteadt, and J.E. Foley. 1983. The regulation of glucose transport by cAMP stimulators via three different mechanisms in rat and human adipocytes. *J Biol Chem*. 258:13685-92.

Kemp, B.E. 2004. Bateman domains and adenosine derivatives form a binding contract. *J Clin Invest*. 113:182-4.

Kemp, B.E., D. Stapleton, D.J. Campbell, Z.P. Chen, S. Murthy, M. Walter, A. Gupta, J.J. Adams, F. Katsis, B. van Denderen, I.G. Jennings, T. Iseli, B.J. Michell, and L.A. Witters. 2003. AMP-activated protein kinase, super metabolic regulator. *Biochem Soc Trans*. 31:162-8.

Kennedy, H.J., A.E. Pouli, E.K. Ainscow, L.S. Jouaville, R. Rizzuto, and G.A. Rutter. 1999. Glucose generates sub-plasma membrane ATP microdomains in single islet beta-cells. Potential role for strategically located mitochondria. *J Biol Chem*. 274:13281-91.

Kern, P.A., M. Saghizadeh, J.M. Ong, R.J. Bosch, R. Deem, and R.B. Simsolo. 1995. The expression of tumor necrosis factor in human adipose tissue. Regulation by obesity, weight loss, and relationship to lipoprotein lipase. *J Clin Invest*. 95:2111-9.

Kersten, S. 2001. Mechanisms of nutritional and hormonal regulation of lipogenesis. *EMBO Rep*. 2:282-6.

Kersten, S., S. Mandard, N.S. Tan, P. Escher, D. Metzger, P. Chambon, F.J. Gonzalez, B. Desvergne, and W. Wahli. 2000. Characterization of the fasting-induced adipose factor FIAF, a novel peroxisome proliferator-activated receptor target gene. *J Biol Chem*. 275:28488-93.

Kim, K.H., F. Lopez-Casillas, D.H. Bai, X. Luo, and M.E. Pape. 1989. Role of reversible phosphorylation of acetyl-CoA carboxylase in long-chain fatty acid synthesis. *Faseb J*. 3:2250-6.

Kim, K.H., M.J. Song, E.J. Yoo, S.S. Choe, S.D. Park, and J.B. Kim. 2004. Regulatory role of glycogen synthase kinase 3 for transcriptional activity of ADD1/SREBP1c. *J Biol Chem*. 279:51999-2006.

Kim, Y.D., K.G. Park, Y.S. Lee, Y.Y. Park, D.K. Kim, B. Nedumaran, W.G. Jang, W.J. Cho, J. Ha, I.K. Lee, C.H. Lee, and H.S. Choi. 2008. Metformin inhibits hepatic gluconeogenesis through AMP-activated protein kinase-dependent regulation of the orphan nuclear receptor SHP. *Diabetes*. 57:306-14.

Kirpichnikov, D., S.I. McFarlane, and J.R. Sowers. 2002. Metformin: an update. *Ann Intern Med*. 137:25-33.

Kirsch, D.M., M. Baumgarten, T. Deufel, F. Rinninger, W. Kemmler, and H.U. Haring. 1983. Catecholamine-induced insulin resistance of glucose transport in isolated rat adipocytes. *Biochem J*. 216:737-45.

Klein, J., S. Westphal, D. Kraus, B. Meier, N. Perwitz, V. Ott, M. Fasshauer, and H.H. Klein. 2004. Metformin inhibits leptin secretion via a mitogen-activated protein kinase signalling pathway in brown adipocytes. *J Endocrinol*. 183:299-307.

Klip, A., T. Ramlal, and E.J. Cragoe, Jr. 1986. Insulin-induced cytoplasmic alkalinization and glucose transport in muscle cells. *Am J Physiol*. 250:C720-8.

Klip, A., T. Ramlal, and U.M. Koivisto. 1988. Stimulation of Na+/H+ exchange by insulin and phorbol ester during differentiation of 3T3-L1 cells. Relation to hexose uptake. *Endocrinology*. 123:296-304.

Knighton, D.R., J.H. Zheng, L.F. Ten Eyck, V.A. Ashford, N.H. Xuong, S.S. Taylor, and J.M. Sowadski. 1991. Crystal structure of the catalytic subunit of cyclic adenosine monophosphate-dependent protein kinase. *Science*. 253:407-14.

Koh, H.J., M.F. Hirshman, H. He, Y. Li, Y. Manabe, J.A. Balschi, and L.J. Goodyear. 2007. Adrenaline is a critical mediator of acute exercise-induced AMP-activated protein kinase activation in adipocytes. *Biochem J*. 403:473-81.

Kola, B., M. Christ-Crain, F. Lolli, G. Arnaldi, G. Giacchetti, M. Boscaro, A.B. Grossman, and M. Korbonits. 2008. Changes in adenosine 5'-monophosphate-activated protein kinase as a mechanism of visceral obesity in Cushing's syndrome. *J Clin Endocrinol Metab*. 93:4969-73.

Komjati, M., G. Kastner, W. Waldhausl, and P. Bratusch-Marrain. 1988. Detrimental effect of hyperosmolality on insulin-stimulated glucose metabolism in adipose and muscle tissue in vitro. *Biochem Med Metab Biol*. 39:312-8.

Kresge, N., R.D. Simoni, and R.L. Hill. 2005. Reversible Phosphorylation and Kinase Cascades: the Work of Edwin G. Krebs. *J. Biol. Chem.* 280:e40-.

Kudo, N., A.J. Barr, R.L. Barr, S. Desai, and G.D. Lopaschuk. 1995. High rates of fatty acid oxidation during reperfusion of ischemic hearts are associated with a decrease in malonyl-CoA levels due to an increase in 5'-AMP-activated protein kinase inhibition of acetyl-CoA carboxylase. *J Biol Chem*. 270:17513-20.

Kumar, N., and C.S. Dey. 2002. Metformin enhances insulin signalling in insulin-dependent and-independent pathways in insulin resistant muscle cells. *Br J Pharmacol*. 137:329-36.

Kurth-Kraczek, E.J., M.F. Hirshman, L.J. Goodyear, and W.W. Winder. 1999. 5' AMP-activated protein kinase activation causes GLUT4 translocation in skeletal muscle. *Diabetes*. 48:1667-71.

Larance, M., G. Ramm, J. Stockli, E.M. van Dam, S. Winata, V. Wasinger, F. Simpson, M. Graham, J.R. Junutula, M. Guilhaus, and D.E. James. 2005. Characterization of the role of the Rab GTPase-activating protein AS160 in insulin-regulated GLUT4 trafficking. *J Biol Chem*. 280:37803-13.

Lee, J., and P.F. Pilch. 1994. The insulin receptor: structure, function, and signaling. *Am J Physiol*. 266:C319-34.

Leff, T. 2003. AMP-activated protein kinase regulates gene expression by direct phosphorylation of nuclear proteins. *Biochem Soc Trans*. 31:224-7.

Lihn, A.S., N. Jessen, S.B. Pedersen, S. Lund, and B. Richelsen. 2004. AICAR stimulates adiponectin and inhibits cytokines in adipose tissue. *Biochem Biophys Res Commun*. 316:853-8.

Lindsay, R.S., T. Funahashi, R.L. Hanson, Y. Matsuzawa, S. Tanaka, P.A. Tataranni, W.C. Knowler, and J. Krakoff. 2002. Adiponectin and development of type 2 diabetes in the Pima Indian population. *Lancet*. 360:57-8.

Lizcano, J.M., O. Goransson, R. Toth, M. Deak, N.A. Morrice, J. Boudeau, S.A. Hawley, L. Udd, T.P. Makela, D.G. Hardie, and D.R. Alessi. 2004. LKB1 is a master kinase that activates 13 kinases of the AMPK subfamily, including MARK/PAR-1. *Embo J*. 23:833-43.

Lochhead, P.A., I.P. Salt, K.S. Walker, D.G. Hardie, and C. Sutherland. 2000. 5-aminoimidazole-4-carboxamide riboside mimics the effects of insulin on the expression of the 2 key gluconeogenic genes PEPCK and glucose-6-phosphatase. *Diabetes*. 49:896-903.

Londos, C., D.L. Brasaemle, C.J. Schultz, J.P. Segrest, and A.R. Kimmel. 1999. Perilipins, ADRP, and other proteins that associate with intracellular neutral lipid droplets in animal cells. *Semin Cell Dev Biol*. 10:51-8.

Lord, G.M., G. Matarese, J.K. Howard, R.J. Baker, S.R. Bloom, and R.I. Lechler. 1998. Leptin modulates the T-cell immune response and reverses starvation-induced immunosuppression. *Nature*. 394:897-901.

Lord, J.M., I.H. Flight, and R.J. Norman. 2003. Metformin in polycystic ovary syndrome: systematic review and meta-analysis. *Bmj*. 327:951-3.

Lowe, E.D., M.E. Noble, V.T. Skamnaki, N.G. Oikonomakos, D.J. Owen, and L.N. Johnson. 1997. The crystal structure of a phosphorylase kinase peptide substrate complex: kinase substrate recognition. *Embo J*. 16:6646-58.

Luiken, J.J., S.L. Coort, J. Willems, W.A. Coumans, A. Bonen, G.J. van der Vusse, and J.F. Glatz. 2003. Contraction-induced fatty acid translocase/CD36 translocation in rat cardiac myocytes is mediated through AMP-activated protein kinase signaling. *Diabetes*. 52:1627-34.

Lund, S., G.D. Holman, O. Schmitz, and O. Pedersen. 1995. Contraction stimulates translocation of glucose transporter GLUT4 in skeletal muscle through a mechanism distinct from that of insulin. *Proc Natl Acad Sci U S A*. 92:5817-21.

Luo, B., G.J. Parker, R.C. Cooksey, Y. Soesanto, M. Evans, D. Jones, and D.A. McClain. 2007. Chronic hexosamine flux stimulates fatty acid oxidation by activating AMP-activated protein kinase in adipocytes. *J Biol Chem*. 282:7172-80.

Lupi, R., F. Dotta, L. Marselli, S. Del Guerra, M. Masini, C. Santangelo, G. Patane, U. Boggi, S. Piro, M. Anello, E. Bergamini, F. Mosca, U. Di Mario, S. Del Prato, and P. Marchetti. 2002. Prolonged exposure to free fatty acids has cytostatic and pro-apoptotic effects on human pancreatic islets: evidence that beta-cell death is caspase mediated, partially dependent on ceramide pathway, and Bcl-2 regulated. *Diabetes*. 51:1437-42.

Maeda, N., I. Shimomura, K. Kishida, H. Nishizawa, M. Matsuda, H. Nagaretani, N. Furuyama, H. Kondo, M. Takahashi, Y. Arita, R. Komuro, N. Ouchi, S. Kihara, Y. Tochino, K. Okutomi, M. Horie, S. Takeda, T. Aoyama, T. Funahashi, and Y. Matsuzawa. 2002. Diet-induced insulin resistance in mice lacking adiponectin/ACRP30. *Nat Med*. 8:731-7.

Maffei, M., J. Halaas, E. Ravussin, R.E. Pratley, G.H. Lee, Y. Zhang, H. Fei, S. Kim, R. Lallone, S. Ranganathan, and et al. 1995. Leptin levels in human and rodent: measurement of plasma leptin and ob RNA in obese and weight-reduced subjects. *Nat Med*. 1:1155-61.

Mahlapuu, M., C. Johansson, K. Lindgren, G. Hjalm, B.R. Barnes, A. Krook, J.R. Zierath, L. Andersson, and S. Marklund. 2004. Expression profiling of the gamma-subunit isoforms of AMP-activated protein kinase suggests a major role for gamma3 in white skeletal muscle. *Am J Physiol Endocrinol Metab*. 286:E194-200.

Manne, J., A.C. Argeson, and L.D. Siracusa. 1995. Mechanisms for the pleiotropic effects of the agouti gene. *Proc Natl Acad Sci U S A*. 92:4721-4.

Manning, G., D.B. Whyte, R. Martinez, T. Hunter, and S. Sudarsanam. 2002. The protein kinase complement of the human genome. *Science*. 298:1912-34.

Marchesini, G., M. Brizi, G. Bianchi, S. Tomassetti, M. Zoli, and N. Melchionda. 2001. Metformin in non-alcoholic steatohepatitis. *Lancet*. 358:893-4.

Marino, E., and S.T. Grey. 2008. A new role for an old player: do B cells unleash the self-reactive CD8+ T cell storm necessary for the development of type 1 diabetes? *J Autoimmun*. 31:301-5.

Marsin, A.S., L. Bertrand, M.H. Rider, J. Deprez, C. Beauloye, M.F. Vincent, G. Van den Berghe, D. Carling, and L. Hue. 2000. Phosphorylation and activation of heart PFK-2 by AMPK has a role in the stimulation of glycolysis during ischaemia. *Curr Biol*. 10:1247-55.

Maslowska, M., T. Scantlebury, R. Germinario, and K. Cianflone. 1997. Acute in vitro production of acylation stimulating protein in differentiated human adipocytes. *J Lipid Res*. 38:1-11.

Matejkova, O., K.J. Mustard, J. Sponarova, P. Flachs, M. Rossmeisl, I. Miksik, M. Thomason-Hughes, D. Grahame Hardie, and J. Kopecky. 2004. Possible involvement of

AMP-activated protein kinase in obesity resistance induced by respiratory uncoupling in white fat. *FEBS Lett*. 569:245-8.

Matthaei, S., A. Hamann, H.H. Klein, H. Benecke, G. Kreymann, J.S. Flier, and H. Greten. 1991. Association of Metformin's effect to increase insulin-stimulated glucose transport with potentiation of insulin-induced translocation of glucose transporters from intracellular pool to plasma membrane in rat adipocytes. *Diabetes*. 40:850-7.

Matthaei, S., J.P. Reibold, A. Hamann, H. Benecke, H.U. Haring, H. Greten, and H.H. Klein. 1993. In vivo metformin treatment ameliorates insulin resistance: evidence for potentiation of insulin-induced translocation and increased functional activity of glucose transporters in obese (fa/fa) Zucker rat adipocytes. *Endocrinology*. 133:304-11.

McBride, A., S. Ghilagaber, A. Nikolaev, and D.G. Hardie. 2009. The glycogen-binding domain on the AMPK beta subunit allows the kinase to act as a glycogen sensor. *Cell Metab*. 9:23-34.

McGarry, J.D. 1995. The mitochondrial carnitine palmitoyltransferase system: its broadening role in fuel homoeostasis and new insights into its molecular features. *Biochem Soc Trans*. 23:321-4.

McGee, S.L., K.J. Mustard, D.G. Hardie, and K. Baar. 2008. Normal hypertrophy accompanied by phosphoryation and activation of AMP-activated protein kinase alpha1 following overload in LKB1 knockout mice. *J Physiol*. 586:1731-41.

McKinney, T.D., and M.A. Hosford. 1992. Organic cation transport by rat hepatocyte basolateral membrane vesicles. *Am J Physiol*. 263:G939-46.

Merrill, G.F., E.J. Kurth, D.G. Hardie, and W.W. Winder. 1997. AICA riboside increases AMP-activated protein kinase, fatty acid oxidation, and glucose uptake in rat muscle. *Am J Physiol*. 273:E1107-12.

Meyre, D., M. Farge, C. Lecoeur, C. Proenca, E. Durand, F. Allegaert, J. Tichet, M. Marre, B. Balkau, J. Weill, J. Delplanque, and P. Froguel. 2008. R125W coding variant in TBC1D1 confers risk for familial obesity and contributes to linkage on chromosome 4p14 in the French population. *Hum Mol Genet*. 17:1798-802.

Miinea, C.P., H. Sano, S. Kane, E. Sano, M. Fukuda, J. Peranen, W.S. Lane, and G.E. Lienhard. 2005. AS160, the Akt substrate regulating GLUT4 translocation, has a functional Rab GTPase-activating protein domain. *Biochem J*. 391:87-93.

Min, J., S. Okada, M. Kanzaki, J.S. Elmendorf, K.J. Coker, B.P. Ceresa, L.J. Syu, Y. Noda, A.R. Saltiel, and J.E. Pessin. 1999. Synip: a novel insulin-regulated syntaxin 4-binding protein mediating GLUT4 translocation in adipocytes. *Mol Cell*. 3:751-60.

Minokoshi, Y., T. Alquier, N. Furukawa, Y.B. Kim, A. Lee, B. Xue, J. Mu, F. Foufelle, P. Ferre, M.J. Birnbaum, B.J. Stuck, and B.B. Kahn. 2004. AMP-kinase regulates food intake by responding to hormonal and nutrient signals in the hypothalamus. *Nature*. 428:569-74.

Minokoshi, Y., Y.B. Kim, O.D. Peroni, L.G. Fryer, C. Muller, D. Carling, and B.B. Kahn. 2002. Leptin stimulates fatty-acid oxidation by activating AMP-activated protein kinase. *Nature*. 415:339-43.

Mizuarai, S., S. Miki, H. Araki, K. Takahashi, and H. Kotani. 2005. Identification of dicarboxylate carrier Slc25a10 as malate transporter in de novo fatty acid synthesis. *J Biol Chem*. 280:32434-41.

Mohamed-Ali, V., S. Goodrick, A. Rawesh, D.R. Katz, J.M. Miles, J.S. Yudkin, S. Klein, and S.W. Coppack. 1997. Subcutaneous adipose tissue releases interleukin-6, but not tumor necrosis factor-alpha, in vivo. *In* J Clin Endocrinol Metab. Vol. 82. 4196-200.

Mokdad, A.H., E.S. Ford, B.A. Bowman, W.H. Dietz, F. Vinicor, V.S. Bales, and J.S. Marks. 2003. Prevalence of obesity, diabetes, and obesity-related health risk factors, 2001. *Jama*. 289:76-9.

Momcilovic, M., S.P. Hong, and M. Carlson. 2006. Mammalian TAK1 activates Snf1 protein kinase in yeast and phosphorylates AMP-activated protein kinase in vitro. *J Biol Chem*. 281:25336-43.

Montague, C.T., I.S. Farooqi, J.P. Whitehead, M.A. Soos, H. Rau, N.J. Wareham, C.P. Sewter, J.E. Digby, S.N. Mohammed, J.A. Hurst, C.H. Cheetham, A.R. Earley, A.H. Barnett, J.B. Prins, and S. O'Rahilly. 1997. Congenital leptin deficiency is associated with severe early-onset obesity in humans. *Nature*. 387:903-8.

Moorhead, G.B., L. Trinkle-Mulcahy, and A. Ulke-Lemee. 2007. Emerging roles of nuclear protein phosphatases. *Nat Rev Mol Cell Biol*. 8:234-44.

Moule, S.K., and R.M. Denton. 1998. The activation of p38 MAPK by the beta-adrenergic agonist isoproterenol in rat epididymal fat cells. *FEBS Lett*. 439:287-90.

Moule, S.K., G.I. Welsh, N.J. Edgell, E.J. Foulstone, C.G. Proud, and R.M. Denton. 1997. Regulation of protein kinase B and glycogen synthase kinase-3 by insulin and beta-adrenergic agonists in rat epididymal fat cells. Activation of protein kinase B by wortmannin-sensitive and -insensitive mechanisms. *J Biol Chem*. 272:7713-9.

Mu, J., J.T. Brozinick, Jr., O. Valladares, M. Bucan, and M.J. Birnbaum. 2001. A role for AMP-activated protein kinase in contraction- and hypoxia-regulated glucose transport in skeletal muscle. *Mol Cell*. 7:1085-94.

Munday, M.R., D.G. Campbell, D. Carling, and D.G. Hardie. 1988. Identification by amino acid sequencing of three major regulatory phosphorylation sites on rat acetyl-CoA carboxylase. *Eur J Biochem*. 175:331-8.

Musi, N., M.F. Hirshman, J. Nygren, M. Svanfeldt, P. Bavenholm, O. Rooyackers, G. Zhou, J.M. Williamson, O. Ljunqvist, S. Efendic, D.E. Moller, A. Thorell, and L.J. Goodyear. 2002. Metformin increases AMP-activated protein kinase activity in skeletal muscle of subjects with type 2 diabetes. *Diabetes*. 51:2074-81.

Newgard, C.B., and J.D. McGarry. 1995. Metabolic coupling factors in pancreatic beta-cell signal transduction. *Annu Rev Biochem*. 64:689-719.

Newton, A.C. 1995. Protein kinase C: structure, function, and regulation. *J Biol Chem*. 270:28495-8.

Nonogaki, K., G.M. Fuller, N.L. Fuentes, A.H. Moser, I. Staprans, C. Grunfeld, and K.R. Feingold. 1995. Interleukin-6 stimulates hepatic triglyceride secretion in rats. *Endocrinology*. 136:2143-9.

Ofei, F., S. Hurel, J. Newkirk, M. Sopwith, and R. Taylor. 1996. Effects of an engineered human anti-TNF-alpha antibody (CDP571) on insulin sensitivity and glycemic control in patients with NIDDM. *Diabetes*. 45:881-5.

Ojuka, E.O., L.A. Nolte, and J.O. Holloszy. 2000. Increased expression of GLUT-4 and hexokinase in rat epitrochlearis muscles exposed to AICAR in vitro. *J Appl Physiol*. 88:1072-5.

Okuno, A., H. Tamemoto, K. Tobe, K. Ueki, Y. Mori, K. Iwamoto, K. Umesono, Y. Akanuma, T. Fujiwara, H. Horikoshi, Y. Yazaki, and T. Kadowaki. 1998. Troglitazone increases the number of small adipocytes without the change of white adipose tissue mass in obese Zucker rats. *J Clin Invest*. 101:1354-61.

Olson, A.L., J.B. Knight, and J.E. Pessin. 1997. Syntaxin 4, VAMP2, and/or VAMP3/cellubrevin are functional target membrane and vesicle SNAP receptors for insulin-stimulated GLUT4 translocation in adipocytes. *Mol Cell Biol*. 17:2425-35.

Orci, L., W.S. Cook, M. Ravazzola, M.Y. Wang, B.H. Park, R. Montesano, and R.H. Unger. 2004. Rapid transformation of white adipocytes into fat-oxidizing machines. *Proc Natl Acad Sci U S A*. 101:2058-63.

Ouchi, N., S. Kihara, Y. Arita, K. Maeda, H. Kuriyama, Y. Okamoto, K. Hotta, M. Nishida, M. Takahashi, T. Nakamura, S. Yamashita, T. Funahashi, and Y. Matsuzawa. 1999. Novel modulator for endothelial adhesion molecules: adipocyte-derived plasma protein adiponectin. *Circulation*. 100:2473-6.

Owen, M.R., E. Doran, and A.P. Halestrap. 2000. Evidence that metformin exerts its anti-diabetic effects through inhibition of complex 1 of the mitochondrial respiratory chain. *Biochem J*. 348 Pt 3:607-14.

Pagano, G., M. Cassader, P. Cavallo-Perin, A. Bruno, P. Masciola, A. Ozzello, A.M. Dall'Omo, and A. Foco. 1984. Insulin resistance in the aged: a quantitative evaluation of in vivo insulin sensitivity and in vitro glucose transport. *Metabolism*. 33:976-81.

Pajvani, U.B., X. Du, T.P. Combs, A.H. Berg, M.W. Rajala, T. Schulthess, J. Engel, M. Brownlee, and P.E. Scherer. 2003. Structure-function studies of the adipocyte-secreted hormone Acrp30/adiponectin. Implications fpr metabolic regulation and bioactivity. *J Biol Chem*. 278:9073-85.

Park, S.H., S.R. Gammon, J.D. Knippers, S.R. Paulsen, D.S. Rubink, and W.W. Winder. 2002. Phosphorylation-activity relationships of AMPK and acetyl-CoA carboxylase in muscle. *J Appl Physiol*. 92:2475-82.

Patel, M.S., and T.E. Roche. 1990. Molecular biology and biochemistry of pyruvate dehydrogenase complexes. *Faseb J*. 4:3224-33.

Peak, M., M. al-Habori, and L. Agius. 1992. Regulation of glycogen synthesis and glycolysis by insulin, pH and cell volume. Interactions between swelling and alkalinization in mediating the effects of insulin. *Biochem J*. 282 (Pt 3):797-805.

Phillips, S.A., T.P. Ciaraldi, A.P. Kong, R. Bandukwala, V. Aroda, L. Carter, S. Baxi, S.R. Mudaliar, and R.R. Henry. 2003. Modulation of circulating and adipose tissue adiponectin levels by antidiabetic therapy. *Diabetes*. 52:667-74.

Polekhina, G., A. Gupta, B.J. Michell, B. van Denderen, S. Murthy, S.C. Feil, I.G. Jennings, D.J. Campbell, L.A. Witters, M.W. Parker, B.E. Kemp, and D. Stapleton. 2003. AMPK beta subunit targets metabolic stress sensing to glycogen. *Curr Biol*. 13:867-71.

Prentki, M., and B.E. Corkey. 1996. Are the beta-cell signaling molecules malonyl-CoA and cystolic long-chain acyl-CoA implicated in multiple tissue defects of obesity and NIDDM? *Diabetes*. 45:273-83.

Proctor, K.M., S.C. Miller, N.J. Bryant, and G.W. Gould. 2006. Syntaxin 16 controls the intracellular sequestration of GLUT4 in 3T3-L1 adipocytes. *Biochem Biophys Res Commun*. 347:433-8.

Pryor, P.R., S.C. Liu, A.E. Clark, J. Yang, G.D. Holman, and D. Tosh. 2000. Chronic insulin effects on insulin signalling and GLUT4 endocytosis are reversed by metformin. *Biochem J*. 348 Pt 1:83-91.

Qin, S., Y. Minami, M. Hibi, T. Kurosaki, and H. Yamamura. 1997. Syk-dependent and -independent signaling cascades in B cells elicited by osmotic and oxidative stress. *J Biol Chem*. 272:2098-103.

Quinn, C.E., P.K. Hamilton, C.J. Lockhart, and G.E. McVeigh. 2008. Thiazolidinediones: effects on insulin resistance and the cardiovascular system. *Br J Pharmacol*. 153:636-45.

Ramm, G., M. Larance, M. Guilhaus, and D.E. James. 2006. A role for 14-3-3 in insulin-stimulated GLUT4 translocation through its interaction with the RabGAP AS160. *J Biol Chem*. 281:29174-80.

Randhawa, V.K., P.J. Bilan, Z.A. Khayat, N. Daneman, Z. Liu, T. Ramlal, A. Volchuk, X.R. Peng, T. Coppola, R. Regazzi, W.S. Trimble, and A. Klip. 2000. VAMP2, but not VAMP3/cellubrevin, mediates insulin-dependent incorporation of GLUT4 into the plasma membrane of L6 myoblasts. *Mol Biol Cell*. 11:2403-17.

Rea, R., and R. Donnelly. 2006. Effects of metformin and oleic acid on adipocyte expression of resistin. *Diabetes Obes Metab*. 8:105-9.

Ren, T., J. He, H. Jiang, L. Zu, S. Pu, X. Guo, and G. Xu. 2006. Metformin reduces lipolysis in primary rat adipocytes stimulated by tumor necrosis factor-alpha or isoproterenol. *J Mol Endocrinol*. 37:175-83.

Ritchie, S.A., M.A. Ewart, C.G. Perry, J.M. Connell, and I.P. Salt. 2004. The role of insulin and the adipocytokines in regulation of vascular endothelial function. *Clin Sci (Lond)*. 107:519-32.

Roach, W.G., J.A. Chavez, C.P. Miinea, and G.E. Lienhard. 2007. Substrate specificity and effect on GLUT4 translocation of the Rab GTPase-activating protein Tbc1d1. *Biochem J*. 403:353-8.

Rorsman, P., L. Eliasson, E. Renstrom, J. Gromada, S. Barg, and S. Gopel. 2000. The Cell Physiology of Biphasic Insulin Secretion. *News Physiol Sci*. 15:72-77.

Rouille, Y., S.J. Duguay, K. Lund, M. Furuta, Q. Gong, G. Lipkind, A.A. Oliva, Jr., S.J. Chan, and D.F. Steiner. 1995. Proteolytic processing mechanisms in the biosynthesis of neuroendocrine peptides: the subtilisin-like proprotein convertases. *Front Neuroendocrinol*. 16:322-61.

Ruan, H., and H.F. Lodish. 2003. Insulin resistance in adipose tissue: direct and indirect effects of tumor necrosis factor-alpha. *Cytokine Growth Factor Rev*. 14:447-55.

Ruderman, N.B., H. Park, V.K. Kaushik, D. Dean, S. Constant, M. Prentki, and A.K. Saha. 2003. AMPK as a metabolic switch in rat muscle, liver and adipose tissue after exercise. *Acta Physiol Scand*. 178:435-42.

Ruderman, N.B., A.K. Saha, D. Vavvas, and L.A. Witters. 1999. Malonyl-CoA, fuel sensing, and insulin resistance. *Am J Physiol*. 276:E1-E18.

Russell, R.R., 3rd, R. Bergeron, G.I. Shulman, and L.H. Young. 1999. Translocation of myocardial GLUT-4 and increased glucose uptake through activation of AMPK by AICAR. *Am J Physiol*. 277:H643-9.

Saha, A.K., P.R. Avilucea, J.M. Ye, M.M. Assifi, E.W. Kraegen, and N.B. Ruderman. 2004. Pioglitazone treatment activates AMP-activated protein kinase in rat liver and adipose tissue in vivo. *Biochem Biophys Res Commun*. 314:580-5.

Sajan, M.P., G. Bandyopadhyay, Y. Kanoh, M.L. Standaert, M.J. Quon, B.C. Reed, I. Dikic, and R.V. Farese. 2002. Sorbitol activates atypical protein kinase C and GLUT4 glucose transporter translocation/glucose transport through proline-rich tyrosine kinase-2, the extracellular signal-regulated kinase pathway and phospholipase D. *Biochem J*. 362:665-74.

Sakagami, H., S. Saito, T. Kitani, S. Okuno, H. Fujisawa, and H. Kondo. 1998. Localization of the mRNAs for two isoforms of Ca2+/calmodulin-dependent protein kinase kinases in the adult rat brain. *Brain Res Mol Brain Res*. 54:311-5.

Sakamoto, K., O. Goransson, D.G. Hardie, and D.R. Alessi. 2004. Activity of LKB1 and AMPK-related kinases in skeletal muscle: effects of contraction, phenformin, and AICAR. *Am J Physiol Endocrinol Metab*. 287:E310-7.

Sakamoto, K., and G.D. Holman. 2008. Emerging role for AS160/TBC1D4 and TBC1D1 in the regulation of GLUT4 traffic. *Am J Physiol Endocrinol Metab*. 295:E29-37.

Sakoda, H., T. Ogihara, M. Anai, M. Fujishiro, H. Ono, Y. Onishi, H. Katagiri, M. Abe, Y. Fukushima, N. Shojima, K. Inukai, M. Kikuchi, Y. Oka, and T. Asano. 2002. Activation of AMPK is essential for AICAR-induced glucose uptake by skeletal muscle but not adipocytes. *Am J Physiol Endocrinol Metab*. 282:E1239-44.

Salpeter, S.R., E. Greyber, G.A. Pasternak, and E.E. Salpeter. 2003. Risk of fatal and nonfatal lactic acidosis with metformin use in type 2 diabetes mellitus: systematic review and meta-analysis. *Arch Intern Med*. 163:2594-602.

Salt, I., J.W. Celler, S.A. Hawley, A. Prescott, A. Woods, D. Carling, and D.G. Hardie. 1998a. AMP-activated protein kinase: greater AMP dependence, and preferential nuclear localization, of complexes containing the alpha2 isoform. *Biochem J*. 334 (Pt 1):177-87.

Salt, I.P., J.M. Connell, and G.W. Gould. 2000. 5-aminoimidazole-4-carboxamide ribonucleoside (AICAR) inhibits insulin-stimulated glucose transport in 3T3-L1 adipocytes. *Diabetes*. 49:1649-56.

Salt, I.P., G. Johnson, S.J. Ashcroft, and D.G. Hardie. 1998b. AMP-activated protein kinase is activated by low glucose in cell lines derived from pancreatic beta cells, and may regulate insulin release. *Biochem J*. 335 (Pt 3):533-9.

Saltiel, A.R., and C.R. Kahn. 2001. Insulin signalling and the regulation of glucose and lipid metabolism. *Nature*. 414:799-806.

Saltiel, A.R., and J.E. Pessin. 2002. Insulin signaling pathways in time and space. *Trends Cell Biol*. 12:65-71.

Samad, F., and D.J. Loskutoff. 1996. Tissue distribution and regulation of plasminogen activator inhibitor-1 in obese mice. *Mol Med*. 2:568-82.

Sanders, M.J., Z.S. Ali, B.D. Hegarty, R. Heath, M.A. Snowden, and D. Carling. 2007a. Defining the mechanism of activation of AMP-activated protein kinase by the small molecule A-769662, a member of the thienopyridone family. *J Biol Chem*. 282:32539-48.

Sanders, M.J., P.O. Grondin, B.D. Hegarty, M.A. Snowden, and D. Carling. 2007b. Investigating the mechanism for AMP activation of the AMP-activated protein kinase cascade. *Biochem J*. 403:139-48.

Sano, H., L. Eguez, M.N. Teruel, M. Fukuda, T.D. Chuang, J.A. Chavez, G.E. Lienhard, and T.E. McGraw. 2007. Rab10, a target of the AS160 Rab GAP, is required for insulin-stimulated translocation of GLUT4 to the adipocyte plasma membrane. *Cell Metab*. 5:293-303.

Sano, H., S. Kane, E. Sano, C.P. Miinea, J.M. Asara, W.S. Lane, C.W. Garner, and G.E. Lienhard. 2003. Insulin-stimulated phosphorylation of a Rab GTPase-activating protein regulates GLUT4 translocation. *J Biol Chem*. 278:14599-602.

Sarbassov, D.D., D.A. Guertin, S.M. Ali, and D.M. Sabatini. 2005. Phosphorylation and regulation of Akt/PKB by the rictor-mTOR complex. *Science*. 307:1098-101.

Saxena, R., B.F. Voight, V. Lyssenko, N.P. Burtt, P.I. de Bakker, H. Chen, J.J. Roix, S. Kathiresan, J.N. Hirschhorn, M.J. Daly, T.E. Hughes, L. Groop, D. Altshuler, P. Almgren, J.C. Florez, J. Meyer, K. Ardlie, K. Bengtsson Bostrom, B. Isomaa, G. Lettre, U. Lindblad, H.N. Lyon, O. Melander, C. Newton-Cheh, P. Nilsson, M. Orho-Melander, L. Rastam, E.K. Speliotes, M.R. Taskinen, T. Tuomi, C. Guiducci, A. Berglund, J. Carlson, L. Gianniny, R. Hackett, L. Hall, J. Holmkvist, E. Laurila, M. Sjogren, M. Sterner, A. Surti, M. Svensson, R. Tewhey, B. Blumenstiel, M. Parkin, M. Defelice, R. Barry, W. Brodeur, J. Camarata, N. Chia, M. Fava, J. Gibbons, B. Handsaker, C. Healy, K. Nguyen, C. Gates, C. Sougnez, D. Gage, M. Nizzari, S.B. Gabriel, G.W. Chirn, Q. Ma, H. Parikh, D. Richardson, D. Ricke, and S. Purcell. 2007. Genome-wide association analysis identifies loci for type 2 diabetes and triglyceride levels. *Science*. 316:1331-6.

Schaffler, A., M. Neumeier, H. Herfarth, A. Furst, J. Scholmerich, and C. Buchler. 2005. Genomic structure of human omentin, a new adipocytokine expressed in omental adipose tissue. *Biochim Biophys Acta*. 1732:96-102.

Schaffler, A., J. Scholmerich, and C. Buchler. 2005. Mechanisms of disease: adipocytokines and visceral adipose tissue--emerging role in intestinal and mesenteric diseases. *Nat Clin Pract Gastroenterol Hepatol*. 2:103-11.

Scheid, M.P., and J.R. Woodgett. 2003. Unravelling the activation mechanisms of protein kinase B/Akt. *FEBS Lett*. 546:108-12.

Schmelzle, T., and M.N. Hall. 2000. TOR, a central controller of cell growth. *Cell*. 103:253-62.

Scott, J.W., S.A. Hawley, K.A. Green, M. Anis, G. Stewart, G.A. Scullion, D.G. Norman, and D.G. Hardie. 2004. CBS domains form energy-sensing modules whose binding of adenosine ligands is disrupted by disease mutations. *J Clin Invest*. 113:274-84.

Scott, J.W., B.J. van Denderen, S.B. Jorgensen, J.E. Honeyman, G.R. Steinberg, J.S. Oakhill, T.J. Iseli, A. Koay, P.R. Gooley, D. Stapleton, and B.E. Kemp. 2008. Thienopyridone drugs are selective activators of AMP-activated protein kinase beta1-containing complexes. *Chem Biol*. 15:1220-30.

Segalen, C., S.L. Longnus, D. Baetz, L. Counillon, and E. Van Obberghen. 2008. 5-aminoimidazole-4-carboxamide-1-beta-D-ribofuranoside reduces glucose uptake via the inhibition of Na+/H+ exchanger 1 in isolated rat ventricular cardiomyocytes. *Endocrinology*. 149:1490-8.

Seger, R., and E.G. Krebs. 1995. The MAPK signaling cascade. *Faseb J*. 9:726-35.

Sell, H., D. Dietze-Schroeder, K. Eckardt, and J. Eckel. 2006. Cytokine secretion by human adipocytes is differentially regulated by adiponectin, AICAR, and troglitazone. *Biochem Biophys Res Commun*. 343:700-6.

Senn, J.J., P.J. Klover, I.A. Nowak, T.A. Zimmers, L.G. Koniaris, R.W. Furlanetto, and R.A. Mooney. 2003. Suppressor of cytokine signaling-3 (SOCS-3), a potential mediator of interleukin-6-dependent insulin resistance in hepatocytes. *J Biol Chem*. 278:13740-6.

Shakur, Y., L.S. Holst, T.R. Landstrom, M. Movsesian, E. Degerman, and V. Manganiello. 2001. Regulation and function of the cyclic nucleotide phosphodiesterase (PDE3) gene family. *Prog Nucleic Acid Res Mol Biol*. 66:241-77.

Shaw, R.J., M. Kosmatka, N. Bardeesy, R.L. Hurley, L.A. Witters, R.A. DePinho, and L.C. Cantley. 2004. The tumor suppressor LKB1 kinase directly activates AMP-activated kinase and regulates apoptosis in response to energy stress. *Proc Natl Acad Sci U S A*. 101:3329-35.

Shaw, R.J., K.A. Lamia, D. Vasquez, S.H. Koo, N. Bardeesy, R.A. Depinho, M. Montminy, and L.C. Cantley. 2005. The kinase LKB1 mediates glucose homeostasis in liver and therapeutic effects of metformin. *Science*. 310:1642-6.

Shepherd, P.R. 2005. Mechanisms regulating phosphoinositide 3-kinase signalling in insulin-sensitive tissues. *Acta Physiol Scand*. 183:3-12.

Shimabukuro, M., Y.T. Zhou, M. Levi, and R.H. Unger. 1998. Fatty acid-induced beta cell apoptosis: a link between obesity and diabetes. *Proc Natl Acad Sci U S A*. 95:2498-502.

Shu, Y., S.A. Sheardown, C. Brown, R.P. Owen, S. Zhang, R.A. Castro, A.G. Ianculescu, L. Yue, J.C. Lo, E.G. Burchard, C.M. Brett, and K.M. Giacomini. 2007. Effect of genetic variation in the organic cation transporter 1 (OCT1) on metformin action. *J Clin Invest*. 117:1422-31.

Shulman, G.I. 2000. Cellular mechanisms of insulin resistance. *J Clin Invest*. 106:171-6.

Sinha, R., G. Fisch, B. Teague, W.V. Tamborlane, B. Banyas, K. Allen, M. Savoye, V. Rieger, S. Taksali, G. Barbetta, R.S. Sherwin, and S. Caprio. 2002. Prevalence of impaired glucose tolerance among children and adolescents with marked obesity. *N Engl J Med*. 346:802-10.

Smith, J.L., P.B. Patil, and J.S. Fisher. 2005. AICAR and hyperosmotic stress increase insulin-stimulated glucose transport. *J Appl Physiol*. 99:877-83.

Smith, U., M. Kuroda, and I.A. Simpson. 1984. Counter-regulation of insulin-stimulated glucose transport by catecholamines in the isolated rat adipose cell. *J Biol Chem*. 259:8758-63.

Solaz-Fuster, M.C., J.V. Gimeno-Alcaniz, M. Casado, and P. Sanz. 2006. TRIP6 transcriptional co-activator is a novel substrate of AMP-activated protein kinase. *Cell Signal*. 18:1702-12.

Soukas, A., P. Cohen, N.D. Socci, and J.M. Friedman. 2000. Leptin-specific patterns of gene expression in white adipose tissue. *Genes Dev*. 14:963-80.

Spurlin, B.A., R.M. Thomas, A.K. Nevins, H.J. Kim, Y.J. Kim, H.L. Noh, G.I. Shulman, J.K. Kim, and D.C. Thurmond. 2003. Insulin resistance in tetracycline-repressible Munc18c transgenic mice. *Diabetes*. 52:1910-7.

Srere, P.A. 1959. The citrate cleavage enzyme. I. Distribution and purification. *J Biol Chem*. 234:2544-7.

Standaert, M.L., Y. Kanoh, M.P. Sajan, G. Bandyopadhyay, and R.V. Farese. 2002. Cbl, IRS-1, and IRS-2 mediate effects of rosiglitazone on PI3K, PKC-lambda, and glucose transport in 3T3/L1 adipocytes. *Endocrinology*. 143:1705-16.

Stapleton, D., K.I. Mitchelhill, G. Gao, J. Widmer, B.J. Michell, T. Teh, C.M. House, C.S. Fernandez, T. Cox, L.A. Witters, and B.E. Kemp. 1996. Mammalian AMP-activated protein kinase subfamily. *J Biol Chem*. 271:611-4.

Stapleton, D., E. Woollatt, K.I. Mitchelhill, J.K. Nicholl, C.S. Fernandez, B.J. Michell, L.A. Witters, D.A. Power, G.R. Sutherland, and B.E. Kemp. 1997. AMP-activated protein

kinase isoenzyme family: subunit structure and chromosomal location. *FEBS Lett*. 409:452-6.

Stock, J.B., A.J. Ninfa, and A.M. Stock. 1989. Protein phosphorylation and regulation of adaptive responses in bacteria. *Microbiol Rev*. 53:450-90.

Stone, S., V. Abkevich, D.L. Russell, R. Riley, K. Timms, T. Tran, D. Trem, D. Frank, S. Jammulapati, C.D. Neff, D. Iliev, R. Gress, G. He, G.C. Frech, T.D. Adams, M.H. Skolnick, J.S. Lanchbury, A. Gutin, S.C. Hunt, and D. Shattuck. 2006. TBC1D1 is a candidate for a severe obesity gene and evidence for a gene/gene interaction in obesity predisposition. *Hum Mol Genet*. 15:2709-20.

Stouthard, J.M., J.A. Romijn, T. Van der Poll, E. Endert, S. Klein, P.J. Bakker, C.H. Veenhof, and H.P. Sauerwein. 1995. Endocrinologic and metabolic effects of interleukin-6 in humans. *Am J Physiol*. 268:E813-9.

Stumvoll, M., N. Nurjhan, G. Perriello, G. Dailey, and J.E. Gerich. 1995. Metabolic effects of metformin in non-insulin-dependent diabetes mellitus. *N Engl J Med*. 333:550-4.

Sullivan, J.E., K.J. Brocklehurst, A.E. Marley, F. Carey, D. Carling, and R.K. Beri. 1994. Inhibition of lipolysis and lipogenesis in isolated rat adipocytes with AICAR, a cell-permeable activator of AMP-activated protein kinase. *FEBS Lett*. 353:33-6.

Sun, X.J., and F. Liu. 2009. Phosphorylation of IRS proteins Yin-Yang regulation of insulin signaling. *Vitam Horm*. 80:351-87.

Tapon, N., N. Ito, B.J. Dickson, J.E. Treisman, and I.K. Hariharan. 2001. The Drosophila tuberous sclerosis complex gene homologs restrict cell growth and cell proliferation. *Cell*. 105:345-55.

Taylor, E.B., D. An, H.F. Kramer, H. Yu, N.L. Fujii, K.S. Roeckl, N. Bowles, M.F. Hirshman, J. Xie, E.P. Feener, and L.J. Goodyear. 2008. Discovery of TBC1D1 as an insulin-, AICAR-, and contraction-stimulated signaling nexus in mouse skeletal muscle. *J Biol Chem*. 283:9787-96.

Terada, S., M. Goto, M. Kato, K. Kawanaka, T. Shimokawa, and I. Tabata. 2002. Effects of low-intensity prolonged exercise on PGC-1 mRNA expression in rat epitrochlearis muscle. *Biochem Biophys Res Commun*. 296:350-4.

Thong, F.S., P.J. Bilan, and A. Klip. 2007. The Rab GTPase-Activating Protein AS160 Integrates Akt, Protein Kinase C, and AMP-Activated Protein Kinase Signals Regulating GLUT4 Traffic. *Diabetes*. 56:414-23.

Thong, F.S., C.B. Dugani, and A. Klip. 2005. Turning signals on and off: GLUT4 traffic in the insulin-signaling highway. *Physiology (Bethesda)*. 20:271-84.

Thornton, C., M.A. Snowden, and D. Carling. 1998. Identification of a novel AMP-activated protein kinase beta subunit isoform that is highly expressed in skeletal muscle. *J Biol Chem*. 273:12443-50.

Tiainen, M., A. Ylikorkala, and T.P. Makela. 1999. Growth suppression by Lkb1 is mediated by a G(1) cell cycle arrest. *Proc Natl Acad Sci U S A*. 96:9248-51.

Tiikkainen, M., A.M. Hakkinen, E. Korsheninnikova, T. Nyman, S. Makimattila, and H. Yki-Jarvinen. 2004. Effects of rosiglitazone and metformin on liver fat content, hepatic insulin resistance, insulin clearance, and gene expression in adipose tissue in patients with type 2 diabetes. *Diabetes*. 53:2169-76.

Tokumitsu, H., H. Inuzuka, Y. Ishikawa, M. Ikeda, I. Saji, and R. Kobayashi. 2002. STO-609, a specific inhibitor of the Ca(2+)/calmodulin-dependent protein kinase kinase. *J Biol Chem*. 277:15813-8.

Tomas, E., T.S. Tsao, A.K. Saha, H.E. Murrey, C. Zhang Cc, S.I. Itani, H.F. Lodish, and N.B. Ruderman. 2002. Enhanced muscle fat oxidation and glucose transport by ACRP30 globular domain: acetyl-CoA carboxylase inhibition and AMP-activated protein kinase activation. *Proc Natl Acad Sci U S A*. 99:16309-13.

Tong, J., M.J. Zhu, K.R. Underwood, B.W. Hess, S.P. Ford, and M. Du. 2008. AMP-activated protein kinase and adipogenesis in sheep fetal skeletal muscle and 3T3-L1 cells. *J Anim Sci*. 86:1296-305.

Tong, L. 2005. Acetyl-coenzyme A carboxylase: crucial metabolic enzyme and attractive target for drug discovery. *Cell Mol Life Sci*. 62:1784-803.

Towler, M.C., and D.G. Hardie. 2007. AMP-activated protein kinase in metabolic control and insulin signaling. *Circ Res*. 100:328-41.

Tsao, T.S., E. Tomas, H.E. Murrey, C. Hug, D.H. Lee, N.B. Ruderman, J.E. Heuser, and H.F. Lodish. 2003. Role of disulfide bonds in Acrp30/adiponectin structure and signaling specificity. Different oligomers activate different signal transduction pathways. *J Biol Chem*. 278:50810-7.

Ubersax, J.A., and J.E. Ferrell, Jr. 2007. Mechanisms of specificity in protein phosphorylation. *Nat Rev Mol Cell Biol*. 8:530-41.

Uchida, T., M.G. Myers, Jr., and M.F. White. 2000. IRS-4 mediates protein kinase B signaling during insulin stimulation without promoting antiapoptosis. *Mol Cell Biol*. 20:126-38.

Ullrich, A., and J. Schlessinger. 1990. Signal transduction by receptors with tyrosine kinase activity. *Cell*. 61:203-12.

Ullrich, K.J. 1994. Specificity of transporters for 'organic anions' and 'organic cations' in the kidney. *Biochim Biophys Acta*. 1197:45-62.

Uysal, K.T., S.M. Wiesbrock, M.W. Marino, and G.S. Hotamisligil. 1997. Protection from obesity-induced insulin resistance in mice lacking TNF-alpha function. *Nature*. 389:610-4.

Vanhaesebroeck, B., S.J. Leevers, G. Panayotou, and M.D. Waterfield. 1997. Phosphoinositide 3-kinases: a conserved family of signal transducers. *Trends Biochem Sci*. 22:267-72.

Vgontzas, A.N., D.A. Papanicolaou, E.O. Bixler, A. Kales, K. Tyson, and G.P. Chrousos. 1997. Elevation of plasma cytokines in disorders of excessive daytime sleepiness: role of sleep disturbance and obesity. *J Clin Endocrinol Metab*. 82:1313-6.

Vidal-Puig, A.J., R.V. Considine, M. Jimenez-Linan, A. Werman, W.J. Pories, J.F. Caro, and J.S. Flier. 1997. Peroxisome proliferator-activated receptor gene expression in human tissues. Effects of obesity, weight loss, and regulation by insulin and glucocorticoids. *J Clin Invest*. 99:2416-22.

Villena, J.A., B. Viollet, F. Andreelli, A. Kahn, S. Vaulont, and H.S. Sul. 2004. Induced adiposity and adipocyte hypertrophy in mice lacking the AMP-activated protein kinase-alpha2 subunit. *Diabetes*. 53:2242-9.

Vincent, M.F., M.D. Erion, H.E. Gruber, and G. Van den Berghe. 1996. Hypoglycaemic effect of AICAriboside in mice. *Diabetologia*. 39:1148-55.

Vincent, M.F., P.J. Marangos, H.E. Gruber, and G. Van den Berghe. 1991. Inhibition by AICA riboside of gluconeogenesis in isolated rat hepatocytes. *Diabetes*. 40:1259-66.

Wajchenberg, B.L. 2000. Subcutaneous and visceral adipose tissue: their relation to the metabolic syndrome. *Endocr Rev*. 21:697-738.

Wakil, S.J. 1989. Fatty acid synthase, a proficient multifunctional enzyme. *Biochemistry*. 28:4523-30.

Wakil, S.J., J.K. Stoops, and V.C. Joshi. 1983. Fatty acid synthesis and its regulation. *Annu Rev Biochem*. 52:537-79.

Wang, D., and H.S. Sul. 1997. Upstream stimulatory factor binding to the E-box at -65 is required for insulin regulation of the fatty acid synthase promoter. *J Biol Chem*. 272:26367-74.

Wang, D.S., J.W. Jonker, Y. Kato, H. Kusuhara, A.H. Schinkel, and Y. Sugiyama. 2002. Involvement of organic cation transporter 1 in hepatic and intestinal distribution of metformin. *J Pharmacol Exp Ther*. 302:510-5.

Wang, X., L. Zhou, G. Li, T. Luo, Y. Gu, L. Qian, X. Fu, F. Li, J. Li, and M. Luo. 2007. Palmitate activates AMP-activated protein kinase and regulates insulin secretion from beta cells. *Biochem Biophys Res Commun*. 352:463-8.

Ward, C.W., and M.C. Lawrence. 2009. Ligand-induced activation of the insulin receptor: a multi-step process involving structural changes in both the ligand and the receptor. *Bioessays*. 31:422-34.

Warne, J.P. 2003. Tumour necrosis factor alpha: a key regulator of adipose tissue mass. *J Endocrinol*. 177:351-5.

Watkins, P.A. 1997. Fatty acid activation. *Prog Lipid Res*. 36:55-83.

Weyer, C., T. Funahashi, S. Tanaka, K. Hotta, Y. Matsuzawa, R.E. Pratley, and P.A. Tataranni. 2001. Hypoadiponectinemia in obesity and type 2 diabetes: close association with insulin resistance and hyperinsulinemia. *J Clin Endocrinol Metab*. 86:1930-5.

White, M.F. 1998. The IRS-signalling system: a network of docking proteins that mediate insulin action. *Mol Cell Biochem*. 182:3-11.

White, M.F. 2002. IRS proteins and the common path to diabetes. *Am J Physiol Endocrinol Metab*. 283:E413-22.

Whitehead, J.P., S.F. Clark, B. Urso, and D.E. James. 2000. Signalling through the insulin receptor. *Curr Opin Cell Biol*. 12:222-8.

Whitehead, J.P., J.C. Molero, S. Clark, S. Martin, G. Meneilly, and D.E. James. 2001. The role of Ca2+ in insulin-stimulated glucose transport in 3T3-L1 cells. *J Biol Chem*. 276:27816-24.

Widberg, C.H., N.J. Bryant, M. Girotti, S. Rea, and D.E. James. 2003. Tomosyn interacts with the t-SNAREs syntaxin4 and SNAP23 and plays a role in insulin-stimulated GLUT4 translocation. *J Biol Chem*. 278:35093-101.

Wiman, B., J. Chmielewska, and M. Ranby. 1984. Inactivation of tissue plasminogen activator in plasma. Demonstration of a complex with a new rapid inhibitor. *J Biol Chem*. 259:3644-7.

Winder, W.W., and D.G. Hardie. 1996. Inactivation of acetyl-CoA carboxylase and activation of AMP-activated protein kinase in muscle during exercise. *Am J Physiol*. 270:E299-304.

Winder, W.W., B.F. Holmes, D.S. Rubink, E.B. Jensen, M. Chen, and J.O. Holloszy. 2000. Activation of AMP-activated protein kinase increases mitochondrial enzymes in skeletal muscle. *J Appl Physiol*. 88:2219-26.

Witczak, C.A., N. Fujii, M.F. Hirshman, and L.J. Goodyear. 2007. Ca2+/calmodulin-dependent protein kinase kinase-alpha regulates skeletal muscle glucose uptake independent of AMP-activated protein kinase and Akt activation. *Diabetes*. 56:1403-9.

Witters, L.A., and B.E. Kemp. 1992. Insulin activation of acetyl-CoA carboxylase accompanied by inhibition of the 5'-AMP-activated protein kinase. *J Biol Chem*. 267:2864-7.

Witters, L.A., A.C. Nordlund, and L. Marshall. 1991. Regulation of intracellular acetyl-CoA carboxylase by ATP depletors mimics the action of the 5'-AMP-activated protein kinase. *Biochem Biophys Res Commun*. 181:1486-92.

Wojtaszewski, J.F., C. MacDonald, J.N. Nielsen, Y. Hellsten, D.G. Hardie, B.E. Kemp, B. Kiens, and E.A. Richter. 2003. Regulation of 5'AMP-activated protein kinase activity and substrate utilization in exercising human skeletal muscle. *Am J Physiol Endocrinol Metab*. 284:E813-22.

Wojtczak, L., and P. Schonfeld. 1993. Effect of fatty acids on energy coupling processes in mitochondria. *Biochim Biophys Acta*. 1183:41-57.

Woods, A., P.C. Cheung, F.C. Smith, M.D. Davison, J. Scott, R.K. Beri, and D. Carling. 1996a. Characterization of AMP-activated protein kinase beta and gamma subunits. Assembly of the heterotrimeric complex in vitro. *J Biol Chem*. 271:10282-90.

Woods, A., K. Dickerson, R. Heath, S.P. Hong, M. Momcilovic, S.R. Johnstone, M. Carlson, and D. Carling. 2005. Ca2+/calmodulin-dependent protein kinase kinase-beta acts upstream of AMP-activated protein kinase in mammalian cells. *Cell Metab*. 2:21-33.

Woods, A., S.R. Johnstone, K. Dickerson, F.C. Leiper, L.G. Fryer, D. Neumann, U. Schlattner, T. Wallimann, M. Carlson, and D. Carling. 2003. LKB1 is the upstream kinase in the AMP-activated protein kinase cascade. *Curr Biol*. 13:2004-8.

Woods, A., I. Salt, J. Scott, D.G. Hardie, and D. Carling. 1996b. The alpha1 and alpha2 isoforms of the AMP-activated protein kinase have similar activities in rat liver but exhibit differences in substrate specificity in vitro. *FEBS Lett*. 397:347-51.

Wu, X., H. Motoshima, K. Mahadev, T.J. Stalker, R. Scalia, and B.J. Goldstein. 2003. Involvement of AMP-activated protein kinase in glucose uptake stimulated by the globular domain of adiponectin in primary rat adipocytes. *Diabetes*. 52:1355-63.

Xiao, B., R. Heath, P. Saiu, F.C. Leiper, P. Leone, C. Jing, P.A. Walker, L. Haire, J.F. Eccleston, C.T. Davis, S.R. Martin, D. Carling, and S.J. Gamblin. 2007. Structural basis for AMP binding to mammalian AMP-activated protein kinase. *Nature*. 449:496-500.

Xing, H., J.P. Northrop, J.R. Grove, K.E. Kilpatrick, J.L. Su, and G.M. Ringold. 1997. TNF alpha-mediated inhibition and reversal of adipocyte differentiation is accompanied by suppressed expression of PPARgamma without effects on Pref-1 expression. *Endocrinology*. 138:2776-83.

Xu, H., K.M. Williams, W.S. Liauw, M. Murray, R.O. Day, and A.J. McLachlan. 2008. Effects of St John's wort and CYP2C9 genotype on the pharmacokinetics and pharmacodynamics of gliclazide. *Br J Pharmacol*. 153:1579-86.

Yaffe, M.B., G.G. Leparc, J. Lai, T. Obata, S. Volinia, and L.C. Cantley. 2001. A motif-based profile scanning approach for genome-wide prediction of signaling pathways. *Nat Biotechnol*. 19:348-53.

Yamada, E., S. Okada, T. Saito, K. Ohshima, M. Sato, T. Tsuchiya, Y. Uehara, H. Shimizu, and M. Mori. 2005. Akt2 phosphorylates Synip to regulate docking and fusion of GLUT4-containing vesicles. *J Cell Biol*. 168:921-8.

Yamagishi, S.I., D. Edelstein, X.L. Du, Y. Kaneda, M. Guzman, and M. Brownlee. 2001. Leptin induces mitochondrial superoxide production and monocyte chemoattractant protein-1 expression in aortic endothelial cells by increasing fatty acid oxidation via protein kinase A. *J Biol Chem*. 276:25096-100.

Yamaguchi, S., H. Katahira, S. Ozawa, Y. Nakamichi, T. Tanaka, T. Shimoyama, K. Takahashi, K. Yoshimoto, M.O. Imaizumi, S. Nagamatsu, and H. Ishida. 2005. Activators of AMP-activated protein kinase enhance GLUT4 translocation and its glucose transport activity in 3T3-L1 adipocytes. *Am J Physiol Endocrinol Metab*. 289:E643-9.

Yamauchi, M., F. Kambe, X. Cao, X. Lu, Y. Kozaki, Y. Oiso, and H. Seo. 2008. Thyroid hormone activates adenosine 5'-monophosphate-activated protein kinase via intracellular calcium mobilization and activation of calcium/calmodulin-dependent protein kinase kinase-beta. *Mol Endocrinol*. 22:893-903.

Yamauchi, T., J. Kamon, Y. Minokoshi, Y. Ito, H. Waki, S. Uchida, S. Yamashita, M. Noda, S. Kita, K. Ueki, K. Eto, Y. Akanuma, P. Froguel, F. Foufelle, P. Ferre, D. Carling, S. Kimura, R. Nagai, B.B. Kahn, and T. Kadowaki. 2002. Adiponectin stimulates glucose utilization and fatty-acid oxidation by activating AMP-activated protein kinase. *Nat Med*. 8:1288-95.

Yang, C., K.J. Coker, J.K. Kim, S. Mora, D.C. Thurmond, A.C. Davis, B. Yang, R.A. Williamson, G.I. Shulman, and J.E. Pessin. 2001. Syntaxin 4 heterozygous knockout mice develop muscle insulin resistance. *J Clin Invest*. 107:1311-8.

Yang, C., R.T. Watson, J.S. Elmendorf, D.B. Sacks, and J.E. Pessin. 2000. Calmodulin antagonists inhibit insulin-stimulated GLUT4 (glucose transporter 4) translocation by preventing the formation of phosphatidylinositol 3,4,5-trisphosphate in 3T3L1 adipocytes. *Mol Endocrinol*. 14:317-26.

Yang, J., A. Hodel, and G.D. Holman. 2002. Insulin and isoproterenol have opposing roles in the maintenance of cytosol pH and optimal fusion of GLUT4 vesicles with the plasma membrane. *J Biol Chem*. 277:6559-66.

Ye, J.M., N. Dzamko, M.E. Cleasby, B.D. Hegarty, S.M. Furler, G.J. Cooney, and E.W. Kraegen. 2004. Direct demonstration of lipid sequestration as a mechanism by which rosiglitazone prevents fatty-acid-induced insulin resistance in the rat: comparison with metformin. *Diabetologia*. 47:1306-13.

Ye, J.M., N. Dzamko, A.J. Hoy, M.A. Iglesias, B. Kemp, and E. Kraegen. 2006. Rosiglitazone treatment enhances acute AMP-activated protein kinase-mediated muscle and adipose tissue glucose uptake in high-fat-fed rats. *Diabetes*. 55:2797-804.

Yeh, L.A., K.H. Lee, and K.H. Kim. 1980. Regulation of rat liver acetyl-CoA carboxylase. Regulation of phosphorylation and inactivation of acetyl-CoA carboxylase by the adenylate energy charge. *J Biol Chem*. 255:2308-14.

Yin, D., S.D. Clarke, J.L. Peters, and T.D. Etherton. 1998. Somatotropin-dependent decrease in fatty acid synthase mRNA abundance in 3T3-F442A adipocytes is the result of a decrease in both gene transcription and mRNA stability. *Biochem J*. 331 (Pt 3):815-20.

Yin, W., J. Mu, and M.J. Birnbaum. 2003. Role of AMP-activated protein kinase in cyclic AMP-dependent lipolysis In 3T3-L1 adipocytes. *J Biol Chem*. 278:43074-80.

Yoon, J.C., T.W. Chickering, E.D. Rosen, B. Dussault, Y. Qin, A. Soukas, J.M. Friedman, W.E. Holmes, and B.M. Spiegelman. 2000. Peroxisome proliferator-activated receptor gamma target gene encoding a novel angiopoietin-related protein associated with adipose differentiation. *Mol Cell Biol*. 20:5343-9.

Young, J., and S. Povey. 1998. The genetic basis of tuberous sclerosis. *Mol Med Today*. 4:313-9.

Young, M.E., G.K. Radda, and B. Leighton. 1996. Activation of glycogen phosphorylase and glycogenolysis in rat skeletal muscle by AICAR--an activator of AMP-activated protein kinase. *FEBS Lett*. 382:43-7.

Zerial, M., and H. McBride. 2001. Rab proteins as membrane organizers. *Nat Rev Mol Cell Biol*. 2:107-17.

Zhang, Y., R. Proenca, M. Maffei, M. Barone, L. Leopold, and J.M. Friedman. 1994. Positional cloning of the mouse obese gene and its human homologue. *Nature*. 372:425-32.

Zheng, D., P.S. MacLean, S.C. Pohnert, J.B. Knight, A.L. Olson, W.W. Winder, and G.L. Dohm. 2001. Regulation of muscle GLUT-4 transcription by AMP-activated protein kinase. *J Appl Physiol*. 91:1073-83.

Zhou, G., R. Myers, Y. Li, Y. Chen, X. Shen, J. Fenyk-Melody, M. Wu, J. Ventre, T. Doebber, N. Fujii, N. Musi, M.F. Hirshman, L.J. Goodyear, and D.E. Moller. 2001. Role of AMP-activated protein kinase in mechanism of metformin action. *J Clin Invest*. 108:1167-74.

Zhou, Y.P., and V. Grill. 1995. Long term exposure to fatty acids and ketones inhibits B-cell functions in human pancreatic islets of Langerhans. *J Clin Endocrinol Metab*. 80:1584-90.

Zigman, J.M., and J.K. Elmquist. 2003. Minireview: From anorexia to obesity--the yin and yang of body weight control. *Endocrinology*. 144:3749-56.

Zong, H., J.M. Ren, L.H. Young, M. Pypaert, J. Mu, M.J. Birnbaum, and G.I. Shulman. 2002. AMP kinase is required for mitochondrial biogenesis in skeletal muscle in response to chronic energy deprivation. *Proc Natl Acad Sci U S A*. 99:15983-7.